

Actions of Cannabinoids on Amoebae

By

Israa Al-hammadi

Lancaster
University



This thesis is submitted for the degree of
Doctor of Philosophy

April 2020

Department of Biomedical and Life Sciences

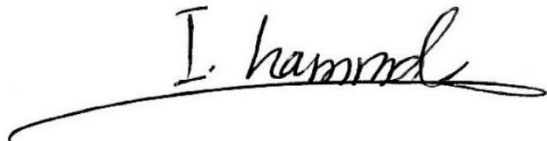
2nd April 2020

To Whom It May Concern:

Declaration

Actions of cannabinoids on amoebae.

This thesis has not been submitted in support of an application for another degree at this or any other university. It is the result of my own work and includes nothing that is the outcome of work done in collaboration except where specifically indicated. Many of the ideas in this thesis were the product of discussion with my supervisor Dr. Jackie Parry and Dr. Karen Wright.

A handwritten signature in black ink, reading "I. hammadi", with a long horizontal flourish underneath.

Israa Al-hammadi MSc. BSc.

Table of contents

Abstract	1
Chapter 1: General Introduction	3
1.1 Introduction	3
1.2 The Endocannabinoid System (ECS) in humans	3
1.2.1 General overview	3
1.2.2 Main ligands of the endocannabinoid system	3
1.2.2.1 Endocannabinoids	4
1.2.2.2 Phytocannabinoids	7
1.2.3 Main cannabinoid receptors	10
1.2.3.1. CB1 and CB2 receptors	10
1.2.3.2 The transient receptor potential vanilloid type 1 (TRPV1)	11
1.2.3.3 G-protein coupled receptor 55 (GPR55)	11
1.2.4 Other receptors	12
1.2.4.1 Peroxisome Proliferator-activated Receptors (PPARs)	12
1.2.4.2 Dopamine Receptors	14
1.2.4.3 Serotonin receptors (5-HT)	16
1.3. Existence of an endocannabinoid system in single-celled eukaryotes	17
1.3.1. Endocannabinoids in <i>Tetrahymena</i>	18
1.3.2. Enzymes in <i>Tetrahymena</i>	19
1.3.3. Receptors in <i>Tetrahymena</i>	19
1.3.4. Response of <i>Tetrahymena</i> to cannabinoids	20
1.4. Cannabinoids and amoebae	21
1.4.1. Overview of amoebae	21
1.4.2. Amoebic response to cannabinoids	21
1.4.3. Amoebic feeding	23
1.4.3.1. General overview	23
1.4.3.2. Receptor-mediated ingestion of prey (Fig. 1.9, stages 1-2)	24
1.4.3.3. Phagosome formation and trafficking (Fig. 1.9, stages 3-6)	27
1.4.3.4. Defecation and membrane recycling (Fig. 1.9, stages 7-9)	28
1.5. Aims of the study	28

Chapter 2: Methods and Materials	30
2.1 Organisms and maintenance	30
2.1.1. <i>Escherichia coli</i>	30
2.1.2. <i>Synechococcus</i> sp. ('Pico')	30
2.1.3. Amoebae	30
2.2. Experimental compounds	31
2.2.1 Fluorescent microspheres ('beads')	31
2.2.2. Agonists	32
2.2.3. Antagonists	32
2.2.4. Sugars	32
2.3. Counting cells and beads	32
2.3.1 Counting <i>E. coli</i> cells	32
2.3.2 Counting <i>Synechococcus</i> cells and beads	33
2.3.3. Counting amoeba cells in suspension	33
2.3.4. Counting amoeba cells on agar plates	33
2.3.5. Counting fluorescent prey inside <i>Vermamoeba vermiformis</i> cells	33
2.4. Amoeba population growth experiments	34
2.4.1. Basic experimental protocol	34
2.4.2. Initial screening of amoebae for sensitivity to the agonists	34
2.4.3. Determining MIC, IC50 and lethal dose of agonists against sensitive amoebae	35
2.4.4. Effect of antagonists on population growth	34
2.5. Feeding experiments involving <i>Vermamoeba vermiformis</i>	34
2.5.1. Basic experimental protocol	34
2.5.2. Effect of AEA and CBD on <i>V. vermiformis</i> feeding	36
2.5.3. Effect of CBD concentration of <i>V. vermiformis</i> feeding	36
2.5.4. Effect of PPAR agonists and antagonists of the feeding of <i>V. vermiformis</i>	36
2.5.5. Effect of blocking amoeba prey recognition receptors, prior to adding CBD on <i>V. vermiformis</i> feeding	37
2.6. Effect of CBD on phagosome processing and defecation in <i>V. vermiformis</i>	37
2.7. Bioinformatic analysis	38

Chapter 3: Sensitivity of amoebae to CBD and AEA	39
3.1. Introduction	39
3.2. Results	39
3.2.1 Initial screening of amoebae for sensitivity to AEA and CBD	39
3.2.2 MIC, IC50 and lethal dose values for AEA and CBD against sensitive amoebae	41
3.3. Discussion	43
3.3.1 Differences in sensitivity of amoebae to AEA and CBD	44
3.3.2 Dose-dependent effect of AEA and CBD on amoebic growth	46
3.4. Conclusions	49
Chapter 4: Effect of CBD and AEA on feeding in <i>Vermamoeba vermiformis</i>	50
4.1. Introduction	50
4.2. Results	51
4.2.1 Effect of AEA and CBD (2µM) on <i>V. vermiformis</i> feeding on indigestible bead and <i>Synechococcus</i> ('Pico')	53
4.2.2 Effect of CBD concentration on the feeding lag and ingestion rate of <i>V. vermiformis</i>	55
4.2.3 Effect of CBD on phagosome trafficking within <i>V. vermiformis</i>	55
4.2.4 Interaction between CBD and the feeding receptors of <i>V. vermiformis</i>	56
4.3. Discussion	59
4.3.1 Effect of particle type on <i>V. vermiformis</i> ingestion rates	59
4.3.2 Effect of AEA on the feeding of <i>V. vermiformis</i>	60
4.3.3 Overall effect of CBD on the feeding of <i>V. vermiformis</i>	61
4.3.4 Effect of CBD on phagosome trafficking and defecation (Fig. 4.8, stages 6-7)	62
4.3.5 Effect of CBD on phagosome formation (Fig. 4.8, stages 3-5)	63
4.3.6 Effect of CBD on phagosome membrane recycling (Fig. 4.8, stages 8-9)	64
4.3.7 Pre-phagosome membrane availability at the site of phagocytosis (Fig. 4.8, stage 1)	65
4.3.8 Effect of CBD on receptor-mediated prey uptake (Fig. 4.8, stages 1-2)	66
4.3.8.1 Prey uptake in the absence of CBD	66
4.3.8.2 Prey uptake in the presence of CBD	68
4.3.9 Working hypothesis on how CBD affects feeding in <i>V. vermiformis</i>	69
4.4. Conclusions	72

Chapter 5: Involvement of Peroxisome Proliferator-Activated Receptors (PPARs)	
in the mode of action of CBD against <i>Veramoeba vermiformis</i>	73
5.1. Introduction	73
5.2. Results	74
5.2.1. Growth experiments	74
5.2.1.1. Response of all amoebae to four PPAR agonists	74
5.2.1.2. Response of all <i>V. vermiformis</i> strains to PPAR agonists in the presence and absence of specific PPAR antagonists	77
5.2.1.3. Response of all <i>V. vermiformis</i> strains to AEA and CBD in the presence and absence of specific PPAR antagonists	78
5.2.1.4. Response of all <i>V. vermiformis</i> strains to CBD in the presence of varying concentrations of specific PPAR antagonists	80
5.2.2. Feeding experiments with <i>V. vermiformis</i> CCAP 1534/14	81
5.3. Discussion	84
5.3.1. Sensitivity of amoebae to PPAR agonists	84
5.3.2. Response of <i>V. vermiformis</i> to PPAR antagonists	86
5.3.2.1. Growth experiments	86
5.3.2.2. Feeding experiments	88
5.3.3. PPAR-induced non-genomic response	89
5.3.4. Signalling cascades responsible for phagosome cup formation (Fig. 4.8, stage 2-3)	91
5.3.4.1. Opsonized phagocytosis in macrophages	91
5.3.4.2. Non-opsonized phagocytosis in macrophages	93
5.3.4.3. Phagocytosis of <i>Mycobacterium</i> spp. and the involvement of PPAR	95
5.4. Conclusion	98
Chapter 6: Involvement of the dopamine and serotonin receptors in the mode of action of CBD against amoebae	100
6.1. Introduction	100
6.2. Results	101
6.2.1. Growth experiments with Haloperidol	101
6.2.2. Feeding experiment with Haloperidol	102
6.2.3. Growth experiments with separate dopamine and serotonin	

receptor blockers	103
6.3. Discussion	105
6.3.1. Effect of CBD on <i>N. gruberi</i> feeding	105
6.3.2. Blocking experiments	106
6.3.2.1. Suitability of the chosen receptor blockers	106
6.3.2.2. Population growth of amoebae in the presence of AEA and CBD with/without Haloperidol	106
6.3.2.3. Population growth of <i>N. gruberi</i> in the presence of CBD with/without S-WAY	107
6.4. Conclusions	108
Chapter 7: General Discussion	109
7.1. Amoebic sensitivity to AEA and CBD	109
7.2. Amoebic response to AEA	110
7.3. Effect of CBD on amoebic feeding	112
7.3.1. Amoebic feeding in the absence of CBD	112
7.3.2. Amoebic feeding response in the presence of CBD	113
7.4. Mode of action of CBD on <i>V. vermiformis</i>	115
7.5. Comparison of <i>V.vermiformis</i> response to cells of higher animals	117
7.6. Involvement of serotonin receptors in the mode of action of CBD against amoebae	118
7.7. Conclusion	119
References	120
Appendix 1: Media formulations	146
Appendix 2: IC50 graphs of all sensitive amoeba strains with AEA and CBD (Section 3.2.2)	147
Appendix 3: IC50 graphs of all sensitive amoeba strains with OEA, PEA, GW0742 and Rosiglitazone (Section 5.2.1.1)	151
Appendix 4: Response of <i>Vermamoeba vermiformis</i> strains to PPAR agonists in the presence and absence of specific PPAR antagonists (Section 5.2.1.2)	158
Appendix 5: Response of <i>Vermamoeba vermiformis</i> strains to CBD in the presence and absence of three PPAR antagonists (Section 5.2.1.3)	164
Appendix 6: Response of <i>Vermamoeba vermiformis</i> strains to CBD in the presence	

and absence of three PPAR antagonists at different concentrations (Section 5.2.1.4)	166
Appendix 7: Response of sensitive amoeba strains to CBD and AEA in the presence and absence of Haloperidol (Section 6.2.1.)	173

Abbreviations

ECS	endocannabinoid system
CBD	Cannabidiol
AEA	Arachidonylethanolamide
OEA	Oleylethanolamide
PEA	Palmitoylethanolamide
PPAR	Peroxisome proliferator-activated receptor
AcEs	Acylethanolamines
AcGs	Acylglycerols
CBRs	Cannabinoid receptors
CB1	Cannabinoid receptor type 1
CB2	Cannabinoid receptor type 2
COX2	Cyclooxygenase subtype 2
DAGL	Diacylglycerol lipase subtype α
DAPI	4',6-diamidino-2-phenylindole
FAAH	Fatty acid amide hydrolase
GPCR	G protein-coupled receptor
GPR55	G-protein-coupled receptor 55
IC50	half maximal inhibitory concentration
MAGL	Monoacylglyceride lipase
MIC	Minimum inhibitory concentration
NAPE-PLD	N-acyl phosphatidylethanolamide selective phospholipase D
THC	Delta-9-Tetrahydrocannabinol
CBGA	cannabigerolic acid
CBDAS	oxidocyclase cannabidiolic acid synthase
TRVP1	Transient receptor potential channel subfamily V member 1
2-AG	2-arachidonoylglycerol
GlcNAc	N-Acetyl-D-glucosamine
GalNAc	N-Acetyl-D-galactosamine
Syk	Tyrosine-protein kinase

LAT	Linker for activation of T cells
PKC	Protein Kinase C

Acknowledgement

First, and most of all, I would like to thank Dr. Jackie Parry and Dr. Karen Wright for their assistance, guidance and patience throughout this study. Without your help this work would not have been possible, I will be always grateful for this opportunity. The thanks extend to the exceptional people in the department of biomedical and life Sciences in Lancaster University. I would like to special thanks Janice Drinkall and Dawn McCracken for many ways they helped me to finish this study. I also would like to acknowledge those who made this PhD possible financially The Higher Committee For Education Development (HCED) in Iraq. Lastly, I would like to say a very big thank you to my husband Ahmed, my parents and everyone in my family who have always offered me their unconditional love and support.

Abstract

Endocannabinoids, such as Anandamide (AEA), are lipid compounds which, together with the receptors they bind to, form the endocannabinoid system (ECS) which, in animals, modulates mood, cognition, appetite etc. The ECS can be activated by phytocannabinoids such as cannabidiol (CBD) and as such, interest in its therapeutic use has grown substantially over recent years. However, not all of CBD's effects can be explained by its binding to cannabinoid receptors and many other targets have been proposed. A better understanding of these alternative targets would increase the therapeutic potential of this phytocannabinoid in the future.

Single-celled protists, such as amoebae, do not possess cannabinoid receptors yet they respond negatively to endo- and phyto-cannabinoids, suggesting they possess alternative targets only. This study therefore examined the involvement of three alternative targets, i.e., the Peroxisome-Proliferator Activated Receptor (PPAR), Dopamine Receptor and Serotonin Receptor, in the action of AEA and CBD on amoebae.

Of the 20-amoeba species tested, only 6 showed a reduction in population growth in the presence of CBD (IC_{50} , 0.98-7.31 μ M), i.e., *Hartmannella cantabrigiensis*, *Naegleria gruberi*, *Vahlkampfia avara*, *Vermamoeba vermiformis*, *Acanthamoeba castellanii* and *Flamella arnhemensis*. All but the latter two species also showed reduced population growth in the presence of AEA (IC_{50} , 0.96-9.89 μ M). The negative effect of AEA could not be alleviated by blocking receptors with antagonists against the three PPAR isoforms (PPARs α , β and γ), the dopamine receptor or the serotonin receptor, suggesting that none were involved in the mode of action of AEA. However, the negative effect of CBD was alleviated with the antagonist for the PPAR α receptor in *V. vermiformis* and that for the serotonin receptor (specifically 5-HT $_{1A}$) in *N. gruberi*. Interestingly, CBD significantly affected the feeding behaviour of these two amoebae (but AEA did not), by stopping amoebic feeding completely (and causing a lag in the ingestion of prey), which was then followed by a reduced ingestion rate; both of which were dose-dependent.

Further work with *V. vermiformis* showed that this CBD-induced cessation in feeding was not due to the halting of phagosome processing and defecation however, there was an interaction between CBD and C-type lectins recognising mannose, N-Acetyl-D-glucosamine (GlcNAc) and

N-Acetyl-D-galactosamine (GalNAc). Receptor-mediated phagocytosis in *V. vermiformis* involved all three C-type lectins and although CBD did not appear to directly interfere (bind) with any of them, its presence (together with sugars to block these receptors) led to a synergistic reduction in ingestion rate with mannose and GalNAc (but no effect on lag) and an extension of the lag with GlcNAc (but no effect on ingestion rate). The 'CBD-receptor' (putative PPAR α) and GlcNAc receptor were therefore considered to be involved with phagosome formation and not prey capture and phagosome filling. It is therefore hypothesised that, because only the three PPAR isoforms exist in vertebrates, *V. vermiformis* possesses a promiscuous PPAR-like molecule that can bind CBD at the same site it binds the PPAR α antagonist. The instantaneous nature of the feeding lag suggests the presence of a non-genomic PPAR response whereby in its ligated state PPAR cannot bind with a necessary protein (possibly Syk, LAT or PKC) to initiate a downstream signaling cascade, which would normally culminate in actin polymerisation and phagocytic cup formation.

In conclusion, amoebae provide an ideal model organism to evaluate the significance of alternative targets in the functioning of the ECS. And, as is the case with animals, multiple alternative targets appear to be present in amoebae; PPAR α (for CBD) in one species, Serotonin Receptor (for CBD) in another species, with the other alternative targets for CBD and indeed AEA currently unknown. And, considering multicellularity originated from free-living single-celled protists, amoebae have also provided an opportunity to investigate the historical functioning of the ECS which appears to be in the main, involved with the feeding response.

Chapter 1: General Introduction

1.1. Introduction

This introduction begins with an overview of the endocannabinoid system in humans which encompasses its role, the receptors involved and their ligands. It then evaluates the phylogenetic and experimental evidence for an endocannabinoid system in single-celled protists, in particular, the ciliate *Tetrahymena*. It then moves on to amoebae, the organism used in this study and, in particular, reviews current knowledge regarding its feeding mechanisms.

1.2. The Endocannabinoid System (ECS) in humans

1.2.1. General overview

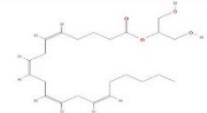
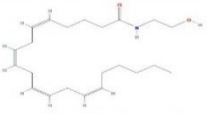
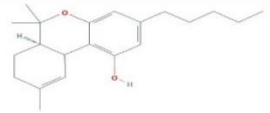
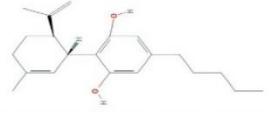
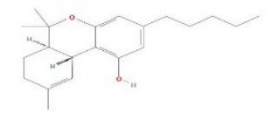
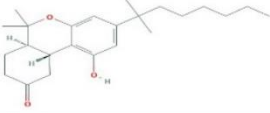
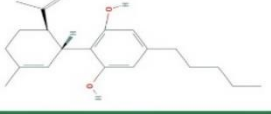
The endocannabinoid system (ECS), also known as the endogenous cannabinoid system, is present in almost all types of vertebrates including mammals, birds, reptiles and fish (Silver 2019). It is one of the most important biological systems within the body with the function of maintaining homeostasis (Bih et al., 2015). As such, it is involved in the control of many processes such as mood, pain, cognition, appetite, memory, inflammation and reproductive function, and if perturbed, can lead to physiological or pathophysiological disorders (Hansen et al. 2006; Ngo et al., 2019). The ECS comprises cannabinoid receptors (CBRs), their endogenous ligands, i.e., endocannabinoids, and the enzymes that synthesise and metabolise them (Battista et al., 2012). Endocannabinoids initiate their action by binding to CBRs (Howlett et al., 2010), however, these receptors can also bind phytocannabinoids such as Δ^9 -tetrahydrocannabinol (THC) and cannabidiol (CBD), present naturally in *Cannabis sativa* (Pertwee et al., 2010; Wu, 2019).

1.2.2. Main ligands of the endocannabinoid system

Ligands for the endocannabinoid system are classified into two main groups; the endogenous endocannabinoids (neurotransmitter compounds formed in the brain and in peripheral tissues) and the exogenous phytocannabinoids (occur naturally in *C. sativa*). In addition, there are many synthetic cannabinoids (Table 1.1) (Svíženská et al. 2008; Madras, 2015). These endogenous, exogenous and synthetic cannabinoids are further classified based on their acyl

chain and, in the main, fall into two groups: N-acylethanolamines (NAEs) and monoacylglycerols (ACGs) (Piscitelli, 2015).

Table 1.1: Common members for the three main cannabinoid groups. Their chemical structure, the enzymes that metabolise them and the receptor(s) they bind to (Bettinger and Chu, 2019).

Table 1: Examples of Types of Cannabinoids.*			
	Potency toward Cannabinoid (CB) Receptors	Metabolism	Chemical Structures**
Endocannabinoids			
2-arachidonoylglycerol	<ul style="list-style-type: none"> Both CB1 and CB2 	<ul style="list-style-type: none"> Primarily MAGL into glycerol and arachidonic acid 	
Anandamide	<ul style="list-style-type: none"> Preferentially CB1 Some activity on TRPV-1 	<ul style="list-style-type: none"> FAAH ethanolamine and arachidonic acid COX-2 into prostaglandins 	
Phytocannabinoids			
Delta-9-tetrahydrocannabinol	<ul style="list-style-type: none"> Both CB1 and CB2 	<ul style="list-style-type: none"> Phase I enzymes including CYP 2C9, 2C19, and 3A4 Phase II enzymes 	
Cannabidiol	<ul style="list-style-type: none"> Preferentially CB2 	<ul style="list-style-type: none"> Phase I enzymes including CYP 2C19 and 3A4 Phase II enzymes including UGT 1A7, 1A9, and 2B7 	
Synthetic Cannabinoids			
Dronabinol (Marinol)	<ul style="list-style-type: none"> Both CB1 and CB2 	<ul style="list-style-type: none"> Phase I enzymes including CYP 2C9, 2C19, and 3A4 Phase II enzymes 	
Nabilone (Cesamet, Syndros)	<ul style="list-style-type: none"> Both CB1 and CB2 	<ul style="list-style-type: none"> Not fully elucidated, however several metabolites have been identified 	
Cannabidiol (Epidiolex)	<ul style="list-style-type: none"> Preferentially CB2 	<ul style="list-style-type: none"> Phase I enzymes including CYP 2C19 and 3A4 Phase II enzymes including UGT 1A7, 1A9, and 2B7 	

1.2.2.1. Endocannabinoids

Endogenous cannabinoids are not synthesised and stored in tissues, but are formed “on demand” and are then released to bind with CBRs in order to elicit a response (Hansen et al. 2006). The biosynthesis and breakdown of two well studied cannabinoids are summarised in Figure 1.1.

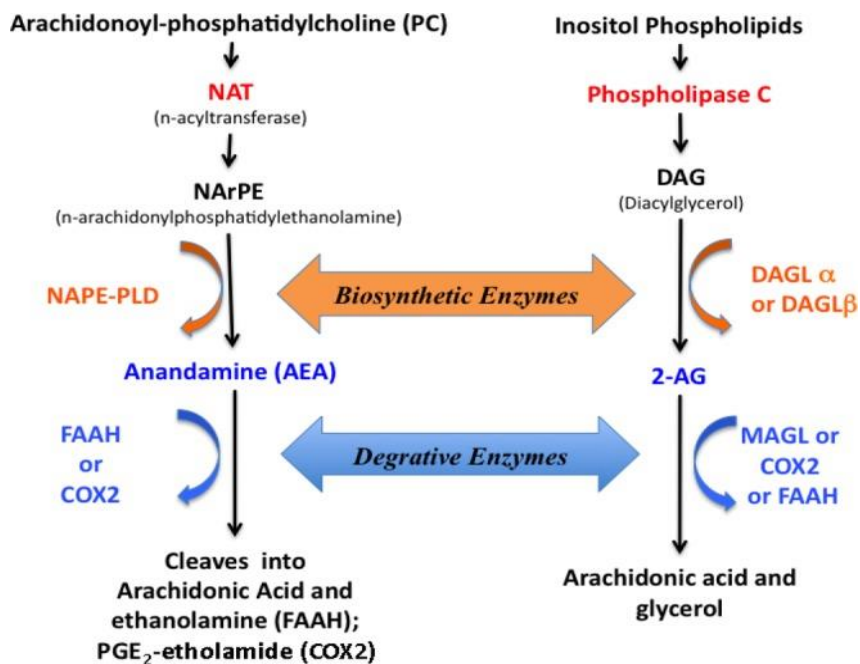


Figure 1.1 Biosynthesis and degradation of the endogenous cannabinoids Anandamide (AEA) and 2-arachidonoylglycerol (2-AG), showing the main enzymes that lead to their synthesis and hydrolysis (Scotchie et al., 2015).

N-arachidonylethanolamine (NAE) was the first endocannabinoid to be isolated (in 1992) from the brain of a pig (Onaivi et al., 2005). It is more commonly known as anandamide (AEA) where “ananda” means bliss (in the Indo-European language Sanskrit) and “amide” originates from its chemical composition (Mechoulam & Fride, 1995). AEA is a long-chain fatty acid ethanolamine and a representative of the NAEs. It is synthesised from N-arachidonoyl phosphatidyl-ethanolamine (NAPE) via hydrolysis with phospholipase D (NAPE-PLD) (Liu et al., 2008) (Fig. 1.1). This process is regulated by the calcium ions and cAMP (Tsuboi et al., 2015). AEA is hydrolysed by the Fatty acid amide hydrolase enzyme (FAAH) into arachidonic acid and ethanolamine (Neelamegan et al., 2012) (Fig. 1.1). Anandamide predominantly influences the central nervous system (CNS) and the peripheral system (PNS) (Pacher et al., 2006). Its actions are mediated by activation of the CB1 receptor in the CNS and the CB2 receptor in the PNS (see 1.2.3.1) (Zou & Kumar, 2018). In addition, AEA can bind to the transient receptor potential channel vanilloid 1 (TRPV1), Dopamine receptor, Peroxisome Proliferator-Activated Receptor (i.e., PPAR α and PPAR γ) and various orphan G protein-coupled receptors (e.g., GPR55) (see 1.2.4) (Pertwee et al., 2010; Lee et al., 2016).

The second endocannabinoid to be isolated in 1995 was 2-arachidonoylglycerol (2-AG) which is a member of the AcGs (Zou and Kumar, 2018). 2-AG is synthesised from diacylglycerol (DAG) which is mediated by two diacylglycerol lipases (DAGL) - DAGL α and DAGL β (Fezza et al., 2014) (Fig. 1.1). It is hydrolysed by monoacylglycerol lipase (MAGL) into arachidonic acid and glycerol although FAAH can also hydrolyse 2-AG (Di Marzo et al., 1998) (Fig. 1.1). Like AEA, 2-AG predominantly influences the CNS and PNS (Kleberg et al., 2014) via activation of the CB1 receptor (Zou & Kumar, 2018). However, it can also activate PPAR α and GPR55, like AEA, (Kozak et al., 2002; Ryberg et al., 2007) but it cannot activate TRPV1 or the Dopamine receptor, unlike AEA (Garbutt, 1983; Starowicz et al., 2007).

There are many other NAEs and AcGs but the current study included two NAEs, alongside AEA, which warrant an introduction: Palmitoylethanolamide (PEA) and Oleoylethanolamide (OEA).

Oleoylethanolamide (OEA) is synthesised from oleic acid and phosphatidylethanolamine and is hydrolyzed by FAAH into oleic acid and ethanolamine (Thabuis et al., 2008). This cannabinoid also exists in many types of food, such as cocoa powder, nuts and oatmeal (Di Marzo et al., 1998; Astarita et al., 2006). In humans, OEA is known to have an essential biological action by regulating food intake, body weight and controlling the balance the lipid metabolism (Thabuis et al., 2011). OEA has a high affinity for the PPAR α receptor (see 1.2.4.1) (Fu et al., 2003).

Palmitoylethanolamide (PEA) is synthesised from N-acylated phosphatidylethanolamine (NAPE)-phospholipase D (Leung et al., 2006). Its degradation is mediated by FAAH to yield palmitic acid and ethanolamine (Skaper et al., 2018). It has been found to have an inhibitory impact on inflammation and cell degeneracy (Aloe et al., 1993; Mazzari et al., 1996; Berdyshev et al., 1998) and has a neuroprotective role in rodents (Lambert et al., 2001; Calignano et al., 1998; Jaggar et al., 1998). Like OEA, PEA predominantly activates PPAR α (see 1.2.4.1) (Lo Verme et al., 2005).

1.2.2.2. Phytocannabinoids

The phytocannabinoids belong to a family of terpenophenolic composites which are derived from the plant *C. sativa* (Happyana et al., 2013). Their chemical structure comprises a terpenoid ring derived structurally from C10 terpenoid subunits of geranyl pyrophosphate (ElSohly, 2007; Kis, et al., 2019). They are biosynthesised within adhesive structures called glandular trichomes (Fig. 1.2), with each trichome containing different cannabinoids (Fischedick et al., 2010; Happyana et al., 2013). Further, cannabinoids comprise a considerable part of the resin and constitute about 30% of the weight of the dried flowering tops (ElSohly, 2007).

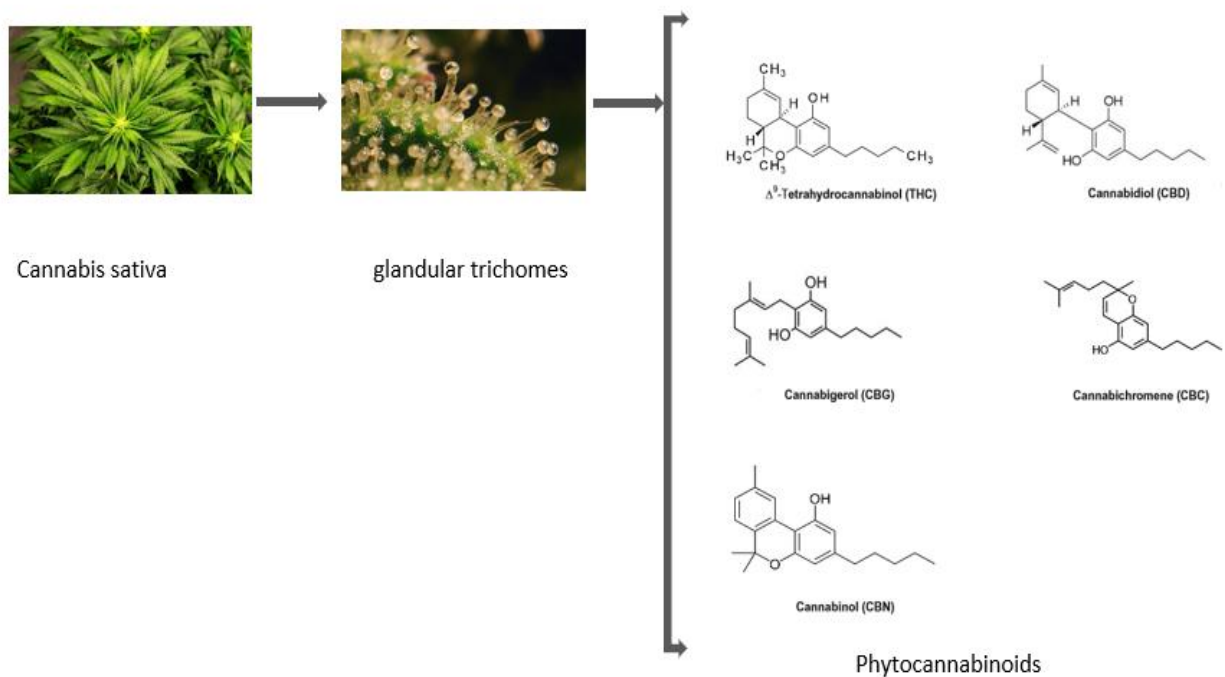


Figure 1.2: Biosynthesis of phytocannabinoids takes place in the glandular trichomes of *Cannabis sativa*. The molecular structure of some of the more common phytocannabinoids is shown (Tambaro et al., 2012; Palazzoli et al. 2018; The weed blog, 2012; www.compassclinics.com).

C. sativa contains more than 85 cannabinoids (El Alfy et al., 2010) but those most common are the psychoactive Delta-9-tetrahydrocannabinol (THC) and its non-psychoactive isomer Cannabidiol (CBD) (Fisar, 2009). THC and CBD are synthesised from cannabigerolic acid (CBGA) which itself is synthesized from olivetolic acid and geranyl diphosphate (Fellermeier and Zenk, 1998; Dewick, 2009) (Fig. 1.3). CBGA is then converted to THC via oxidocyclase

tetrahydrocannabinidiolic acid synthase (THCAS) whereas CBD is formed by oxidocyclase cannabidiolic acid synthase (CBDAS) (Sirikantaramas et al., 2004; Taura et al., 2007) (Fig. 1.3).

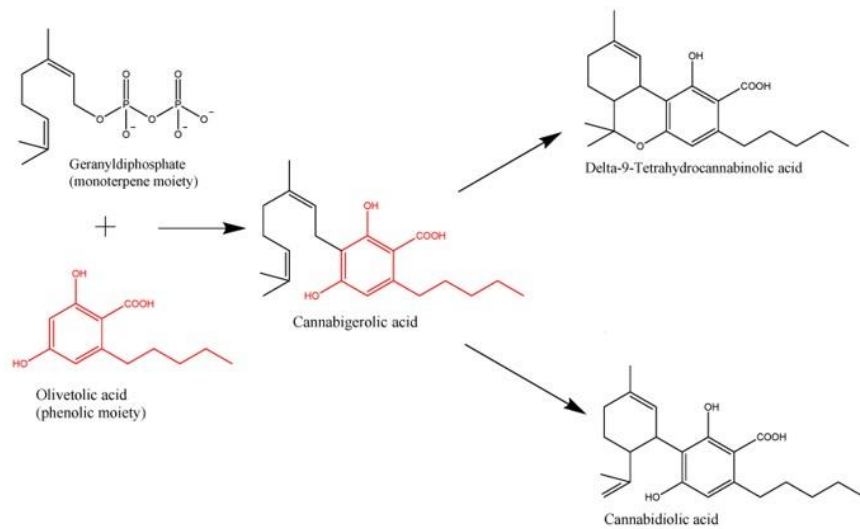


Figure 1.3: Synthetic pathway of Delta-9-tetrahydrocannabinol (THC) Cannabidiol (CBD) (Kis et al., 2019).

The exact function of phytocannabinoids in plants is still unclear, however the most supported theory is that they play a protective role by responding to an external physical or biological effect such as UV light, drying conditions, insects and bacterial infection (Bernstein et al., 2019). Plants do not possess cannabinoid receptors or any endocannabinoids, however the endocannabinoid-like composites can be produced by plants such as PEA and MEA (N-myristoylethanolamine). Those compounds can bind and activate CB-like receptors (Onaivi, 2005). As for PEA, it can be found in various plants, for example, soybean and peanut and binds to unknown CB2-like receptor (Chapman, 2000). MEA is reported to be present in tobacco and *Medicago truncatula*, and acts as anti-alkalization agent as a means of immunity that depends on the rapid inflow of calcium ions (Ca^{2+}) and rapid outflow of potassium ions (K^+) (Chapman, 2000). This reaction is similar to that of the human immune cell response whereby suppression of calcium - potassium channels is mediated by cannabinoid receptors (Mackie et al., 1995). Tripathy et al. (2003) also demonstrated that CBR-like proteins are present in the membrane of plant cells and mediate the signalling pathways of the NAEs

compounds. Moreover, sequences of NAPE-PLD synthesising enzymes have been found in tobacco (Chapman, 2000).

Phytocannabinoids (in particular THC, CBD and CBG) have multiple therapeutic effects which are summarised in (Table 1.2).

Table 1.2: Examples of the therapeutic effects of Delta-9-tetrahydrocannabinol (THC), Cannabidiol (CBD) and Cannabigerol (CBG).

Phytocannabinoid	Pharmacological effect	References
THC	Pain relief Antioxidation Bronchodilation Anti-inflammation (with Alzheimer) Relaxation of muscles	Rahn and Hohmann, 2009 Hampson et al., 1998 William et al., 1976 Currais et al., 2016 Kavia et al., 2010
CBD	Antioxidation Anti-anxiety Anti-spasm Breast cancer Inhibition Anti-bacterial (MRSA)	Hampson et al., 1998 Russo et al., 2005 Jones et al., 2010 Ligresti et al., 2006 Appendino and Gibbons, 2008
CBG	Anti-inflammation Anti-proliferation Growth inhibition of carcinoma Breast cancer inhibition Inhibition of melanoma cell	Formukong and Evans, 1988 Diaz-Laviada, 2010 Baek et al., 1998 McAllister et al., 2007 Baek et al., 1996

Fungi, like plants, do not possess the main endocannabinoid receptors but they do possess the enzymes that synthesise and metabolise them (McPartland et al., 2006). The sequences of NAE synthesising enzymes (NAPE-PLD and MAGL) and hydrolysing enzymes (FAAH and DAGL) have been identified in the yeast *Saccharomyces cerevisiae* (McPartland et al., 2006) and in the fruiting body of *Tuber melanosporum* (truffle) (Pacioni et al., 2015). In addition, Muccioli et al. (2009) found that *S. cerevisiae* produces inactive PEA in a quantity similar to that produced in mouse brain (650 and 100-500 pmol/g, respectively) and Pacioni et al. (2015) found that the truffle of *T. melanosporum* contained high quantities of AEA (7.0 ± 5.8 pmol/mg).

1.2.3. Main cannabinoid receptors (CBRs)

According to genome databases, Protists do not possess the main cannabinoid receptors (see 1.3) so only a brief introduction on them follows.

1.2.3.1. CB1 and CB2 receptors

Many cannabinoids initiate their action by interacting with CBRs in many parts of the CNS and PNS (Howlett et al., 2010). Ligands include AEA, 2-AG, CBD, THC and synthetic cannabinoids (Pertwee et al., 2010). The two main CBRs, CB1 and CB2, differ according to their chemical structure, characteristics of their binding to the ligand and their transduction signal system (Pertwee, 1995; Howlett et al., 2002). The CB1 receptor is found mainly on neurons in the brain and progressive loss of CB1 is an early sign for Huntington's disease (Blázquez et al., 2010). CB2 is more abundant in peripheral tissues and macrophages (Grotenhermen, 2004); although CB1 has also been described in many peripheral tissues within reproductive, gastrointestinal and cardiovascular systems (Pertwee, 2001; Szabo et al., 2001; Wagner et al., 2001).

CB1 and CB2 belong to a group of receptors that cross the cell membrane seven times and combine with proteins that bind guanine-nucleotide (Svíženská et al., 2008). They have an N-terminal extracellular area which has glycosylation locations, a C-terminal intracellular area bound to the G protein complex (therefore are G-coupled protein receptors), and 7 transmembrane domains connected by three extracellular and three intracellular loops

(Duvernay et al., 2005). In humans, CB1 and CB2 are 48% similar with regards to amino acid composition (Munro et al., 1993).

1.2.3.2. The transient receptor potential vanilloid type 1 (TRPV1)

The transient receptor potential vanilloid type 1 (TRPV1) belongs to the transient receptor potential (TRP) superfamily and its natural ligand is capsaicin, found in chili peppers (Caterina et al., 1997). This receptor is primarily expressed in sensory neurons where it co-localises with CB1 and CB2, and is involved in temperature sensing, pain and nociception (Caterina et al., 2000). Ligand binding leads to an influx of calcium (Ca^{2+}) and sodium (Na^+) causing the depolarization of the cells which induces the physical/neural effects (Liedtke et al., 2010). AEA, CBD and OEA act as full agonists (Bisogno et al., 2001; Zou and Kumar, 2018) but 2-AG does not bind to it (Starowicz et al., 2007). TRPV1 differs from both CB1 and CB2 in that it has six transmembrane domains and consists of an extra intramembrane loop which conjoins both the fifth and sixth transmembrane domains and shapes the pore channel region (Caterina et al., 1997; Iannotti et al., 2016).

1.2.3.3. G-protein coupled receptor 55 (GPR55)

GPR55 is the third true cannabinoid receptor and can bind all three groups of cannabinoids (endocannabinoids, phytocannabinoids and synthetic cannabinoids) (Ryberg et al., 2007). GPR55 is widely expressed in the CNS and PNS, often co-localising with CB1 (Sawzdargo et al., 1999). Although AEA targets both CB1 and CB2, it has an even higher affinity for GPR55 (Ryberg et al., 2007). THC, 2-AG, PEA are also agonists for GPR55 while CBD is an antagonist (Ryberg et al., 2007). Despite being the target for many cannabinoids, GPR55 displays low sequence identity to both CB1 (13.5%) and CB2 (14.4%) (Pertwee et al., 2010).

There is another G coupled receptor, GPR119, which is found in the gastrointestinal tract and pancreas, where it stimulates the insulin secretion pathway (Li et al., 2018). It is only activated by fatty acid amides, including AEA, OEA and PEA, with OEA being the most efficacious (Overton et al., 2006).

1.2.4. Other receptors

Many non-CBR receptors have been proposed to bind to cannabinoids (Bih et al., 2015) (Table 1.3). Of those, the Serotonin receptor, Dopamine receptor and PPARs were considered putative cannabinoid receptors in protists (see 1.3.3).

Table 1.3: Receptors, other than CB1, CB2, GPR55 and TRVP1, that have been shown to bind cannabinoids (Bih et al., 2015)

Target receptor	Binding cannabinoids
PPARs	CBD, AEA, OEA, PEA, THC, 2-AG
Opioid	CBD, AEA, THC
glycine	CBD, AEA, THC
Serotonin	CBD, AEA
dopamine	CBD, AEA
Nicotinic Acetylcholine	CBD, AEA, 2-AG, CP55940, WIN55, 212-2
Adenosine	CBD

1.2.4.1. Peroxisome Proliferator-activated Receptors (PPARs)

PPARs belong to the family of the nuclear receptor and exist in three isoforms (α , β/δ , and γ) (Ferguson et al. 2018). OEA, PEA, AEA, 2-AG predominantly bind to PPAR α (although they can also bind to PPAR γ , O'Sullivan, 2016), while CBD and THC only bind to PPAR γ (Kasten and Boehm, 2016). Only the break-down products of endocannabinoids activate PPAR β/δ , so many synthetic agonists have been manufactured for this receptor, e.g., GW0742 (Sznajdman et al. 2003). Ligand binding activates the metabolism of lipids and glucose (Haile and Kosten 2017; Ferguson et al. 2018) and this occurs via two routes: the well-studied genomic route (see below) and the poorly studied non-genomic route (see Chapter 5).

In the classic genomic response, a PPAR is ligand-activated then transported to the nucleus where it forms a heterodimer with another nuclear hormone, the retinoid X-receptor (RXR). The dimer binds to peroxisome proliferator-response elements (PPREs) located on the regulatory regions of target genes and carries out transcription (Fig. 1.4) (Chinetti-Gbaguidi

and Staels, 2009; Grygiel-Górniak, 2014). PPAR targeted genes are primarily involved in the regulation of metabolism and energy homeostasis, cell differentiation, inflammation and proliferation (Tyagi et al., 2011).

PPAR activation is thought to occur via three main mechanisms (Fig. 1.4): 1) Direct binding of cannabinoids to the PPAR, 2) indirect binding through the conversion of cannabinoid into PPAR-active metabolites (for e.g. PPAR β/δ) and 3) activation of a cannabinoid cell surface receptor which results in activation through a cell signalling cascade (O'Sullivan, 2007). This signalling cascade has not been well researched but it is known that, in macrophages for example, the binding of *Mycobacterium tuberculosis* and *M. leprae* to the mannose receptor activates PPAR γ alongside the activation of the p38 mitogen activated protein kinase (MAPK) pathway (Rajaram et al., 2010; Mahajan et al., 2012; Guirado et al., 2018; Diaz Acosta et al., 2018) (discussed further in 5.3.4.3.).

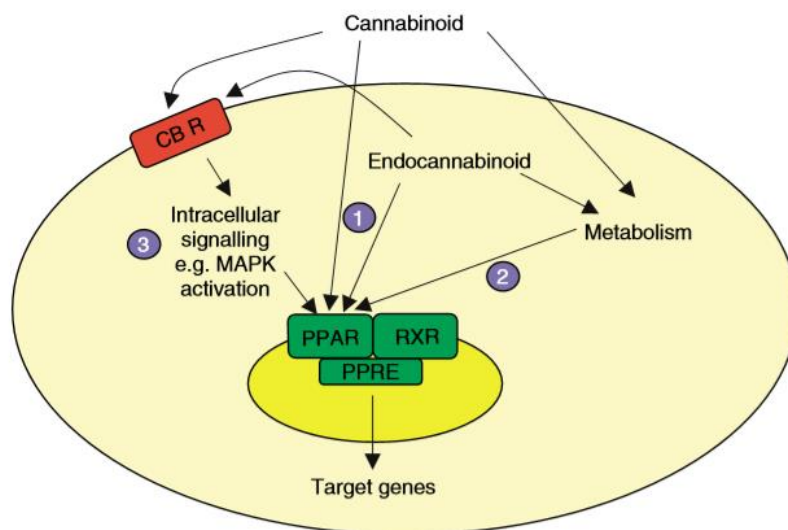


Figure 1.4: Schematic of the three main ways in which Peroxisome-Proliferator Activated Proteins (PPARs) are activated prior to forming a heterodimer with the Retinoid X-Receptor (RXR), and then binding to Peroxisome Proliferator-Response Elements (PPREs). 1) Binding of the endocannabinoid/cannabinoid, 2) binding of endocannabinoid/cannabinoid metabolites, 3) activation of a cannabinoid cell surface receptor (CB R) which results in PPAR activation through a cell signalling cascade (O'Sullivan, 2007).

A 4th mechanism has also been proposed whereby fatty acid binding proteins (FABPs) chaperone cannabinoids from the outer cell membrane to the nucleus where they bind to PPARs (O'Sullivan, 2016). Specifically, binding of the PPAR α ligands oleic acid, fenofibrate and GW7647 to FABP1 and FABP2 (Hughes et al., 2015), and OEA to FABP5 (Kaczocha et al., 2012),

promotes nuclear localisation and the activation of PPAR α . THC and CBD have also been shown to be chaperoned by FABPs 3, 5 and 7, with equivalent binding to 3 and 7 but with CBD binding more strongly to FABP5 (Elmes et al., 2015).

AEA and 2-AG activation of PPAR α has been shown to induce neuroprotective properties (Sun et al., 2007) while OEA and PEA affect various physiological and pathophysiological functions, notably feeding and anti-inflammatory pain (Sun & Bennett, 2007; Hind et al., 2015; O'Sullivan, 2016). Activation of PPAR γ by CBD has shown anti-carcinogenic properties by inhibiting tumour viability and metastasis (Fernández-Ruiz et al., 2015; Payandemehr et al., 2015) while THC causes the dilation of blood vessels (Sun et al., 2006). In addition to phytocannabinoids, synthetic cannabinoids such as Thiazolidinediones (glitazones), a family of drugs used for Type 2 diabetes treatment, are common PPAR γ agonists, particularly Rosiglitazone, which has a high affinity and specificity for this PPAR (Lehmann et al., 1995). Only the break down products of endocannabinoids, especially of the NAEs, have been shown to activate PPAR β/δ , for example, arachidonic acid (AA) from AEA (Yu et al., 2014) and oleamide from OEA (Dionisi et al., 2012).

PPAR activation can therefore be achieved with endocannabinoids, phytocannabinoids and their derivatives, and synthetic cannabinoids.

1.2.4.2. Dopamine receptors

Dopamine is a member of a group of neurotransmitters known as catecholamines that is produced by dopaminergic neurons in the CNS and is also present in the PNS, particularly in the kidney where it is involved in nephritic vasodilation (Romanelli et al., 2009). The primary function of dopamine is to control actions in the brain concerned with movement, cognition, feeding, sleeping and mood (Marsden, 2006). The dopamine receptors it binds to are divided into five subtypes (D1 to D5) and all are coupled to Gi and Gs mediated systems of transduction and are therefore GPCRs (Rashid et al., 2007). These subtypes are further classified into two sub-classes (D1-like and D2-like) (Beaulieu and Gainetdinov, 2011) depending on their affinities for agonists and antagonists, their mechanisms of effectors and their patterns of distribution (Mishra et al., 2018). The D1 receptor (in D1-like class)

dominates the dopamine receptors in the CNS while D2 dominates those in the PNS, with D3, D4 (D2-like) and D5 (D1-like) being present at much lower levels (Romanelli et al., 2009). Ligand binding to D1 and D2 result in opposite effects (Fig. 1.5) with, for example, activated D1 causing the upregulation of cAMP while activated D2 causes its down-regulation (Neve et al., 2004; Guevara Lora, et al, 2016).

AEA, CBD and THC are known to bind to dopamine receptors with THC binding to D1 (Miyamoto et al., 1996) while CBD and AEA bind to D2 (Beltramo et al., 2000; Seeman, 2016). A recent study has shown that THC and CBD can bind to a heterodimer of D1-D2 receptors within the brain, with THC only binding to D1 but addition of CBD (ratio 1:3) prevented THC binding to D1 and upregulated mRNA expression in D2 (Hasbi et al., 2020).

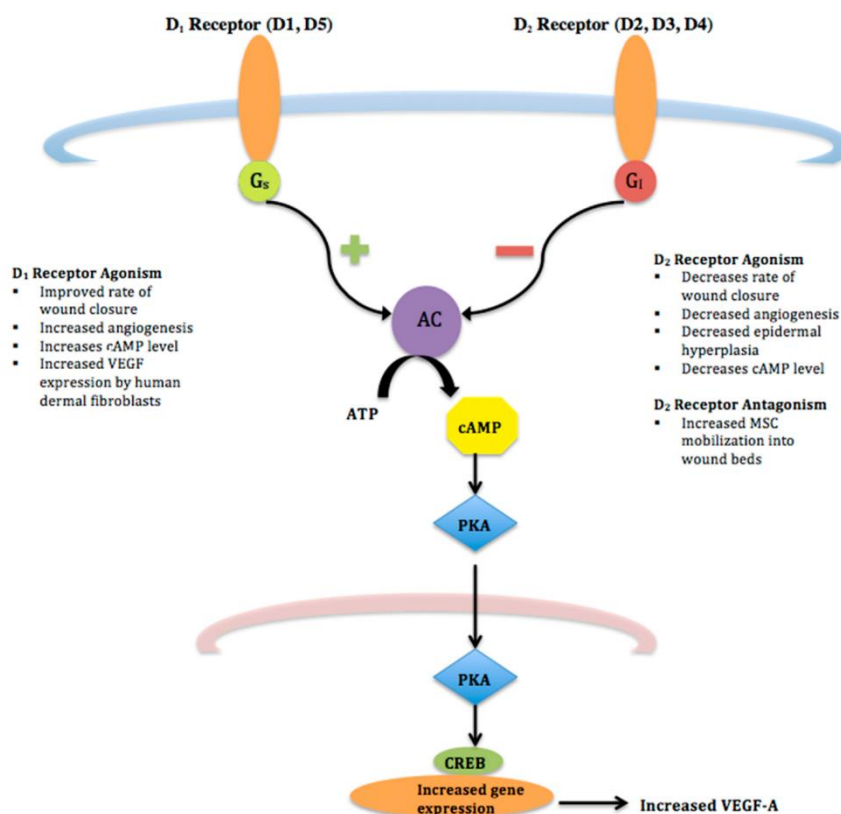


Figure 1.5: Dopamine receptor pathway and cellular effects (Vaughn et al., 2018).

1.2.4.3 Serotonin receptors (5-HT)

Serotonin (5-HT) is a monoamine neurotransmitter biosynthesized in the CNS and PNS (Mazák et al., 2009). It is synthesized by a two-stage enzymatic process: firstly, hydroxylation of tryptophan by the enzyme tryptophan hydroxylase and secondly, decarboxylation of the side chain by aromatic amino acid decarboxylase (Nakamura and Hasegawa, 2009).

The term serotonin is derived from the Greek word serum “ser” in combination with the Latin word tonic “tonin” because it was first isolated from serum and had the ability to cause a rise in blood pressure (Mohammad-Zadeh et al., 2008; Nichols and Nichols, 2008). Serotonin acts locally as a hormone in the different tissues within the digestive system, the cardiovascular system and the immune system (Pithadia, and Jain, 2009). It has been identified as being involved in psychological diseases, for instance, depression and anxiety, as well as in Alzheimer’s disorder (Masson et al., 2012). This large number of roles has led to the development of several therapeutic composites such as antidepressants, antipsychotics and different anti-vomiting medicines (Cirillo et al., 2011).

The pharmaceutical properties of serotonin are complicated, as its activities are mediated through a large number of 5-HT receptors (Celada et al., 2004). There are at least seven distinct receptor families (5-HT₁ up to 5-HT₇) with each family placed in different areas of the body and each instigating a different response (Frazer and Hensler, 1999). Apart from 5-HT₃ (a ligand-ion channel), all 5-HT receptor subtypes are GPCRs (Mazák et al., 2009) and ligand binding initiates the signaling cascade depicted in Figure 1.6.

AEA and CBD have been shown to bind to a serotonin receptor. The activation of 5-HT_{1A} by CBD reduces the damage of neurotransmitters that occurs as a result of neuropathic pain disorder (De Gregorio et al., 2019) while the activation of 5-HT₃ by AEA has caused stimulation of pain relief (Racz et al., 2008).

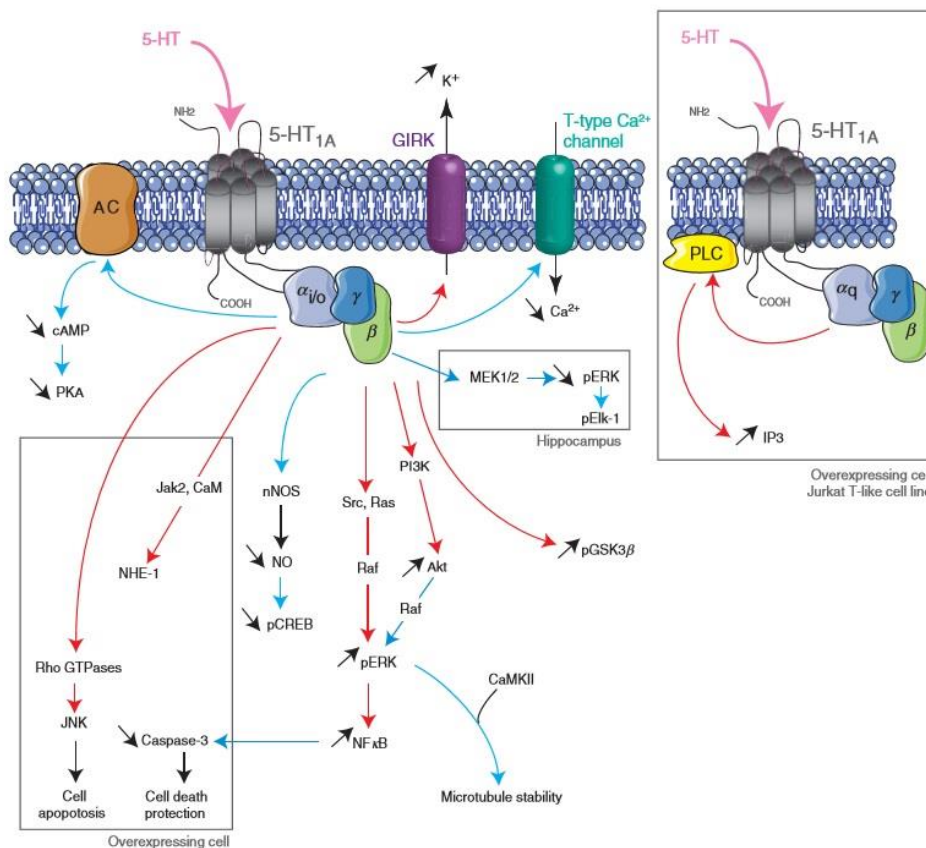


Figure 1.6 Signalling pathway of the 5-HT receptor (Masson et al., 2012).

1.3. Existence of an endocannabinoid system in single-celled eukaryotes

A phylogenetic study by McPartland et al. (2006) examined whether all eukaryotes possessed known receptors and enzymes which participated in the endocannabinoid system (ECS) (Fig. 1.7). The unicellular organisms included the yeast *Saccharomyces cerevisiae*, the obligate *Plasmodium falciparum* and the ciliate *Tetrahymena thermophila*. The first conclusion of the study was that these protists did not contain homologues to the four main cannabinoid receptors (CB1, CB2, GPR55 and TRPV1). The second was that they all contained sequences for the enzymes Fatty Acid Amide Hydrolase (FAAH) and Monoacylglycerol Lipase (MAGL) which hydrolyse NAEs and 2-AcGs, respectively. Differences were then evident with regards to the synthesizing enzymes, with sequences for DAGL (synthesis of AcGs) being present in *T. thermophila* and *S. cerevisiae* (but not *P. falciparum*) while sequences for NAPE-PLD (synthesis

of NAEs) were present in *P. falciparum* and *S. cerevisiae* (but not in *T. thermophila*) (McPartland et al., 2006). Experimental evidence to substantiate these observations was mainly attained from work on the ciliate *Tetrahymena*; reviewed below.

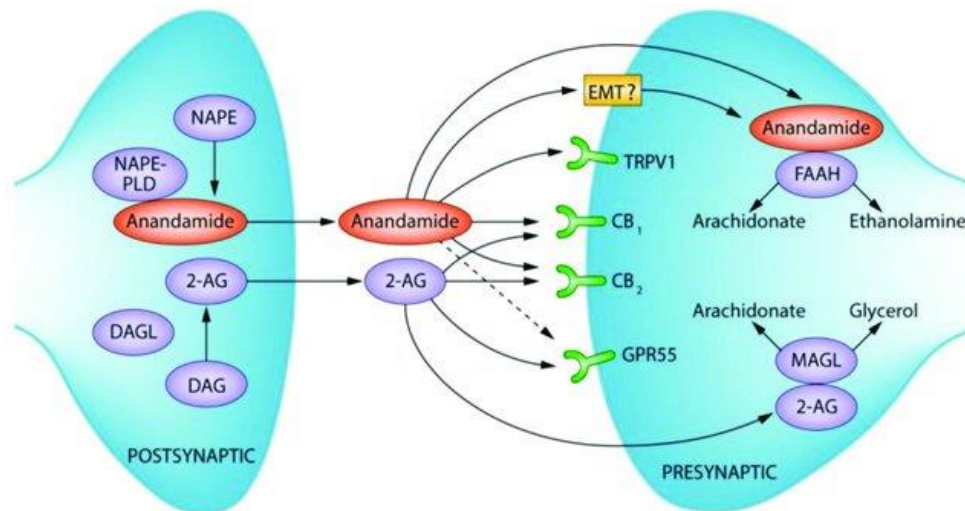


Figure 1.7: A summary of the main components of the AEA and 2-AG cannabinoid system showing their synthesis (left), the four main cannabinoid receptors and their metabolizing enzymes (right) (Zhou et al., 2019).

1.3.1. Endocannabinoids in *Tetrahymena*

Anagnostopoulos et al. (2010) identified a suite of *N*-acylethanolamines (NAEs) and 2-acylglycerols (2-AcGs) in *Tetrahymena thermophila* (Table 1.4) together with free fatty acids (FFAs). The concentrations of 2-AcGs were higher than NAEs and only small amounts of AEA and 2-AG were detected. Of the NAEs detected, GLEA, SEA and EEA are present in only trace amounts in mammals (Kleberg et al., 2014; Gaitán et al., 2018) while LEA, along with PEA and OEA, are more common and are primarily in the GI tract where they exhibit similar anorexic functions; activating mainly PPARs and TRPV1 (Kleberg et al., 2014).

Table 1.4: Presence of N-acylethanolamines (NAEs) and 2-acylglycerols (2-AcGs) in the ciliate *Tetrahymena thermophila* together with their cellular concentration (Anagnostopoulos et al., 2010).

Endocannabinoid	Class	Concentration (pM/mg of protein at 27°C)
Linolenylethanolamine (LEA)	NAE	2.3±0.8
Oleoylethanolamine (OEA)	NAE	0.6±0.3
Palmitoylethanolamine (PEA)	NAE	1.8 ± 0.3
Stearoylethanolamine (SEA)	NAE	0.3 ± 0.1
Eicosenoylethanolamine (EEA)	NAE	3.2±1.5
γ-Linolenylethanolamine (GLEA)	NAE	2.3±0.8
γ-Linolenoylglycerol (2-GLG)	2-AcG	5100±620
2-Palmitoylglycerol (2-PG)	2-AcG	770±120
2-Linolenoylglycerol (2-LG)	2-AcG	4000±560
2-Oleoylglycerol (2-OG)	2-AcG	1600±240
2-Eicenoylglycerol (2-EG)	2-AcG	1500±290

1.3.2. Enzymes in *Tetrahymena*

Karava et al. (2001) were first to detect an enzyme in *Tetrahymena pyriformis* which had the same function as FAAH (hydrolysing AEA to arachidonic acid and ethanolamine). Karava et al. (2005) then went on to reveal the presence of 2 isoforms of FAAH in this species: a 66 kDa isoform (close in size to that reported for mammalian FAAH [63 or 67 kDa] [Giang and Cravatt, 1997]) and a 45 kDa isoform (close to the 46 kDa of amide hydrolase in invertebrates [Matias et al., 2001]). Two isoforms of MAGL have also been found in *T. thermophila*; 40kDa and 45kDa (Evagorou et al., 2010).

1.3.3. Receptors in *Tetrahymena*

To date, no homologues of CB1, CB2, GPR55 and TRVP1 have been detected in protists. However, they do respond to cannabinoids (see 1.6.4 and 1.7.2) suggesting a cellular target

is present. Bih et al. (2015) reviewed the literature for evidence of the involvement of other receptors that could bind CBD and found seven. Table 1.5 lists these seven receptors and evaluates whether they might be present in *Tetrahymena*.

Table 1.5: CBD receptors identified by Bih et al., (2015) and whether the receptor, or orthologues, are present in *Tetrahymena* (www.ciliate.org).

Receptors	Cannabinoid ligands	Present in <i>Tetrahymena</i> ?
Opioid	CBD, AEA, THC	Yes, μ Opioid
Dopamine	CBD, AEA	Yes, D1 receptor
Serotonin	CBD, AEA	Yes
Adenosine	CBD	Possible, produces cAMP
PPARs	CBD, AEA, OEA, PEA, THC, 2-AG	Possible, possess peroxisomes
Nicotinic Acetylcholine	CBD, AEA, 2-AG, CP55940, WIN55,212-2	Possible- possess acetylcholinesterase
Glycine	CBD, AEA, THC	Possible – possess chemotaxis towards 5-Gly

1.3.4. Response of *Tetrahymena* to cannabinoids

Only two studies have evaluated the effect of cannabinoids on *Tetrahymena*. McClean and Zimmerman (1976) were the first to show that THC caused the cells of *T. pyriformis* to become round and move in a sluggish manner. It was then found that THC caused a dose-dependent delay in cell division, with cells being most sensitive in their G2 phase of cell division (Zimmerman et al., 1981). In both studies, cells recovered after a few hours.

In addition to these, there have been two studies on amoebae (see 1.6.2) but as yet, the presence of ECS enzymes or endocannabinoids in amoeba cells has not been evaluated.

1.4. Cannabinoids and amoebae

1.4.1. Overview of amoebae

Amoeba represent an important component of surface-associated communities (biofilms) as their trophozoites can only feed on surface-associated prey (Parry, 2004). Free living amoebae (FLA) are prevalent in water and soil (Lorenzo-Morales et al., 2013) and although several species are opportunistic pathogens, the majority are non-pathogenic (Thomas et al., 2009). Amoebae are divided into naked and testate amoebae; testate amoebae possess an external shell-like structure (teste) with one compartment and one aperture (Esteban et al., 2014). Naked amoebae exist in three forms; a cyst which forms under unfavourable conditions (lack of food and osmotic stress), a moving trophozoite (the feeding form) and a 'floating form' (a non-feeding form suspended in liquid) (Figure 1.8). Also, a fourth form has been identified as a 'round body' (a pre-cyst form) (Pickup et al., 2007).

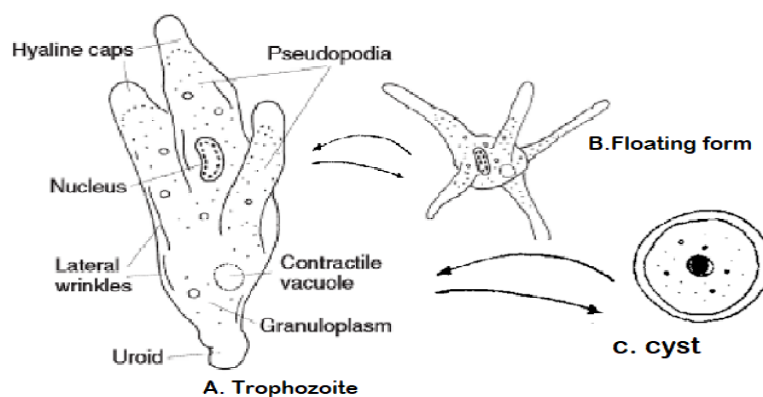


Figure 1.8: Life cycle of an amoeba (Smirnov, 2008).

1.4.2. Amoebic response to cannabinoids

To date, only two studies have examined the response of amoebae to cannabinoids. Pringle et al. (1979) studied the growth of *Naegleria fowleri* for 3 days with/without three phytocannabinoids: Delta-9-tetrahydrocannabinol (THC), Cannabidiol (CBD) and Cannabinol (CBN). *N. fowleri* was affected by all treatments and results showed that, at an equivalent concentration, THC was more potent than CBN or CBD (Table 1.6). Moreover, THC prevented

the trophozoites from transforming into flagellates or cysts, but had no effect on cell shape or speed of movement (Pringle et al., 1979).

Table 1.6: The influence of the phytocannabinoids Delta-9-tetrahydrocannabinol (THC), Cannabidiol (CBD) and Cannabinol (CBN), on population growth of the amoeba *Naegleria fowleri* (Pringle et al., 1979).

Phytocannabinoid	Concentration (μM)	% Population growth compared to control	Experimental Conditions
delta-9-tetrahydrocannabinol (THC)	15.9	47	Grown up from 1×10^4 - 5×10^4 cells/ml for 72 h at 37°C
	31.8	79	
	63.6	88	
	159	No growth	
Cannabidiol (CBD)	15.9	73	
	31.8	87	
	63.6	94	
Cannabinol (CBN)	16.1	57	
	32.2	80	
	64.4	93	

The second study was carried out by Dey et al. (2010) who tested N-arachidonylethanolamine (AEA) and 2-O-arachidonoylglycerol (2-AG) on the growth of three amoebae over 3 days: *Acanthamoeba castellanii*, *Willertia magna* and *Vermamoeba (Hartmannella) vermiformis* (Table 1.7). Results indicated that reduced population growth occurred with $5.75\mu\text{M}$ AEA (MIC $<5.75\mu\text{M}$) and 100% cell death occurred at $57.5\mu\text{M}$ (Table 1.7) *V. vermiformis* was more sensitive to AEA treatment than *A. castellanii* and *W. magna* with IC_{50} s of 14, 17 and $20\mu\text{M}$, respectively. In addition, all amoebae were affected by 2-AG at $26.4\mu\text{M}$ (only concentration tested) and showed the same pattern of sensitivity as that with AEA, i.e., *V. vermiformis* $>$ *A. castellanii* $>$ *W. magna*. This study also demonstrated that it was 2-AG *per se* that caused the reaction (and not its breakdown products) as the same reduction in population growth was recorded with 2-AG-ether which is a non-hydrolysable form of 2-AG (Table 1.7) (Dey et al., 2010).

Both studies then, found that two endocannabinoids and three phytocannabinoids reduced amoebic population growth after 3 days. Successful population growth of amoebae requires successful ingestion and metabolism of prey, yet no study to date has examined the effect of cannabinoids on amoebic feeding.

Table 1.7: Sensitivity of three amoebae to different doses of N-arachidonylethanolamine (AEA), 2-O-arachidonoylglycerol (2-AG) and 2-AG-ether under similar condition (cells were grown up from 2×10^5 cells/ml initial dose for 72 h, at 37°C) (Dey et al., 2010).

Amoeba sp.	Cannabinoid	Concentration (μM)	% Population growth compared to Control
<i>Acanthamoeba castellanii</i>	AEA	5.75	Inhibition of growth
		17.0	50
		28.8	68
		57.5	Cell death
	2-AG	26.4	reduction 75.2%
	2- AG ether	27.4	reduction 75.4%
<i>Willertia magna</i>	AEA	5.75	Inhibition of growth
		20.0	50
		28.8	58
		57.5	death
	2- AG	26.4	reduction 56.6%
	2- AG ether	27.4	reduction 56.2%
<i>Hartmannella vermiformis</i>	AEA	5.75	Inhibition of growth
		14.0	50
		28.8	96
		57.5	death
	2- AG	26.4	reduction 95.6%
	2- AG ether	27.4	reduction 87.8%

1.4.3. Amoebic feeding

1.4.3.1. General overview

Amoebic trophozoites use extended pseudopodia for motility and the engulfment of prey via phagocytosis (Bogitsh et al., 2018). Phagocytosis refers to a biological process that organizes the absorption of particles into cellular vacuoles (phagosomes) from the cell membrane (Levin et al., 2016). The mechanism of phagosomal formation and maturation in protists is still poorly described but is thought to be similar to that of macrophages. Briefly, the process begins when the phagocytic cell recognises the binding ligands of the prey cell in a receptor-dependent way (Fig. 1.9, stages 1-2). This recognition leads to signal pathways that stimulate the re-shaping of the actin cytoskeleton and the extension of pseudopodia to enclose the prey in a phagocytic cup (Duhon and Cardelli, 2002; Cosson and Soldati, 2008; Pauwels et al., 2017) (Fig. 1.9, stage 3). The complete closing of the phagocytic cup leads to the formation of the phagosome (Fig. 1.9, stages 4-5), which is inert until it matures via a complicated series of fusion events with endosomes (to reduce the pH) and then with lysosomes (which contain digestive enzymes) (Haas, 2007; Pauwels et al., 2017) (Fig. 1.9, stage 6). The process ends with

the defecation of waste materials (Fig. 1.9, stage 7) and the recycling of the phagosome membrane to make new phagosomes (Allen and Fok, 1980; Gotthardt et al., 2002) (Fig. 1.9, stages 8-9).

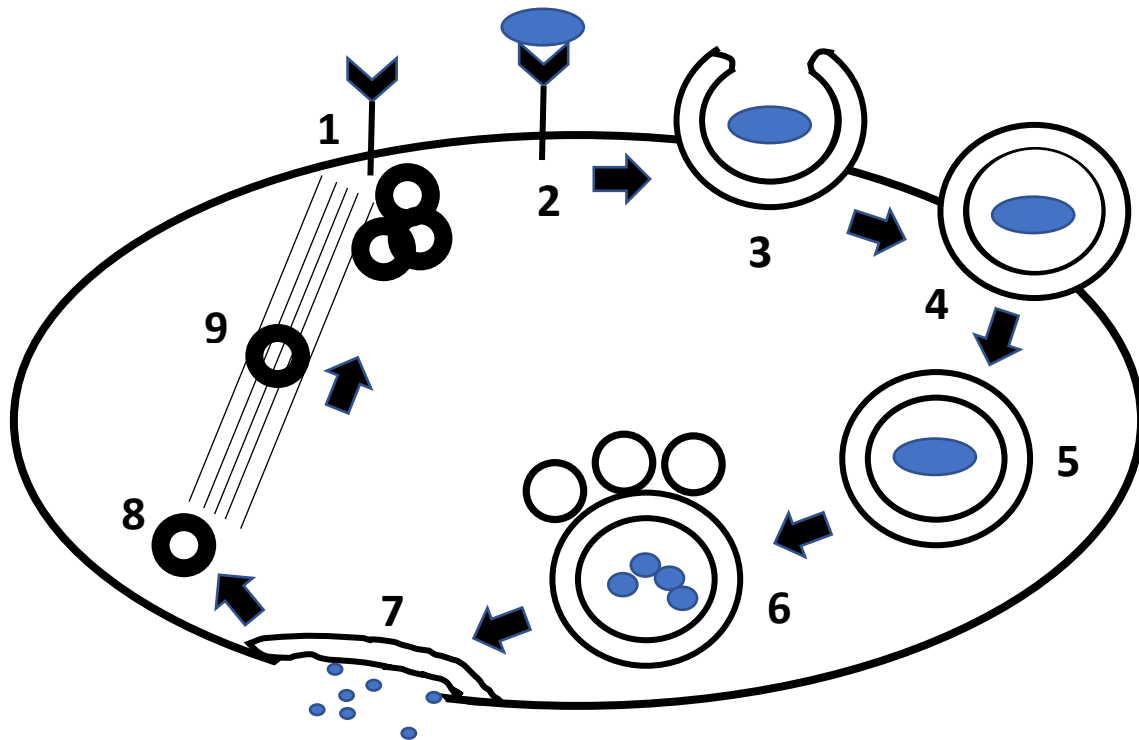


Figure 1.9: Diagrammatic representation of membrane dynamics in the phagocytic cycle. 1) Receptors and membrane are available for prey uptake and phagosome formation. 2) Binding of prey to receptors (e.g. C-type lectins) leads to 3), actin polymerisation and formation of pseudopodia which surround the prey. 4) Myosin is recruited to help seal the ends of the pseudopods together. 5) Dynamin is recruited to allow detachment of the phagosome into the cytoplasm. 6) The phagosome matures via a series of fusions with endosomes and lysosomes and the contained material is digested. 7) Phagosome membrane fuses with the plasma membrane and releases undigested material. 8) Plasma membrane is endocytosed to form vesicles. 9) Vesicles are transported to the site of phagocytosis by microtubule ribbons and used to form new phagosomes. Stages 3 to 7 are known to be reliant on activation of the Arp2/3 system.

1.4.3.2. Receptor-mediated ingestion of prey (Fig. 1.9, stages 1-2)

C-type lectins have been shown to be key receptors for prey capture in amoebae (Ravdin and Guerrant, 1981; Bracha et al., 1982; Ravdin et al., 1985; Petri et al., 1987; Allen and Davidowicz, 1990; Venkataraman et al., 1997; Harb et al., 1998; Garate et al. 2004; Alsam et al., 2005; Bär et al., 2015). C-type lectins are glycoproteins that are part of a protein super family which includes 17 sub-groups; divided according to phylogenetic and structural properties of binding domain (Boskovic et al., 2006; Drickamer & Taylor, 2015). They primarily

bind carbohydrate ligands on bacteria, in a calcium dependent manner, via a conserved extracellular carbohydrate recognition domain (CDR) (Kerrigan & Brown, 2009; Hoving et al., 2014; Alenton et al., 2017). The carbohydrates they recognize include mannose, N-acetylglucosamine (GlcNAc), L-fucose, glucose, galactose and N-acetylgalactosamine (GalNAc) (Drickamer and Fadden, 2002).

C-type lectins are functionally diverse and are involved in the recognition of pathogens, phagocytosis, activation of platelets, cell binding, transporting substance into the cell and cell differentiation (Ramoino et al., 2001; Wormald & Sharon, 2004; Cambi et al., 2005; Roberts et al., 2006; Gupta, 2012). The majority of these lectins exist on the cell surface however they can also be found associated with organelles such as the Golgi complex, phagosome and nuclear envelope (Ramoino, 1997; Roberts et al., 2006).

The role of specific C-type lectins in amoebic feeding has been studied using sugar blocking experiments whereby the amoeba is pre-incubated with a specific sugar, to block a specific receptor, and then the uptake of prey is compared in the presence/absence of the blocking. Using this technique, a mannose receptor has long been known play a role in amoebic feeding. Bracha et al. (1982) first demonstrated that the uptake of *Escherichia coli* and *Serratia marcescens* by *Entamoeba histolytica* was reduced by 66% with 100mM mannose. Alsam et al. (2005) also showed that the feeding of *Acanthamoeba castellanii* on *E. coli* was reduced by 80% in the presence of 100mM mannose. Allen and Davidowicz (1990) tested various mannose concentrations on *A. castellanii* whilst feeding on the yeast *Saccharomyces cerevisiae* and found the IC₅₀ to be 10mM.

The *A. castellanii* mannose receptor has been cloned and is a 400-kDa protein, comprising multiple 130-kDa subunits (Garate et al. 2004). Despite extensive BLAST searches, this receptor lacks sequence identity to any well characterized lectin receptor in other cell types. For example, in mammals the mannose receptor is 180-kDa (Stahl and Ezekowitz, 1998). Mannose residues are present in many Gram-negative cell wall structures such as O-antigens, core polysaccharide, Type I fimbriae, S-layers, capsules, slime (Ofek et al., 1993; Hamrick et al., 2000; Lagoumintzis et al., 2003; Veremeichenko et al., 2005; Bradshaw et al., 2018) and in the mannose-capped lipoarabinomannan (ManLAM) of *Mycobacterium tuberculosis* (Kang et al., 2005). Gram-positive cells do not possess mannose residues (Mirelman et al., 1980).

There is also evidence for a Gal/GalNAc receptor in amoebae. *Entamoeba histolytica* primarily uses this 170 kDa transmembrane lectin as an adherence molecule to bind to host cells (Ravdin and Guerrant, 1981; Petri et al., 1987) and it can be blocked with 4.5mM GalNAc and 56mM galactose (Ravdin et al., 1985). *E. histolytica* has also been shown to use this lectin to bind Gal/GalNAc-rich bacterial strains, e.g. *E. coli* serotype O55 (Bär et al., 2015). *Vermamoeba vermiformis* possesses a similar 170kDa transmembrane lectin to bind and internalize *Legionella pneumophila* which can be 70-89% blocked with 100mM GalNAc (Venkataraman et al., 1997; Harb et al., 1998). In mammalian cells, the membrane galactose ligand (MGL) is only ca. 40 KDa but produces dimers and trimers (80-120KDa) (Napoletano et al. 2012). It binds only GalNAc and blocking with 100mM GalNAc prevents of the uptake of *Neisseria gonorrhoeae* (van Vliet et al., 2009). GalNAc residues are present in the cell walls of both Gram-positive and Gram-negative bacteria where they form part of the glycosaminoglycans, teichoic acids, O-antigens, and slime (Speert et al., 1988; Abeygunawardana et al., 1989; Michael et al., 2002; Bogomolnaya et al. 2008).

To date, there have been no reports of true amoebae possessing a GlcNAc receptor. Indeed, no specific GlcNAc receptor has been found in professional phagocytes, with GlcNAc instead binding to either the mannose receptor (East et al., 2002), Peptidoglycan Recognition Proteins (PGRPs) (Liu et al., 2001) or DC-SIGN (van Kooyk and Geijtenbeek, 2003). To date, there are no reports of protists possessing homologues of PGRPs or DC-SIGN so GlcNAc might bind to the mannose receptor instead. However, one study has argued that a specific GlcNAc receptor is one of three lectins in the slime mould *Dictyostelium discoideum* (which has an amoebic stage in its growth cycle). Here, all three are used for the adhesion of cells to a surface (Bozzaro & Roseman, 1983). GlcNAc is one of the main cell surface carbohydrates in bacteria which, together with N-acetylmuramic acid, forms the peptidoglycan layer of Gram-negative and Gram-positive cells (Rogers et al., 1980). It is also found in the core polysaccharide of the lipopolysaccharide layer (van Kooyk and Geijtenbeek, 2003).

In addition to C-type lectins, a recent study by Sattler et al. (2018) has shown that *D. discoideum* possesses homologous receptors to the mammalian class B scavenger receptors, LIMP-2 and CD36, i.e. LmpA and LmpB, respectively. Scavenger receptors are another class of surface membrane glycoprotein used for the recognition of carbohydrates in phagocytosis

(Perún et al., 2016). The Class B scavenger receptors bind to the lipoteichoic acid of Gram-positive bacteria (Stuart et al., 2005; Hoebe et al., 2005) and the lipid A of the lipopolysaccharide layer of Gram-negative bacteria (Baranova et al., 2008). In *D. discoideum*, LmpA was found in endosomes and phagolysosomes and played a role in the binding and phagocytosis of bacteria (particularly Gram-positive strains) while LmpB was localized to the plasma membrane and early phagosomes and was exclusively involved in the uptake of Gram-positive bacteria (Sattler et al. 2018).

1.4.3.3. Phagosome formation and trafficking (Fig. 1.9, stages 3-6)

Little is known about the formation of phagosomes in protists but it is thought to be similar to that of macrophages. Here, phagosome formation is a complex molecular process but in its simplest terms: Upon prey-receptor binding, actin polymerisation is activated and two pseudopodia extend out from the cell to surround the prey particle. Myosin is then recruited to help seal the ends of the pseudopods together and then the recruitment of dynamin leads to the detachment of the phagosome from the cell surface to the cytoplasm (Levin et al., 2016). The whole process (and indeed phagosome trafficking [Duleh and Welch, 2010]) is reliant on activation of the Arp2/3 system (Seven-transmembrane-actin-related proteins 2 and 3) which itself is activated via a plethora of molecules and signalling cascades (Levin et al. 2016) (see Chapter 5).

Studies on protists have confirmed that actin, myosin and dynamin play a role in the formation of the phagocytic cup, migration of newly formed phagosomes into the cell, trafficking of phagosomes within the cell, and their fusion with lysosomes (Tiggemann and Plattner, 1981; Tiggemann et al., 1981; Allen and Fok, 1983; Méténier, 1984). In addition, all sequenced protists to date have been shown to possess the Arp2/3 complex, including amoebae; *Acanthamoeba castellanii*, *Naegleria fowleri*, *Entamoeba histolytica*, *E. dispar*, *E. invadens* and *E. moshkovskii* (www.amoebadb.org). Defecation in *D. discoideum* is also dependent on the activation of the Arp2/3 system (Carnell et al., 2011).

1.4.3.4. Defecation and membrane recycling (Fig. 1.9, stages 7-9)

There is very little information on the recycling of phagosome membrane in amoebae and most work has been performed on ciliates; though this is still very little. Ciliates are known to possess a limited volume of membrane with which to form phagosomes (Allen, 1974) and the constant recycling of 'old' phagosome membrane from the cytoproct (cell 'anus') to the cytostome (cell 'mouth') is essential to ensure membrane availability for newly developing phagosomes (Allen, 1974). The actual process by which 'expended' phagosome membrane is recycled has only been studied in the ciliate *Paramecium* (Allen and Fok, 1980). Here, the membrane of a defecated phagosome fuses with the plasma membrane and is then retrieved at the cytoproct by endocytosis. The resulting endosomes become flattened and disk-shaped ('discoidal vesicles'). Within 3 min these vesicles become aligned to a bundle of microtubule ribbons which join the cytoproct to the cytostome, and the vesicles then travel along it and reach the cytostome by 4 min (Allen and Fok, 1980). This is an example of 'direct recycling', i.e., no involvement of the lysosomal or Golgi systems on the vesicle's journey back to the cytostome (Allen and Fok, 1980). Direct membrane recycling has also been observed in the ciliates *Tetrahymena* (Grønlien et al., 2002) and *Ophrydium* (Goff and Stein, 1981) but it is currently unknown whether amoebae also employ direct membrane recycling.

1.5. Aims of the study

The overall aim of this study was to evaluate the sensitivity of amoebae to the endocannabinoid AEA and the phytocannabinoid CBD by examining their population growth and feeding response in their presence. It also aimed to evaluate whether three receptors (PPAR, Dopamine, Serotonin) could be involved in their mode of action to investigate the evolutionary, and non-receptor-based, functioning of the ECS in amoeba.

Specific objectives were to:

- 1) Determine the extent of AEA and CBD sensitivity within freshwater naked amoebae by evaluating population growth in their presence, in a range of species. Determine the MIC, IC₅₀ and lethal doses with those sensitive strains.

- 2) Characterise the feeding behaviour of untreated *Veramoeba vermiformis* and determine whether it possesses C-type lectin prey-recognition receptors for mannose, N-Acetyl-D-glucosamine (GlcNAc) and N-Acetyl-D-galactosamine (GalNAc).
- 3) Compare the feeding behaviour of *V. vermiformis* in 2) to that in the presence of the cannabinoid and evaluate whether any effects (specifically feeding lags and ingestion rates) are density-dependent, and whether cannabinoids interact with the prey-recognition receptors.
- 4) Determine whether cannabinoids affect phagosome trafficking and defecation in *V. vermiformis* using a pulse-chase experiment.
- 5) Determine whether PPARs are a possible cannabinoid receptor in amoebae.
 - a. Evaluate how many amoebic species are sensitive to agonists for the three PPAR isoforms (α , β/δ and γ). Determine the MIC, IC₅₀ and lethal doses for population growth of the sensitive strains and whether the effects can be abolished in the presence of their respective PPAR antagonist (α , β/δ and γ).
 - b. Determine whether the PPAR agonists (at their IC₅₀s) mirror the effects of cannabinoids on *V. vermiformis* feeding and whether these effects can be abolished with the use of their respective PPAR antagonist. Determine whether any of the PPAR antagonists can abolish the cannabinoid feeding effect.
- 6) Determine whether the Dopamine and/or Serotonin receptors are possible cannabinoid receptors in amoebae.
 - a. Evaluate whether the AEA/CBD effect on the population growth of sensitive strains can be blocked with Haloperidol (a dopamine/serotonin antagonist).
 - b. If a responsive strain is something other than *V. vermiformis*, perform a feeding experiment in the presence of the cannabinoid with/without haloperidol.
 - c. Using more specific blockers, determine whether any Haloperidol effect is due to receptors for dopamine, serotonin or both.

Chapter 2: Methods and Materials

2.1 Organisms and maintenance

2.1.1. *Escherichia coli*

Escherichia coli (*E. coli*) DH5 α (Dr Karen Tait) was maintained as streak plates on Diagnostic Sensitivity Test Agar (DST) containing chloramphenicol at 30 $\mu\text{g/ml}$ (to retain a bacterial plasmid containing a gene for a lactonase, which was required for a separate study) (see Appendix 1). The bacterium was grown at 25°C for 3 days prior to an experiment, after which, a bacterial suspension was prepared by flooding two plates with sterile distilled water and scraping the cells into suspension with a sterile spreader. The number of cells/ml was then determined (see 2.3.1).

2.1.2. *Synechococcus* sp. ('Pico')

Synechococcus sp. S-KH3 (Dillon and Parry, 2009) was cultured in a flask containing Blue-green 11 broth (BG11, see Appendix 1). Cells were sub-cultured 3 days prior to an experiment and incubated at room temperature (23°C), in a 16:8 natural light: dark cycle, on a rotary shaker (0.00118 *g*). The number of cells/ml was then determined (see 2.3.2).

2.1.3. Amoebae

Twenty-seven strains of amoeba (Table 2.1) were maintained on Non-Nutrient Agar (NNA, see Appendix 1) with a thin streak of *E. coli* DH5 α down the center of the plate. They were sub-cultured by removing a plug of agar from a previously cultured amoeba plate and placing this, cell-side-down, on the streak of *E. coli* on a fresh NNA plate. Plates were incubated at room temperature (*ca.* 23°C) for 7 days prior to an experiment. Then, the agar plug together with any residual *E. coli* streak and areas with cysts, were removed from the plate prior to flooding with Amoeba Saline (AS, see Appendix 1) and suspending the cells using a sterile spreader. The suspension was collected in a 50 ml tissue culture flask which was placed on a rotary shaker (0.00118 *g*) to promote the amoebic 'floating form' and avoid the formation of cysts. When very high concentrations of an amoeba were required (feeding experiments [see 2.5] and pulse-chase experiments [see 2.6]), a suspension was made from 7-10 plates.

Table 2.1: Sources of amoebae used in the study. CCAP (Culture Collection of Algae and Protozoa), ATCC (American Type Culture Collection).

Amoeba	Source	Isolated from...	Year
<i>Acanthamoeba castellanii</i>	CCAP1501/1A	Soil; California, USA	1957
<i>Acanthamoeba polyphaga</i>	CCAP1501/18	Freshwater; cooling tower, Lincoln, England, UK	1985
<i>Amoeba borokensis</i>	CCAP1503/7	Freshwater; pond, Borok, Russia	1974
<i>Allovahlkampfia nedeslanaiensis</i>	CCAP2502/3	Soil; pasture, Veluwe, The Netherlands	2011
<i>Cochliopodium minus</i>	CCAP1537/1A	Freshwater; pond, Madison, Wisconsin, USA	1965
<i>Dermamoeba algensis</i>	CCAP1524/1	Freshwater; Pond, St Petersburg, Russia	2000
<i>Echinamoeba silvestris</i>	CCAP1519/1	Soil; Wandlebury Wood, England, UK	1964
<i>Flamella arnhemensis</i>	CCAP1525/2	Freshwater; cooling tower, Arnhem, Netherlands	2004
<i>Hartmannella cantabrigiensis</i>	CCAP1534/8	Freshwater; ditch, Cambridge, England	1972
<i>Hartmannella cantabrigiensis</i>	CCAP1534/11	Freshwater; ditch, Cambridge, England	1972
<i>Mayorella cantabrigiensis</i>	CCAP1547/11	Freshwater; Cambridge Univ., England, UK	1981
<i>Naegleria gruberi</i> NEG-M	ATCC30224	No data	?
<i>Phalansterium filosum</i>	CCAP1576/1	Soil; Khao Yai National Park, Thailand	2001
<i>Saccamoeba limax</i>	CCAP1572/3	Freshwater, Scotland, UK	1977
<i>Stygamoeba regulata</i>	CCAP1580/1	Brackish; Nivå Bay, The Sønd, Denmark	1994
<i>Tetramitus aberdonicus</i>	CCAP1588/4	Soil; garden, Macauley Institute, Aberdeen, UK	1972
<i>Thecamoeba quadrilineata</i>	CCAP1583/10	Freshwater; roof gutter, Melsbach, Germany	1998
<i>Vahlkampfia avara</i>	CCAP1588/1A	Freshwater; ditch, Schneider, Indiana, USA	1964
<i>Vannella placida</i>	CCAP1565/2	Freshwater; stream, Wisconsin, USA	1964
<i>Vermamoeba vermiformis</i>	CCAP1534/7A	Freshwater; Pigeon Lake, Wisconsin, USA	1964
<i>Vermamoeba vermiformis</i>	CCAP1534/13	Freshwater; sediment, Siegburg, Germany	1967
<i>Vermamoeba vermiformis</i>	CCAP1534/14	Freshwater; lake, Großer Barchsee, Germany	2008
<i>Vermamoeba vermiformis</i> 137	Dr Sutherland McIvor	Soil, North Berwick, Scotland, UK	2000
<i>Vermamoeba vermiformis</i> 172	Dr Sutherland McIvor	Soil, Byron Bay, East Australia	2013
<i>Vermamoeba vermiformis</i> 173	Dr Sutherland McIvor	Soil, Byron Bay, East Australia	2013
<i>Vermamoeba vermiformis</i> 174	Dr Sutherland McIvor	Soil, Byron Bay, East Australia	2013
<i>Vexillifera bacillipedes</i>	CCAP1590/1	Freshwater; Rock River, Wisconsin, USA	1968

2.2. Experimental compounds

2.2.1 Fluorescent microspheres ('beads')

A suspension of yellow-green fluorescent microspheres of 0.49µm diameter (Fluoresbrite, Polyscience Inc.) was stored at 4°C. The number of beads/ml was determined (see 2.3.2).

2.2.2. Agonists

Stock solutions of all agonists (obtained from TOCRIS) were prepared in ethanol and stored at -20°C. Cannabidiol (CBD), N-oleoylethanolamine (OEA), N-palmitoylethanolamine (PEA), GW0742 and Rosiglitazone stocks were 10mM while Anandamide (AEA) was 14.4mM. When necessary, stocks were 10-fold diluted in AS prior to use.

2.2.3. Antagonists

Stock solutions of all antagonists (obtained from TOCRIS) were prepared at 10mM in ethanol and stored at -20°C. These included the PPAR antagonists GW6471 (PPAR α), GSK3787 (PPAR β) and T0070907 (PPAR γ), the dopamine receptor antagonists Haloperidol chloride, LE 300 and L-741,626 and the serotonin receptor antagonist (S)-WAY 100135 dihydrochloride. When necessary, stocks were 10-fold diluted in AS prior to use.

2.2.4. Sugars

Three sugars were used to block amoebic C-type lectin feeding receptors prior to the addition of CBD. D (+)-Mannose, N-Acetyl-D-glucosamine (GlcNAc) and N-Acetyl-D-galactosamine (GalNAc) (Sigma). Stock solutions (1M) were freshly prepared in sterile water on the day of an experiment.

2.3. Counting cells and beads

2.3.1 Counting *E. coli* cells

An *E. coli* suspension (see 2.1.1) was 10-fold diluted in sterile water down to 10⁻³ in eppendorfs (volume 100 μ L). A drop of the DNA stain, 4',6-dimidino-2-phenylindol (DAPI), was added to each dilution and left to stain for 30 min at room temperature. A known volume, of a known dilution, was filtered onto a white 0.2 μ m pore-size filter (Millipore) under low suction. The filter was then placed onto a drop of immersion oil on a glass slide. A drop of oil was placed on the center of the filter, followed by a coverslip and then a final drop of oil was placed on the cover slip. The filter was examined with an epifluorescence microscope (1250x magnification), under UV excitation, which makes the cells appear blue.

A whipple grid (WG) was located in the eye piece of the microscope and cells were counted in randomly selected WGs until at least 400 cells had been counted. The average number of cells per WG was deduced and multiplied by 23068 to give the number of cells on the filter. Knowing the volume and dilution filtered, the concentration of *E. coli* cells in the undiluted sample (cells/ml) could be calculated.

2.3.2 Counting *Synechococcus* cells and beads

The same method was performed as described in 2.3.1. but in the absence of DAPI staining because *Synechococcus* cells naturally fluoresce red under green excitation (due to the presence of Chlorophyll *a*) and beads fluoresce yellow under blue excitation.

2.3.3. Counting amoeba cells in suspension

Two haemocytometer slides, each containing two haemocytometer grids, were loaded with a suspension of the amoeba (see 2.1.3.). The number of cells in the medium-sized squares (9 per grid) were determined (36 squares in total) using a light microscope (x40 magnification). The average number of cells per square was multiplied by 10,000 to give the number of cells/ml in the suspension.

2.3.4. Counting amoeba cells on agar plates

All experimental plates, inoculated with amoeba cells, had a piece of acetate glued to the back of the plate, which contained 5 counting squares (area of each = 1.44 cm²). When the plate was viewed with a light microscope (x40 magnification) the squares were visible, along with the amoeba cells on the surface of the plate. The number of cells were counted in each square, divided by 1.44 and then averaged to give the number of amoebic cells/cm².

2.3.5. Counting fluorescent prey inside *Vermamoeba vermiformis* cells

A fixed suspension of the amoeba, obtained in feeding and pulse-chase experiments (see 2.5 and 2.6), was loaded into a haemocytometer slide and viewed with an epifluorescence microscope using a combination of white light (to locate amoeba cells) and either blue or green excitation (to count ingested beads and *Synechococcus*, respectively). The haemocytometer grid lines aided the location of the very small cells of *V. vermiformis*. A total of 20 cells in each sample were viewed and the number of ingested prey/cell determined.

2.4. Amoeba population growth experiments

2.4.1. Basic experimental protocol

E. coli was prepared and counted as described in 2.1.1. and 2.3.1. Amoebae were prepared and counted as described in 2.1.3 and 2.3.3. All experiments employed NNAg plates (see Appendix 1) which was AS solidified with agarose as opposed to agar N^o2 (which contains a carbon source). This prevented the growth of *E. coli* during the experiment. Furthermore, NNAg plates were prepared on a spirit-level-checked surface in the Class 2 cabinet.

The desired starting concentrations of an amoeba and *E. coli* were 15 cells/cm² and 5x10⁶ cells/cm², respectively. Since the surface area of the agar in the 9 cm diameter Petri dish was 63.63 cm², this demanded that the inoculum (which was always 1ml) contained 954 amoebic cells and 3.18x10⁸ *E. coli* cells. For a control inoculum, the amoeba and *E. coli* were added to the eppendorf and the volume was made up to 1ml with AS. For test inocula, the cells and compound were added and then made up to 1ml with AS.

All the 1ml inocula were vortexed before pouring onto a NNAg agar plate, swirling the plate to ensure full coverage and then leaving the plate to dry on a spirit-level-checked surface in a Class 2 cabinet. A piece of acetate containing 5 counting grids was then fixed onto the back of the plate and a T_{zero} count was performed (see 2.3.4) before incubating the plates at 16°C. The amoeba cells on the Control plate were counted every day and only when the population had divided at least three times were the cells on the Test plates counted (normally 3 days).

2.4.2. Initial screening of amoebae for sensitivity to the agonists

These experiments employed a very high concentration of each agonist (200µM) with the view that, if the amoeba did not respond at this concentration it was unlikely to be sensitive to the agonist. Experiments followed that described in 2.4.1. To achieve an agonist concentration of 200µM in the 1ml inoculum, 20µL of undiluted CBD, OEA, PEA, GW0742 and Rosiglitazone stocks, and 13.9 µL of undiluted AEA stock, were used. These experiments were repeated at least twice. Experiments that utilised the same controls were grouped for statistical analysis, i.e., (i) CBD and AEA vs a common Control and, (ii) OEA, PEA, GW0742 and Rosiglitazone vs a common Control. Each group was analysed using a one-way Analysis of

Variance (ANOVA). If $P \leq 0.05$, a post-hoc Tukey test was carried out to discern which treatment was giving the significant result.

2.4.3. Determining the MIC, IC₅₀ and lethal dose of agonists against sensitive amoebae

These experiments employed a range of agonist concentrations and the procedure followed that described in 2.4.1. Experiments were repeated three times. The %population growth (compared to the Control) in each replicate of each test was deduced and plotted against agonist concentration in Qtiplot, which calculated the IC₅₀ value and slope. The MIC and lethal dose values were estimated from the graphs by extrapolating the linear decline in % population growth to 100% (for MIC) and 0% (for lethal dose) (see Figure 3.2 as an example).

2.4.4. Effect of antagonists on population growth

These experiments tested AEA/CBD/PPAR agonists at either 2 μ M or their IC₅₀ value (see relevant Chapters), in the presence and absence of 10 μ M antagonists for PPARs, Dopamine and Serotonin receptors. Each antagonist was added 20 mins before the addition of the agonist. Experiments were performed three times and the % population growth of the Tests (compared to the Control) were analysed with a one-way ANOVA. Those that gave significant results ($P \leq 0.05$) were subjected to dose-response experiments whereby the antagonist concentrations were 10, 1, 0.1, 0.01 and 0.001 μ M. These experiments were repeated three times and data (% population growth compared to Control) were analysed with a one-way ANOVA and those that gave significant results ($P \leq 0.05$) were further analysed using a post-hoc Tukey test.

2.5. Feeding experiments involving *Vermamoeba vermiformis*

2.5.1. Basic experimental protocol

The prey used for feeding experiments were either fluorescent microspheres (beads) or *Synechococcus* due their fluorescent characteristics allowing their visualization within amoeba cells. Inoculation of experimental plates followed the procedure described in 2.4.1., i.e., 1ml inoculum, but the concentration of prey was increased to 3x10⁷ particles/cm² (this concentration was optimised to ensure enough prey were consumed/cell in a relatively short

time period). Also, a denser suspension of the amoeba was required (see 2.1.3). Test inocula were variable and contained the agonist and/or antagonist and/or sugars (see 2.5.2 to 2.5.5). As soon as the plates had dried (considered T_{zero}), four plugs of agar were removed with a sterile cork borer (6mm diameter) and placed into a 15ml centrifuge tube contained 1ml of AS and 50 μ L of 10% glutaraldehyde (final conc. 0.5% v/v) to fix the cells. Further samples (4 plugs) were removed and fixed every 20 min for a given period of time. The cells were dislodged from the agar surface into suspension by vortexing for 2 min. The suspension was loaded into a haemocytometer slide and the number of prey/cell determined (see 2.3.5).

The average prey/cell was plotted against time (min) to provide a visual depiction of the response. The linear portion of the increase in prey/cell, for each treatment, were compared with an Analysis of Covariance (ANCOVA). Ingestion rate (prey/cell/min) was determined as the gradient of the linear increase of prey/cell over time. The lag phase (min) was estimated from the point at which this linear increase crossed the x axis (where prey/cell is zero). Ingestion rates and feeding lags were deduced for each replica and then averaged.

2.5.2. Effect of AEA and CBD on *V. vermiformis* feeding

The experiment followed that described in 2.5.1. using only AEA and CBD at a concentration of 2 μ M and both beads and *Synechococcus* as prey. It was only performed once for the latter prey so limited statistical analysis were carried out, while it was performed three times for former with full statistical analysis of the data.

2.5.3. Effect of CBD concentration of *V. vermiformis* feeding

The experiment followed that described in 2.5.1. using CBD at 0, 0.1, 1, 2 and 5 μ M and beads as the prey. These experiments were performed twice and full statistical analysis was carried out.

2.5.4. Effect of PPAR agonists and antagonists of the feeding of *V. vermiformis*

The experiment followed that described in 2.5.1. using CBD at 2 μ M, beads as the prey, and the PPAR agonists (OEA, PEA, GW0742 and Rosiglitazone) at their IC_{50} values. Experiments were performed in the presence/absence of a specific PPAR antagonist at 10 μ M, added 20

min before agonist. These experiments were performed three times, and full statistical analysis was carried out.

2.5.5. Effect of blocking amoeba prey recognition receptors, prior to adding CBD, on *V. vermiformis* feeding

The experiment followed that described in 2.5.1. except that the amoeba was pre-incubated for 20 min with 100mM of D (+)-Mannose, N-Acetyl-D-glucosamine (GlcNAc) and N-Acetyl-D-galactosamine (GalNAc), to block amoebic C-type lectins. Then, the experiment was inoculated as normal with CBD at 2 μ M and using *Synechococcus* as the prey. These experiments were performed three times and full statistical analysis was carried out.

2.6. Effect of CBD on phagosome processing and defecation in *V. vermiformis*

Pulse-chase experiments were performed to monitor the fate of ingested prey (beads) in the presence and absence of 2 μ M CBD. Two dense suspensions of *V. vermiformis* (1 ml) were mixed with beads (at 5x10⁷ particles/ml) and each poured onto a level NNAg plate. Once dry, four plugs of agar were removed from each plate and fixed at 0, 5 and 10 min (see 2.5.1).

Immediately after this, the chase was performed, i.e., 1 ml of AS was poured onto the surface of each plate, the cells were dislodged into suspension then added to 24 ml AS in a tissue culture flask. CBD was added to one of these flasks at 2 μ M (Test). Then, each flask was used to inoculate eight large NNAg plates (140 cm diameter) with 1ml of the suspension. The suspension was quickly spread across the surface. This dilution into 25ml AS coupled with spreading the amoebae across a large area was intended to stop further ingestion of beads and only allow only the fate of the pre-ingested prey (up to 10 min) to be monitored.

A whole plate, for Control and Test, was sacrificed at T = 15, 20, 25 and 30 min, then every 10 min up to 70 min, by adding 1ml of glutaraldehyde (0.5% v/v) to the plate and dislodging the cells into suspension. Twenty cells in each sample were viewed and the number of ingested prey/cell recorded (see 2.3.5). This experiment was performed three times and full statistical analysis was carried out. Ingestion rates and defecation rates were deduced for each replica and then averaged. Rates were statistically compared with an ANCOVA.

2.7. Bioinformatic analysis

Published genome databases were explored to verify whether the gene sequences of cannabinoid putative receptors and the degradation enzymes of cannabidiol existed in single-celled eukaryotes or not. Three databases were used; www.amoebadb.org , www.ciliate.org and www.dictybase.org .

Chapter 3: Sensitivity of amoebae to CBD and AEA

3.1. Introduction

The effect of cannabinoids on amoebae has not been extensively researched. There is only one publication (Pringle et al. 1979) which has examined the effect of THC and CBD on *Naegleria fowleri* and one (Dey et al., 2010) which has examined the effect of AEA and 2-AG on *Vermamoeba vermiformis*, *Acanthamoeba castellanii* and *Wilertia magna*. Some work has been performed on the effects of THC and CBD on the slime mould *Dictyostelium discoideum* (Bram and Brachet, 1976; Perry et al. 2020). This mould has an amoebae stage in its growth cycle but upon starvation the cells do not form cysts, as do true amoebae, instead they aggregate to form a slug followed by a fruiting body (Hayes et al., 2013).

The first aim of the current study was to evaluate the extent to which true naked amoebae respond to cannabinoids. Considering the taxonomy of amoebae is still very fluid (Kang et al., 2017), it was necessary to obtain strains from reputable culture collections so that if their genus/species name changed, their catalogue number would not; allowing others to repeat the experiments if necessary. A representative strain of all the 20 species of non-marine naked amoebae available in culture (at 2017) were tested here. Two species of *Acanthamoeba* were included as this genus is well studied and of medical significance (Thomas et al., 2009). Each amoeba was first subjected to a high concentration (200 μ M) of CBD and AEA to determine whether they were sensitive or insensitive to these compounds. Those strains that were sensitive were further tested to deduce their MIC, IC₅₀ and lethal dose values.

3.2. Results

3.2.1 Initial screening of amoebae for sensitivity to AEA and CBD

Exposure of the 20 species of amoeba (27 strains) to 200 μ M AEA or CBD resulted in 14 insensitive species (Table 3.1) and 6 sensitive species (Table 3.2).

Table 3.1: Strains considered insensitive to AEA or CBD (at 200µM). ANOVAs for each of two experiments show no significant effect of the compounds on population growth, compared to the Control (P>0.05).

Amoeba	ANOVA P values
<i>Acanthamoeba polyphaga</i> CCAP1501/18	0.08/0.50
<i>Amoeba borokensis</i> CCAP1503/7	0.14/0.35
<i>Allovahlkampfia nedeslanaiensis</i> CCAP2502/3	0.68/0.81
<i>Cochliopodium minus</i> CCAP1537/1A	0.81/0.92
<i>Dermamoeba algensis</i> CCAP1524/1	0.46/0.50
<i>Echinamoeba silvestris</i> CCAP1519/1	0.41/0.42
<i>Mayorella cantabrigiensis</i> CCAP1547/11	0.43/0.68
<i>Phalansterium filosum</i> CCAP1576/1	0.89/0.99
<i>Saccamoeba limax</i> CCAP1572/3	0.29/0.92
<i>Stygamoeba regulata</i> CCAP1580/1	0.14/0.19
<i>Tetramitus aberdonicus</i> CCAP1588/4	0.12/0.89
<i>Thecamoeba quadrilineata</i> CCAP1583/10	0.16/0.58
<i>Vannella placida</i> CCAP1565/2	0.77/0.77
<i>Vexillifera bacillipedes</i> CCAP1590/1	0.18/0.53

Of the 6 sensitive species (Table 3.2) all strains were sensitive to CBD and all but *Flamella arnhemensis* and *Acanthamoeba castellanii* were sensitive to AEA.

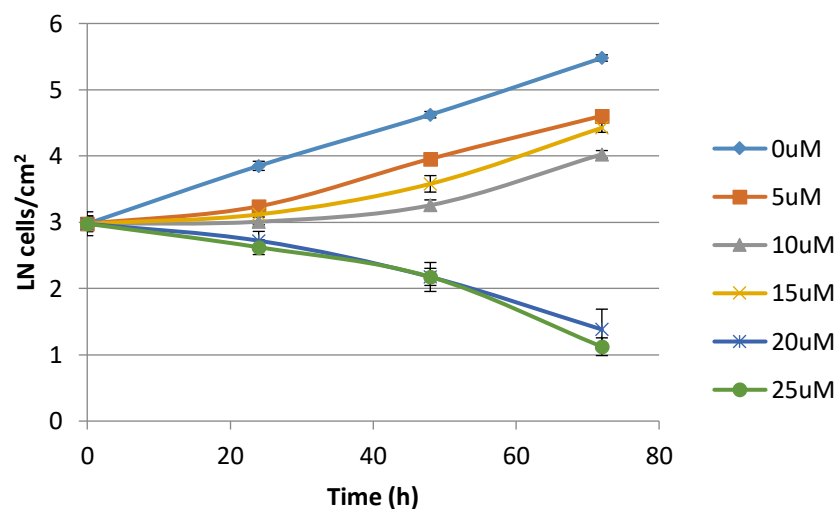
Table 3.2: Strains considered sensitive to AEA or CBD (at 200µM). ANOVAs for each of two experiments were significant (P<0.05) and post-hoc Tukey tests identified which compound affected population growth, compared to the control. All were sensitive to CBD and all but two (*A. castellanii* and *F. arnhemensis*) were sensitive to AEA.

Amoeba	Post-hoc (vs Control) P values	
	CBD	AEA
<i>Acanthamoeba castellanii</i> CCAP1501/1A	0.001/0.036	0.25/0.90
<i>Flamella arnhemensis</i> CCAP1525/2	0.002/0.007	0.18/0.29
<i>Hartmannella cantabrigiensis</i> CCAP1534/8	0.001/0.005	0.001/0.003
<i>Hartmannella cantabrigiensis</i> CCAP1534/11	0.001/0.001	0.001/0.001
<i>Naegleria gruberi</i> NEG-M ATCC30224	0.001/0.001	0.001/0.001
<i>Vahlkampfia avara</i> CCAP1588/1A	0.001/0.007	0.001/0.006
<i>Vermamoeba vermiformis</i> CCAP1534/7A	0.001/0.001	0.001/0.001
<i>Vermamoeba vermiformis</i> CCAP1534/13	0.001/0.001	0.001/0.001
<i>Vermamoeba vermiformis</i> CCAP1534/14	0.001/0.001	0.001/0.001
<i>Vermamoeba vermiformis</i> 137	0.001/0.001	0.001/0.001
<i>Vermamoeba vermiformis</i> 172	0.001/0.001	0.001/0.001
<i>Vermamoeba vermiformis</i> 173	0.001/0.001	0.001/0.001
<i>Vermamoeba vermiformis</i> 174	0.001/0.001	0.001/0.001

There appeared to be no strain differences in amoebic response, with all 7 strains of *Vermamoeba vermiformis*, and both strains of *Hartmannella cantabrigiensis*, showing the same response. Species difference were evident within the genus *Acanthamoeba* with *A. castellanii* being sensitive to CBD (Table 3.2) while *A. polyphaga* was not (Table 3.1).

3.2.2. MIC, IC₅₀ and lethal dose values for AEA and CBD against sensitive amoebae

All 13 sensitive strains (Table 3.2) were subjected to dose response experiments with CBD and AEA. There now follows an example of the analysis carried out on each strain, using *Vermamoeba vermiformis* CCAP 1534/7A with AEA as an example (Fig. 3.1).



	Specific growth rate (/h)	Lag phase (min)
0uM	0.035±0.002	0
5uM	0.028±0.001	14.65±2.08**
10uM	0.022±0.002*	26.79±2.21**
15uM	0.027±0.002*	21.39±1.54**

Figure 3.1: The effect of AEA concentration on the population growth of *Vermamoeba vermiformis* CCAP 1534/7A at 23°C together with calculated specific growth rates (/h) and lag phases (min). Significant difference to Control [0µM] *P<0.05, ** P<0.01.

Fig 3.1 shows the population growth of *Vermamoeba vermiformis* 7A over 3 days in the presence of various concentrations of AEA (0 to 25µM). At 5µM, AEA induced a significant lag (P<0.01) after which the specific growth rate equaled that of the Control (P=0.10) (Fig. 3.1).

At 10 and 15µM AEA the specific growth rates were equal ($P=0.10$) but significantly lower than the Control and 5µM AEA ($P<0.05$). The lag period with these concentrations was also equal ($P=0.15$) and significantly longer than at 5µM AEA ($P<0.01$). AEA was lethal to the amoeba at concentrations of 20µM and above (Fig. 3.1).

Vermamoeba vermiformis 7A was subjected to further experiments using various AEA concentrations and the % survival compared to control (after the control had divided at least three times) was plotted against AEA concentration (µM) in QtiPlot (Fig. 3.2). The Qtiplot automatically generates two parameters (IC_{50} and Slope). The MIC and lethal dose (LD) values were estimated from this graph (Fig. 3.2 blue lines). The parameter values were; $IC_{50} = 2.63 \pm 1.26\mu\text{M}$, Slope = 1.04 ± 0.05 , MIC = $0.3\mu\text{M}$ and LD $\geq 20\mu\text{M}$ (Table 3.3).

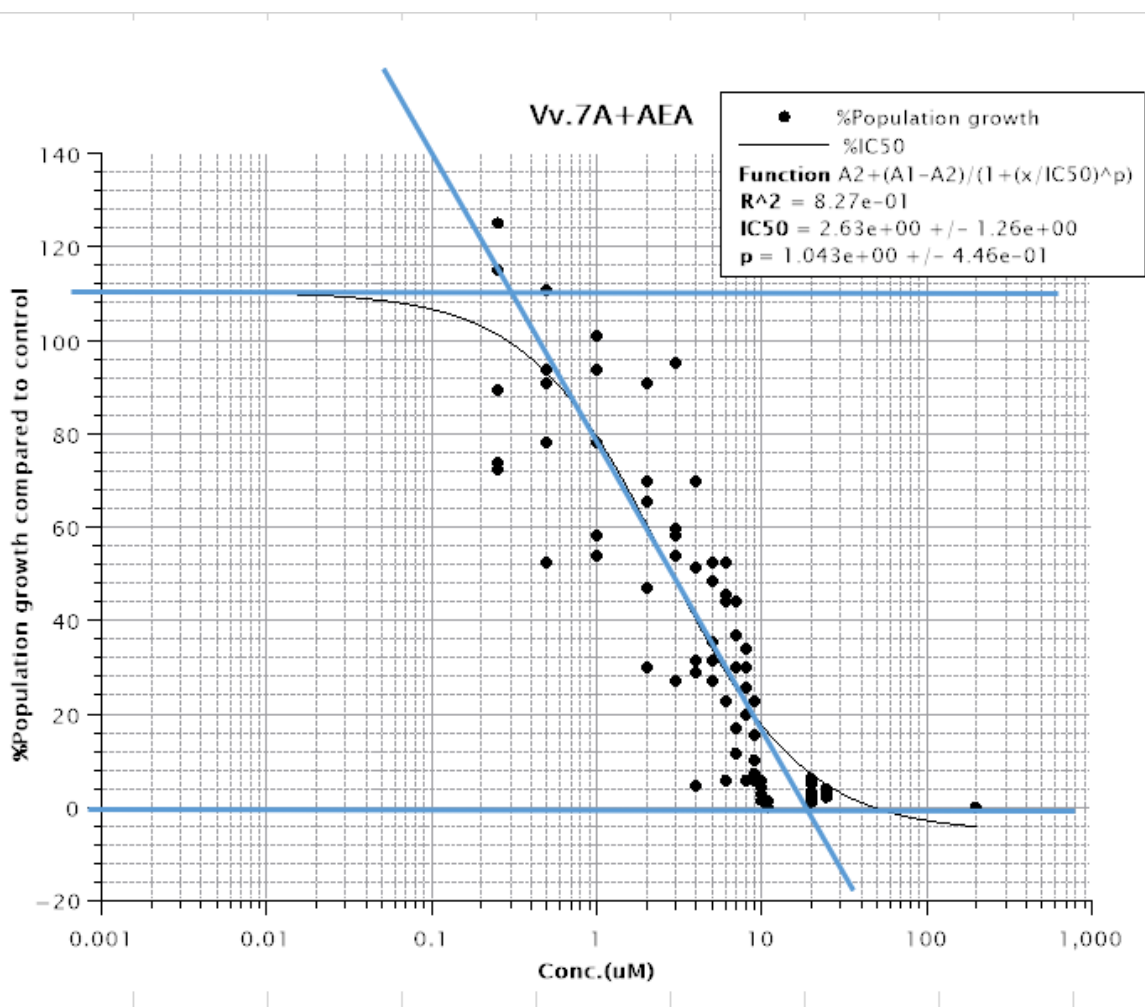


Figure 3.2: Qtiplot of % population growth (compared to the Control) against AEA concentration (µM) for *Vermamoeba vermiformis* CCAP 1534/7A. The programme generates values for IC_{50} (2.63µM) and Slope (1.043), while MIC (0.3µM) and lethal dose (20µM) are estimated from where the linear decline crosses the the '100%' (MIC) and 0% (Lethal Dose).

The above analysis was performed for all sensitive strains and data for the four parameters are summarised in Table 3.3 (individual IC₅₀ plots can be found in Appendix 2). Based on comparison of IC₅₀ values (Table 3.3) *Naegleria gruberi* was the most sensitive strain to CBD followed by *Vahlkampfia avara* and *Flamella arnhemensis*. The least sensitive strain was *Acanthamoeba castellanii*. *V. vermiformis* and *Hartmannella cantabrigiensis* strains showed varying degrees of sensitivity, with *V. vermiformis* 173 being the most sensitive and 137 being the least sensitive (Table 3.3).

N. gruberi and *V. avara* were less sensitive to AEA compared to CBD (Table 3.3) and this was also the case for all *V. vermiformis* and *H. cantabrigiensis* strains except for *V. vermiformis* 173 which displayed equal sensitivity to AEA and CBD (based on IC₅₀) (Table 3.3).

Table 3.3: Calculated MIC, IC₅₀, lethal dose (µM) and slope values for AEA and CBD acting on 13 strains of amoebae.

Sensitive amoeba strains	CBD				AEA			
	MIC	IC ₅₀	Slope	Lethal	MIC	IC ₅₀	Slope	Lethal
<i>Acanthamoeba castellanii</i> CCAP 1501/1A	10	16.37	4.59	>27	N/A	N/A	N/A	N/A
<i>Flamella arnhemensis</i> CCAP 1525/2	0.4	0.97	2.47	>4	N/A	N/A	N/A	N/A
<i>Hartmannella cantabrigiensis</i> CCAP 1534/11	15	17.93	18.15	>21	0.1	3.63	0.53	>100
<i>Hartmannella cantabrigiensis</i> CCAP 1534/8	1.5	4.1	1.96	>13	14	23.71	3.46	>41
<i>Naegleria gruberi</i> NEG-M ATCC 3022	0.2	0.72	1.63	>3	0.21	1.15	1.25	>6
<i>Vahlkampfia avara</i> CCAP 1588/1A	0.08	0.78	0.94	>9	2.1	7.52	1.76	>40
<i>Vermamoeba vermiformis</i> 137	4	7.31	3.77	>14	1.3	9.89	1.01	>50
<i>Vermamoeba vermiformis</i> 172	0.3	1.78	1.23	>10	5	7.33	5.45	>12
<i>Vermamoeba vermiformis</i> 173	0.08	0.98	0.87	>10	0.06	0.96	0.72	>13
<i>Vermamoeba vermiformis</i> 174	1.6	2.98	3.86	>5	1.2	5.41	1.23	>25
<i>Vermamoeba vermiformis</i> CCAP 1534/7A	0.2	1.99	0.89	>16	0.3	2.63	1.04	>20
<i>Vermamoeba vermiformis</i> CCAP 1534/13	3	5.05	3.79	>9	1.5	7.69	1.32	>35
<i>Vermamoeba vermiformis</i> CCAP 1534/14	0.15	1.01	1.05	>8	0.15	2.33	0.74	>30

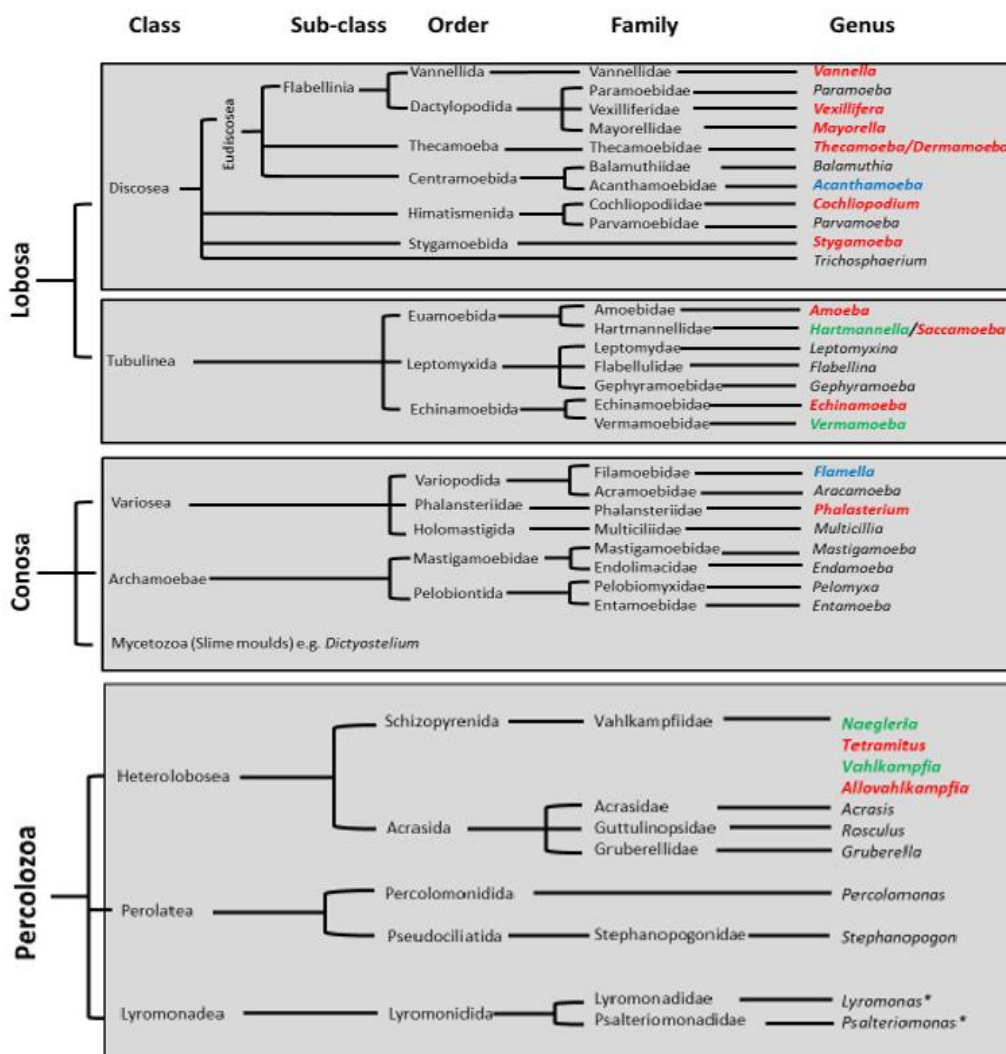
3.3. Discussion

This study investigated the sensitivity of 20 amoebic species (27 strains) to the cannabinoids CBD and AEA. Fourteen species were insensitive to both, four were sensitive to both and two were sensitive to CBD only. Results showed no strain differences within a given species, however differences within the genus *Acanthamoeba* were evident with *A. castellanii* being sensitive to CBD while *A. polyphaga* was not. Also, the data suggest that amoebae are generally more sensitive to CBD than AEA.

3.3.1. Differences in sensitivity of amoebae to AEA and CBD

There appears to be no pattern regarding the phylogenetic position of an amoeba and its sensitivity to AEA and CBD. Of those that were sensitive, *V. vermiformis*, *H. cantabrigiensis*, *A. castellanii* and *F. arnhemensis* are within the supergroup Amoebozoa (sub-phylum Lobosa), while *V. avara* and *N. gruberi* belong to the Excavata (sub-phylum Percolozoa) (Fig. 3.3). Also, *Echinamoebida* and *Vermamoeba* are within the same order (Echinamoebida) (Fig. 3.3) but the former was insensitive to both AEA and CBD while the latter was sensitive.

Figure 3.3: Phylogenetic position of the 19 amoeba genera used in this study (adapted from Smirnov et al., 2011). **Green** = susceptible to CBD and AEA, **blue** = susceptible to CBD only, **red** = not susceptible. *Flagellate.



Saccamoeba and *Hartmannella* are within the same family (*Hartmannellidae*) (Fig. 3.3) yet the former was insensitive to AEA and CBD while the latter was sensitive. *Allovahlkampfia*, *Tetramitus*, *Vahlkampfia* and *Naegleria* are also in the same family (*Vahlkampfiidae*) (Fig. 3.3) but the former two were insensitive to AEA and CBD while the latter two were sensitive. There is also a difference within the genus *Acanthamoeba* (not shown in Fig. 3.3) whereby *A. polyphaga* was not sensitive to AEA and CBD while *A. castellanii* was sensitive to CBD only. In addition, *V. vermiformis* was previously described as *Hartmannella vermiformis* until 2011, when Smirnov et al. described it as a new genus under the newly described order Echinamoebida (Figure 3.3). However, both these genera responded similarly to CBD and AEA suggesting that they might behave the same and did not warrant such separation (but see Chapter 5 where their separation does appear warranted).

Considering their taxonomic position did not appear to govern sensitivity, attention turned to the size of the amoebae (Table 3.4) and where they were isolated from (Table 2.1).

Table 3.4: Comparison of cell sizes between amoeba species. Sensitive strains in bold. Adapted from Page, 1988; Marciano-Cabral et al., 2003; Garstecki et al., 2005; Walochnik and Mulec, 2009; Tymł et al., 2016; www.microworld; www.nies.go.jp.

Amoeba	Cell length (µM)
<i>Phalansterium filiosum</i>	6.3-8.5
<i>Echinamoeba silvestris</i>	7-21
<i>Hartmannella cantabrigiensis</i>	10-30
<i>Naegleria gruberi</i>	10-36
<i>Vexillifera bacillipedes</i>	10-70
<i>Acanthamoeba castellanii</i>	12-35
<i>Flamella arnhemensis</i>	13-34
<i>Vermamoeba vermiformis</i>	14-31
<i>Vahlkampfia avara</i>	14-33
<i>Cochliopodium minus</i>	16-42
<i>Stygamoeba regulata</i>	19-38
<i>Allovahlkampfia sp.</i>	20-40
<i>Acanthamoeba polyphaga</i>	25-40
<i>Tetramitus aberdonicus</i>	30-65
<i>Thecamoeba quadrilineata</i>	35-80
<i>Saccamoeba limax</i>	35-85
<i>Vannella placida</i>	40-75
<i>Dermamoeba algensis</i>	50-100
<i>Mayorella cantabrigiensis</i>	55-180
<i>Amoeba borokensis</i>	210-545

Cell measurements of the strains in the current study were not determined but Table 3.4 indicates (using published data) that those susceptible strains (in bold) are generally at the lower end of the cell size spectrum. However, if cell size was a determinant of sensitivity, a concentration of 200 μ M would have been expected to significantly affect the very small cells of *P. filosum* and *E. silvestris* (Table 3.4), but they did not.

There was also no obvious relationship between the source of the amoebae with regards to freshwater vs soil, country of origin or year of isolation (see Table 2.1). For example, *V. vermiformis* strains were isolated from both soil and freshwater in four countries, between the years 1964 and 2013, and all were susceptible to CBD and AEA (see Table 2.1).

It was interesting to note that even though there were no strain differences in the responses of different strains of *V. vermiformis* or *H. cantabrigiensis* to CBD/AEA there was a difference in response observed between species of *Acanthamoeba*. Here, the similarly sized (Table 3.4) *A. castellanii* was sensitive to CBD while *A. polyphaga* was not. The author cannot find evidence from previous studies of the former being sensitive to a compound while the latter was not, but differences between these species in their response to a particular compound has been reported. For example, Henriquez, et al. (2008) showed that *A. castellanii* was more sensitive to chlorhexidine (IC₅₀ 1.56-3.13 μ M) compared to *A. polyphaga* (IC₅₀ 3.13-6.25 μ M). Also, McBride et al. (2005) found that *A. castellanii* was far more sensitive to hexadecyl-PC and octadecyl-PC (IC₅₀s both 3.91-7.81 μ M) compared to *A. polyphaga* (IC₅₀s of 31.25-62.5 μ M and 15.63-31.25 μ M, respectively). So, there is evidence that they are 'different' but in the current study their difference with regards to susceptibility to CBD was very striking.

3.3.2 Dose-dependent effect of AEA and CBD on amoebic growth

The MICs of CBD ranged from 0.08 to 15 μ M, IC₅₀s from 0.72 to 18 μ M and lethal doses from ca. 3 to 21 μ M (Table 3.3). Comparison to previously published work is limited, as only one study has examined the effect of CBD on amoebae. Pringle et al. (1979) found that the population growth of *Naegleria fowleri* (LEE) was suppressed by 47% and 73% after 3 days incubation with 15.9 μ M THC and CBD, respectively. In the current study, a concentration of 15.9 μ M CBD would be lethal to *N. gruberi* NEG-M (Lethal dose \geq 3 μ M, Table 3.3) suggesting that *N. gruberi* is far more sensitive to CBD than *N. fowleri*.

The MICs of AEA ranged from 0.06 to 14 μ M, IC₅₀s from 0.96 to 24 μ M and lethal doses from *ca.* 6 to 100 μ M (Table 3.3). Once again, only one study has examined the effect of AEA on amoebae. Dey et al. (2010) showed that the population growth of three amoebae, after 3 days, was negatively affected by AEA, 2-AG but not 2-AG-ether. The latter is a non-hydrolysable form of 2-AG therefore showing that it was the 2-AG itself, and not a breakdown product, that caused this negative effect. The IC₅₀s of *V. vermiformis* (Ax.5.2e4b), *A. castellanii* (By 02.2.4) and *Wilertia magna* c2c Maky (ATCC PTA-7824) with AEA were 14, 17 and 20 μ M, respectively (Dey et al., 2010). Their IC₅₀ for *V. vermiformis* (14 μ M) is outside the range of that recorded for the seven *V. vermiformis* strains tested in the current study (0.96-9.89 μ M, Table 3.3). Also, the *A. castellanii* used in the current study (CCAP1501/1A) was not sensitive to AEA (Tables 3.2 and 3.3), unlike the strain of Dey et al. (2010). This difference might be due to the use of a different strain, although in the current study there was no difference recorded between several strains of *V. vermiformis* and *H. cantabrigiensis*. However, there is evidence of strain differences in susceptibility to Polyhexamethylene biguanide (PHMB) within the species *A. castellanii* (Huang et al., 2015).

Data showed that, in general, amoebae were more sensitive to CBD than AEA. With such little amoebic data with which to make comparisons, amoebic sensitivity was compared to those of mammalian cells (Table 3.6). Firstly, it appears that the CBD and AEA concentrations required to elicit a response in amoebae are of the same order as those required to elicit a response in mammalian cells (Table 3.6). Secondly, there is some evidence to suggest that mammalian cells are more sensitive to CBD than AEA. For example, Grimaldi et al. (2006) showed that 10 μ M AEA was not toxic to MDA-MB-231 breast cancer cells (after 24h) but Sultan et al. (2018) recorded CBD-induced apoptosis in these cells (after 24h), with an IC₅₀ of 2.2 μ M (Table 3.6). Ligresti et al. (2006) also found these cells to be sensitive to CBD at 8.2 μ M (after 4d) (Table 3.6). Studies on C6 glioma cells (Table 3.6) have shown that CBD-induced apoptosis occurs (after 4d) with an IC₅₀ of 8.5 μ M (Ligresti et al., 2006) while a concentration of 15 μ M AEA only suppressed their growth by 66% (after 5d) (Ortega et al., 2015).

Table 3.6: The effect, and the effective concentrations, of CBD and AEA on mammalian cells.

Cannabinoid	Cell type	Concentration	Effect	Time after treatment	Reference
CBD	MDA-MB-231 h-breast cancer T-47D h-breast cancer	IC ₅₀ = 2.2µM IC ₅₀ = 5µM	Induced apoptosis	24h	Sultan et al., 2018
	Caco-2 cells	10µM	Activated arrangement of autophagosome	4-6h	Koay et al., 2014
		25µM	Cell death	4-6h	
	h-carcinoma	1-10µM	Induced apoptosis	24h	De Petrocellis et al., 2013
	MDA-MB-231 h-breast	IC ₅₀ = 8.2µM	Induced apoptosis	4d	Ligresti et al., 2006
C6 cells of glioma	IC ₅₀ = 8.5µM	Induced apoptosis	4d	Ligresti et al., 2006	
AEA	cardiac endothelioma in rat, h-breast cancer	IC ₅₀ = 0.5-6 µM	Inhibition of G1/S phase	48-96h	De Petrocellis et al., 2000
	H460 h- lung cancer	20µM	Induced apoptosis	2h	Athanasiou et al., 2007
	h- melanoma	IC ₅₀ = 5.8µM	Induction of cytotoxicity	24h	Adinolfi et al., 2013
	MDA-MB-231 h-breast	10µM	No effect	24h	Grimaldi et al., 2006
	C6 cells of glioma	15µM	Growth inhibition	5d	Ortega et al., 2015

3.4. Conclusions

This study set out to determine the sensitivity of 20 naked amoeba species to CBD and AEA. Fourteen species (70%) were insensitive while 6 species (30%) were sensitive. There appeared to be no correlation between sensitivity and phylogenic position, cell size or habitat. For the sensitive strains, (i) CBD and AEA reduced population growth over 3 days in a dose-dependent manner and, (ii) higher concentrations proved lethal but lower concentrations induced a lag followed by reduced growth rate which was dose-dependent.

Chapter 4 now looks at one strain in more detail (*Vermamoeba vermiformis* CCAP 1534/14) with regards to the effect of AEA and CBD on its feeding behaviour, to see if disrupted feeding is the reason for the lag phase followed by reduced population growth in the presence of these compounds.

Chapter 4: Effect of CBD and AEA on feeding in *Vermamoeba vermiformis*

4.1. Introduction

The results of Chapter 3 indicated that CBD and AEA reduces the population growth of sensitive amoebae in a dose dependent manner. *Vermamoeba vermiformis* CCAP 1534/7A (Fig 3.1) showed two features that are evident during the early stage of cannabinoid (at sub-lethal concentrations). Firstly, there is a lag phase with no effect on subsequent population growth and then there is a longer lag phase accompanied by a reduction in population growth.

Successful amoebic population growth requires successful ingestion and metabolism of prey, so this part of the study examined whether it was the amoebic feeding process which was being affected by the cannabinoids and causing the lag and reduced growth rates. The feeding process in amoebae was described in Section 1.6.3 but a brief summary follows. The process begins when the phagocytic cell recognises the binding ligands of the prey cell in a receptor-dependent manner. In protists, these receptors have been identified as C-type lectins which bind carbohydrate residues (e.g. mannose, GalNAc, GlcNAc) on the bacterial cell (e.g. Allen and Davidowicz, 1990; Venkataraman et al., 1997). Actin polymerisation is activated and two pseudopodia extend out from the cell to surround the prey particle then myosin is recruited to help seal the ends of the pseudopodia together (Levin et al., 2016). The recruitment of dynamin leads to the detachment of the phagosome from the cell surface and into the cytoplasm (Levin et al., 2016) where it matures via a complicated series of fusion events with endosomes and lysosomes (Haas, 2007; Pauwels et al., 2017). Fusion of the phagosome membrane with the outer membrane then leads to the defecation of any undigested material and then the spent phagosome membrane is endocytosed and used to make new phagosomes (Allen and Fok, 1980).

Although *V. vermiformis* strain 173 was the most sensitive to CBD and AEA (Table 3.3), feeding experiments employed the second most sensitive strain, *V. vermiformis* CCAP 1534/14, as it is held within a culture collection and available to other researchers. Two fluorescent prey were used: live *Synechococcus* sp. S-KH3 (Dillon and Parry, 2009) and polystyrene microspheres (beads); both of which are indigestible to *V. vermiformis* (Pickup et al., 2007). The concentration of CBD/AEA was 2 μ M which is close to the IC₅₀ values of both cannabinoids (Table 3.3), and would allow a direct comparison of their effects on amoeba cells.

4.2. Results

4.2.1. Effect of AEA and CBD (2 μ M) on *V. vermiformis* feeding on indigestible beads and *Synechococcus* ('Pico')

These experiments were only performed once, alongside each other, with three replicas (see 2.5.2). The same controls were used for Fig. 4.1a and b.

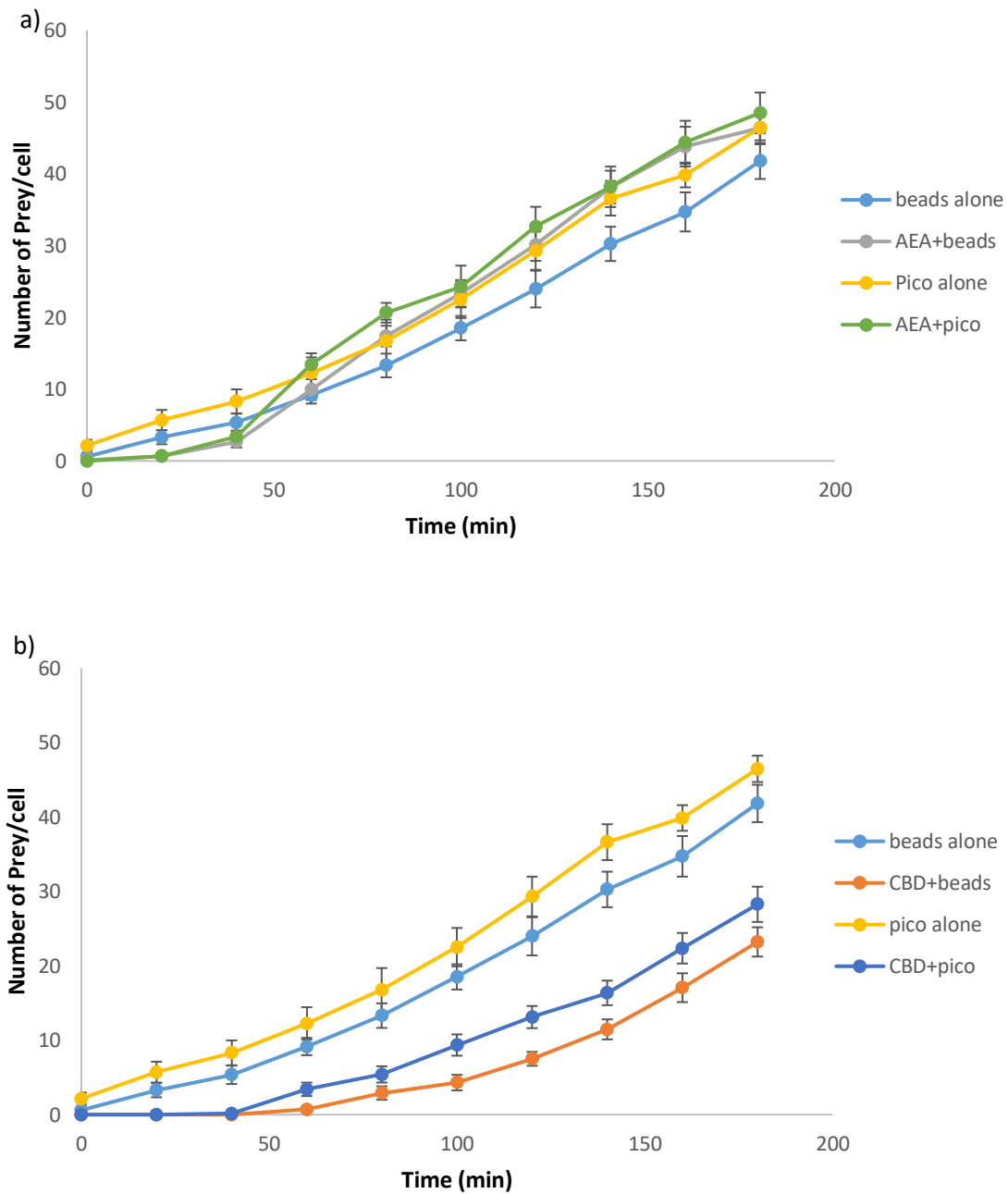


Figure 4.1: Effect of a) AEA and b) CBD (both at 2 μ M) on the feeding of *Vermamoeba vermiformis* CCAP1534/14 on beads and live *Synechococcus* ('Pico'). Experiment was performed once.

Although it appears from Fig. 4.1 that *V. vermiformis* CCAP1534/14 ingests beads to a lesser extent than *Synechococcus* (in the Controls), there was no significant difference in their uptake ($P=0.91$). Estimated ingestion rates were *ca.* 0.26 and 0.28 prey/cell/min for beads and *Synechococcus*, respectively.

AEA induced a lag in feeding (Fig 4.1a); *ca.* 31 min for beads and *ca.* 21 min for *Synechococcus*, yet surprisingly only the latter was significantly different to the Control ($P<0.05$). After this, feeding in the presence of AEA was higher than the Control with both beads and *Synechococcus* ($P<0.01$), which was also surprising. This disruption of feeding (firstly a negative effect followed by a positive effect) appeared unlikely to be the reason for reduced population growth of *V. vermiformis* with AEA (Fig. 3.1) but before removing AEA from the feeding study, this experiment was repeated a further two times with beads as the prey (Fig. 4.2). Composite data, and a full statistical analysis, confirmed that AEA did *not* induce a significant lag phase ($P=0.17$) and did *not* result in an elevated ingestion rate, compared to the Control ($P=0.77$). AEA was therefore considered to have no significant effect on *V. vermiformis* feeding and experiments with AEA ceased.

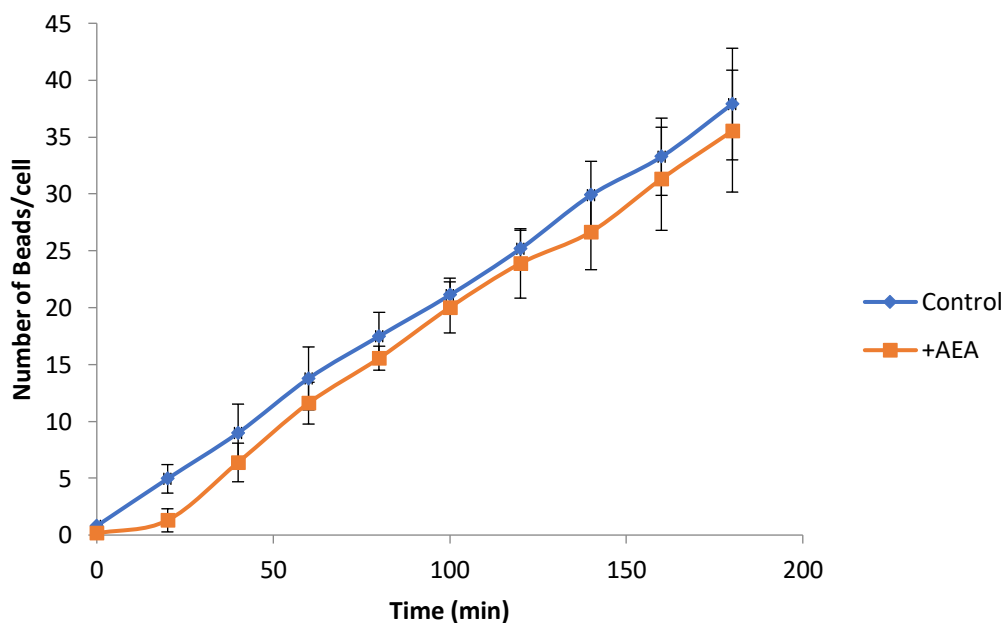


Figure 4.2: Effect of AEA (2 μ M) on the feeding of *Vermamoeba vermiformis* CCAP1534/14 on beads. Experiment performed three times.

CBD caused a significant ($P < 0.01$) lag in the uptake of both beads (*ca.* 86 min) and *Synechococcus* (*ca.* 59 min) followed by a resumption of feeding, at rates equivalent to the Control, with *Synechococcus* ($P = 0.37$) but lower than the Control, with beads ($P < 0.05$) (Fig. 4.1). This disruption in feeding might therefore contribute to reduced population growth of *V. vermiformis* in the presence of CBD after 3 days so further studies on CBD were performed.

4.2.2. Effect of CBD concentration on the feeding lag and ingestion rate of *V. vermiformis*

V. vermiformis CCAP1534/14 was fed with beads at 3×10^7 particles/cm² in the absence and presence of CBD (0.1–5 μ M) (see 2.5.3) and the number of beads/cell recorded over time (Fig. 4.3). This experiment was performed twice. Ingestion rates (prey/cell/min) and feeding lags (min) were deduced for each replicate ($n = 6$) and averaged. In these experiments the Control showed a *ca.* 42 min lag in feeding (Fig. 4.3) so this was subtracted from Test lag times to provide net lag times (Fig. 4.4a).

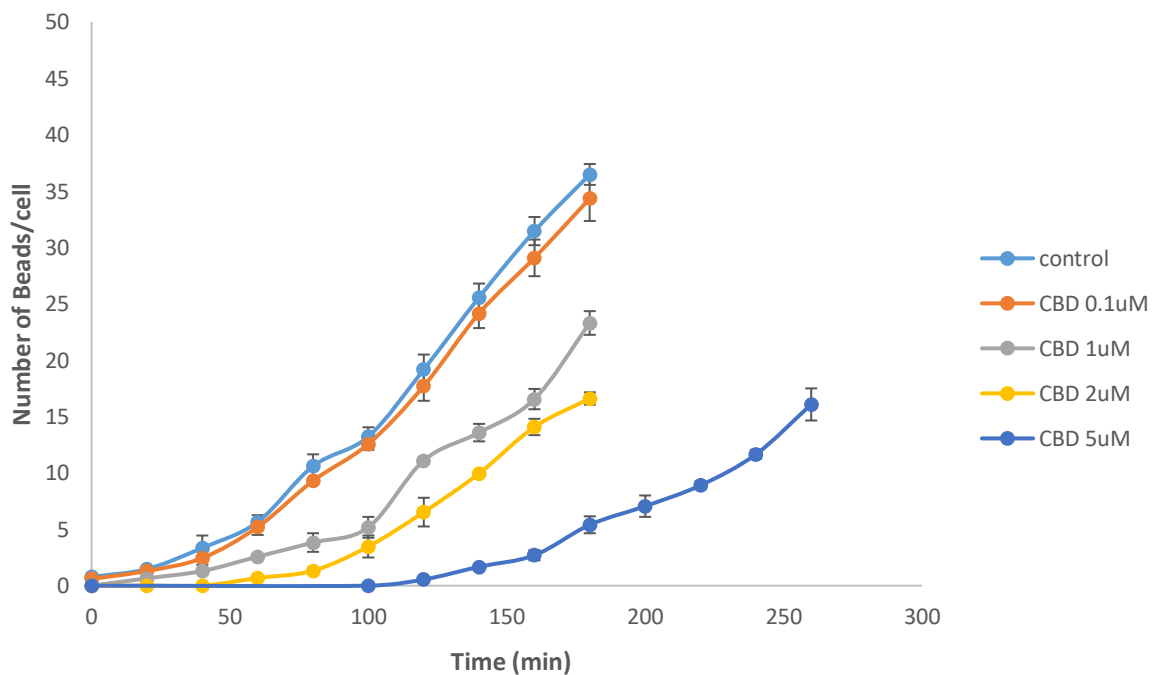


Figure 4.3: Consumption of beads (as beads/cell) by *Vermamoeba vermiformis* CCAP1534/14 in the absence (Control) and presence of CBD at concentrations ranging from 0.1 to 5 μ M.

Figure 4.4a shows that CBD did not induce a significant feeding lag until 1 μ M ($P<0.05$), after which the lag duration appeared to be dose-dependent. The ingestion rates at 0.1 and 1 μ M were not significantly different to the Control ($P=0.89$), but those at $\geq 2\mu$ M were significantly lower than the Control ($P<0.05$) (Fig 4.4b).

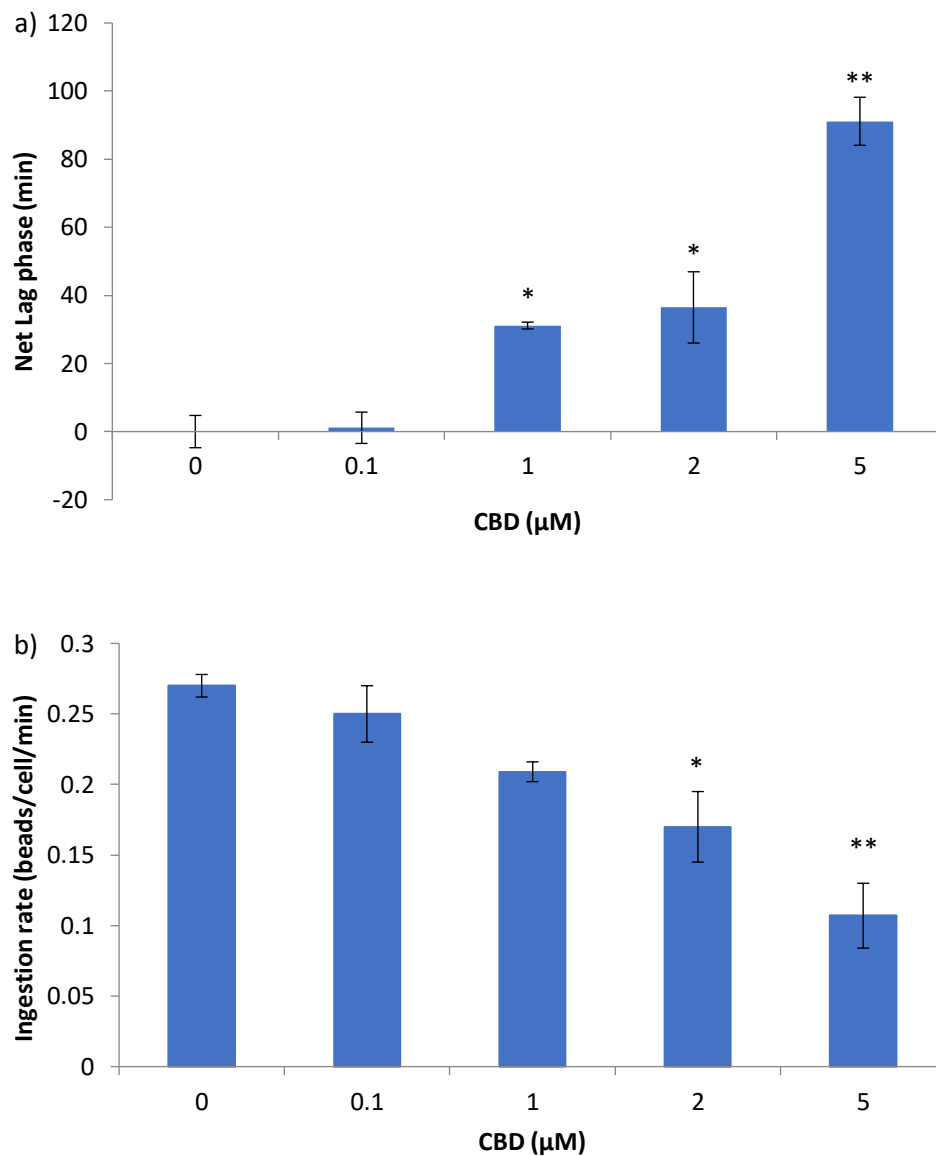


Figure 4.4: Effect of CBD concentration (0.1-5.0 μ M) on a) the feeding lag (min) and b) subsequent ingestion rates (beads/cell/min) of *Vermamoeba vermiformis* CCAP1534/14 feeding on beads. Significant difference to Control, *= $P<0.05$ **= $P<0.01$.

Plotting the net lag phase against ingestion rate (Fig. 4.5) shows a strong inverse relationship, whereby the longer the lag the lower the subsequent ingestion rate. Data therefore suggest that the immediate negative effect of CBD is to stop feeding completely, i.e., induce a lag, then when feeding resumes it does so at a slower rate. A complete cessation in feeding could be due to CBD (i) blocking ingestion mechanisms such as feeding receptors and/or the formation of new phagosomes or, (ii) blocking the trafficking of phagosomes in the cell so that no membrane becomes recycled to form new phagosomes. The latter was tested first (see 4.2.3)

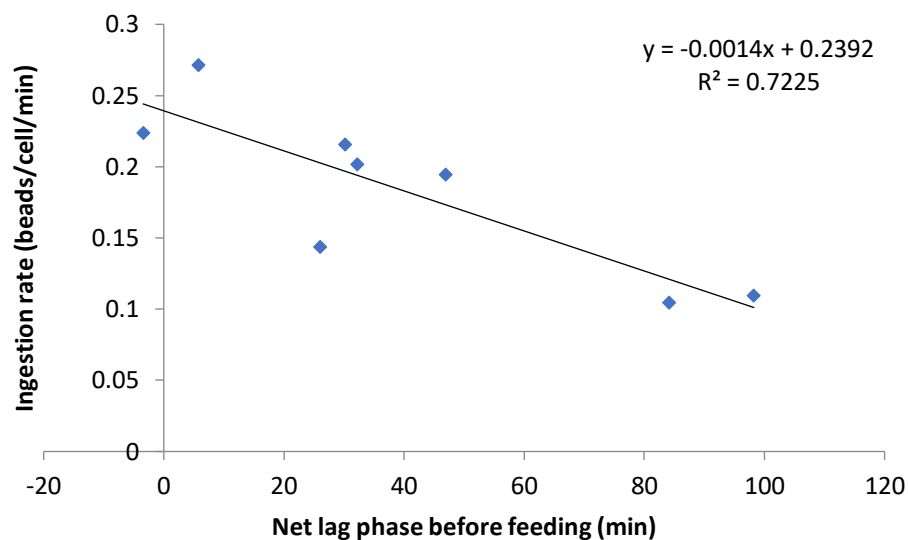


Figure 4.5: Relationship between the duration of a CBD-induced feeding lag and subsequent ingestion rate in *Vermamoeba vermiformis* CCAP1534/14 feeding on beads.

4.2.3. Effect of CBD on phagosome trafficking within *V. vermiformis*

Pulse-chase experiments were performed three times, using beads as the prey, in the absence and presence of CBD at 2 μ M (see 2.6). This CBD concentration yields a *ca.* 36 min lag in feeding (Fig. 4.4a). During the first 10 min (no CBD in either treatment), ingestion of the beads was evident and by 10 min *V. vermiformis* CCAP1534/14 cells contained *ca.* 23 beads. At 10 min, both treatments were diluted (to prevent further uptake of beads) and CBD was added to one treatment (Test). The loss of beads in pre-formed phagosomes over time was then monitored. If CBD stopped phagosome processing and defecation inside the cell for *ca.* 36 min the graphical response would mirror that shown by the orange dotted line (Fig. 4.6). It did not. And although the presence of CBD appeared to ‘empty’ the amoeba of beads quicker

than the Control, with defecation rates of 4.17 ± 0.46 and 3.74 ± 0.37 beads/cell/min for Test and Control respectively, these rates were not significantly different ($P=0.50$). It therefore appears that CBD does not affect the trafficking and defecation of phagosomes, so attention turned to its potential effect on the ingestion process.

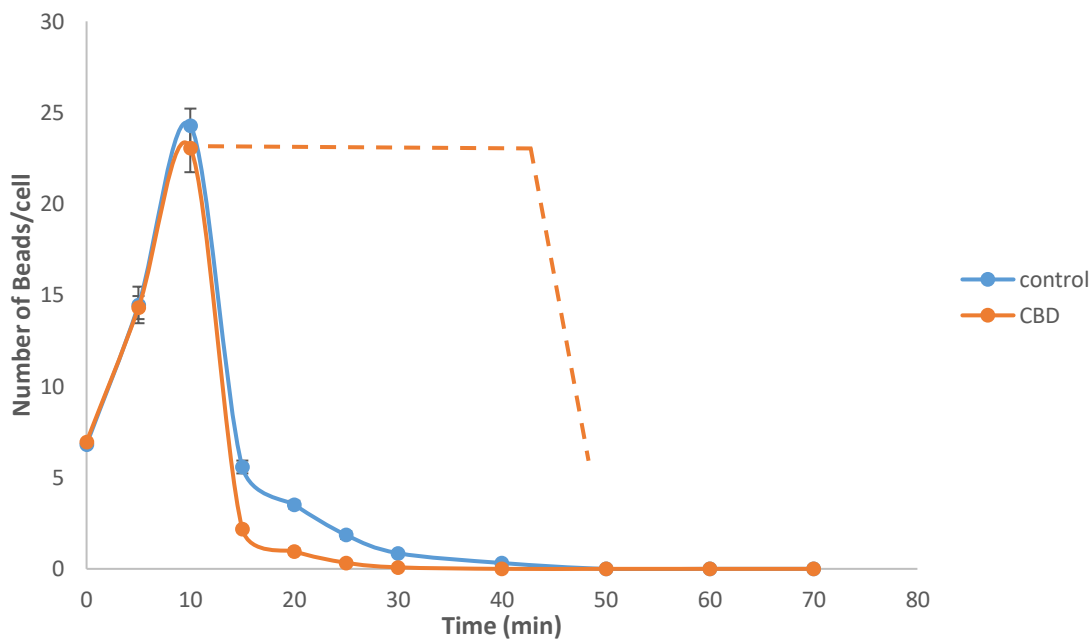


Figure 4.6: Effect of CBD on the defecation of beads in phagosomes formed over the first 10 min in *Vermamoeba vermiformis* CCAP1534/14. The amoeba was diluted at 10 min and CBD ($2\mu\text{M}$) added to one treatment. If CBD halted phagosome trafficking and defecation, the loss of beads would begin at ca. 46 min; it did not. Experiment repeated three times.

4.2.4. Interaction between CBD and the feeding receptors of *V. vermiformis*

V. vermiformis CCAP1534/14 was incubated for 20 min with 100mM of D (+)-mannose, N-Acetyl-D-glucosamine (GlcNAc) or N-Acetyl-D-galactosamine (GalNAc), to block C-type lectins, before performing feeding experiments with *Synechococcus* in the absence and presence of CBD ($2\mu\text{M}$) (see 2.5.5). These experiments were performed three times (Fig. 4.7). Any feeding lag exhibited by the Control was subtracted from Test lag times to provide net lag times (Table 4.1).

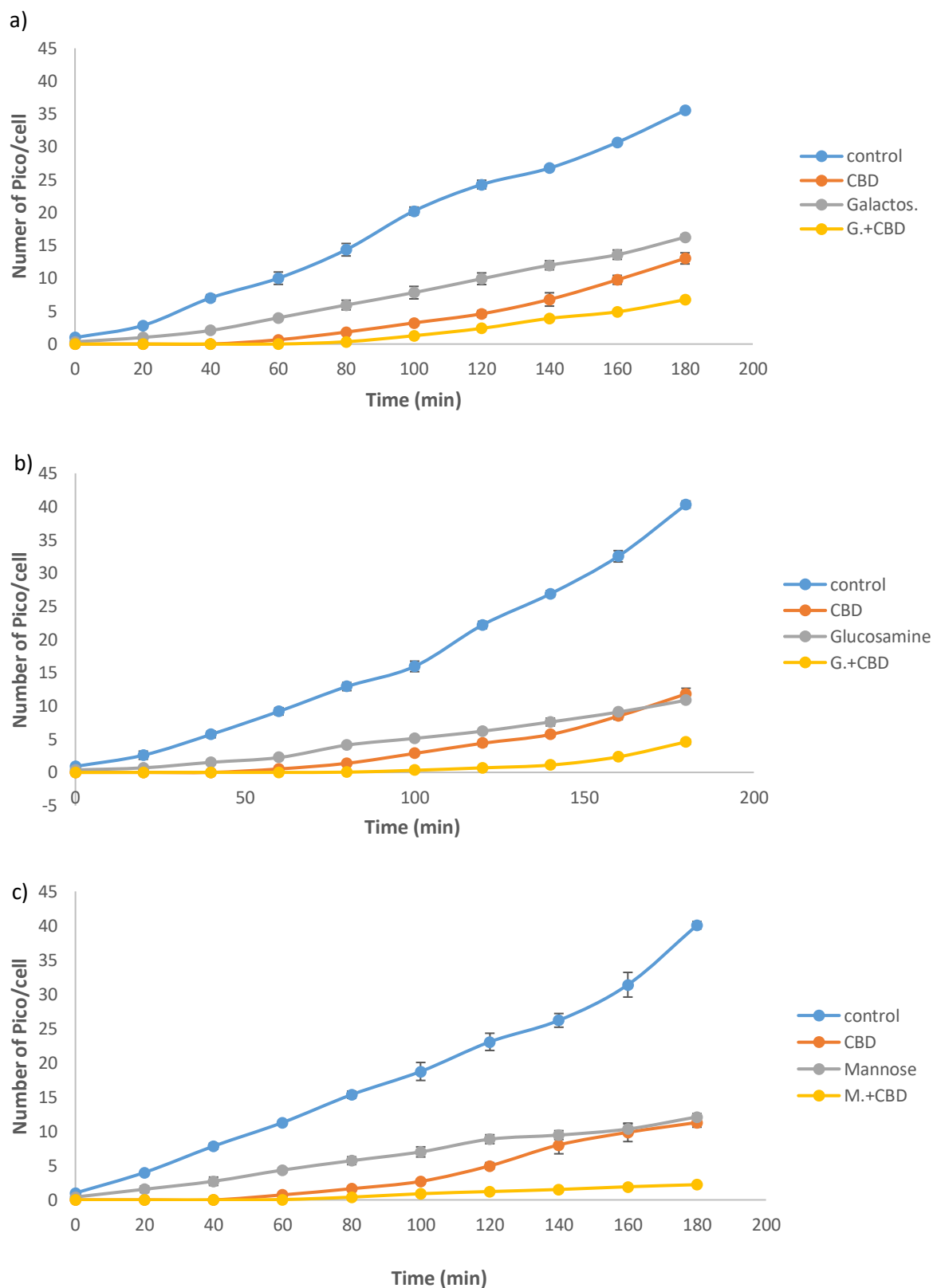


Figure 4.7: Feeding of *Vermamoeba vermiformis* CCAP1534/14 on *Synechococcus* (Pico) in the absence (Control) and presence of CBD (at 2 μ M) with/without a 20-minute pre-incubation with a) GalNAc b) GlcNAc and c) mannose (100mM). Feeding in the presence of the sugar alone is also shown.

CBD alone caused a significant lag which was quite variable (50.32-74.41 min) (Table 4.1) but the subsequent ingestion rates were less variable (0.104-0.112 pico/cell/min) (Table 4.1). These ingestion rates were significantly lower (by 44-58%) than those of the Controls (P<0.01).

The presence of the sugars alone caused no significant lag phase but did significantly reduce ingestion rate (Table 4.1) suggesting that all three are involved in the feeding process of this amoeba. The presence of GalNAc, GlcNAc and mannose significantly (P<0.01) reduced prey ingestion rate by 53%, 73% and 66%, respectively (compared to the Control). GalNAc alone reduced ingestion rate to the same level as CBD alone (P=0.25) while GlcNAc and mannose alone caused a significantly lower ingestion rate than with CBD alone (P<0.01).

Table 4.1: Feeding lags (min) and subsequent ingestion rates (prey/cell/min) of *Vermamoeba vermiformis* CCAP1534/14 feeding on *Synechococcus* in the presence/absence of CBD (2µM) with/without a 20-minute pre-incubation with a sugar (GalNAc, GlcNAc or mannose) at 100mM. Significant difference (P<0.05) to *Control, "sugar alone, ^CBD alone.

Sugar/Parameter	Control	CBD alone	Sugar alone	Sugar then CBD
GalNAc				
Net lag phase (min)	0	65.62±11.51**	11.02±1.06	74.61±6.39**
Ingestion rate (prey/cell/min)	0.205±0.004	0.112±0.022*	0.096±0.006*	0.065±0.007*^
GlcNAc				
Net lag phase (min)	0	50.32±7.71**	0	101.25±3.48**^
Ingestion rate (prey/cell/min)	0.247±0.014	0.104±0.007**	0.066±0.001*^	0.087±0.010*
Mannose				
Net lag phase (min)	0	74.41±7.70**	5.71±4.21	53.38±5.88**
Ingestion rate (prey/cell/min)	0.190±0.012	0.106±0.009**	0.065±0.003*^	0.018±0.001**^

The effect of pre-incubating the amoeba with sugars, and then adding CBD, differed with each of the sugars (Fig. 4.7). The CBD-induced lag phase was not affected by pre-incubating with GalNAc (P=0.76) or mannose (P=0.44) (Table 4.1) but it was significantly (P<0.01) increased (2-fold) upon pre-incubation with GlcNAc (Table 4.1).

Addition of CBD had no effect on the ingestion rates of GalNAc- and GlcNAc-pre-treated cells as rates (with CBD) were equivalent to those in the presence of the sugar alone (P=0.35, P=0.81, respectively) (Table 4.1). However, addition of CBD to mannose-pre-treated cells significantly (P<0.05) reduced ingestion rate compared to both mannose alone and CBD alone (Table 4.1).

To summarise, all three sugar treatments significantly reduced the ingestion rate of *V. vermiformis* to varying degrees (GlcNAc [by 73%], mannose [by 66%], GalNAc [by 53%]) but none induced a lag phase. A lag phase was *only* induced in the presence of CBD and pre-blocking the GalNAc and mannose receptors had no effect on its duration whereas blocking the GlcNAc receptor doubled its duration. CBD did not affect the ingestion rates of GalNAc- and GlcNAc-pre-treated cells but did significantly reduce that of mannose-pre-treated cells.

4.3. Discussion

4.3.1. Effect of particle type on *V. vermiformis* ingestion rates

V. vermiformis CCAP1534/14 was able to successfully ingest 0.49 μ m diameter beads (0.065 μ m³ volume) and live *Synechococcus* S-KH3 cells (1.04 μ m³ volume, Dillon and Parry, 2009) at equivalent rates (Fig. 4.1). In these, and subsequent experiments (see later Chapters), ingestion rates only ranged from 0.17 to 0.28 prey/cell/min (or 11.4-16.8 prey/cell/h) irrespective of particle type (at 3×10^7 particles/cm², 23°C); further suggesting no effect of prey type.

These rates are within the range of some previously published ingestion rates (Table 4.2), although data are scarce on the ingestion of *Synechococcus*. However, one study (Dillon and Parry, 2009) recorded an ingestion rate of 1.68 prey/cell/h when *Echinamoeba* sp. fed on *Synechococcus* S-KH3 (at 1×10^7 cells/cm², 23°C), which is the same prey used in the current study. Their ingestion rate is lower than that obtained here with *V. vermiformis* CCAP1534/14 which might be due to their lower prey concentration and/or the smaller size of *Echinamoeba* (7-21 μ m) compared to *V. vermiformis* (14 x 31 μ m) (Table 3.4).

The author cannot find a study which has directly compared the ingestion rates of beads versus live prey in amoebae. However, such studies have been performed with other protists, with differing results. Some studies have shown that ciliates and flagellates ingest beads at a lower rate than live or heat-killed bacteria (Sherr et al., 1987; Nygaard et al., 1988; Jürgens and Šimek, 2000; Boenigk et al., 2001a; Parry et al., 2001) while other studies have shown they are consumed at equivalent rates (Sherr et al., 1987; Dolan and Šimek, 1997; Boenigk et al. 2001b).

Table 4.2: Published ingestion rates (IR) of various amoebae. Adapted from Rogerson et al., 1996; Butler and Rogerson, 1997; Mayes et al., 1997; Heaton et al., 2001; Huws et al., 2004, Xinyao et al., 2006; Pickup et al., 2007; Dillon and Parry, 2009.

Amoeba	Bacterial prey	Bacterial Concentration	Temperature (°C)	IR (prey/cell/h)
<i>Platyamoeba australis</i>	Gram -ve	4-350x10 ⁶ cells/ml	4	1.2-28.6
Isolate 5	Gram -ve	4-350x10 ⁶ cells/ml	4	0.86-34.59
<i>Platyamoeba</i> sp.	<i>Planococcus</i>	2.5x10 ⁸ cells/ml	20	0.2
<i>Vahlkampfia damariscottae</i>	<i>Planococcus</i>	2.5x10 ⁸ cells/ml	20	9.7
<i>Vannella caledonica</i>	<i>Planococcus</i>	2.5x10 ⁸ cells/ml	20	2.2
<i>Trichosphaerium sieboldi</i>	<i>Planococcus</i>	ca 1.4x10 ⁷ cells/cm ²	20	1465
Unidentified filose	<i>Planococcus</i>	ca 1.4x10 ⁷ cells/cm ²	20	10
<i>Stereomyxa ramose</i>	<i>Planococcus</i>	ca 1.4x10 ⁷ cells/cm ²	20	111
<i>Saccamoeba limax</i>	<i>Escherichia coli</i>	7x10 ⁶ cells/cm ²	20	58
<i>Hartmannella cantabrigiensis</i>	<i>E. coli</i>	7x10 ⁶ cells/cm ²	20	243
<i>Vermamoeba vermiformis</i>	<i>E. coli</i>	1x10 ⁶ cells/cm ²	20	139
<i>Acanthamoeba castellanii</i>	<i>E. coli</i>	1x10 ⁶ cells/cm ²	20	964
<i>Echinamoeba</i> sp.	<i>Synechococcus</i> spp.	1x10 ⁷ cells/cm ²	23	0.6-2.9
<i>Acanthamoeba</i> sp.	<i>Synechococcus</i> spp.	1x10 ⁷ cells/cm ²	23	7.6-14
<i>Naegleria</i> sp.	<i>Synechococcus</i> sp.	?	28	5.6
<i>Naegleria</i> sp.	<i>Anacystis nidulans</i>	?	28	136
<i>Naegleria</i> sp.	<i>Microcystis aeruginosa</i>	?	28	3.3
<i>Naegleria</i> sp.	<i>Aphanocapsa elachista</i>	?	28	8.3

4.3.2. Effect of AEA on the feeding of *V. vermiformis*

AEA (2µM) was found to have no significant effect on the feeding of *V. vermiformis* CCAP1534/14, even though a slight lag was evident in its presence (Fig. 4.2). And, although it was removed from the current feeding studies there may be merit in revisiting this because the AEA concentration might have been too low to give a significant result. A concentration of 2µM AEA and CBD was chosen as this value was close to their IC₅₀ values and would allow

a direct comparison of their effect. But, 2 μ M is above the IC₅₀ for CBD (IC₅₀ = 1.01 μ M) and below the IC₅₀ for AEA (IC₅₀ = 2.33 μ M) (Table 3.3). Experiments should be repeated with higher concentrations of AEA to confirm/deny any effect on feeding in this amoeba.

4.3.3. Overall effect of CBD on the feeding of *V. vermiformis*

CBD (at 2 μ M) induced a significant feeding lag followed by a reduced ingestion rate when *V. vermiformis* CCAP1534/14 fed on beads (Fig. 4.4) and *Synechococcus* (Table 4.1). The effect of CBD was dose-dependent, with the lag being induced at a lower CBD concentration (1 μ M) then the reduction in feeding (2 μ M) (Fig 4.4); a response also recorded with population growth (Fig. 3.1). A longer lag resulted in lower ingestion rates (Fig. 4.5); implying there are connected in some way. It also suggests that the effect of CBD is long-lasting; >260 min at 5 μ M. This contrasts to the response of the ciliate *Tetrahymena pyriformis*, whereby the effect is relatively short-lived; 40-60 min at 4 μ M (Parry, personal communication).

It is unknown whether these protists differ in their ability to degrade CBD, which might affect its longevity in their cells. In all human cells, CBD is metabolised by cytochrome P450 oxidases, sulfotransferases and glucuronyl transferases (Ujváry and Hanus, 2016). Most work has been performed on P450 oxidases (CYPs) which are enzymes necessary for the metabolism of drugs (Šrejber et al., 2018). Even though more than 50 CYP enzymes exist, only six of them (CYP1A2, CYP2C9, CYP2C19, CYP2D6, CYP3A4, and CYP3A5) are responsible for metabolising 90% of medicinal drugs (Lynch and Price, 2007). Of these, CYP2C9 metabolises THC and CBN, CYP2C19 metabolises CBD, and CYP3A4 can metabolise all three (Stout and Cimino, 2014). Interestingly, *Tetrahymena thermophila* possesses 102 CYP homologues (www.ciliate.org), the slime mould *Dictyostelium discoideum* possesses 9 (www.dictybase) whilst *Acanthamoeba castellanii* possesses only 1 and *Entamoeba* spp. and *Naegleria fowleri* possess none (www.amoebadb.org). None of the above protists possess glucuronyl transferases but they all possess sulfotransferases, although there is very little information on the latter with regards to metabolism of CBD/THC (Ujváry and Hanus, 2016). Therefore, it might be that *V. vermiformis*, like other amoebae, possesses a limited ability to degrade CBD within their cells and this might explain the longevity of the drug action on *V. vermiformis*, compared to *T. pyriformis*.

Whether CBD is metabolised or not, amoebic feeding was affected by this phytocannabinoid, but which stage of the feeding process was being targeted (Fig. 4.8 [same as Fig. 1.9 but inserted here to accompany the discussion of each stage]).

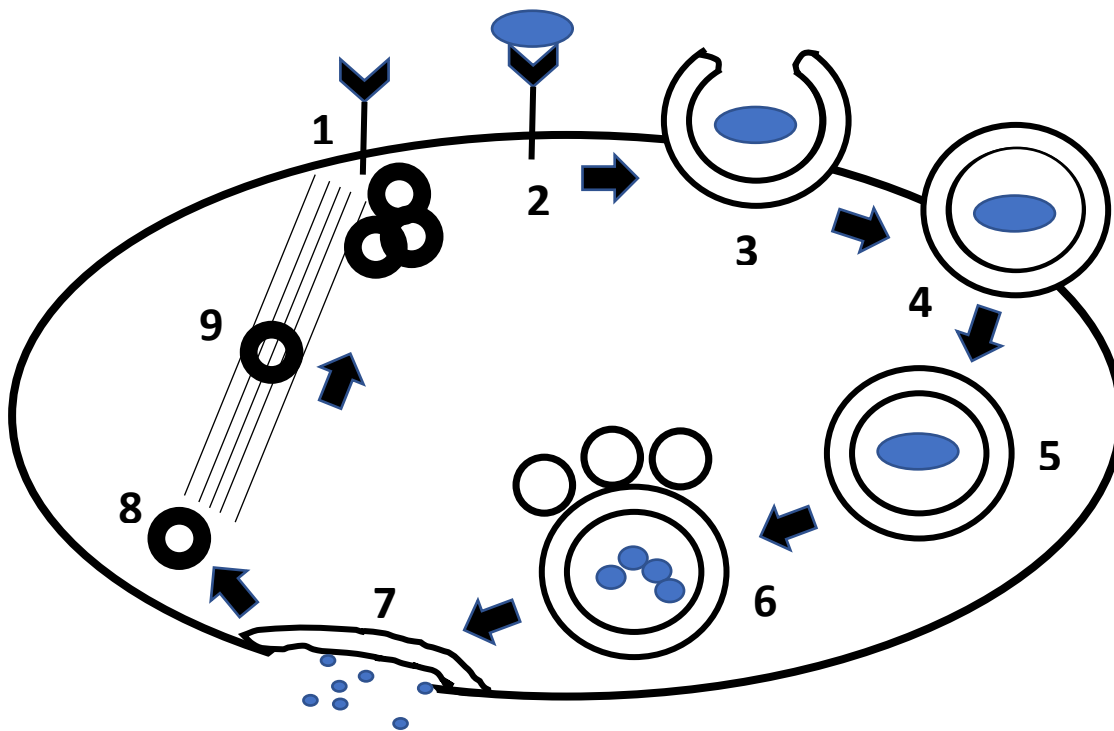


Figure 4.8: Diagrammatic representation of membrane dynamics in the phagocytic cycle. 1) Receptors and membrane are available for prey uptake and phagosome formation. 2) Binding of prey to receptors (e.g. C-type lectins) leads to 3), actin polymerisation and formation of pseudopodia which surround the prey. 4) Myosin is recruited to help seal the ends of the pseudopods together. 5) Dynamin is recruited to allow detachment of the phagosome into the cytoplasm. 6) The phagosome matures via a series of fusions with endosomes and lysosomes and the contained material is digested. 7) Phagosome membrane fuses with the plasma membrane and releases undigested material. 8) Plasma membrane is endocytosed to form vesicles. 9) Vesicles are transported to the site of phagocytosis by microtubule ribbons and used to form new phagosomes. Stages 3 to 7 are known to be reliant on activation of the Arp2/3 system.

4.3.4. Effect of CBD on phagosome trafficking and defecation (Fig. 4.8, stages 6-7)

Pulse-chase experiments with *V. vermiformis* CCAP1534/14 showed that CBD did not affect the processing of pre-formed phagosomes (Fig. 4.8, stages 6-7), i.e., they were trafficked through the cell and defecated at the same rate as the Control (Fig. 4.6). The vacuole passage time (VPT) was less than 10 min, as demonstrated by an immediate loss of prey from the cell

upon the chase at 10 min. Published VPTs are rare for comparison, but Thurman and Parry (2010) reported that the VPT in the ciliate *T. pyriformis*, feeding on *Synechococcus* sp. S-KH5, was variable but that the minimum VPT was 30 min. Ciliates possess a single rudimentary mouth (cytostome) at one end of the cell, where all the ingestion of prey takes place, and a single rudimentary anus (cytoproct) at the other end of the cell, where undigested material is expelled from the cell. Because phagosomes travel along the whole length of the cell, it will take time, and because there is only one exit point, pre-formed phagosomes have to queue before their contents are expelled which results in variable VPTs (Thurman and Parry, 2010). Amoebae, on the other hand, have no defined cytostome and cytoproct and appear to ingest and defecate prey at any point in their outer membrane (Page, 1988), which might explain their shorted VPT. However, the slime mould *D. discoideum* exhibited a VPT of 80 min when feeding on the yeast *Cryptococcus neoformans* (Watkins et al. 2018).

The lack of effect of CBD on phagosome trafficking and defecation (Fig. 4.8, stages 6-7) mirrors the results obtained with *T. pyriformis* (Parry, personal communication), and suggests that CBD's target is something involved with the initial stages of prey ingestion. The potential target(s) could be, (i) prey capture (Fig. 4.8, stages 1-2), (ii) formation of the phagosome (Fig. 4.8, stages 3-5) and/or, (iii) phagosome membrane recycling after defecation (Fig. 4.8, stages 8-9). Separating these out is difficult as if just one of these processes fails, no ingestion of prey takes place; and this is what was measured in all experiments (as prey/cell).

4.3.5. Effect of CBD on phagosome formation (Fig. 4.8, stages 3-5)

Upon prey-receptor binding, actin polymerisation is activated and two pseudopodia extend out from the cell to surround the prey particle. Myosin is then recruited to help seal the ends of the pseudopods together and then the recruitment of dynamin leads to the detachment of the phagosome from the cell surface to the cytoplasm (Levin et al., 2016). The whole process (and indeed phagosome trafficking [Duleh and Welch, 2010]) is reliant on activation of the Arp2/3 system (Seven-transmembrane-actin-related proteins 2 and 3) which itself is activated via a plethora of molecules and signalling cascades (Levin et al. 2016) (discussed further in Chapter 5).

Phagosome formation therefore appears to use the same cytoskeletal machinery, and the same Arp 2/3 complex, as that used for phagosome trafficking and defecation, which were *not* affected by CBD in *V. vermiformis* CCAP1534/14. This implies that at least the machinery for phagosome formation might have been fully functional in the presence of CBD in this amoeba. In addition, CBD is known to become incorporated into the plasma membrane of cells and increase membrane fluidity (Watkins, 2019). Increased membrane fluidity, by decreasing the saturated:unsaturated fatty acid ratio, has been shown to increase phagocytosis in both macrophages (Schumann, 2016) and *A. castellanii* (Avery et al., 1995). Thus, one might have expected an *increase* in feeding in the presence of CBD, with functional machinery present, but this was not recorded. However, even functional machinery would only be able to form phagosomes if the prey recognition receptors were fully functional and/or there was enough membrane available at the site of prey-receptor binding.

4.3.6. Effect of CBD on phagosome membrane recycling (Fig. 4.8, stages 8-9)

The constant recycling of phagosome membrane in ciliates is essential to ensure membrane availability for newly developing phagosomes (Allen, 1974). Ciliates use ‘direct recycling’, i.e., no involvement of the lysosomal or Golgi systems on the vesicle’s journey from the cytoproct to the cytostome (Allen and Fok, 1980; Goff and Stein, 1981; Grønlien et al., 2002).

It is currently unknown whether direct recycling occurs in amoebae but a membrane recycling process has been shown to be imperative for the correct formation of pseudopodia (for locomotion) in *D. discoideum* (Zanchi et al. 2010). Here, SecA mutants (with no ability to defecate) became paralysed within minutes and cells shrunk in size. This was because the block in defecation resulted in a net endocytosis of plasma membrane and an accumulation of small vesicles that remained close to the plasma membrane. This ultimately reduced the outer cell membrane area, reducing cell size and restricting pseudopodia expansion (Zanchi et al. 2010). This does imply then, that membrane recycling would also be imperative for phagosome formation, as expansion of pseudopodia around a particle is part of the process (Fig. 4.8). If this recycling was somehow affected by CBD, there would be limited membrane available for the functional cytoskeletal machinery to form phagosomes.

Observations of CBD-treated *V. vermiformis* CCAP1534/14 cells in feeding experiments did not show an obvious difference in cell size between the Control cells and those treated with CBD. No difference in cell size has also been recorded for Control and CBD-treated *T. pyriformis* cells (Parry, personal communication). In both cases, the CBD-treated cells of these protists would have been defecating normally (known from pulse-chase experiments) and thus, constantly adding membrane to the outer plasma membrane. If subsequent endocytosis (Fig. 4.8, stage 8) was blocked (with no phagocytosis was taking place) the cells would be expected to *increase* in size; but they did not. So, endocytosis might therefore be functional and, in the presence of CBD, the cell size would not be expected to change (which was recorded). But this lack of cell size change does not clarify whether the endosomes remain at the site of defecation or whether they are transported to the site of new phagocytosis, i.e., whether the transport system is functional (Fig. 4.8, stage 9), as cell size would not change in either case. However, with such little published information on stage 9 it is difficult to discuss this further.

4.3.7. Pre-phagosome membrane availability at the site of phagocytosis (Fig. 4.8, stage 1)

An observation made throughout the current study was that the CBD-induced lag phase durations in *V. vermiformis* CCAP1534/14 were highly variable *between* experiments. This has also been observed with *T. pyriformis* (Parry, personal communication) possibly indicating that CBD's target is highly variable in the cells at the start of an experiment. This might be due to the amount of membrane available at the site of phagocytosis. For example, in well-fed cells the majority of membrane might already be used up in pre-existing phagosomes, leaving only a small volume for new phagosomes; which would be demonstrated by a low ingestion rate in Control cells. Conversely, if the cell is 'empty' of pre-existing phagosomes, there would be more membrane available for new phagosomes (yielding a high ingestion rate in Control cells). Indeed, others have observed that starved cells feed faster than well-fed cells and the accepted explanation is that it is due to variations in the nutritional and physiological conditions of the protist at the start of the experiment (Boenigk et al., 2001).

Although *V. vermiformis* was prepared in the same way for each experiment (grown to stationary phase for 7 days on a streak of *E. coli*), these cells would *not* be *exactly* the same between experiments and their membrane availability for phagocytosis might have differed.

Indeed, ingestion rates of *V. vermiformis* Control cells ranged from 0.17 to 0.28 prey/cell/min, with 3×10^7 prey/cm², which is not a great deal but does suggest that membrane availability might have been different at the start of each experiment. When these ingestion rates (as a proxy for membrane availability) are plotted against the lag phase duration in corresponding CBD-treated cells, there is a *small* trend towards shorter CBD-induced lag times occurring when *more* membrane is available. This is opposite to what was expected, but it might be suggesting a dose-response at the molecular level whereby binding of CBD to a larger area of nascent phagosome membrane might be diluting its effectiveness. However, this is just speculation at present.

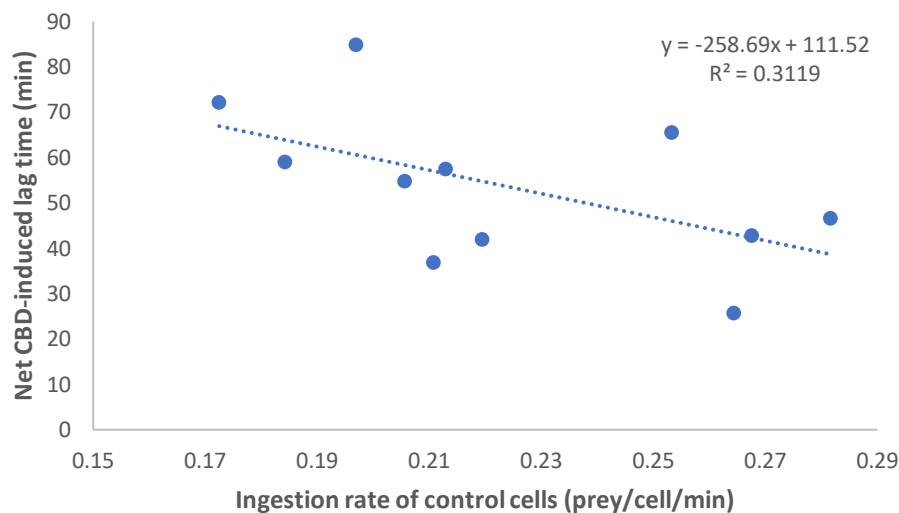


Figure 4.9: Relationship between ingestion rate of Control *Vermamoeba vermiformis* CCAP1534/14 cells (as a proxy for the level of membrane available in the cells for the formation of phagosomes) against the length of a 2µM-CBD-induced lag phase (min). High ingestion rate is a proxy for low membrane availability and *vice versa*.

4.3.8. Effect of CBD on receptor-mediated prey uptake (Fig. 4.8, stages 1-2)

4.3.8.1. Prey uptake in the absence of CBD

Previous studies have shown that C-type lectins are involved in the ingestion of prey by amoebae, particularly lectins for mannose (Bracha et al., 1982; Allen and Davidowicz, 1990; Garate et al. 2004; Alsam et al., 2005) and GalNAc (Ravdin and Guerrant, 1981; Ravdin et al., 1985; Petri et al., 1987; Venkataraman et al., 1997; Harb et al., 1998; Bär et al., 2015). The

current study found that ingestion of *Synechococcus* by *V. vermiformis* CCAP1534/14 was reduced in the presence of mannose, GalNAc and GlcNAc, but no lag phase was induced. GlcNAc was the most potent sugar blocker (73% reduction in feeding), followed by mannose (66% reduction) and then GalNAc (53% reduction). This might suggest that either, (i) this amoeba possesses three distinct receptors for these sugar ligands, as does *D. discoideum* (Bozzaro & Roseman, 1983) or, (ii) it might only have only two receptors (mannose and GalNAc), as do professional phagocytes, because although the mannose receptor preferentially binds mannose (and fucose) it can, to a lesser extent, bind GlcNAc (Largent et al., 1984; Lobst and Drickamer, 1994; Roseman and Baenziger, 2000).

The binding of GlcNAc led to the strongest inhibition of ingestion in *V. vermiformis* suggesting it was not only binding 'weakly' to a mannose receptor but also/instead binding 'strongly' to its own receptor. In addition, blocking with GlcNAc affected the duration of the CBD-induced lag phase whereas blocking with mannose did not (Table 4.1). These data therefore support the case for three distinct sugar receptors in *V. vermiformis*, as has been suggested for *D. discoideum* (Bozzaro & Roseman, 1983) and more recently, for *T. pyriformis* (Boboc, 2019).

The location of carbohydrate-binding receptors in cells can be visualized with fluorescent derivatives of plant lectins such as ConcanavalinA (ConA) which binds D-mannose (Goldstein et al., 1965), wheat germ agglutinin (WGA) which binds GlcNAc (Wright, 1992), and peanut agglutinin (PNA) which binds GalNAc (Macartney, 1986). A handful of studies have used such techniques to detect these receptors in ciliates and dinoflagellates. The mannose receptor has been shown to be associated with the whole feeding process, i.e., prey capture, phagosome formation, phagosome trafficking, defecation and membrane recycling (Scott and Hufnagel, 1983; Wilks and Sleight, 2004; Roberts et al., 2006; Wootton et al., 2007; Dürichen et al., 2016). Wilks and Sleight (2004) showed a distinct series of events of ConA staining in *Euplotes mutabilis*, starting with the staining of the cytostome only, then simultaneous staining of the cytostome and phagosomes, then staining of the phagosomes only, followed by no staining. In *T. pyriformis*, the mannose receptor has been shown to affect phagosome trafficking by detecting the nature of the internalised prey, i.e., inducing early exocytosis or full trafficking (Dürichen et al., 2016) and has also been shown to be important in defecation (preventing membrane defecation alongside the cargo) and the endocytosis of plasma membrane at the cytoproct (Scott and Hufnagel, 1983).

Staining ciliates with WGA (binds to GlcNAc) has shown it to be associated with early phagosomes near the cytostome (Wilks and Sleigh, 2004; Dürichen et al., 2016). In *T. pyriformis*, WGA bound to patches of these early phagosome membranes whereas ConA bound to the whole membrane (Dürichen et al., 2016). Its role in prey capture is less clear as Wilkes and Sleigh (2004) detected WGA binding at the cytostome of *E. mutabilis* but Roberts et al. (2006) and Dürichen et al. (2016) did not detect cytostome binding in *Euplotes vannus* and *T. pyriformis*, respectively. With regards to GalNAc, Roberts et al. (2006) found that the binding of PNA occurred only in the phagosomes of *E. vannus* whereas Wilks and Sleigh (2004) recorded binding at the cytostome in addition to phagosomes of *E. mutabilis*.

4.3.8.2. Prey uptake in the presence of CBD

The most striking feature of CBD was its ability to completely arrest feeding in *V. vermiformis* CCAP1534/14 for 50-74 min; but *not* arrest subsequent phagosome trafficking. Addition of mannose, GalNAc and GlcNAc alone did not induce such a lag phase suggesting that these are *not* the receptors involved in inducing a lag. Pre-blocking cells with mannose or GalNAc prior to adding CBD did not affect this CBD-induced lag suggesting no interaction with CBD. Indeed, receptors for both GalNAc and mannose are associated with the full life-span of a phagosome (Wilkes and Sleigh, 2004; Roberts et al., 2006; Dürichen et al., 2016), and the mannose receptor itself is important for defecation and membrane recycling (Scott and Hufnagel, 1983), yet the trafficking and defecation of these phagosomes were not affected by CBD; further suggesting no interaction between these receptors and CBD.

The GlcNAc receptor on the other hand, is not associated with mature phagosomes and defecation and is only associated with newly formed phagosomes at the cytostome (Wilkes and Sleigh, 2004; Dürichen et al., 2016). When GlcNAc was added to *V. vermiformis* prior to the addition of CBD, the lag phase was doubled, suggesting some level of interaction between the GlcNAc receptor and CBD during the stage of phagosome formation. The GlcNAc receptor itself appeared to be the dominant feeding receptor in *V. vermiformis*. When it was blocked, feeding was reduced by 73% compared to the blocking of the mannose and GalNAc receptors which reduced feeding by 66% and 53%, respectively. However, it is unknown whether the GlcNAc was binding to the GlcNAc receptor alone, or whether it was also binding weakly to the mannose receptor (to yield a cumulative 73%

reduction in feeding). Addition of CBD after blocking with GlcNAc did not affect this reduced feeding rate.

One could therefore make an initial assumption that CBD might possibly be binding to the GlcNAc receptor (to cause a reduction in feeding rate) and to a yet unidentified 'other' receptor (to cause a lag). When both receptor types are available, CBD binds to both and causes a 50 min lag with a 53% reduction in feeding. When the GlcNAc receptor is blocked with GlcNAc, CBD can only bind to the 'other' (giving a longer lag) and the reduction in feeding is due to GlcNAc binding to the GlcNAc receptor. However, this is *highly* speculative and there is already evidence against this theory.

Firstly, there is no evidence to date that C-type lectins can bind cannabinoids. Secondly, if CBD does not bind to the GalNAc or mannose receptors (as hypothesised) it would only be able to bind to the 'other' receptor and this should have yielded a lag of 100 min, but it did not. Thirdly, a CBD-induced lag (and reduced feeding) was recorded when the prey were polystyrene beads and these do not possess surface carbohydrate moieties for recognition by C-type lectins. Indeed, the mannose receptor has been shown *not* to be involved in the uptake of beads in *A. castellanii* (Allen and Davidowicz, 1990); no data on GlcNAc and GalNAc receptors.

However, in slight defense of the theory, there is some evidence that C-type lectins can bind lipids (Cummings and McEver, 2006). For example, the macrophage inducible C-type lectin (Mincle) typically binds mannose and glucose residues but possesses hydrophobic pockets which can bind lipids (Chiffolleau, 2018). To the authors knowledge, no-one has actually tested whether cannabinoids can bind to C-type lectins so it is not known for certain whether they can or not. There have also been a couple of reports of C-type lectins being involved in the uptake of beads in professional phagocytes, via hydrophobic interactions, specifically the mannose receptor (Ichinose and Sawada, 1996) and the GlcNAc receptor (Shinzaki et al., 2016); no reports of the GalNAc receptor being involved.

4.3.9. Working hypothesis on how CBD affects feeding in *V. vermiformis*

A hypothesis is proposed whereby CBD *only* binds to 'another' receptor and *does not* bind to the GlcNAc receptor. It does however require an acknowledgement that the process of

phagosome formation *is not* necessarily controlled by those receptors that capture prey and move them into the phagosome. To the author's knowledge, this has not been properly discussed in the literature to date and 'ingestion rate' has been used as an all-encompassing term which combines both processes. Here, we separate them out and suggest that the receptors for CBD and GlcNAc are involved with phagosome formation whereas receptors for mannose and GalNAc are involved with prey capture and phagosome filling.

It is proposed that CBD *only* binds to a yet unidentified receptor which firstly stops phagosome formation completely and then causes phagosome formation to proceed at a slower rate than normal, i.e., at *ca.* half the rate seen in Control cells. Even though C-type lectins, which do not bind CBD, may have bound many prey cells, they can only fill the phagosome at the same rate at which it is being formed; so CBD is governing overall 'ingestion rate'. Now, if any of these C-type lectins are blocked by their respective sugar there will be less prey captured and phagosomes will be filled with less prey. If this is coupled with a reduced phagosome formation rate due to the presence of CBD, one would expect a *synergistic negative* effect on ingestion rate, and this is what was observed when the mannose and GalNAc receptors were blocked (Table 4.1). Ingestion rates for cells treated with both the sugar and CBD were significantly lower than rates with CBD alone in both cases, and lower than rates with the sugar alone (but this was only significant for mannose, Table 4.1).

As for the GlcNAc receptor, it is proposed that this is predominantly involved in controlling phagosome *formation rate*. When blocked with GlcNAc, no lag was formed but the formation rate was reduced by 73% that of the Control; more so than with CBD alone (after its lag). In the presence of both GlcNAc and CBD there was a lag which was twice the duration of that with CBD alone, suggesting some level of synergistic negative effect on lag duration. However, it is proposed that the CBD-induced lag itself was not prolonged but that instead, the combination of a 73% reduction in phagosome formation rate (by blocking with GalNAc) together with a 50% reduction in rate due to the presence of CBD led to a phagosome formation rate that was *so* slow there was very limited ingestion occurring, and so it *appeared* as if the CBD-induced lag had been prolonged. Why after 100h this combined 'lag' was lost, and phagosome formation rate reverted to that equivalent to

blocking with GalNAc alone, is currently unclear as the action of CBD would be expected to persist as it did in experiments involving mannose and GalNAc.

A feature which lends weight to the GlcNAc receptor being specifically associated with phagosome formation is the observation of Dürichen et al. (2016) whereby WGA (for GlcNAc) bound to patches of early phagosome membranes whereas ConA (for mannose) bound to the whole membrane. This implies some level of specificity as to the location of GlcNAc receptors in phagosome membranes. It is also interesting that both Wilks and Sleight (2004) and Dürichen et al. (2016) *only* found GlcNAc receptors to be associated with early phagosomes, after which they disappeared (unlike mannose and GalNAc receptors). Where do GlcNAc receptors go? Are they recycled to nascent vesicles to help control the formation of new phagosomes?

As for the identity of the CBD receptor, this could be anything involved in stages 9 through to 5 (Fig. 4.8). However, further observations suggest it is not involved with stages 4 (phagosome closure) and 5 (phagosome detachment into the cytoplasm). The reason for this is that, *if* these were the targets, phagosomes would still have developed and become filled with prey, in the presence of CBD. This would have been observed and prey/cell counts would have increased; this was not the case.

With regards to phagocytic cup formation (Fig. 4.8, stage 3), it was noted that phagosome formation and trafficking utilise the same cytoskeletal machinery and considering the latter was unaffected by CBD it implied that *V. vermiformis* had the functional machinery in place to form phagosome. However, no evidence of phagocytic cup formation was recorded which might suggest that this machinery was *not activated* between stages 2 and 3 (Fig. 4.8). Actin polymerisation is reliant on activation of the Arp2/3 system which itself is activated via a plethora of molecules and signalling cascades; cascades which can differ depending on cytoskeletal function/location in the cell (Levin et al. 2016). So, because CBD stopped phagocytic cup formation (Fig. 4.8, stage 3), components of the signalling cascade *between* stages 2 and 3 continue to be a possible target for CBD.

4.4. Conclusions

V. vermiformis CCAP1534/14 was able to ingest inert beads and live *Synechococcus* at equivalent rates. These rates were reduced in the presence mannose, GalNAc and GlcNAc suggesting that this amoeba possesses three corresponding C-type lectins. It was proposed that the former two receptors are involved with prey capture and phagosome filling while the latter is involved with controlling phagosome formation rate.

AEA had no effect on *V. vermiformis* feeding but CBD induced a feeding lag (MIC <1 μ M) followed by a reduced ingestion rate (MIC <2 μ M). The longer the lag, the lower the subsequent ingestion rate suggesting they are coupled in some way. The long-term effect of CBD on *V. vermiformis*, compared to *T. pyriformis*, was thought to be due to a reduced capacity for metabolizing CBD within the amoebic cell (possibly due to the lack of CYPs).

It was proposed that CBD's target was not the C-type lectins but a yet unidentified receptor. Based on experimental evidence, this receptor was not considered to be involved in the following stages of feeding (Fig. 4.8): phagosome closure (stage 4), phagosome detachment (stage 5), phagosome trafficking (stage 6), phagosome defecation (stage 7) and endocytosis (stage 8). So, the current hypothesis is that CBD acts on a target between stages 8 and 3 (Fig. 4.8) and that it is involved in controlling phagosome formation rather than prey capture and phagosome filling. Further speculation now stops until additional evidence is obtained. In Chapters 5 and 6 the effects of blocking putative CBD receptors is performed to see if this eliminates the effects of CBD and which could offer clues as to the mechanism by which CBD affects amoebic feeding between stages 8 to 3.

Chapter 5: Involvement of Peroxisome Proliferator-Activated Receptors (PPARs) in the mode of action of CBD against *Vermamoeba vermiformis*

5.1. Introduction

The working hypothesis from Chapter 4 was that, at sub-lethal concentrations, CBD acts on *Vermamoeba vermiformis* CCAP1534/14 by binding to a yet unidentified receptor which leads to a complete cessation of ingestion followed by a reduced ingestion rate. It was considered that CBD acted on phagosome formation (along with the GlcNAc receptor), rather than prey capture and phagosome filling. Phagosome formation relies on effective membrane recycling to the site of phagocytosis (Fig. 4.8, stage 9), effective prey-receptor binding (Fig. 4.8, stages 1-2) and the activation of actin polymerisation via a signalling cascade (in-between stages 2 and 3), for the formation of the phagocytic cup (Fig. 4.8, stage 3). The target for CBD is considered to lie somewhere between these stages.

As for the identity of the CBD receptor, 11 receptors for CBD have been reported in the literature (Bih et al., 2015). Protists are already known *not* to possess homologues of the main receptors CB1, CB2, GPR55 and TRPV1 (McPartland et al., 2006), which reduces the number of potential receptors to seven, i.e., receptors for Nicotinic Acetylcholine, Adenosine, Glycine, Opioids, Serotonin, Dopamine, and Peroxisome Proliferation. Homologues of the latter, Peroxisome Proliferator-Activated Receptors (PPARs), have not been identified in protists to date *but* protists do possess peroxisomes (Ludewig-Klingner et al., 2017) and PPARs in animals are known to be involved in controlling their feeding behaviour (Romano et al., 2015; Satta et al., 2018). Since feeding in *V. vermiformis* was affected by CBD (in Chapter 4) these receptors were investigated first.

In animals, the predominant ligands for PPARs are the endocannabinoids Oleoylethanolamide (OEA) and Palmitoylethanolamide (PEA) (Sullivan, 2016). OEA and PEA are known to be synthesised by the ciliate *Tetrahymena thermophila* (Anagnostopoulos et al., 2010) and the slime mould *Dictyostelium discoideum* (Hayes et al., 2013). OEA has a strong anorexiant effect on mice, i.e., it can stop feeding completely and then reduce food intake; PEA is less potent than OEA and AEA has no effect on feeding at all (Rodríguez de Fonseca et al., 2001; Diep et al., 2011). The effect of OEA on mice is remarkably similar to the effect of CBD on *V.*

vermiformis, in that feeding completely stops and then resumes at a slower rate (and AEA has no effect) (Chapter 4). Although PPARs exist in three isoforms (α , β/δ and γ), OEA and PEA have highest affinities for PPAR α (Romano et al., 2015) while CBD binds to PPAR γ (O'Sullivan, 2016).

OEA's mode of action in animals is not completely understood, but elevated concentrations of OEA appear to 'trick' animals into thinking they are full (satiated), which stops them feeding (Rodríguez de Fonseca et al., 2001; Diep et al., 2011). This mode of action might also be pertinent to protists, in that, if membrane is limited for phagosome formation (at satiation), or there are defunct receptor-driven signalling cascades, protists cannot produce pseudopodia to feed (Boenigk et al., 2001).

The following experiments tested the involvement of 'PPARs' in the creation of the CBD-induced feeding lag and reduced feeding rate in *V. vermiformis* CCAP1534/14, which ultimately leads to a reduced population growth rate. It involved the use of four known PPAR agonists, OEA and PEA (for PPAR α), GW0742 (for PPAR β/δ) and Rosiglitazone (for PPAR γ) to see if they gave the same amoebic response as that exhibited with CBD. The latter two agonists are synthetic. Rosiglitazone is a member of a Thiazolidinediones (Lehmann et al., 1995) and, because only break-down products of endocannabinoids activate PPAR β/δ , GW0742 has been specifically manufactured as a selective agonist for this receptor (Sznajdman et al. 2003). Experiments then blocked the PPAR receptors with antagonists specific for each PPAR isoform to see if this alleviated the effect of the PPAR agonists and CBD. All amoebae (20 species) were subjected to 3-day growth experiments whereas feeding experiments were only performed with *V. vermiformis* CCAP 1534/14.

5.2. Results

5.2.1. Growth experiments

5.2.1.1. Response of all amoebae to four PPAR agonists

All amoebae that had been tested for their sensitivity to AEA and CBD in Chapter 3 (Table 3.1) were subjected to 200 μ M of OEA, PEA, GW0742 and Rosiglitazone, and amoebic growth after three divisions (normally 3 days) was compared to the Control (no agonist). Experiments were performed twice (for AEA/CBD sensitive strains) and once (for AEA/CBD non-sensitive strains).

All the strains which had been shown to be insensitive to CBD and AEA at 200µM (Table 3.1) were also found to be insensitive to the four PPAR agonists (Table 5.1). However, some of those strains that were sensitive to AEA/CBD, were insensitive to the four PPAR agonists, i.e., *Naegleria gruberi*, *Vahlkampfia avara*, *Flamella arnhemensis*, *Acanthamoeba castellanii* and *Hartmannella cantabrigiensis* (Table 5.1, bold).

Table 5.1: Amoebae that proved insensitive to PPAR agonists OEA, PEA, GW0742 and Rosiglitazone (at 200µM). One-way ANOVA P values shown. Experiments performed once (for strains not sensitive to AEA/CBD) or twice (for strains sensitive to AEA/CBD – in bold).

Amoeba	ANOVA P value
<i>Acanthamoeba castellanii</i> CCAP1501/1A	0.08/0.72
<i>Acanthamoeba polyphaga</i> CCAP1501/18	0.47
<i>Amoeba borokensis</i> CCAP1503/7	0.99
<i>Allovahlkampfia nedeslanaiensis</i> CCAP2502/3	0.74
<i>Cochliopodium minus</i> CCAP1537/1A	0.96
<i>Dermamoeba algensis</i> CCAP1524/1	0.69
<i>Echinamoeba silvestris</i> CCAP1519/1	0.63
<i>Flamella amhemensis</i> CCAP1525/2	0.33/0.48
<i>Hartmannella cantabrigiensis</i> CCAP1534/8	0.16/0.57
<i>Hartmannella cantabrigiensis</i> CCAP1534/11	0.89/0.90
<i>Mayorella cantabrigiensis</i> CCAP1547/11	0.79
<i>Naegleria gruberi</i> NEG-M	0.71/0.75
<i>Phalansterium filosum</i> CCAP1576/1	0.53
<i>Saccamoeba limax</i> CCAP1572/3	0.9
<i>Stygamoeba regulata</i> CCAP1580/1	0.75
<i>Tetramitus aberdonicus</i> CCAP1588/4	0.77
<i>Thecamoeba quadrilineata</i> CCAP1583/10	0.89
<i>Vahlkampfia avara</i> CCAP1588/1A	0.45/0.55
<i>Vannella placida</i> CCAP1565/2	0.99
<i>Vexillifera bacillipedes</i> CCAP1590/1	0.58

Only strains of *V. vermiformis* showed a response to the four PPAR agonists (Table 5.2). All strains were sensitive to 200µM OEA, PEA (PPARα) and GW0742 (PPARβ/δ) and all but two strains (CCAP1534/13 and 137) were sensitive to Rosiglitazone (PPARγ) (Table 5.2).

Table 5.2: All *V. vermiformis* strains were sensitive to PPAR agonists at 200µM (One-way ANOVA, P<0.01). Subsequent post-hoc Tukey test P values show which agonist affected which strain (P<0.05) and which ones did not (P>0.05 – in bold). The effect on the majority of strains was *ca.* 0% survival, except for CCAP1534/7A where Rosiglitazone and PEA yielded 53% and 60% survival, respectively*.

<i>Vermamoeba vermiformis</i> strain	Post-hoc (vs Control) P values			
	GW742	Rosiglitazone	OEA	PEA
CCAP1534/7A	0.001/0.001	0.003/0.003*	0.001/0.001	0.013/0.009*
CCAP1534/13	0.010/0.003	0.107/0.840	0.011/0.005	0.050/0.039
CCAP1534/14	0.001/0.015	0.001/0.012	0.001/0.012	0.013/0.016
137	0.001/0.001	0.097/0.061	0.001/0.001	0.013/0.004
172	0.001/0.001	0.001/0.001	0.025/0.001	0.001/0.001
173	0.001/0.001	0.001/0.001	0.001/0.001	0.001/0.001
174	0.001/0.001	0.001/0.001	0.001/0.001	0.001/0.001

Further growth experiments, with each *V. vermiformis* being subjected to different concentrations of each PPAR agonist (except for CCAP1534/7A with Rosiglitazone and PEA, Table 5.2*), were performed to deduce the MIC, IC₅₀, slope and lethal dose (Table 5.3). Individual IC₅₀ graphs can be found in Appendix 3.

Table 5.3: Calculated MIC, IC₅₀, lethal dose (µM) and slope values for four PPAR agonists (OEA, PEA, GW0742, Rosiglitazone) acting on the population growth of 7 strains of *Vermamoeba vermiformis*.

<i>Vermamoeba vermiformis</i> strain	OEA				PEA			
	MIC	IC50	Slope	Lethal	MIC	IC50	Slope	Lethal
CCAP 1534/7A	0.6	0.94	1.17	>6	ND	<i>ca.</i> 200	ND	ND
CCAP 1534/13	0.20	2.60	0.85	>23	0.75	2.87	1.69	>10
CCAP 1534/14	0.19	0.81	1.51	>5	0.25	2.55	0.91	>23
137	0.08	2.12	0.67	>35	3.10	4.79	5.78	>8
172	2.70	4.28	8.79	>9	2.70	3.68	7.00	>5
173	0.04	0.63	0.81	>10	0.04	0.50	0.85	>8
174	1.00	4.77	1.32	>24	3.20	4.62	6.89	>7
<i>Vermamoeba vermiformis</i> strain	GW0742				Rosiglitazone			
	MIC	IC50	Slope	Lethal	MIC	IC50	Slope	Lethal
CCAP 1534/7A	2.5	6.31	2.24	>17	ND	<i>ca.</i> 200	ND	ND
CCAP 1534/13	0.29	2.50	1.01	>20	ND	ND	ND	ND
CCAP 1534/14	0.60	1.75	2.10	>5	0.16	0.78	1.41	>3
137	2.00	1.80	1.83	>20	ND	ND	ND	ND
172	0.25	1.89	1.09	>14	4.00	6.2	5.5	>9
173	0.01	0.48	0.5	>20	0.14	1	1	>8
174	1.50	5.00	1.75	>19	0.90	2.35	3.33	>6

The most sensitive strain to the PPAR agonists (based on IC₅₀ data) was strain 173 followed by CCAP 1534/14 which was the same pattern as with AEA and CBD sensitivity (Table 3.3). Apart from this, there was no obvious patterns between strains or between agonists.

5.2.1.2. Response of all *V. vermiformis* strains to PPAR agonists in the presence and absence of specific PPAR antagonists

Antagonists (blockers) specific for each of each PPAR isoform (α , β/δ and γ), at 10 μ M, were tested against all the *V. vermiformis* strains in the presence/absence of the four agonists at their IC₅₀ value (Table 5.3). Experiments were performed three times. Results for *V. vermiformis* CCAP 1534/14 are shown in Figure 5.1 (data for other strains are in Appendix 4).

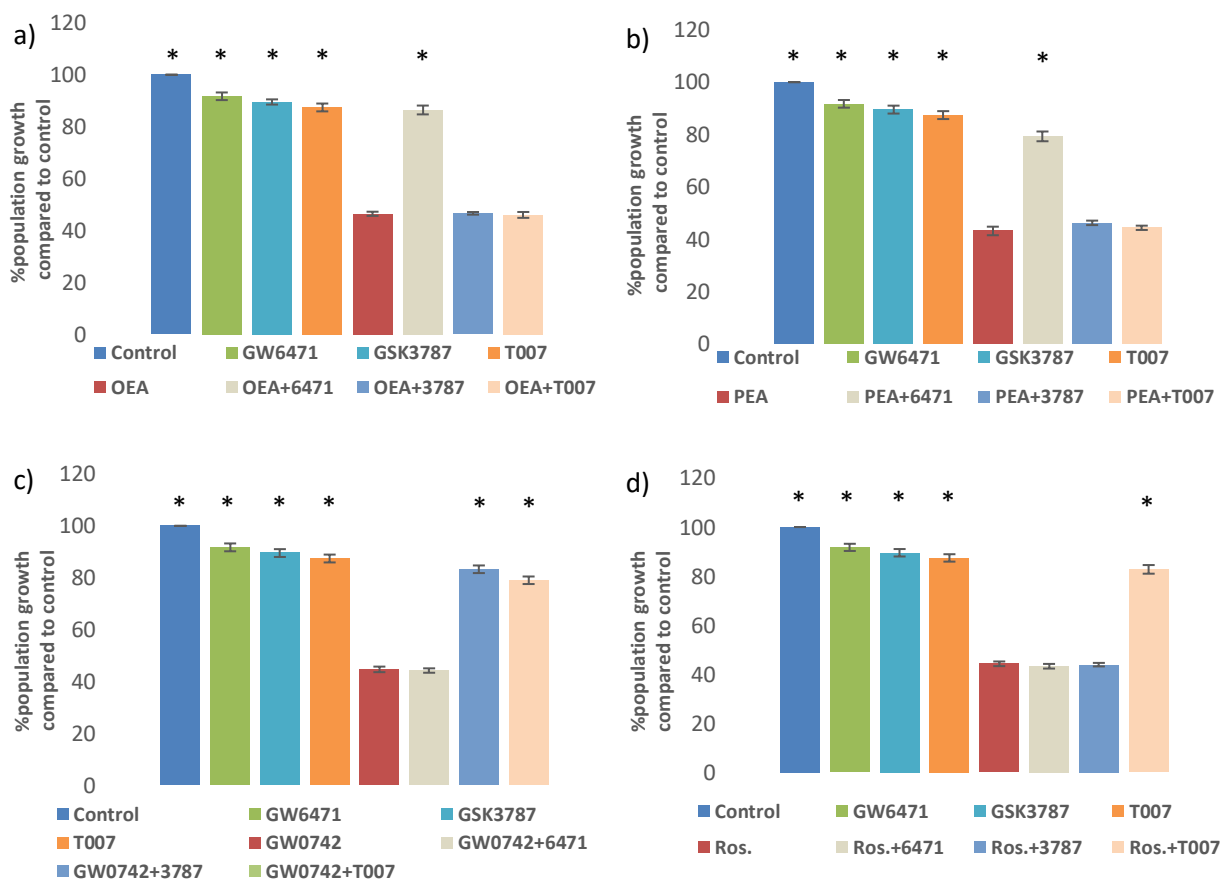


Figure 5.1: Three-day population growth (compared to the Control) of *Vermamoeba vermiformis* CCAP1534/14 in the presence of a) OEA, b) PEA, c) GW0742 and d) Rosiglitazone (each at their IC₅₀ value [Table 5.3]), with/without a pre-incubation with 10 μ M of the PPAR antagonists GW6471 (blocks PPAR α), GSK3787 (blocks PPAR β/δ) and T007 (blocks PPAR γ). Growth in the presence of each antagonist alone is also shown. *significant difference to agonist alone (P<0.01).

None of the antagonists on their own had a significant negative effect on amoebic growth, compared to the Control ($P=0.12$) (Fig. 5.1). The negative action of OEA and PEA on *V. vermiformis* growth was only blocked by GW6471 ($P<0.01$), the specific PPAR α antagonist (Fig. 5.1. a-b). The blocking was 100% effective with GW6471 + OEA or PEA being equivalent to GW6471 alone ($P=0.59$ and 0.25 , respectively). This response was recorded with all *V. vermiformis* strains (Appendix 4).

The action of Rosiglitazone was only blocked by T007 ($P<0.01$), the specific PPAR γ antagonist (Fig. 5.1 d). The blocking was also 100% effective with Rosiglitazone in the presence of T007 being equivalent to T007 alone ($P=0.33$). This response was recorded with all *V. vermiformis* strains (Appendix 4).

The action of GW0742 was expected to be blocked by GSK3787 only, the specific PPAR β/δ antagonist, but it was blocked by this *and* T007 ($P<0.01$), the PPAR γ antagonist (Fig 5.3 c). In both cases, the blocking was 100% effective with GW0742 in the presence of GSK3787 and T007 being equivalent to GSK3787 and T007 alone ($P=0.44$ and 0.25 , respectively). This response was recorded with all *V. vermiformis* strains (Appendix 4).

5.2.1.3. Response of all *V. vermiformis* strains to AEA and CBD in the presence and absence of specific PPAR antagonists

Each *V. vermiformis* strain was pre-incubated with 10 μ M of each PPAR antagonist to see if it blocked the negative effect of AEA and CBD (at 2 μ M). Experiments were performed three times. Results for *V. vermiformis* CCAP 1534/14 are shown in Figure 5.2 (data for other strains are in Appendix 5).

The action of CBD was only blocked by 10 μ M GW6471 (PPAR α) ($P<0.01$) (Fig. 5.2 a). Blocking was 100% effective as there was no difference between GW6471 with or without CBD ($P=0.33$). This response was recorded with all *V. vermiformis* strains (Appendix 5) and suggests an interaction between CBD and a PPAR α -like receptor for this species.

The action of AEA was also significantly blocked by GW6471 ($P<0.01$), but it was far from being 100% blocked (as with CBD) (Fig 5.2 b). The interaction between AEA and these antagonists was only tested on *V. vermiformis* CCAP 1534/14 as AEA was not the major cannabinoid being

studied (based on data from Chapter 4). Further work on its interaction with PPAR antagonists was not carried out.

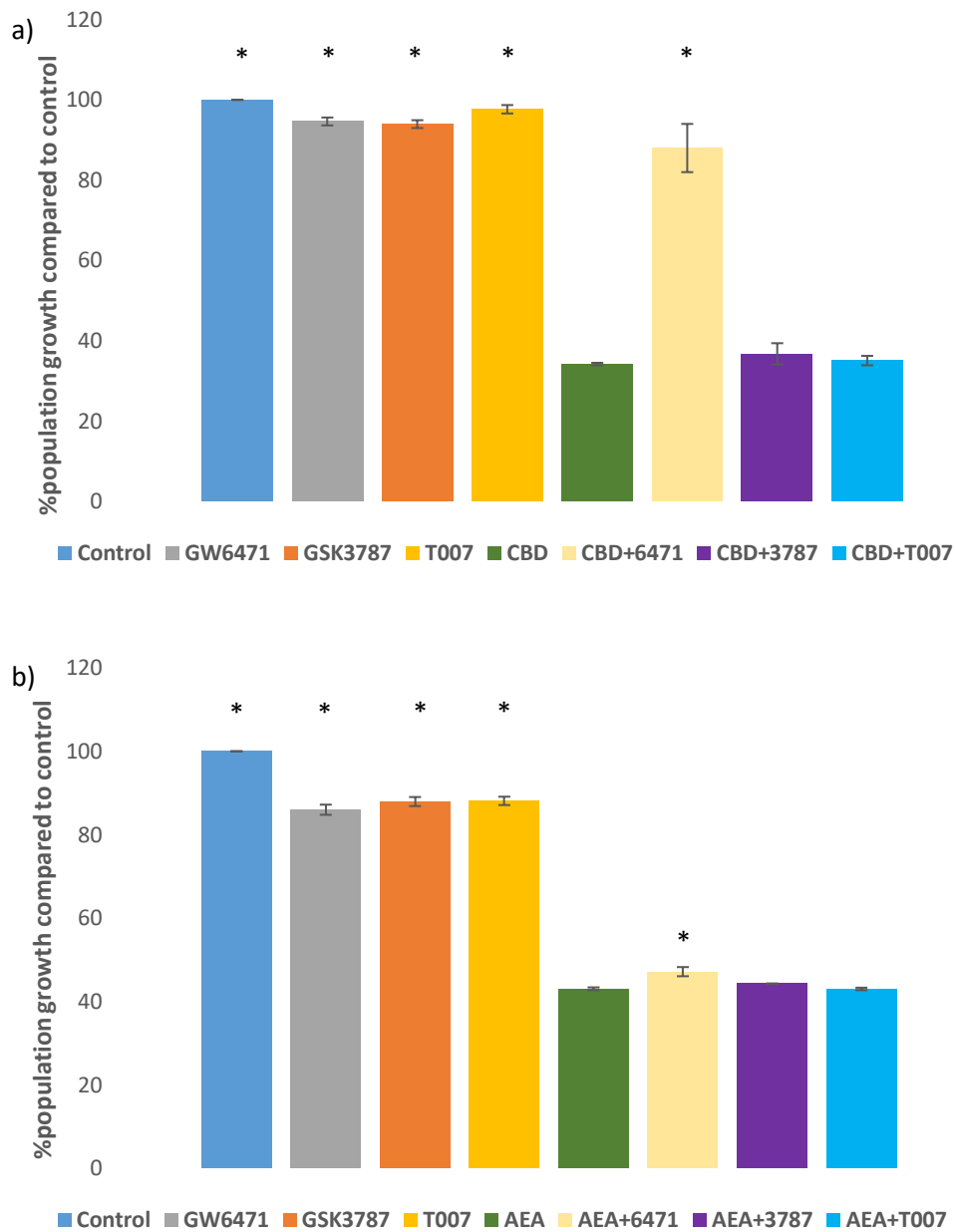


Figure 5.2: Three-day population growth (compared to the Control) of *Vermamoeba vermiformis* CCAP1534/14 in the presence of a) CBD and b) AEA (each at 2 μ M), with/without a pre-incubation with 10 μ M of the PPAR antagonists GW9471 (blocks PPAR α), GSK3787 (blocks PPAR β) and T007 (blocks PPAR γ). Growth in the presence of each antagonist alone is also shown. *Significant difference to agonist alone (P<0.01).

5.2.1.4. Response of all *V. vermiformis* strains to CBD in the presence of varying concentrations of specific PPAR antagonists

Dose-response experiments with *V. vermiformis* CCAP 1534/14, and all antagonists, confirmed that there was only an interaction between CBD and PPAR α (Fig. 5.3) and no interaction between CBD and GSK3787 (ANOVA P=0.67) and T007 (ANOVA P=0.24) (Appendix 5). The action of CBD was blocked at all GW6471 concentrations except 0.01 μ M (P=0.35) and 0.001 μ M (P=0.09) (Fig. 5.3) suggesting an MIC <0.1 μ M. There was a strong dose response with each antagonist concentration (+CBD), being significantly different to each other (P<0.05). A concentration of 10 μ M GW6471 completely blocked the effect of CBD (GW6471 with and without CBD, P=0.84). All other *V. vermiformis* strains showed the same dose-response as that exhibited by strain CCAP1534/14, i.e., all gave 100% blocking at 10 μ M and the MIC was <0.1 μ M (Appendix 6).

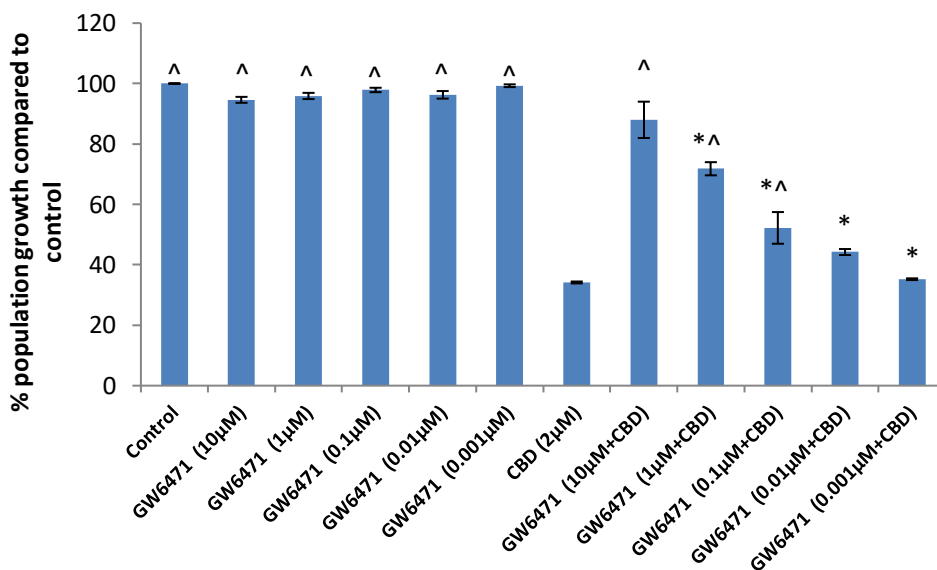
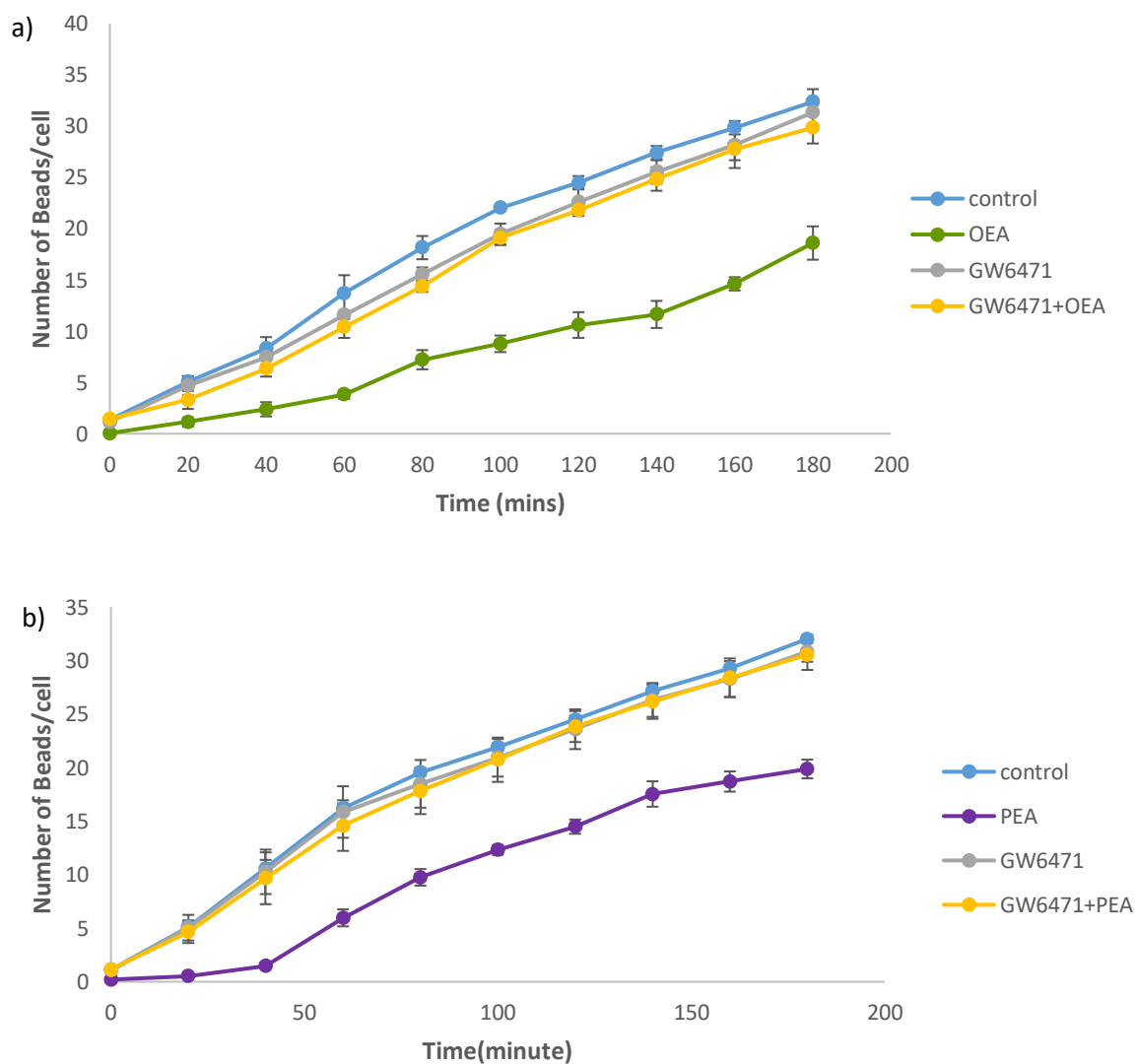


Figure 5.3: Population growth (compared to the Control) of *Vermamoeba vermiformis* CCAP1534/14 in the presence of CBD (at 2 μ M), with/without a pre-incubation with different concentrations (0.001-10 μ M) of the PPAR α antagonist GW6471. Growth in the presence of each concentration of GW6471 alone is also shown. Significant difference (P<0.05) to CBD alone[^] or GW6471 alone*.

5.2.2. Feeding experiments with *V. vermiformis* CCAP 1534/14

The feeding of *V. vermiformis* on beads was monitored in the presence of CBD (2 μ M) and the four PPAR agonists, OEA, PEA, GW0742 and Rosiglitazone (at their IC₅₀ concentration), in the presence and absence of their respective PPAR antagonist (at 10 μ M). Experiments were performed three times.

Figure 5.4 shows that all the agonists had a negative effect of amoebic feeding, i.e., they induced a lag phase and then a reduced ingestion rate, compared to the Control. These effects were eradicated in the presence of the respective PPAR antagonist (Tables 5.4 and 5.5).



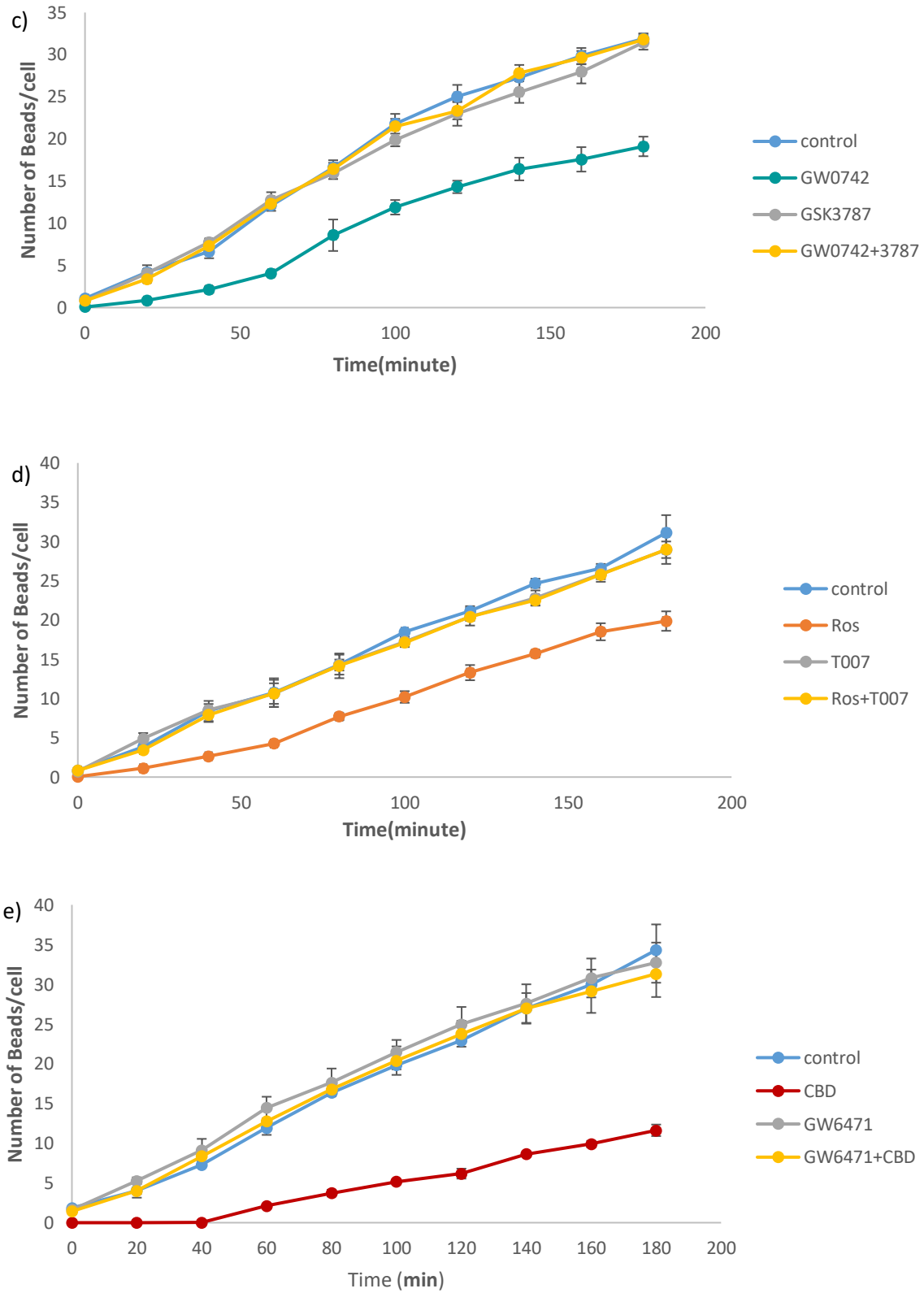


Figure 5.4: Feeding of *Vermamoeba vermiformis* CCAP1534/14 on beads in the presence/absence of a) OEA, b) PEA, c) GW0742, d) Rosiglitazone (each at their IC_{50} value [Table 5.3]) and e) CBD (at $2\mu M$), with/without a pre-incubation with $10\mu M$ of the PPAR antagonist GW6471 (blocks PPAR α), GSK3787 (blocks PPAR β) and T007 (blocks PPAR γ). Feeding in the presence of each antagonist alone is also shown.

All PPAR agonists induced a feeding lag with an equivalent duration (Table 5.4, $P=0.46$) at their IC_{50} values for reduced population growth (OEA, PEA, GW0742, Rosiglitazone at 0.81, 2.55, 1.75 and 0.78 μM , respectively). However, visual examination of the graphical data (Fig. 5.4) clearly showed that CBD completely stopped feeding for up to 40 mins (at 2 μM) whilst the PPAR agonists (at 0.78-2.55 μM) allowed some level of feeding to occur.

Table 5.4: Significant ($P<0.01$) feeding lags in *Vermamoeba vermiformis* CCAP1534/14, induced by each agonist alone. No significant difference between the agonist-induced lag times ($P=0.46$). No lags were recorded in the Control, blocker (antagonist) alone and agonist with blocker. GW6471 = blocker for CBD, OEA and PEA (PPAR α), GSK3787 = blocker for GW0742 (PPAR β/δ) and T007 = blocker for Rosiglitazone (PPAR γ).

Treatment	Lag phase (min)				
	OEA	PEA	GW0742	Rosiglitazone	CBD
Control	0.00 \pm 0.00	0.00 \pm 0.00	0.00 \pm 0.00	0.00 \pm 0.00	0.00 \pm 0.00
Blocker alone	0.00 \pm 0.00	0.00 \pm 0.00	0.00 \pm 0.00	0.00 \pm 0.00	0.00 \pm 0.00
Agonist alone	19.66 \pm 5.31	22.97 \pm 2.26	26.65 \pm 3.64	26.71 \pm 5.18	34.42 \pm 1.58
Agonist and blocker	0.00 \pm 0.00	0.00 \pm 0.00	0.00 \pm 0.00	0.00 \pm 0.00	0.00 \pm 0.00

With regards to subsequent ingestion rates, all PPAR agonists significantly reduced ingestion rate compared to the Control (Table 5.5); a response that was also recorded with CBD. This negative effect was 100% blocked with the respective antagonist (Figure 5.4, Table 5.5).

Table 5.5: Significant reductions (compared to the Control) in ingestion rates of *Vermamoeba vermiformis* CCAP1534/14, induced by each agonist alone ($*P<0.05$, $**P<0.01$). No reduction in rate was recorded with blocker (antagonist) alone and agonist with blocker. GW6471 = blocker for CBD, OEA and PEA (PPAR α), GSK3787 = blocker for GW0742 (PPAR β/δ) and T007 = blocker for Rosiglitazone (PPAR γ).

Treatment	Ingestion rate (beads/cell/min)				
	OEA	PEA	GW0742	Rosiglitazone	CBD
Control	0.211 \pm 0.006	0.169 \pm 0.003	0.183 \pm 0.004	0.166 \pm 0.011	0.185 \pm 0.009
Blocker alone	0.183 \pm 0.004	0.163 \pm 0.002	0.172 \pm 0.006	0.153 \pm 0.005	0.178 \pm 0.014
Agonist alone	0.105 \pm 0.004**	0.139 \pm 0.021*	0.151 \pm 0.009**	0.141 \pm 0.010**	0.079 \pm 0.003**
Agonist and blocker	0.180 \pm 0.001	0.165 \pm 0.004	0.183 \pm 0.004	0.156 \pm 0.007	0.174 \pm 0.017

In order to compare the effect of each agonist on amoebic ingestion rate, *between* experiments (although the agonist concentrations used were variable), ingestion rate was converted to % ingestion rate compared to the relevant Control in each experiment (Fig. 5.5) and data were analysed using a one-way ANOVA. Feeding in the presence of CBD (2 μ M) and OEA (0.81 μ M) were equivalent ($P=0.90$) suggesting that, in reality, OEA is more detrimental to feeding than CBD. Feeding in the presence of OEA and CBD was significantly ($P<0.01$) lower than with PEA (2.55 μ M), Rosiglitazone (0.78 μ M) and GW0742 (1.75 μ M), which were themselves equivalent ($P=0.79$); although it is unknown whether Rosiglitazone (at *ca.* 2 μ M) would have yielding reduce feeding comparable to CBD.

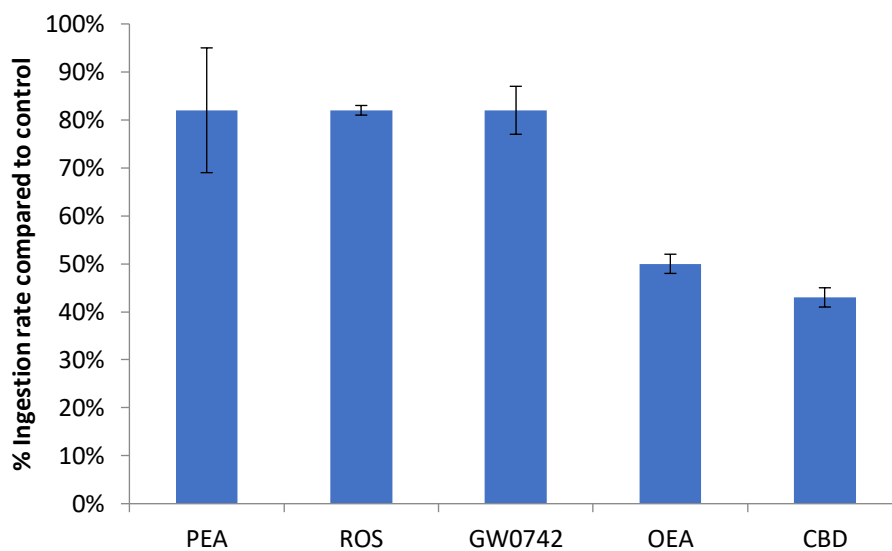


Figure 5.5: % ingestion rates of *Vermamoeba vermiformis*, compared to the Control, in the presence of PEA, Rosiglitazone (ROS), GW0742 and OEA (each at their IC_{50} value [Table 5.3]) and CBD (at 2 μ M). All were significantly ($P<0.001$) lower than the Control. Rates with OEA and CBD were equivalent ($P=0.90$) but significantly ($P<0.01$) lower than those with PEA, Rosiglitazone and GW0742 (which were themselves equivalent $P=0.79$).

5.3. Discussion

5.3.1. Sensitivity of amoebae to PPAR agonists

All those amoebae that were not sensitive to AEA and CBD (Table 3.1) were also not sensitive to the four PPAR agonists. This suggests that they might not be susceptible to any form of N-acylethanolamine (NAE), although it remains to be seen whether they are susceptible other ligands of the endocannabinoid system, such as monoacylglycerols (AcGs), N-acyldopamines,

N-acylserotonin, Fatty acids amides of amino acids (FAAAs) or COX2-derivatives (Piscitelli, 2015). But this is future work.

Of those species that were sensitive to AEA/CBD, only *V. vermiformis* strains were sensitive to the PPAR agonists. Those that were not, were: *Naegleria gruberi* and *Vahlkampfia avara* (both in the sub-Phylum Percolozoa), *Flamella amhemensis* (in the sub-Phylum Conosa), *Acanthamoeba castellanii* (in the sub-phylum Lobosa, Class Discosea) and *Hartmannella cantabrigiensis* (in the sub-Phylum Lobosa, Class Tubulinea, alongside *V. vermiformis*) (Fig. 3.3). *V. vermiformis* was previously described as *Hartmannella vermiformis* until it was reclassified in 2011 due to (i) differences in shape, length/breadth ratio and its tendency to branch when changing the direction of locomotion and, (ii) the fact that it always grouped with *Echinamoeba*, and not with other hartmannellids, in published phylogenetic trees (Smirnov et al., 2011). Now, we have recorded that these genera also differ in their response to PPAR agonists which lends further weight to the re-classification of *H. vermiformis* to *V. vermiformis*.

A recent phylogenomic study of amoeba, comparing 325 protein genes from 98 taxa, has resulted in some slight changes to the amoeba taxonomic tree (as depicted in Fig. 3.3), but *Vermamoeba* is still most closely related to *Echinamoeba* and distinct from *Hartmannella* (Kang et al., 2017). There is also no evidence to suggest that *Vermamoeba* has evolved earlier or later than other genera (Kang et al., 2017) so why it is the *only* genus that is susceptible to PPAR agonists remains a mystery. However, it might *not* be the only genus, but without any trend whatsoever in susceptibility/non-susceptibility one would have to test every single genus of amoeba to confirm this. This study has already tested all the available genera of non-marine naked amoebae available in culture; other genera are currently unculturable.

All *V. vermiformis* strains responded to AEA, CBD, OEA and GW0742 but there were strain differences with regards to their susceptibility to PEA and Rosiglitazone. Strains CCAP1534/13 and 137 were not sensitive to Rosiglitazone (at 200 μ M) and CCAP1534/7A required very high concentrations of PEA and Rosiglitazone to elicit a response (Table 5.3). All these combinations were deemed 'insensitive'. Of those sensitive combinations, strain differences were evident with regards to MIC, IC₅₀ and lethal dose (Table 5.3) but values were within the same range and were similar to those obtained for CBD (Table 3.3). For example, IC₅₀ values

ranged from 0.63-4.77 μ M (OEA), 0.5-4.79 μ M (PEA), 0.48-6.31 μ M (GW0742) and 0.78-6.2 μ M (Rosiglitazone) (Table 5.3) while those for CBD were 0.98-7.31 μ M (CBD) (Table 3.3); all were below 10 μ M.

5.3.2. Response of *V. vermiformis* to PPAR antagonists

5.3.2.1. Growth experiments

There were no *V. vermiformis* strain differences evident in their responses to PPAR antagonists blocking the action of an agonist. In all cases the action of OEA and PEA was 100% blocked with 10 μ M GW6471 only, the specific PPAR α antagonist, Rosiglitazone was 100% blocked with 10 μ M T007 only, the specific PPAR γ antagonist but, GW0742 was unexpectedly 100% blocked by both GSK3787, the specific PPAR β/δ antagonist, and T007 (at 10 μ M). Lee et al. (2002) examined T007 binding selectivity using adipocyte differentiation assays in HEK293 cell lines and found it blocked the effect of Rosiglitazone with an IC₅₀ of 0.01 μ M but could also block the action of PPAR α ligands (IC₅₀ of 0.85 μ M) and PPAR β/δ ligands (IC₅₀ of 1.8 μ M). Since this antagonist was used at 10 μ M it might be expected to block all agonists but it did not. And, if higher concentrations are required to block amoebic PPARs then one would expect T007 to possibly block PPAR α before PPAR β/δ , but it did not. This unexpected result is discussed further below.

The results might suggest that the majority of *V. vermiformis* strains contain three PPAR isoforms but this is difficult to believe as to date, the three isoforms have only been reported in bony fish, mammals, birds and amphibians; not invertebrates (Zhou et al. 2015). Phylogenetic analysis has also shown that PPAR α and PPAR β/δ cluster together, whereas the branch of PPAR γ is distinct, suggesting the latter is the earliest ancestor of the PPAR gene family (Zhou et al., 2015). However, not all *V. vermiformis* strains responded to Rosiglitazone and if PPAR γ was the ancestral form of PPAR, one would expect this isoform to be present in all these primitive cells. It is therefore more likely that *V. vermiformis* possesses a single promiscuous PPAR-like molecule which can bind each PPAR agonist and each PPAR antagonist.

Structurally, a PPAR molecule is divided into five distinct functional regions; a DNA-binding domain (DBD), a ligand-binding domain (LBD), activation function 1 (AF1), activation function

2 (AF2), and a variable hinge region (Zhou et al., 2015). The LBD is unusually large and spacious in PPARs and, as a consequence, they are relatively promiscuous (O'Sullivan, 2007; Itoh et al., 2008). It might therefore be that the PPAR agonists/antagonists bind to the amoeba's PPAR-like molecule at different sites in the LBD. For example, the PPAR α antagonist might bind to the same site(s) as OEA and PEA and the PPAR β/δ antagonist might bind to the same site as GW0742. However, the PPAR γ antagonist (which also seems to block GW0742 as well as Rosiglitazone) might span the binding sites of both Rosiglitazone *and* GW0742 in this 'PPAR'.

The agonists themselves can also be promiscuous. For example, in addition to binding to PPAR α , PEA can bind to the CB2 receptor (Facci et al., 1995) and OEA can bind to TPRV1 and GPR119 (Overton et al., 2006; Kleberg et al., 2014; Piscitelli, 2015). A very promiscuous agonist is CBD which, to date, has 11 reported receptors (Bih et al., 2015). In the current study, all *V. vermiformis* strains showed the same response with CBD in that its action was 100% blocked with 10 μ M GW6471 only (PPAR α antagonist) and there was a dose-response, yielding an MIC of <0.1 μ M. CBD is not known to bind to PPAR α in animals, instead it is reported to bind to PPAR γ with an IC₅₀ of 5 μ M (O'Sullivan et al., 2009b); a concentration within the range of IC₅₀ values (0.98-7.31 μ M) reported for CBD binding to 'PPAR α ' in the current study.

The IC₅₀ values for CBD with *V. vermiformis* were shown to be within the same range as those concentrations required to elicit a response in mammalian cells (see 3.3.2) and indeed, the IC₅₀s for the four PPAR agonists are also within the same range as mammalian cells. For example, Lueneberg et al. (2011) showed that 0.1 μ M of OEA caused no cell death in mouse granule neuron cells over 24h while the same concentration of PEA induced 50% cell death. Di Marzo et al. (2001) showed that 5 μ M PEA caused a 30-40% decrease in MCF-7 breast cancer cells after 4 days of treatment. OEA has also been found to suppress the migration of metastatic tumour cells in mice at 2-100 μ M (Sailler et al., 2014). Girroir et al. (2008) tested the effect of GW0742 on the growth of human UACC903 melanoma cells after 4 days of treatment and 1 μ M caused a 77% reduction while 10 μ M caused 100% cell death. With regards to Rosiglitazone, many studies have investigated the effect of this PPAR γ agonist on human cancer cells such as bladder cancer and colorectal cancer cells (e.g. Miao et al., 2011; Cerbone et al., 2012; Xu et al., 2017), with all studies agreeing that concentrations higher than 10 μ M cause 100% cell death.

5.3.2.2. Feeding experiments

The unique characteristic of CBD in Chapter 4 was that it caused an immediate lag/cessation in *V. vermiformis* CCAP 1534/14 feeding whereas the addition of sugars (to block feeding receptors) did not. However, in this Chapter, it has been shown that a lag can also be induced with agonists for the three PPAR isoforms (Table 5.4) at their IC₅₀ concentration. These concentrations were variable (OEA, PEA, GW0742, Rosiglitazone at 0.81, 2.55, 1.75 and 0.78 μM, respectively) and therefore a true comparison to CBD (at 2μM) cannot be made. However, at these IC₅₀ concentrations the lag times were equivalent to each other (Table 5.4) and to that with CBD which was close to its IC₅₀ of 1.01μM (Table 3.3). After this lag, CBD and all the PPAR agonists caused a reduction in ingestion rate compared to the Control (Table 5.5) but OEA was the most potent, followed by CBD. In addition, these negative effects could be abolished by 10μM of their respective PPAR antagonist. The action of CBD was only blocked by GW6471 (for PPARα).

Therefore, it appears that the whole PPAR-like molecule (α, β/δ and γ binding sites) in *V. vermiformis* might be involved, in some way, in the feeding process of *V. vermiformis* and that CBD behaves most like the ligands that bind the α-site, particularly OEA. Indeed, there are striking similarities between OEA and CBD with regards to their mode of action in animals and *V. vermiformis*.

Firstly, OEA has an anorexiant effect in mice, i.e., it can stop feeding completely and then reduce food intake (Rodríguez de Fonseca et al., 2001; Diep et al., 2011). The same response was recorded in *V. vermiformis* with all PPAR agonists and CBD. Secondly, PEA is significantly less potent than OEA and AEA has no effect (Rodríguez de Fonseca et al., 2001; Diep et al., 2011). This response was also recorded with *V. vermiformis*. Thirdly, administration of OEA in mice causes a dose-dependent delay in the feeding onset (Gaetani et al., 2003; Karimian Azari et al., 2014). The effect of CBD on the feeding lag and ingestion rates of *V. vermiformis* was dose-dependent (dose-responses of PPAR agonists were not performed). Fourthly, OEA does not reduce feeding in animals if they lack a functional PPARα gene, suggesting that PPARα activation is crucial for mediating its hypophagic actions (Fu et al., 2003). In the current study, all agonist-induced lags and reduced feeding rates were abolished with PPAR antagonists, and for OEA and CBD, this was the blocking of the PPARα receptor only.

It is also interesting to note that OEA only evokes a delayed feeding onset and reduced meal size in food-deprived rats (only the former in well fed mice) (Gaetani et al., 2003; Karimian Azari et al., 2014). In the current study, *V. vermiformis* would have also been food-deprived after 7 days culturing prior to experiments. It would be interesting to repeat experiments with well-fed cells to see if only a lag phase is induced.

The underlying mechanisms of OEA-induced anorexia in animals is currently unclear although much work is being carried out as it has potential therapeutic uses for the treatment of obesity (Fernández-Ruiz et al., 2015). OEA acts as a satiety signal, which is generated in the intestine upon the ingestion of fat (Provencia et al., 2013). It then induces a 'satiety status' signalling pathway which is transferred to the hypothalamic nuclei of the brain where different neuronal pathways, including oxytocinergic, noradrenergic, and histaminergic neurons, seem to mediate its hypophagic action (Romano et al., 2015). It is considered that upon binding to PPAR α , it induces 'several transcriptional changes' to activate this signaling cascade (Romano, et al., 2015), suggesting that it is a PPAR genomic response (see 1.2.4.1).

However, the observed effects of PPAR agonists and CBD in both *V. vermiformis* (current study) and *T. pyriformis* (Parry, personal communication) appear to be instantaneous; a feature which is considered too rapid to be attributed to the biosynthesis of mRNA or protein in the classical PPAR genomic response (Falkenstein et al., 2000). In addition, no homologues of RXR have been found in protists to date (see 1.2.4.1). It is therefore possible that a non-genomic PPAR response might be occurring in these protists, although this has not been studied as extensively as the genomic response to date.

5.3.3 PPAR-induced non-genomic response

PPAR non-genomic responses are rapid (Falkenstein et al., 2000) and do not involve the binding of PPARs to RXR, but instead, PPARs bind to other proteins (Unsworth et al. 2018). Non-genomic functions occur if PPARs are associated with the cytosol, plasma membrane or intracellular organelles, such as mitochondria, whilst genomic functions are restricted to when they are localized in the nucleus (Unsworth et al. 2018).

Most work on the PPAR-induced non-genomic responses have been performed on anucleate platelets and the mechanism of action of PPAR α and PPAR β/δ appears to be very similar whilst that of PPAR γ is distinct (Figure 5.6). The former two isotopes inhibit ADP-stimulated platelet activation by binding to PKC α (Protein Kinase C α) which then limits its availability to facilitate downstream signalling events; which then increases the level of cAMP (Ali et al, 2006, 2009a). PPAR β/δ can also be activated by the prostaglandin PGI₂ (Ali et al., 2009b) but its involvement in platelet inactivation has yet to be tested (Unsworth et al. 2018).

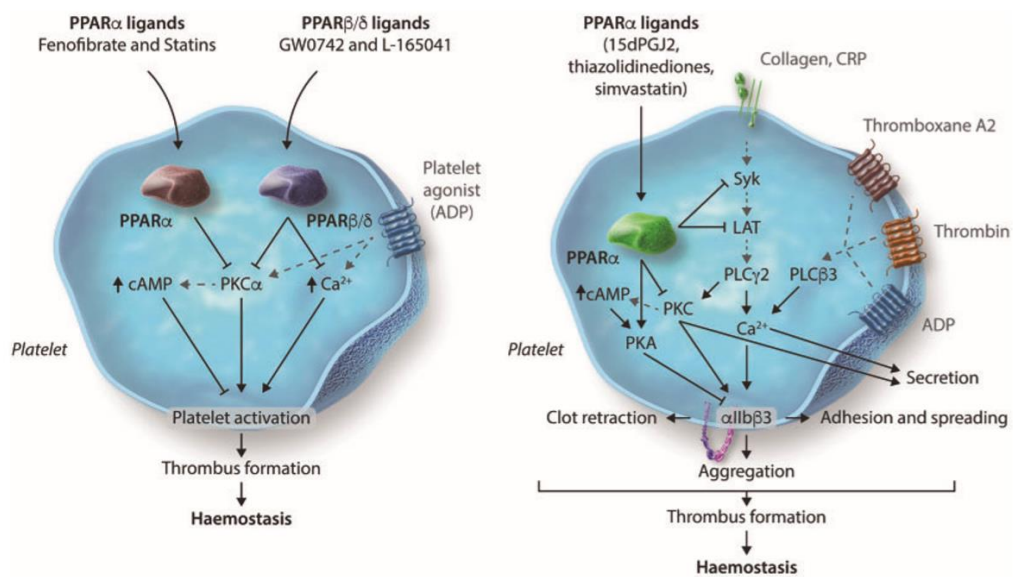


Figure 5.6: Non-genomic regulation of platelets by PPAR ligands. PPAR α and PPAR β/δ ligands cause a reduction in intracellular calcium mobilization and platelet activation. This inhibition is due to the attenuation of PKC α through its interaction with PPAR α or PPAR β/δ , which limits its availability to facilitate signalling downstream. Treatment with PPAR γ ligands inhibits the phosphorylation of Syk and LAT that mediate signalling initiated by the collagen receptor GPVI (Unsworth et al. 2018).

Activation of PPAR γ , on the other hand, inhibits collagen-stimulated platelet function through modulation of signalling downstream of the collagen receptor GPVI (Moraes et al., 2010). Specifically, in its un-ligated state, PPAR γ interacts with Syk (Spleen tyrosine kinase) and LAT (a transmembrane adaptor protein Linker for Activation of T-cells) and their phosphorylation leads to the activation of proteins downstream, e.g. PI3-K (Phosphoinositide 3-kinase). Upon ligation of PPAR γ , an interaction with Syk and LAT is prevented, so no phosphorylation takes place and downstream signalling stops (Moraes et al., 2010). The authors have yet to discover

if PPAR γ is recruited to a signalling protein complex (with both Syk and LAT) or whether interaction with Syk and LAT occurs independently.

What is interesting is that Syk, LAT and PKC are involved in the initial stages of phagosome formation in macrophages; specifically the signaling cascade between stages 2 and 3 (Fig. 4.8).

5.3.4. Signalling cascades responsible for phagosome cup formation (Fig. 4.8, stage 2-3)

Current evidence suggests that a non-genomic response can occur via binding of PPAR α or β/δ to PKC α and binding of PPAR γ to Syk, LAT or a Syk-LAT complex. Considering *V. vermiformis* might possess one promiscuous PPAR molecule, evidence for the involvement of these four molecules (PPAR, Syk, LAT and PKC α) in phagocytosis is reviewed.

5.3.4.1. Opsonized phagocytosis in macrophages

Syk is the first of the four molecules to be involved in phagosome formation in macrophages (Figure 5.7, Stage ii) and is particularly associated with the activation of feeding receptors (Levin et al., 2016). Upon ligand binding to the receptor binding domain, the receptor tail (which extends into the cytosol) initiates the signaling cascade which culminates in the extension of pseudopods (Levin et al., 2016). Receptor tails contain tyrosine residues within a tyrosine-based activation motif (ITAM) and it is the phosphorylation of these residues by Src-family tyrosine kinases (SFKs) that starts the signaling cascade (Fitzner-Attas et al., 2000). To safeguard their phosphorylation, receptors move laterally within the membrane via cytoskeletal remodeling (Jaumouillé et al., 2014) and cluster together in order to exclude Protein Tyrosine Phosphatases (PTPs) such as SHP-1 and SJP-2 (Yamauchi et al., 2012).

Phosphorylated tyrosines then serve as a docking site for the tandem SH2 domains of **Syk** (Johnson et al., 1995). Syk amplifies signaling by (i) further phosphorylating nearby tail tyrosine residues (Mócsai et al., 2010) and (ii) by recruiting and phosphorylation adapter proteins such as growth factor receptor bound protein 2 (Grb2), Grb2-associated-binding protein 2 (Gab2), the Src homology 3 (SH3) domain-binding protein 2 (SH3BP2) and linker of activated T cells (**LAT**) (Tridandapani et al., 2000; Yu et al., 2006). It is these adapter proteins

that then recruit cytosolic effectors to carry out the extensive lipid and cytoskeletal remodeling that accompanies the phagocytic process (Levin et al., 2016).

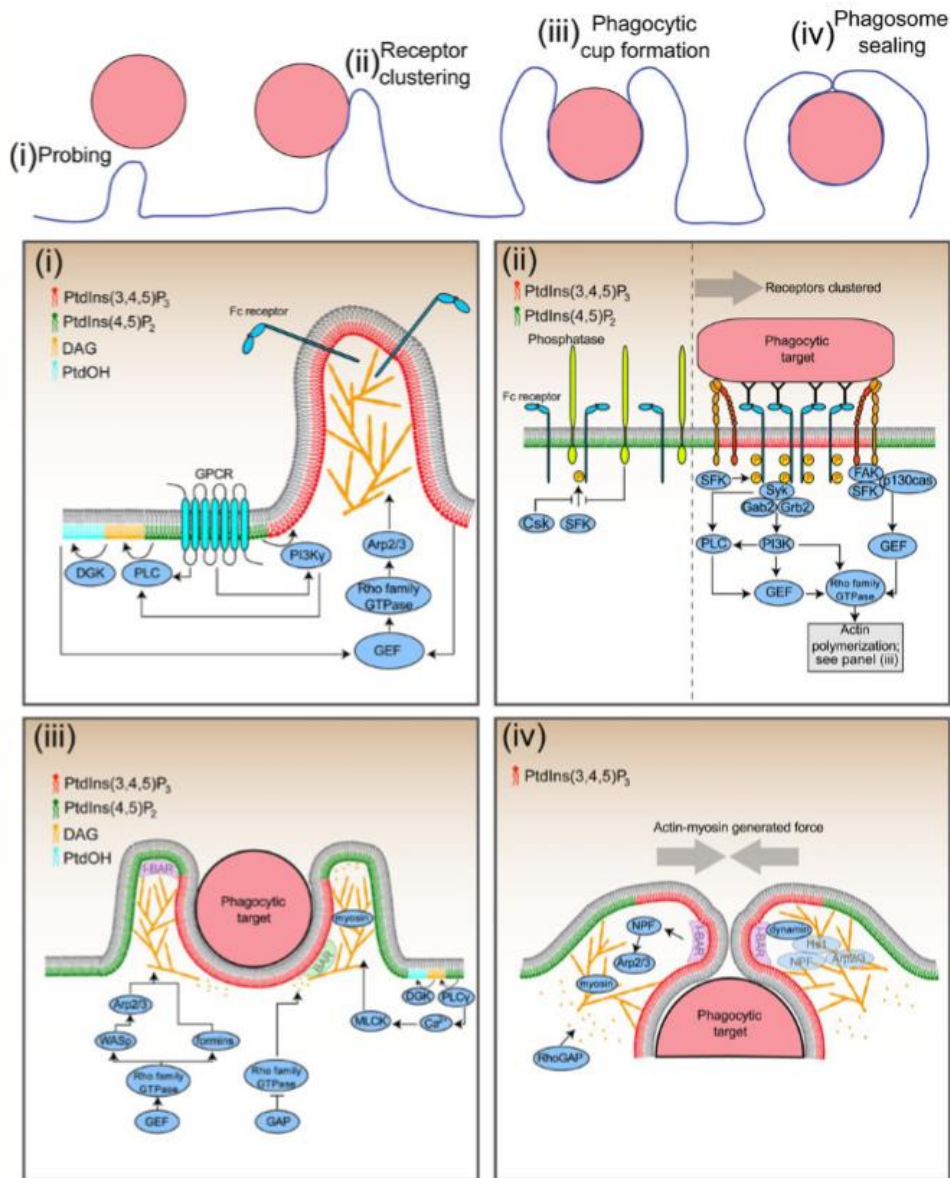


Figure 5.7. Cellular events that lead to vacuole formation in macrophages (Levin et al., 2016). See text for details of stages ii and iii.

One of the first major lipid-remodeling events to occur is a local increase in phosphatidylinositol 4,5-bisphosphate [PtdIns(4,5)P₂] (Botelho et al., 2000), mediated by phosphatidylinositol 4-phosphate 5-kinases (PIP5Ks) whose recruitment is bolstered by the local activation of phospholipase D (Iyer et al., 2004). Shortly after accumulating however,

PtdIns(4,5)P₂ is significantly depleted from sites of phagosome formation through its conversion into PtdIns(3,4,5)P₃ by phosphoinositide 3-kinases (PI3K) (Marshall et al., 2001).

PtdIns(4,5)P₂ can also be broken down into diacylglycerol (DAG) and inositol (1,4,5)-trisphosphate (IP₃) by phospholipase C α (PLC α) (Marshall et al., 2001). DAG and intracellular calcium regulate a number of effectors involved in phagocytosis, including members of the **protein kinase C (PKC) family** and myosin light chain kinase (Larsen et al., 2002). PKC has a range of downstream targets that are implicated in phagocytosis. For example, plekstrin, the major PKC phosphorylation target in platelets, is expressed in macrophages and recruited to the phagosome membrane during receptor-mediated phagocytosis (Brumell et al., 1999), although its role there is unknown.

The culmination of this signaling cascade downstream of receptor tails, together with the generation of lipid intermediates at the site of receptor engagement, leads to the spatial and temporal activation of Arp2/3 by the local recruitment of nucleation-promoting factors (NPFs) (Goley et al., 2004). Specifically, Arp2/3 binds to both PtdIns(4,5)P₂ and Rho-family GTPases particularly Cdc42 or Rac (Levin et al., 2016). These GTPases are activated locally by GEFs, which are themselves recruited by signals at the plasma membrane such as PtdOH and PtdIns(3,4,5)P₃. This then gives rise to the elaborate branched actin networks associated with phagocytosis (Levin et al., 2016).

The above signaling cascade describes that which is induced upon ligand binding to Fc receptors, which are single span transmembrane proteins involved in opsonized phagocytosis (Huber et al., 1976). Opsonized phagocytosis involves Fc receptor-binding to particles coated with opsonins, i.e., soluble molecules such as antibodies, surfactant proteins, mannose binding proteins (Stuart and Ezekowitz, 2005). Compared to opsonized phagocytosis, non-opsonized phagocytosis has received far less attention but it is the type of phagocytosis carried out by protists.

5.3.4.2. Non-opsonized phagocytosis in macrophages

Non-opsonised phagocytosis involves the internalisation of particles via the direct recognition of bacterial ligands (Pathogen-Associated Molecular Patterns [PAMPs]) without the need of enhanced stimuli given by opsonins (Zeng et al., 2016). Two main families of receptors are

involved in non-opsonic phagocytosis: C-type lectins (Harb et al., 1998) and Scavenger Receptors (Peruń et al., 2016). Most information on the signaling cascade, post receptor binding, is available for the mannose receptor (MR/CD206) which exists in both macrophages (Drickamer and Fadden, 2002) and amoebae (Allen and Davidowicz, 1990). However, even though activation of **PKC** by MR-ligand binding has been known for some time (Allen and Aderem, 1996) details of the other components of the signalling cascade have only come to light recently (Rajaram et al., 2017).

The MR is a type I 180-kDa transmembrane C-type lectin that consists of five domains which includes a binding domain and a tail (Stahl et al., 1980). The tail is crucial for phagocytic functions and its removal can significantly reduce the uptake of prey (Ezekowitz et al., 1990). The MR cytoplasmic tail does not contain an ITAM motif and possesses only one tyrosine residue. However, a FcR γ -chain (which contains an ITAM motif) is constitutively bound to it (Schweizer et al., 2000) (Fig. 5.8).

Phagocytosis

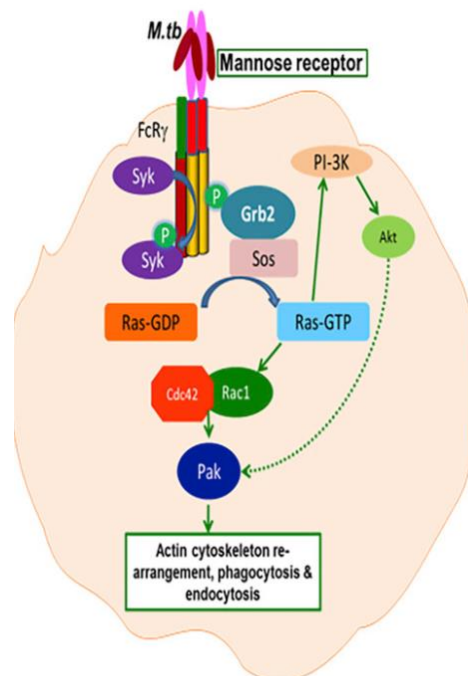


Figure 5.8: Main components of the signaling cascade induced upon the binding of *Mycobacterium tuberculosis* (*M.tb*) to the mannose receptor in macrophages. See text for details (Rajaram et al., 2017).

In a study by Rajaram et al. (2017), it was thought that Src kinase-mediated phosphorylation of the tyrosine residues was occurring in the MR, but this was not confirmed. However, the authors did confirm that **Syk** became phosphorylated and co-localized with the MR early upon MR activation. They considered that Syk might be activated by a recruited Src kinase or alternatively by binding to a constitutively-bound FcR γ -chain. The study then went on to show that the adaptor protein Grb2 (see Fig. 5.7ii) was recruited and phosphorylated by Syk. Another 47 proteins were detected but their identity was undisclosed (Rajaram et al., 2017) so it is unknown at present whether one of these might have been **LAT**. The study also confirmed that Grb2 activated the Rac-1, Cdc42 and PAK-1 which are important for F-actin polymerization (Rajaram et al., 2017).

So, it is beginning to look as if the signaling cascades induced by receptors involved in both opsonized and non-opsonized phagocytic cup formation are similar and involve Syk and PKC (and possibly LAT). What is also interesting, is that the ligand Rajaram et al. (2017) used for activating the MR was *Mycobacterium tuberculosis* (*M.tb*) (Fig. 5.8) and there are reports of PPAR γ being involved in enhancing its survival within host cells.

5.3.4.3. Phagocytosis of *Mycobacterium* spp. and the involvement of PPAR

Mycobacterium tuberculosis infection begins with entry into macrophages where they multiply within the phagosomes, by preventing phagosome fusion with lysosomes (Armstrong and d'Arcy Hart, 1971). The mannose-capped lipoarabinomannan (ManLAM) from the *M. tuberculosis* cell surface has mannose and GlcNAc residues and interacts strongly with the mannose receptor (Kang et al., 2005).

Rajaram et al. (2010) were the first to identify a 'MR-mediated signaling pathway' in macrophages that linked engagement of the mannose receptor by *M. tuberculosis* (or ManLAM) with PPAR γ activation; alongside the activation of the p38 MAPK pathway (Fig. 5.9). PPAR γ activation enhanced bacterial growth within the phagosome (Rajaram et al., 2010) while PPAR γ silencing decreased it (Mahajan et al., 2012). The latter response was also confirmed to occur *in vivo*, using a macrophage-specific PPAR γ knock out mouse model (Guirado et al., 2018). Thus, PPAR γ activation in macrophages *increases* the susceptibility of host cells to *M. tuberculosis* infection.

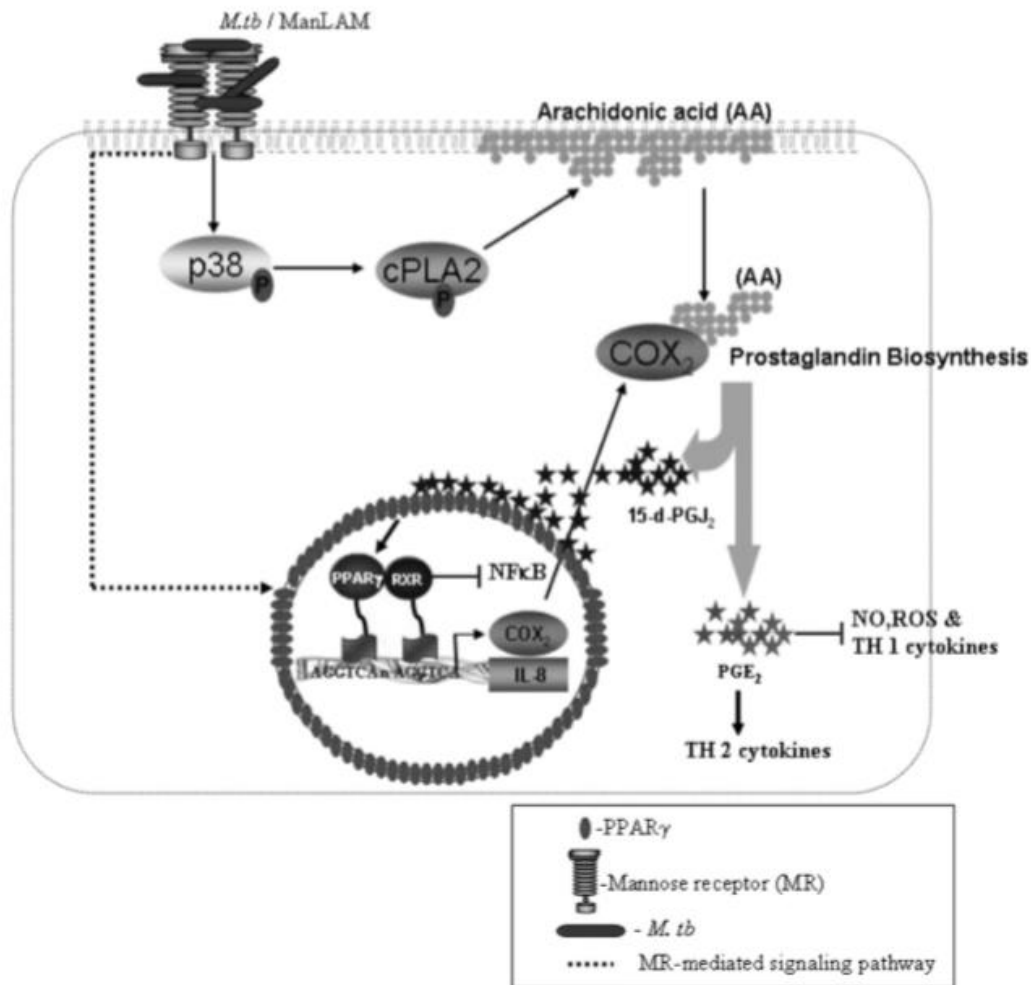


Figure 4.9: A model proposing mannose receptor/PPAR γ crosstalk in *Mycobacterium tuberculosis* infection (Rajaram et al., 2010).

More recently, Diaz Acosta et al. (2018) studied the infection of Schwann cells (SCs) with *Mycobacterium leprae*. An active crosstalk between the mannose receptor (CD206) and PPAR γ was detected that led to the induction of lipid droplet (LD) formation and prostaglandin E2 (PGE2), which are fundamental players in bacterial pathogenesis (Diaz Acosta et al., 2018). A model proposing a key role for the phenolic glycolipid I (PGL I)-induced CD206 (mannose receptor)/PPAR γ crosstalk in *M. leprae* neuropathogenesis was proposed (Fig. 5.10).

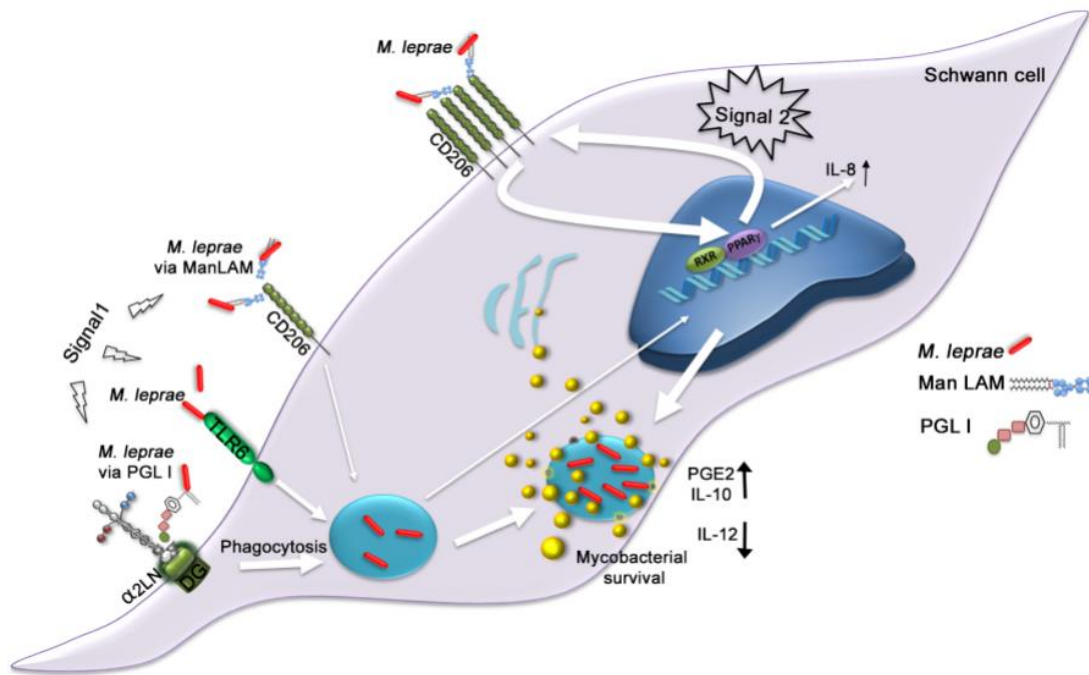


Figure 5.10: A model proposing a key role for the phenolic glycolipid I (PGL I)-induced CD206 (mannose receptor)/PPAR γ crosstalk in *Mycobacterium leprae* neuropathogenesis (Diaz Acosta et al., 2018). See text for details.

The model states that the recognition of *M. leprae* ManLAM by baseline levels of CD206 allows some bacterial entry and weak activation of PPAR γ (Diaz Acosta et al., 2018). Then, CD206 is up-regulated, more bacteria are sensed which triggers a stronger signal ('signal 2', Fig. 5.10), where internalized *M. leprae* promotes the amplification of CD206/ PPAR γ crosstalk (Diaz Acosta et al., 2018). Details of the signalling cascades are absent or vague in this study but the insinuation is that as PPAR γ is upregulated, so too is the phagocytosis of *M. leprae*.

Indeed, stimulation of PPAR γ with the agonist MDG548 has been shown to increase phagocytosis in the murine microglial cell line MMGT12 and increase the levels of the mannose receptor and a scavenger receptor (CD68) (Lecca et al., 2018). Interestingly, when cells were not pre-stimulated with bacterial lipopolysaccharide (LPS), PPAR γ activation increased phagocytosis of necrotic neurons but not latex beads. Only when cells were pre-stimulated with LPS was there an increase in bead consumption (Lecca et al., 2018).

In the current study, activation of the *V. vermiformis* PPAR-like molecule with known agonists, and CBD, did *not* result in increased phagocytosis; quite the opposite. The reason for this is currently unknown. However, it is interesting that both models (Figs. 5.9 and 5.10), and the study of Lecca et al. (2018), involve a PPAR-induced *genomic* response in the nucleus and therefore appear to be describing PPAR activation via mechanism 3 (See 1.2.4.1. and Fig. 1.4). There has been no mention to date of a possible link between the mannose receptor (or indeed any other receptor) and a PPAR-induced *non-genomic* response, which we hypothesise to occur in protists. This might be the reason for the different responses obtained here although this will require further study.

5.4. Conclusions

Of the 19 amoeba genera tested, it was only *V. vermiformis* that responded to PPAR agonists. All seven *V. vermiformis* strains were susceptible to OEA and GW0742 but there were strain differences with regards to their susceptibility to PEA and Rosiglitazone. Each PPAR agonist induced the same feeding response as CBD, i.e., a feeding lag followed by reduced ingestion rate. These negative responses were eliminated by blocking the PPAR with a specific antagonist. Only the blocking with the PPAR α antagonist eliminated the negative effect of CBD.

It is hypothesised that *V. vermiformis* does not contain three separate PPAR isoforms but contains a promiscuous PPAR-like molecule which can bind PPAR agonists and antagonists; and CBD at the α -binding site. It is also hypothesised that, due to the instantaneous effect of PPAR activation of amoebic feeding, PPAR induces a non-genomic response whereby PPAR does not bind to RXR in the nucleus but binds to other proteins outside the nucleus. From the limited information available on this response, potential proteins for PPAR-binding included Syk, LAT and PKC which are all involved in the very early stages of receptor-mediated phagocytosis (whether opsonized or non-opsonized).

Amoebae feed by non-opsonized phagocytosis and receptors for mannose, GalNAc and GlcNAc exist in *V. vermiformis* but CBD did not appear to interact directly with any of them (Chapter 4). There is however evidence for cross-talk between the mannose receptor and PPAR γ in macrophages, with the activation of both leading to increased phagocytosis, possibly

via a PPAR-induced genomic response (information on GalNAc and GlcNAc receptors is unavailable). However, in *V. vermiformis*, activation of PPAR did not increase phagocytosis, it completely stopped feeding for a given period of time. Therefore, the nature of any cross-talk between a feeding receptor and a PPAR in an amoeba appears to be different and might be due to it being a non-genomic response. It might be that un-ligated PPAR binds to a given protein (Syk/LAT/PKC) allowing its phosphorylation and downstream signaling to occur, but on ligation this binding is prohibited, no phosphorylation takes place and the signalling cascade, which would normally culminate in actin polymerisation and phagocytic cup formation, becomes non-functional (in the lag) and less functional (after the lag).

Chapter 6: Involvement of the dopamine and serotonin receptors in the mode of action of CBD against amoebae

6.1. Introduction

The serotonin and dopamine receptors are neurotransmitters that are involved in physiological processes such as appetite, emotion, movement and cognition (de Pedro et al., 1998a, b; Frazer and Hensler, 1999; Mishra et al., 2018). There are at least seven distinct serotonin receptor families (5-HT₁ up to 5-HT₇) (Frazer and Hensler, 1999) with all but 5-HT₃ (a ligand-ion channel) being GPCRs (Mazák et al., 2009). CBD has been shown to bind to 5-HT_{1A} (De Gregorio et al., 2019) while AEA has been shown to bind 5-HT₃ (Racz et al., 2008). Dopamine receptors are all GPCRs and the family consists of D1, D2, D3, D4 and D5 receptors (Rashid et al., 2007). AEA and CBD have been shown to bind to D2 (Beltramo et al., 2000; Seeman, 2016) while THC has been shown to bind to D1 (Miyamoto et al., 1996).

Dopamine receptor D1 has been identified in the ciliate *Tetrahymena thermophila* and serotonin receptors have been identified in *Tetrahymena pyriformis* (Csaba et al., 2010; Ud Daula et al., 2012). So, this part of the study evaluated whether amoebae might have them, and whether they played a role in the AEA/CBD-induced reduction in population growth (observed in Chapter 3) and CBD-induced feeding lag and reduced ingestion rate (observed in Chapters 4 and 5).

The following experiments used four blockers. Haloperidol is considered 'general' blocker, as it blocks both receptor types. However, it does possess a higher affinity for serotonin receptors (particularly 5-HT₂) over dopamine receptors (Kroeze et al., 2003; Li et al., 2016). It also exhibits selectivity for D2-like dopamine receptors with K_i values of 1.2, 1.7, 2.3, 80 and 100nM for D2, D3, D4, D1 and D5, respectively (Lindsley and Hopkins, 2017). Two blockers were specific for dopamine receptors. The first, LE 300, is a potent D1 antagonist with K_i values of 0.08-1.9nM and 6-45nM for D1 and D2, respectively, although it does also display a moderate affinity for the 5-HT_{2A} receptor (K_i value of of 20nM) (Kassack et al., 2002). The second was L741,626, which exhibits a strong antagonistic affinity for D2 with K_i values of 2.4, 100 and 220nM for D2, D3 and D4, respectively (Strange, 2008). The final blocker was (S)-WAY 100135 dihydrochloride, a potent and selective inhibitor of the serotonin receptor 5-HT_{1A} (IC₅₀

of 15nM) with very little sensitivity towards 5-HT_{1B}, 1C, 2, α 1, α 2 and D2 (IC₅₀ > 1000nM) (Fletcher et al., 1993).

6.2. Results

6.2.1. Growth experiments with Haloperidol

All strains that were sensitive to AEA and/or CBD (Table 3.2) were subjected to population growth experiments (with AEA and CBD at their IC₅₀, Table 3.3) in the presence/absence of 10 μ M Haloperidol (added 20 min prior to agonist). Haloperidol was slightly toxic to amoebae at this concentration and induced a significant (P<0.05) 5-10% reduction in growth, compared to the Control, in most amoebae. The only exceptions were *Acanthamoeba castellanii*, *Flamella arnhemensis*, *Hartmannella cantabrigiensis* (CCAP1534/11) (see Appendix 7) and *Naegleria gruberi* (Fig. 6.1).

Only *N. gruberi* showed 100% blocking (P<0.01) by Haloperidol of the negative effect of CBD; it did not block the negative effect of AEA (Fig. 6.1) (data for other strains in Appendix 7).

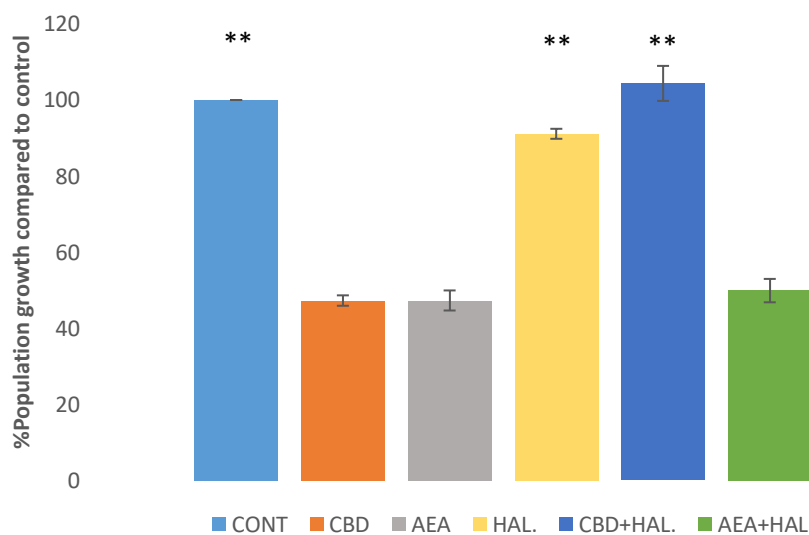


Fig 6.1: Blocking putative dopamine and serotonin receptors in *Naegleria gruberi* with Haloperidol (10 μ M) pre-incubation abolished the negative effect of CBD (at 0.72 μ M) on population growth but did not affect the action of AEA (at 1.15 μ M). **Significant difference (P<0.01) to agonist alone.

A dose response experiment, performed three times, showed that the population growth of *N. gruberi* with CBD alone (0.72 μ M) was significantly lower than in the presence of 10 μ M and 1 μ M Haloperidol ($P < 0.01$) but was equivalent in the presence of 0.1 μ M Haloperidol ($P = 0.75$), suggesting an MIC $< 1\mu$ M (Fig. 6.2).

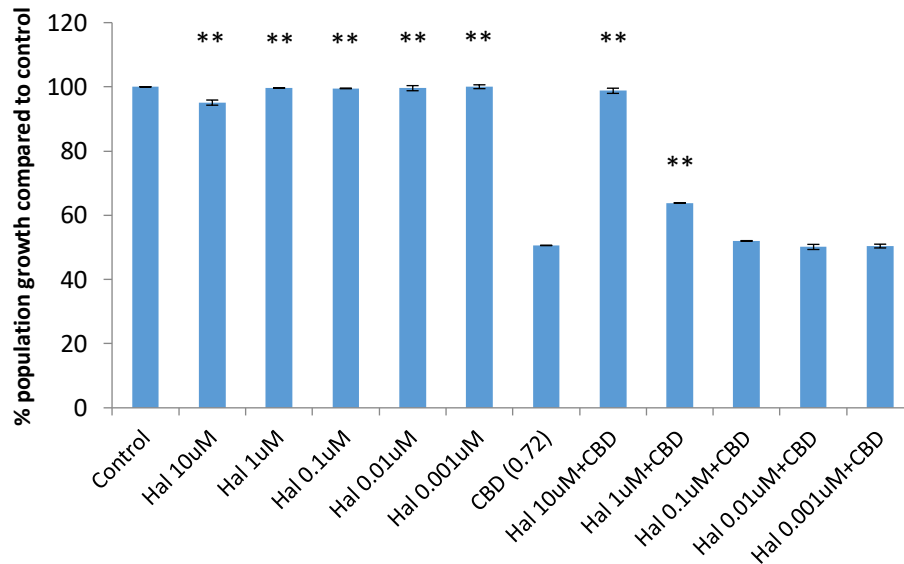
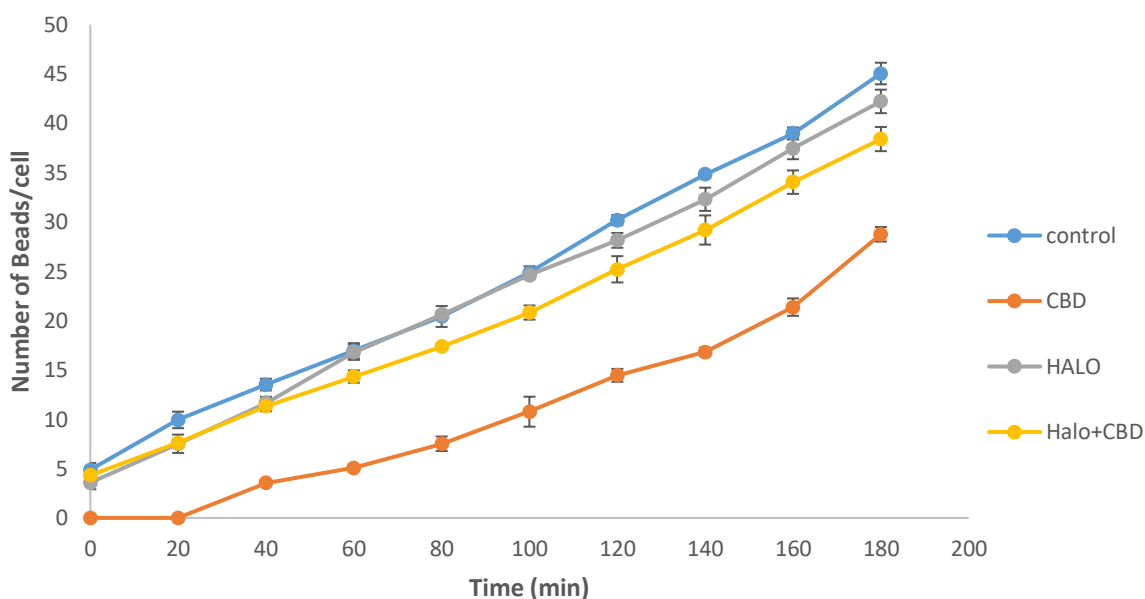


Figure 6.2: Population growth (compared to the Control) of *Naegleria gruberi* in the presence of CBD (at 0.72 μ M), with/without a pre-incubation with different concentrations (0.001-10 μ M) of Haloperidol. Growth in the presence of Haloperidol alone is also shown. **Significant difference ($P < 0.01$) to CBD alone.

6.2.2. Feeding experiment with Haloperidol

The feeding of *N. gruberi* on beads was monitored in the presence of CBD (0.72 μ M) with/without 10 μ M Haloperidol. Experiments were performed three times. CBD induced a lag of 24 min (Fig. 6.3) and then ingestion rate was significantly lower compared to the other three treatments ($P < 0.01$). The presence of Haloperidol, with CBD, abolished the lag phase and alleviated the negative effect on ingestion rate, although it was not 100% alleviated as rates for Haloperidol alone and Haloperidol with CBD were significantly different ($P < 0.01$).

Thus, either the blocking of the dopamine receptor or serotonin receptor (or both) were considered responsible for this alleviation of the negative effect of CBD. Experiments went on to try and separate out these two receptors using more specific blocking agents.



Treatment	Ingestion rate (prey/cell/min)	Lag Phase (min)
Control	0.217±0.001	0.00±0.00
Haloperidol only	0.211±0.009	0.00±0.00
CBD	0.150±0.006**	24.16±2.72**
CBD + Haloperidol	0.190±0.008	0.00±0.00

Figure 6.3: Feeding of *Naegleria gruberi* on beads in the presence/absence of CBD (at 0.72µM), with/without a pre-incubation with 10µM Haloperidol. Feeding in the presence of Haloperidol alone is also shown. Calculated specific ingestion rates (prey/cell/min) and lag phases (min) also shown. **Significant difference (P<0.01) to Control [0µM].

6.2.3. Growth experiments with separate dopamine and serotonin receptor blockers

Growth experiments were carried out with *N. gruberi* and CBD (0.72µM) in the presence/absence of three blockers at concentrations ranging from 0.001 to 10µM. Experiments were performed three times. Experiments with LE300, specific for dopamine D1, were unsuccessful because the blocker itself was toxic to *N. gruberi* even at 0.001µM. At this concentration it was more toxic than CBD alone at its IC₅₀ (Fig. 6.4a).

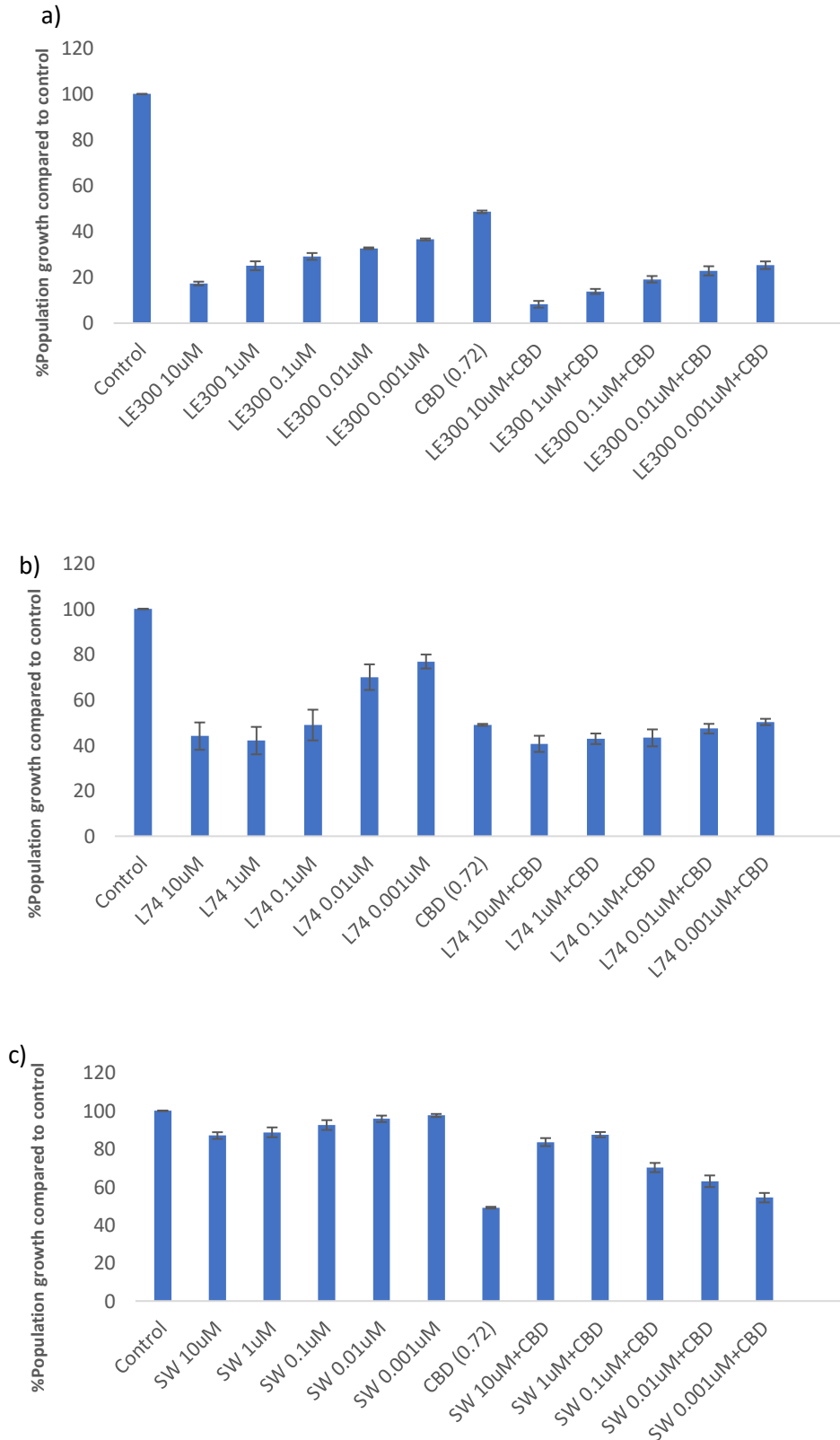


Figure 6.4: Effect of different concentrations of a) LE300 (dopamine D1 blocker), b) L741,626 (dopamine D2 blocker) and c) (S)-WAY 100135 (serotonin 5-HT_{1A} blocker) on *Naegleria gruberi* population growth in the presence/absence of CBD (at 0.72 μM).

L741,626, which specifically blocks D2, was also toxic to *N. gruberi* and yielded a 40-50% population growth, compared to the Control, in the presence of 10, 1 and 0.1 μ M (Fig 6.4b). It was less toxic at 0.01 and 0.001 μ M which allowed some level of statistical analysis to be carried out. It appeared that blocking this receptor at 0.001-0.01 μ M had no significant effect on the action of CBD (ANOVA $P=0.11$).

The final blocker was (S)-WAY 100135 dihydrochloride which is a potent and selective 5-HT_{1A} antagonist (Fig. 6.4c). This blocker was not as toxic to *N. gruberi* as the dopamine receptor blockers but it did significantly reduce population growth by 15% at 10 and 1 μ M S-WAY ($P<0.01$) but not at 0.1 μ M ($P=0.11$). CBD alone (at 0.72 μ M) reduced population growth by 50% and this was alleviated by S-WAY concentrations of 10 to 0.01 μ M ($P<0.01$) but not at 0.001 μ M ($P=0.54$) suggesting an MIC $<0.01\mu$ M. The blocking of CBD by S-WAY was 100% effective at concentrations of 10 and 1 μ M with no significant difference between the effect of S-WAY alone and S-WAY+CBD ($P = 0.27$ and 0.69 , respectively). Blocking was not 100% effective at 0.1 μ M and 0.01 μ M, indicating that a dose-response exists here.

6.3. Discussion

6.3.1. Effect of CBD on *N. gruberi* feeding

The feeding of un-treated *N. gruberi* showed no feeding lag and gave an ingestion rate of 0.217 ± 0.001 beads/cell/min (Fig. 6.3). This is within the range recorded for the similar-sized (Table 3.4) *V. vermiformis* feeding on the same concentration of beads (0.17-0.28 prey/cell/min, Chapters 4 and 5). The presence of CBD (at 0.72 μ M) induced a feeding lag of ca. 24 min and reduced the ingestion rate compared to the Control (Fig. 6.3). The lag was shorter than those recorded by *V. vermiformis*, but these themselves were highly variable (34.42-74.41, Chapters 4 and 5); a feature of the response that is currently unexplainable.

However, what this experiment showed was that CBD's negative effect on feeding occurs in a different species to *V. vermiformis* and so evidence is starting to build up that the reduction in amoebic population growth over three days might be primarily due to its effect on feeding. However, this cannot be said for AEA, as demonstrated by a lack of effect on *V. vermiformis* feeding with this cannabinoid (Figure 4.2).

6.3.2. Blocking experiments

6.3.2.1. Suitability of the chosen receptor blockers

Of the four blockers used in this study, data from only two were reliable enough for robust statistical analysis, i.e., Haloperidol and S-WAY. The dopamine receptor blockers were very toxic to *N. gruberi* and induced a reduction in population growth at concentrations of 0.001 μ M (LE 300) and 0.01 μ M (L741,626). These were lower than the toxic concentrations of S-WAY (0.1 μ M) and Haloperidol (10 μ M). The supplier's safety data sheet (TOCRIS) has no available data on the toxicity of LEE 300, L741,626 and S-WAY but classifies Haloperidol (the least toxic to amoebae) as being acutely toxic. Although these experiments gave encouraging results with regards to the presence of a putative serotonin receptor in *N. gruberi*, less toxic dopamine receptor blockers should be sought in order to repeat these experiments.

6.3.2.2. Population growth of amoebae in the presence of AEA and CBD with/without Haloperidol

The population growth of 6 amoeba species (13 strains, Table 3.3) were monitored in the presence of AEA/CBD with/without 10 μ M Haloperidol. Only one species, *N. gruberi*, showed an alleviation of the CBD effect, but not the AEA effect (Fig. 6.1). Haloperidol blocking was then shown to act in a dose-dependent manner ($\text{MIC} > 0.1 \leq 1 \mu\text{M}$, Fig. 6.2). This was a species that had not been responsive to PPAR agonists (Table 5.1). Conversely, all seven *V. vermiformis* strains responded PPAR blocking (see 5.2.1.2) but none responded to Haloperidol.

This might suggest an either/or situation with regards to what cannabinoid receptor is present in amoebae, as opposed to their cells possessing multiple targets, but it is far too early to say for definite. But it was expected that *V. vermiformis* would show a response to Haloperidol because there are some studies which have reported a link between OEA, PPAR α and the dopamine receptor (Melis et al., 2008; Luchicchi et al. 2010; Tellez et al. 2013; Hankir et al. 2017). The proposed mechanism also involves a non-genomic effect whereby PPAR α receptor activation by OEA, activates protein kinases responsible for the phosphorylation status of the nicotinic acetylcholine receptors (nAChRs). This then modifies the response of dopaminergic neurons to nicotine (Melis et al. 2008; Luchicchi et al. 2010). Considering the action of CBD

on *V. vermiformis* was most like OEA, it involved 'PPAR α ' and we considered PPAR-induced non-genomic effects to occur in amoebae (Chapter 4), this study expected a concomitant dopamine receptor to be present, but it was not. However, it would be worth testing this amoeba species again with specific (non toxic!) dopamine receptor blocker as Haloperidol, even though it can block dopamine receptors, has a much higher affinity for serotonin receptors (Kroeze et al., 2003; Li et al., 2016); and it was a putative serotonin receptor that was identified in *N. gruberi* with both Haloperidol and S-WAY.

Also, Haloperidol is described as a classic antipsychotic that employs its action mainly via dopamine D2 receptor antagonism and slow receptor dissociation kinetics (Li et al., 2016). In addition, Haloperidol is a subtype-selective N-methyl-D-aspartate antagonist that belongs to the first generation of antipsychotic drugs which can be classified into different chemical classes such as phenothiazines (Samara et al., 2014), thioxanthenes (Fux and Belmaker, 1991) and diphenylbutylpiperidines (Gunduz-Bruce et al., 2013). It is the most common antipsychotics drug used in the treatment of patients diagnosed with chronic or acute schizophrenia disorder (Geddes et al., 2000). Haloperidol is also used in the therapy of other disorders, for instance, psychosis, bipolar and behavioural disorders (i.e. hyperactivity) (Kudo and Ishizaki, 1999). However, there is evidence that it does not alleviate the effect of CBD in patients. Zuardi et al. (1995) studied the administering of Haloperidol in patients with schizophrenia who had been given CBD. Haloperidol had no effect on the antipsychotic action of CBD.

6.3.2.3. Population growth of *N. gruberi* in the presence of CBD with/without S-WAY

A putative serotonin receptor was identified in *N. gruberi* based on the fact that Haloperidol and S-WAY both blocked the negative effect of CBD on population growth. This was an interesting result because CBD is known to bind to 5-HT_{1A} in animals (De Gregorio et al., 2019) and S-WAY is a potent and *very* selective inhibitor of 5-HT_{1A} (Fletcher et al., 1993). Indeed, De Gregorio et al. (2019) showed that rats treated with a repetitive low dose of CBD exhibited a reduction in anxiety symptoms after activation of the 5-HT_{1A} receptor, and that this anti-anxiety effect was alleviated by a potent 5-HT_{1A} antagonist (WAY 100635). Others have found similar responses in different animal models (Hind et al., 2016; Sartim et al., 2016; Lee et al., 2017).

Considering a serotonin receptor has been reported to be present in *Tetrahymena pyriformis* (Csaba et al., 2010) it is not inconceivable that *N. gruberi* might possess one too. The study of Csaba et al. (2010) however is vague, and little can be gained regarding any direct cellular effect of receptor-ligand binding. Phagocytes of the immune system possess serotonin receptors and have been studied more extensively; although there is still very little with regards to their role in phagocytosis. Macrophages possess serotonin receptors of the 5-HT₂ class (Sternberg et al., 1986) while monocytes possess receptors from five of the seven families (5-HT₁ up to 5-HT₅) (Hellstrand and Hermodsson, 1993; Dürk et al., 2005). With regards to feeding, Nannmark et al. (1992) showed that direct treatment of polymorphonuclear leukocytes with serotonin suppressed zymosan-induced phagocytosis. In contrast, Northover (1961) showed that serotonin stimulated polymorphonuclear leukocyte phagocytosis of staphylococci and Schuff-Werner and Spletstoesser (1999) went on to show that this was dose-dependent. And, *in vivo*, CBD has been shown to stop the hyperphagia behaviour in rats that is activated by 5-HT_{1A} receptor agonist 8-OH-DPAT (Scopinho et al., 2011).

6.4. Conclusions

Of the 6 amoeba species (13 strains) tested, it was only *N. gruberi* that responded to the antagonistic action of Haloperidol and S-WAY, in the presence of CBD. Both blockers abolished the effect of CBD on population growth at 10 and 1µM, but not at 0.1µM. CBD induced a feeding lag and reduced ingestion rates, as had been previously recorded with *V. vermiformis*. This now shows that the feeding of at least two amoeba species is affected by CBD, and is the possible reason for reduced population growth over three days. Haloperidol abolished the feeding lag and reduced ingestion rate at 10µM. It is hypothesised that CBD is binding to the 5-HT_{1A} receptor, as it does in higher animals.

Chapter 7: General Discussion

Endocannabinoids, e.g. Anandamide (AEA), are lipid compounds which together with their receptors (e.g. CB1, CB2), and metabolizing enzymes, form the human endocannabinoid system (ECS) (Greydanus et al. 2013); affecting mood, cognition, appetite, pain, memory etc. Similar effects are activated by Cannabis due to Δ 9-tetrahydrocannabinol (THC, psychoactive) and cannabidiol (CBD, non-psychoactive) receptor-binding. However, many of their effects cannot be attributed solely to binding to these receptors and another 63 molecular targets have been proposed (Bih et al. 2015). Further knowledge regarding these alternative targets could increase the potential therapeutic use of phytocannabinoids.

Single-celled protists such as amoebae and ciliates do not possess any of the main cannabinoid receptors (CB1, CB2, GPR55 and TRPV1) (McPartland et al. 2006) yet they respond to cannabinoids, often showing a reduction in motility and arrest in cell division (McClellan & Zimmerman 1976; Pringle et al. 1979; Zimmerman et al. 1981; Dey et al. 2010). Accordingly, these protists offer an opportunity to examine the role of alternative molecular targets in the action of cannabinoids on cells. This study therefore evaluated the role of three such targets (PPAR, Dopamine, Serotonin) on the action of CBD and AEA on naked amoebae.

7.1. Amoebic sensitivity to AEA and CBD

A total of 27 amoeba strains, which comprised 20 species, were tested for their sensitivity to AEA and CBD. Fourteen species (70%) were insensitive while 6 species (30%) were sensitive. All 6 were sensitive to CBD but only 4 were also sensitive to AEA. There appeared to be no correlation between sensitivity and phylogenetic position, with differences in sensitivity being evident within a single order (e.g. Order Echinamoebida - *Vermamoeba* “sensitive”, *Echinamoeba* “not sensitive”). Also, differences within a single family were recorded (e.g. family Hartmannellidae - *Hartmannella* “sensitive”, *Saccamoeba* “not sensitive”) and even a difference within the same genus (e.g. *Acanthamoeba* – *A. castellanii* “sensitive”, *A. polyphaga* “not sensitive”).

Regarding cell size, in general, the susceptible strains were at the lower end of the cell size spectrum (Table 3.4), However, the very high concentration used (200 μ M) would have been

expected to significantly affect the very small cells of *P. filosum* and *E. silvestris* if cell size was a compounding factor, but it did not.

Lastly, there was no relationship between sensitivity and the source of the amoeba, for example, *V. vermiformis* strains were isolated from different environments (soil and freshwater) in four different countries and all were sensitive to CBD and AEA.

For those sensitive strains, CBD and AEA reduced population growth over 3 days in a dose-dependent manner and, higher concentrations proved lethal. Lower concentrations induced a lag followed by reduced growth rate which was dose dependent. It was discovered that, for CBD, this reduction in population growth was due to the disruption of amoebic feeding (Section 7.3) however, this was not the case for AEA (Section 7.2).

7.2. Amoebic response to AEA

AEA, at 2 μ M, had no significant effect on *V. vermiformis* feeding, although a slight lag was evident. However, the AEA concentration might have been too low to give a significant result. A concentration of 2 μ M AEA (and CBD) was chosen as this value was close to their IC₅₀ values and would allow a direct comparison of their effect. But, 2 μ M is above the IC₅₀ for CBD (IC₅₀ = 1.01 μ M) and below the IC₅₀ for AEA (IC₅₀ = 2.33 μ M) (Table 3.3). Experiments should be repeated with higher concentrations of AEA to confirm/deny any effect on feeding in this amoeba.

AEA, at 2 μ M, did have a significant effect on *V. vermiformis* population growth however, and considering this is not due to reduced feeding the reason for this remains unknown. Population growth relies on successful ingestion and assimilation of prey so the mode of action of AEA might be at the assimilation stage, and not the ingestion phase.

Assimilation is the process by which digested material in the food vacuole/phagosome is absorbed into the cytoplasm of the cell to generate progeny (Verma, 2001). In protists, assimilation efficiency, or more commonly termed Gross Growth Efficiency (GGE), is defined as the volume of carbon produced (in protists) from the volume of prey consumed (Rose et al., 2009). GGEs are always <100% because protists notoriously convert much of the organic carbon, nitrogen and phosphorus in their prey to inorganic forms, then release them in a process known as remineralisation (Coull and Chandler, 2001).

GGE estimates for amoebae are rare but one study (Butler and Rogerson, 1996) provided estimates for 10 species at 20°C which is close to the 23°C used in the current study. GGEs ranged from 13.7% to 56% with variations within a genus being evident: 13.7-20.8% (*Stereomyxa ramosa*, *Dactydamoeba* sp., *Rhizamoeba* sp.), 26.6-36.1% (*Vannella caledonica*, *Paraflabellula reniformis*, *Vahlkampfia baltica*) and 41.1-56% (*Clydonella rosenfieldi*, *Platyamoeba* sp., *Vahlkampfia damariscottae*, *Vannella* sp.) (Butler and Rogerson, 1996). Zubkov and Sleigh (1998) recorded a GGE of 60% for *Vannella septentrionalis* but no temperature was stated, and it is known that GGEs increase with increasing temperature which suggests that amoebae convert food into biomass with increased efficiency at higher temperatures (Butler and Rogerson, 1996).

The energy required for assimilation and cellular respiration is provided by mitochondria. It has been reported the AEA can directly inhibit the function of mitochondria in rats and decreased the sensitivity of Ca^{2+} in a dose-dependent manner (Catanzaro et al., 2009). The study continued to indicate that these effects are not due to AEA receptor binding, but due to its direct effect on mitochondria and it was accompanied with decreasing of membrane potential and increasing the fluidity of the membrane. Moreover, AEA has been proposed to inhibit the synthesis of ATP (Zaccagnino et al., 2011). In addition, treatment with AEA reduced the respiration of mouse brain mitochondria by 30% mediated by CB1 receptor (Bénard et al., 2012). Anandamide also inhibited the activity of complexes I, II/III and IV of transport chain in pig brain mitochondria (Singh et al., 2015). Other studies indicate that AEA negatively affects the function of mitochondria in different tissues such as the nerve cells and sperm resulting in an inability to perform their functions properly (Rossato et al., 2005; Zaccagnino et al., 2011). In addition, AEA has been shown to reduce oxygen consumption and decrease the potential of the mitochondrial membrane, and its permeability, in rats (Epps et al., 1982; Athanasiou et al., 2007).

Considering amoeba possess mitochondria, they could be a possible target for AEA. Further studies on the effect of AEA on mitochondria in amoebae should be performed to evaluate whether AEA is targeting the mitochondria or not, and this could be carried out by measuring the ATP molecules produced and the activity of the ATPase enzyme. Zaccagnino et al. (2011) examined the effect of AEA on mitochondria by direct measurements of mitochondrial FoF1 ATP synthase complex. This study concluded that AEA inhibited the oxidative phosphorylation

and reduced the releasing of ATP, resulting in dysfunction of mitochondria. Repeating such a study Including measurements of oxygen consumption with amoeba would be beneficial

Alternatively, AEA might directly target the cell cycle of amoeba as it has been reported to cause anti-proliferation action on mammalian carcinoma cells (Xie et al., 2012). This study indicated that AEA caused inhibition of proliferation in the Huh7 cell line by causing cell cycle arresting at the G1 phase and stimulated apoptosis. In addition, AEA can inhibit cancerous cells in the gastric gland to arresting the cell cycle in the G2/M phase (Dong et al., 2014). Furthermore, other cannabinoids such as CBD have been shown to have anti-proliferation and anti-differentiation effects on *Dictyostelium discoideum* (Bram et al., 1976).

Whatever the mode of action, it did not appear to involve the binding of AEA to receptors for PPAR, Dopamine or Serotonin, as when these receptors were blocked with antagonists there was no alleviation of the AEA-induced reduction in population growth. AEA therefore seems to act on cells in a very different manner to CBD and future work should look at whether any of the other molecular targets summarised in Bih et al (2015), such as opioid and acetylcholine, are involved.

7.3. Effect of CBD on amoebic feeding

7.3.1. Amoebic feeding in the absence of CBD

Feeding experiments with *V. vermiformis* showed that it could ingest inert beads and live *Synechococcus* at equivalent rates. These rates were reduced in the presence mannose, GalNac and GlcNac suggesting that this amoeba possesses three corresponding C-type lectins.

Many studies have indicated that C-type lectin receptors are involve in the feeding of amoeba, particularly lectins for mannose (Bracha et al., 1982; Allen and Davidowicz, 1990; Garate et al. 2004; Alsam et al., 2005) and GalNac (Ravdin and Guerrant, 1981; Ravdin et al., 1985; Petri et al., 1987; Venkataraman et al., 1997; Harb et al., 1998; Bär et al., 2015). The current study recorded a reduction in ingestion of *Synechococcus* by *V. vermiformis* in the presence of mannose, GalNac and GlcNac, however, no lag phase was induced. GlcNac was the most potent sugar blocker (73% reduction in feeding), followed by mannose (66% reduction) and then GalNac (53% reduction).

Treatment with GlcNAc led to the strongest inhibition of ingestion in *V. vermiformis* suggesting it was not only binding 'weakly' to a mannose receptor but also/instead binding 'strongly' to its own receptor. In addition, blocking with GlcNAc affected the duration of the CBD-induced lag phase whereas blocking with mannose and GalNAc did not. These data therefore support the case for presence of three distinct sugar receptors in *V. vermiformis*, as has been suggested for *D. discoideum* (Bozzaro & Roseman, 1983) and more recently, for *T. pyriformis* (Boboc, 2019). Future work could look at other amoebae and see if this is a common feature between them.

In addition to C-type lectins, another group of receptors (Scavenger receptors, SRs), that are also surface membrane glycoproteins, are used for the recognition of carbohydrates in prey to facilitate phagocytosis (Perún et al., 2016). The Class B scavenger receptors bind to the lipoteichoic acid of Gram-positive bacteria (Hoebe et al., 2005; Stuart et al., 2005) and the lipid A of the lipopolysaccharide layer of Gram-negative bacteria (Baranova et al., 2008). In 2018, Sattler et al reported that *D. discoideum* possesses homologous receptors to the mammalian class B scavenger receptors, LIMP-2 and CD36, i.e. LmpA and LmpB, respectively. The LmpA was found in endosomes and phagolysosomes and played a role in the binding and phagocytosis of bacteria (particularly Gram-positive strains) while LmpB was localized to the plasma membrane and early phagosomes and was exclusively involved in the uptake of Gram-positive bacteria (Sattler et al. 2018).

An unpublished study in Lancaster university also investigated the participation of SRs in the feeding of protist, specifically, in the ciliate *T. pyriformis* (Parry, unpublished). The study concluded that SRs were not involved in the uptake of *Pseudomonas aeruginosa* however, they appear to be involved in the uptake of live *Synechococcus* cells. Since the current study employed the same prey (live *Synechococcus* cells) in amoebic feeding experiments, it would be interesting to see if CBD interacts with these receptors in *V. vermiformis* (using Dextran Sulphate to block the scavenger receptors).

7.3.2. Amoebic feeding response in the presence of CBD

CBD induced a feeding lag followed by a reduced ingestion rate in both *V. vermiformis* and *N. gruberi*. This should be tested on the other 4 susceptible amoeba strains to confirm that this

is the inherent effect of CBD on amoebae (and not just the specific effect on these two species).

The long-term effect of CBD on *V. vermiformis*, compared to *T. pyriformis*, was thought to be due to a reduced capacity for metabolizing CBD within the amoebic cell (possibly due to the lack of CYPs). It is unknown whether these protists differ in their ability to degrade CBD, which might affect its longevity in their cells. In all human cells, CBD is metabolised by cytochrome P450 oxidases, sulfotransferases and glucuronyl transferases (Ujváry and Hanus, 2016). Most work has been performed on P450 oxidases (CYPs) which are enzymes necessary for the metabolism of drugs (Šrejber et al., 2018). Even though more than 50 CYP enzymes exist, only six of them (CYP1A2, CYP2C9, CYP2C19, CYP2D6, CYP3A4, and CYP3A5) are responsible for metabolising 90% of medicinal drugs (Lynch and Price, 2007). Of these, CYP2C19 metabolises CBD, (Stout and Cimino, 2014). Interestingly, *Tetrahymena thermophila* possesses 102 CYP homologues (www.ciliate.org), the slime mould *Dictyostelium discoideum* possesses 9 (www.dictybase) whilst *Acanthamoeba castellanii* possesses only 1 and *Entamoeba* spp. and *Naegleria fowleri* possess none (www.amoebadb.org). Although there is very little information on the amoeba with regards to metabolism of CBD (Ujváry and Hanus, 2016), it might be that *V. vermiformis*, like other amoebae, possesses a limited ability to degrade CBD within their cells and this might explain the longevity of the drug action on *V. vermiformis*, compared to *T. pyriformis*.

Moreover, the longevity of drug in the cell is depending on the efficiency of dissociation of drug from its corresponding receptor (Vauquelin and Charlton, 2010). Therefore, the rate of dissociation is considered a crucial element to determine the effectiveness of drugs, the slower the dissociation rate, the longer the effect will last (Holdgate, 2017). This rate depends on different factors including temperature and the existence of the catalysis enzymes (Cooper, 2000).

The enzymes responsible for catalysis and metabolism of lipids are present dominantly in the endoplasmic reticulum (ER) (Raff et al., 2002). Since CBD is a lipid molecule, it raises the possibility that the effect of CBD on amoeba might be occurring within the ER, leading to a slow dissociation of this cannabinoid and long lasting activity in these cells. Also, it has been reported that CBD causes apoptosis of Hepatic stellate cells (HSC) in mice by evoking stress

activity on the ER by stimulating Protein kinase R-like endoplasmic reticulum kinase (Lim et al., 2011). Thus, a study to examine the effect of CBD on the ER in amoeba would be interesting step to evaluate the extent of CBD potency on them.

The fact that a longer feeding lag resulted in a lower subsequent ingestion rate suggested the two responses are coupled in some way. CBD did not appear to directly interact with *V. vermiformis*'s feeding receptors, so it was proposed that CBD's target was a yet unidentified receptor. When the C-type lectins were individually blocked (mannose, GalNAc and GlcNAc) in the presence of CBD, there was no interaction between mannose and GalNAc receptors and CBD. However, the GlcNAc receptor 'interacted' with CBD, as blocking this receptor in the presence of CBD led to double the duration of feeding lag. It was hypothesised that the unidentified CBD receptor and GlcNAc receptor were both involved with controlling phagosome formation rate whereas receptors for mannose and GalNAc are involved with prey capture and phagosome filling. No other studies have been carried out on this process to which the results of this study can be compared.

7.4. Mode of action of CBD in *V. vermiformis*

There are many stages involved in the successful formation and processing of phagosomes and a 'CBD-receptor' could be involved in any of these stages. But, based on experimental evidence, this receptor was not considered to be involved in phagosome closure, detachment, trafficking, defecation and endocytosis. Instead, it was considered to be involved in phagosome formation) and/or membrane recycling.

The mechanism of phagosome formation and maturation in protists is still poorly described but is considered to be similar to that of macrophages. the process begins when the phagocytic cell recognises the binding ligands of the prey cell in a receptor-dependent way (Levin et al., 2016). This recognition leads to signal pathways that stimulate the re-shaping of the actin cytoskeleton and the extension of pseudopodia to enclose the prey in a phagocytic cup (Duhon and Cardelli, 2002; Cosson and Soldati, 2008; Pauwels et al., 2017). The complete closing of the phagocytic cup leads to the formation of the phagosome, which is inert until it matures via a complicated series of fusion events with endosomes and then with lysosomes (which contain digestive enzymes) (Haas, 2007; Pauwels et al., 2017). The final stage is the defecation of waste materials and the recycling of the phagosome membrane to make new

phagosomes (Allen and Fok, 1980; Gotthardt et al., 2002). It has been highlighted that Syk, LAT and PKC are involved in the initial stages of phagosome formation in macrophages; in specific, the signaling cascade in the recognition of prey and signalling pathway of extension of pseudopodia to form the phagocytic cup (Unsworth et al. 2018).

As far as the possible identity of the CBD-receptor was concerned, three potential targets were evaluated (PPAR, Serotonin, Dopamine). Of the three, only the blocking of PPAR α resulted in the alleviation of the CBD effect in *V. vermiformis*. This was a very specific interaction as, out of all 20 amoebic species tested, it was only *V. vermiformis* that responded to PPAR agonists. All seven *V. vermiformis* strains were susceptible to OEA and GW0742 but there were strain differences with regards to their susceptibility to PEA and Rosiglitazone. Each PPAR agonist induced the same feeding response as CBD, i.e., a feeding lag followed by reduced ingestion rate. These negative responses were eliminated by blocking the PPAR with a specific antagonist. Only the blocking with the PPAR α antagonist eliminated the negative effect of CBD.

PPARs have been shown to interact with Syk, LAT and PKC proteins in the Non-genomic regulation of platelets (Unsworth et al. 2018), whereas PPAR α and PPAR β ligands result in a decrease in intracellular mobilization of calcium and activation of platelets (Unsworth et al. 2017). This inhibition is due to the reduction of PKC α potency through its interaction with PPAR α or PPAR β , which determines its availability to facilitate downstream signalling (Ali et al., 2009). Treatment with PPAR γ ligands inhibit Syk and LAT phosphorylation that mediate signaling initiated by the GPVI collagen receptor (Unsworth et al. 2018).

Therefore, it is hypothesised that *V. vermiformis* contains a promiscuous PPAR-like molecule which can bind PPAR agonists and antagonists, and CBD at the α -binding site. Due to the instantaneous effect of CBD on amoebic feeding, it suggests that PPAR induces a non-genomic response whereby PPAR binds to proteins outside the nucleus. Potential proteins for PPAR-binding included Syk, LAT and PKC which are all involved in the early stages of receptor-mediated phagocytosis. It might be that un-ligated PPAR binds to this protein allowing its phosphorylation and downstream signaling to occur, but on ligation this binding is prohibited, no phosphorylation takes place and the signalling cascade, which would normally culminate

in actin polymerisation and phagocytic cup formation, becomes non-functional (in the lag) and less functional (after the lag).

Protein phosphorylation is a distinctive sign of signalling cascades and has a crucial role in different biological activities in the cell, such as detection of activation and deactivation of receptors (McCance and Huether, 2014). Therefore, further studies to confirm the highlighted hypothesis should be performed on this amoeba by detecting the protein phosphorylation and measure its level using a suitable protein detecting method such as Kinase Activity Assays or ELISA. Also, sequencing could give a deeper understanding on what this amoeba has in its genome.

Although protists do not perform opsonised phagocytosis, complement proteins (CPs) have been found in the cytoplasm of single-cell eukaryotes (Elvington et al., 2016). Vinculin is one such CP, and is an actin binding protein which plays an important role, with Talin and F-actin, in forming stable cell matrix adhesion (De Beco et al., 2012). Vinculin is also a key factor for phagosome formation, and interacts with cascades involving Syk, FAK, Pyk2, and Src (Allen and Aderem, 1996; Jaumouillé et al., 2019). Moreover, it has been indicated that the mechanism of action of alpha-M beta-2 integrins couple to actin cytoskeleton to form the phagocytic cup is mediated by Talin and Vinculin (Allen and Aderem, 1996).

Interestingly, *V. vermiformis* possesses a gene for the Vinculin (Kang et al., 2020) and there is some evidence in other cells, that Vinculin interacts with CBD (Elbaz et al., 2015). Thus, it could be that CBD interacts with Vinculin in *V. vermiformis*, resulting in an inhibition of phagosome formation but this requires testing.

7.5. Comparison of *V. vermiformis* response to cells of higher animals

There are significant similarities between OEA and CBD with regards to their mode of action in animals and *V. vermiformis*. These similarities can be summarised in that OEA has an anorexiant effect in mice, i.e., it can stop feeding completely and then reduce food intake (Rodríguez de Fonseca et al., 2001; Diep et al., 2011). The same response was recorded in *V. vermiformis* with all PPAR agonists and CBD. Moreover, PEA is significantly less potent than OEA and AEA has no effect (Rodríguez de Fonseca et al., 2001; Diep et al., 2011). This response was also recorded with *V. vermiformis*. Furthermore, administration of OEA in mice causes a

dose-dependent delay in the feeding onset (Gaetani et al., 2003; Karimian Azari et al., 2014). Also, the effect of CBD on the feeding lag and ingestion rates of *V. vermiformis* was dose-dependent (dose-responses of PPAR agonists were not performed). In addition, OEA does not reduce feeding in animals if they lack a functional PPAR α gene, suggesting that PPAR α activation is crucial for mediating its hypophagic actions (Fu et al., 2003). Similarly, in the current study, all agonist-induced lags and reduced feeding rates were abolished with PPAR antagonists, and for OEA and CBD, this was the blocking of the PPAR α receptor only.

It is also interesting to note that OEA only evokes a delayed feeding onset and reduced meal size in food-deprived rats (only the former in well fed mice) (Gaetani et al., 2003; Karimian Azari et al., 2014). In the current study, *V. vermiformis* would have also been food-deprived after 7 days culturing prior to experiments. It would be interesting to repeat experiments with well-fed cells to see if only a lag phase is induced.

However, the mode of action of OEA in animals is not completely understood, but it has been reported that an elevated concentration of OEA appears to 'trick' animals into thinking they are full (satiated), which stops them feeding (Rodríguez de Fonseca et al., 2001; Diep et al., 2011). This mode of action might also be pertinent to protists, in that, if membrane is limited for phagosome formation (at satiation), or there are defunct receptor-driven signalling cascades, protists cannot produce pseudopodia to feed (Boenigk et al., 2001).

7.6. Involvement of serotonin receptors in the mode of action of CBD against amoebae

Only *N. gruberi* responded to the antagonistic action of Haloperidol and S-WAY, in the presence of CBD. Both blockers abolished the effect of CBD on population growth at 10 and 1 μ M, but not at 0.1 μ M. CBD induced a feeding lag and reduced ingestion rates, as had been previously recorded with *V. vermiformis*. This showed that the feeding of at least two amoeba species is affected by CBD, and is the possible reason for reduced population growth over three days.

There is very little on the role of serotonin receptors and phagocytosis, however, serotonin has been found to increase the phagocytic action of macrophages in mouse; mediated by the 5-HT_{1A} receptor (Freire-Garabal et al., 2003). Moreover, CBD has been shown to stop the

hyperphagia behaviour in rats when the 5-HT_{1A} receptor is activated by the agonist 8-OH-DPAT (Scopinho et al., 2011). The current study proposed that *N. gruberi* possesses a 5-HT_{1A} serotonin receptor but due to lack of time, the current study could not continue studying the effect of serotonin receptor and CBD on the feeding of *N. gruberi*. This needs further examination to understand the mechanism in which serotonin receptors mediated feeding processes in this amoeba.

7.7. Conclusions

Overall, the study concludes that CBD is more potent against amoebae than AEA and that there is no correlation between sensitivity and amoebic phylogeny. CBD affects amoebic feeding (by targeting vacuole formation/membrane recycling) while AEA might possibly affect processes involved with the assimilation of prey. The study suggests that *V. vermiformis* possesses a promiscuous PPAR-like molecule that can bind CBD at a potential alpha-type site and instigate a non-genomic response which prevents phagocytic cup formation. It is hypothesised that *N. gruberi* possesses a 5-HT_{1A} serotonin-type receptor which can bind CBD but the phagocytic stage which is targeted has yet to be confirmed.

The study has therefore identified that at least two 'alternative' CBD receptors proposed by Bih et al. (2015) are involved in amoebic feeding and population growth. These simple, and easy to culture, cells now provide a viable cell model for further studies on the interaction of these receptors with CBD; as these cells do not possess the 'complication' of having cannabinoid receptors CB_{1/2}, GPR55 and TRPV1, as do other eukaryotic cells. In addition, further work on these amoebae will provide important information on the ancestry of the ECS in eukaryotic cells.

References

- Acosta, C.C.D., Dias, A.A., Rosa, T.L.S.A., Batista-Silva, L.R., Rosa, P.S., Toledo-Pinto, T.G., Costa, F.D.M.R., Lara, F.A., Rodrigues, L.S., Mattos, K.A. and Sarno, E.N., 2018. PGL I expression in live bacteria allows activation of a CD206/PPAR γ crosstalk that may contribute to successful *Mycobacterium leprae* colonization of peripheral nerves. *PLoS pathogens*, 14(7), p.e1007151.
- Adinolfi, B., Romanini, A., Vanni, A., Martinotti, E., Chicca, A., Fogli, S. and Nieri, P., 2013. Anticancer activity of anandamide in human cutaneous melanoma cells. *European Journal of Pharmacology*, 718(1-3), pp.154-159.
- Alenton, R.R.R., Koiwai, K., Miyaguchi, K., Kondo, H. and Hirono, I., 2017. Pathogen recognition of a novel C-type lectin from *Marsupenaeus japonicus* reveals the divergent sugar-binding specificity of QAP motif. *Scientific reports*, 7, p.45818.
- Ali, F.Y., Davidson, S.J., Moraes, L.A., Traves, S.L., Paul-Clark, M., Bishop-Bailey, D., Warner, T.D., Mitchell, J.A., 2006. Role of nuclear receptor signaling in platelets: antithrombotic effects of PPARbeta. *FASEB J*, 20, pp326–328.
- Ali, F.Y., Hall, M.G., Desvergne, B., Warner, T.D. and Mitchell, J.A., 2009. PPAR β/δ agonists modulate platelet function via a mechanism involving PPAR receptors and specific association/repression of PKC α —brief report. *Arteriosclerosis, thrombosis, and vascular biology*, 29(11), pp.1871-1873.
- Allen, P.G. and Dawidowicz, E.A., 1990. Phagocytosis in *Acanthamoeba*: I. A mannose receptor is responsible for the binding and phagocytosis of yeast. *Journal of Cellular Physiology*, 145(3), pp.508-513.
- Allen, L.A. and Aderem, A., 1996. Molecular definition of distinct cytoskeletal structures involved in complement- and Fc receptor-mediated phagocytosis in macrophages. *The Journal of Experimental Medicine*, 184(2), pp.627-637.
- Allen, R.D., Ueno, M.S. and Fok, A.K., 1988. A Survey of Lectin Binding in *Paramecium* 1. *The Journal of Protozoology*, 35(3), pp.400-407.
- Amorós, I., Barana, A., Caballero, R., Gómez, R., Osuna, L., Lillo, M.P., Tamargo, J. and Delpón, E., 2010. Endocannabinoids and cannabinoid analogues block human cardiac Kv4. 3 channels in a receptor-independent manner. *Journal of Molecular and Cellular Cardiology*, 48(1), pp.201-210.
- Appendino, G., Gibbons, S., Giana, A., Pagani, A., Grassi, G., Stavri, M., Smith, E. and Rahman, M.M., 2008. Antibacterial cannabinoids from *Cannabis sativa*: a structure– activity study. *Journal of Natural Products*, 71(8), pp.1427-1430.

- Apple, J.K., Strom, S.L., Palenik, B. and Brahamsha, B., 2011. Variability in protist grazing and growth on different marine *Synechococcus* isolates. *Applied and environmental Microbiology*, 77(9), pp.3074-3084.
- Astarita, G., Di Giacomo, B., Gaetani, S., Oveisi, F., Compton, T.R., Rivara, S., Tarzia, G., Mor, M. and Piomelli, D., 2006. Pharmacological characterization of hydrolysis-resistant analogs of oleoylethanolamide with potent anorexiatic properties. *Journal of Pharmacology and Experimental Therapeutics*, 318(2), pp.563-570.
- Athamna, A.B.E.D., Ofek, I.T.Z.H.A.K., Keisari, Y., Markowitz, S., Dutton, G.G. and Sharon, N., 1991. Lectinophagocytosis of encapsulated *Klebsiella pneumoniae* mediated by surface lectins of guinea pig alveolar macrophages and human monocyte-derived macrophages. *Infection and immunity*, 59(5), pp.1673-1682.
- Athanasiou, A., Clarke, A.B., Turner, A.E., Kumaran, N.M., Vakilpour, S., Smith, P.A., Bagiokou, D., Bradshaw, T.D., Westwell, A.D., Fang, L., Lobo, D.N., Constantinescu, C.S., Calabrese, V., Loesch, A., Alexander, S.P., Clothier, R.H., Kendall, D.A. and Bates, T.E. (2007) Cannabinoid receptor agonists are mitochondrial inhibitors: a unified hypothesis of how cannabinoids modulate mitochondrial function and induce cell death. *Biochem Biophys Res Commun*. 364(1), pp.131-7.
- Auriti, C., Prencipe, G., Moriondo, M., Bersani, I., Bertaina, C., Mondì, V. and Inglese, R. (2017). Mannose-Binding Lectin: Biologic Characteristics and Role in the Susceptibility to Infections and Ischemia-Reperfusion Related Injury in Critically Ill Neonates. *Journal of Immunology Research*, 2017, p.7045630.
- Avery, S.V., Lloyd, D. and Harwood, J.L., 1995. Temperature-dependent changes in plasma-membrane lipid order and the phagocytotic activity of the amoeba *Acanthamoeba castellanii* are closely correlated. *Biochemical Journal*, 312(3), pp.811-816.
- Bakolitsa, C., de Pereda, J.M., Bagshaw, C.R., Critchley, D.R. and Liddington, R.C., 1999. Crystal structure of the vinculin tail suggests a pathway for activation. *Cell*, 99(6), pp.603-613.
- Barnes, N.M. and Neumaier, J.F., 2011. Neuronal 5-HT receptors and SERT. *Tocris Biosci Sci Rev Ser*, 34, pp.1-16.
- Battista, N., Di Tommaso, M., Bari, M. and Maccarrone, M., 2012. The endocannabinoid system: an overview. *Frontiers in Behavioral Neuroscience*, 6, p.9.
- Beaulieu, J.M. and Gainetdinov, R.R., 2011. The physiology, signaling, and pharmacology of dopamine receptors. *Pharmacological Reviews*, 63(1), pp.182-217.
- Beltramo, M., de Fonseca, F.R., Navarro, M., Calignano, A., Gorriti, M.A., Grammatikopoulos, G., Sadile, A.G., Giuffrida, A. and Piomelli, D., 2000. Reversal of dopamine D2 receptor responses by an anandamide transport inhibitor. *Journal of Neuroscience*, 20(9), pp.3401-3407.

- Bénard, G., Massa, F., Puente, N., Lourenço, J., Bellocchio, L., Soria-Gómez, E., Matias, I., Delamarre, A., Metna-Laurent, M., Cannich, A. and Hebert-Chatelain, E., 2012. Mitochondrial CB 1 receptors regulate neuronal energy metabolism. *Nature Neuroscience*, 15(4), pp.558-564.
- Berdyshev, E., Boichot, E., Corbel, M., Germain, N. and Lagente, V., 1998. Effects of cannabinoid receptor ligands on LPS-induced pulmonary inflammation in mice. *Life Sciences*, 63(8), pp.PL125-PL129.
- Bernstein, N., Gorelick, J. and Koch, S., 2019. Interplay between chemistry and morphology in medical cannabis (*Cannabis sativa* L.). *Industrial Crops and Products*, 129, pp.185-194.
- Bih, C.I., Chen, T., Nunn, A.V., Bazilot, M., Dallas, M. and Whalley, B.J., 2015. Molecular targets of cannabidiol in neurological disorders. *Neurotherapeutics*, 12(4), pp.699-730.
- Bisogno, T., Maurelli, S., Melck, D., De Petrocellis, L., & Di Marzo, V. (1997). Biosynthesis, uptake, and degradation of anandamide and palmitoylethanolamide in leukocytes. *Journal of Biological Chemistry*, 272(6), 3315-3323.
- Boenigk, J., Matz, C., Jürgens, K. and Arndt, H. (2001). The Influence of Preculture Conditions and Food Quality on the Ingestion and Digestion Process of Three Species of Heterotrophic Nanoflagellates. *Microbial Ecology*, 42(2), pp.168–176.
- Bogitsh, B.J., Carter, C.E. and Oeltmann, T.N., 2018. *Human parasitology*. Academic Press.
- Borrelli, F., Romano, B., Petrosino, S., Pagano, E., Capasso, R., Coppola, D., Battista, G., Orlando, P., Di Marzo, V. and Izzo, A.A., 2015. Palmitoylethanolamide, a naturally occurring lipid, is an orally effective intestinal anti-inflammatory agent. *British Journal of Pharmacology*, 172(1), pp.142-158.
- Boskovic, J., Arnold, J.N., Stilion, R., Gordon, S., Sim, R.B., Rivera-Calzada, A., Wienke, D., Isacke, C.M., Martinez-Pomares, L. and Llorca, O., 2006. Structural model for the mannose receptor family uncovered by electron microscopy of Endo180 and the mannose receptor. *Journal of Biological Chemistry*, 281(13), pp.8780-8787.
- Botelho, R.J., Teruel, M., Dierckman, R., Anderson, R., Wells, A., York, J.D., Meyer, T. and Grinstein, S., 2000. Localized biphasic changes in phosphatidylinositol-4, 5-bisphosphate at sites of phagocytosis. *The Journal of Cell Biology*, 151(7), pp.1353-1368.
- Bozzaro, S. and Roseman, S., 1983. Adhesion of *Dictyostelium discoideum* cells to carbohydrates immobilized in polyacrylamide gels. I. Evidence for three sugar-specific cell surface receptors. *Journal of Biological Chemistry*, 258(22), pp.13882-13889.
- Bramblett, R. D., Panu, A. M., Ballesteros, J. A., & Reggio, P. H. (1995). Construction of a 3D model of the cannabinoid CB1 receptor: determination of helix ends and helix orientation. *Life Sciences*, 56(23), pp.1971-1982.

- Brumell, J.H., Howard, J.C., Craig, K., Grinstein, S., Schreiber, A.D. and Tyers, M., 1999. Expression of the protein kinase C substrate pleckstrin in macrophages: association with phagosomal membranes. *The Journal of Immunology*, 163(6), pp.3388-3395.
- Burri, L., Thoresen, G.H. and Berge, R.K., 2010. The role of PPAR activation in liver and muscle. *PPAR research*, 2010.
- Butler, H. and Rogerson, A., 1996. Growth potential, production efficiency and annual production of marine benthic naked amoebae (gymnamoebae) inhabiting sediments of the Clyde Sea area, Scotland. *Aquatic Microbial Ecology*, 10(2), pp.123-129.
- Butler, H. and Rogerson, A., 1997. Consumption rates of six species of marine benthic naked amoebae (*Gymnamoebia*) from sediments in the Clyde Sea area. *Journal of the Marine Biological Association of the United Kingdom*, 77(4), pp.989-997.
- Calignano, A., La Rana, G., Giuffrida, A. and Piomelli, D., 1998. Control of pain initiation by endogenous cannabinoids. *Nature*, 394(6690), pp.277-281.
- Cambi, A., Koopman, M. and Figdor, C.G., 2005. How C-type lectins detect pathogens. *Cellular Microbiology*, 7(4), pp.481-488.
- Capelli, D., Cerchia, C., Montanari, R., Loiodice, F., Tortorella, P., Laghezza, A., Cervoni, L., Pochetti, G. and Lavecchia, A., 2016. Structural basis for PPAR partial or full activation revealed by a novel ligand binding mode. *Scientific reports*, 6, p.34792.
- Carnell, M., Zech, T., Calaminus, S. D., Ura, S., Hagedorn, M., Johnston, S. A., et al. (2011). Actin polymerization driven by WASH causes V-ATPase retrieval and vesicle neutralization before exocytosis. *J. Cell Biol.* 193, pp.831–839.
- Celada, P., Puig, M.V., Amargós-Bosch, M., Adell, A. and Artigas, F., 2004. The therapeutic role of 5-HT_{1A} and 5-HT_{2A} receptors in depression. *Journal of Psychiatry and Neuroscience*, 29(4), p.252.
- Cerbone, A., Toaldo, C., Minelli, R., Ciamporcero, E., Pizzimenti, S., Pettazzoni, P., Roma, G., Dianzani, M.U., Ullio, C., Ferretti, C. and Dianzani, C., 2012. Rosiglitazone and AS601245 decrease cell adhesion and migration through modulation of specific gene expression in human colon cancer cells. *PLoS One*, 7(6), pp.9-13.
- Cirillo, C., Vanden, P.B. and Tack, J., 2011. Role of serotonin in gastrointestinal physiology and pathology. *Minerva Endocrinologica*, 36(4), pp.311-324.
- Cluny, N.L., Keenan, C.M., Lutz, B., Piomelli, D. and Sharkey, K.A., 2009. The identification of peroxisome proliferator-activated receptor alpha-independent effects of oleoylethanolamide on intestinal transit in mice. *Neurogastroenterology & Motility*, 21(4), pp.420-429

- Compassclinics.com.au. 2020. Sativa - Everything You Need To Know About Cannabis Sativa | Compass Lifestyle Clinics. [online] Available at: <<https://www.compassclinics.com.au/blogs/sativa-everything-you-need-to-know-about-cannabis-sativa>> [Accessed 31 March 2020].
- Condie, R., Herring, A., Koh, W. S., Lee, M., & Kaminski, N. E. (1996). Cannabinoid inhibition of adenylate cyclase-mediated signal transduction and interleukin 2 (IL-2) expression in the murine T-cell line, EL4. IL-2. *Journal of Biological Chemistry*, 271(22), pp.13175-13183.
- Cooper, G., 2000. *The Cell. A Molecular Approach. Bioenergetics and Metabolism-Mitochondria, Chloroplasts, and Peroxisomes.*
- Cosson, P. and Soldati, T., 2008. Eat, kill or die: when amoeba meets bacteria. *Current Opinion in Microbiology*, 11(3), pp.271-276.
- Costa, B., Conti, S., Giagnoni, G. and Colleoni, M., 2002. Therapeutic effect of the endogenous fatty acid amide, palmitoylethanolamide, in rat acute inflammation: inhibition of nitric oxide and cyclo-oxygenase systems. *British Journal of Pharmacology*, 137(4), pp.413-420.
- Coull, B.C.&Chandler,G.T.(2001).Meiobenthos*.In J. H. Steele (Ed.), *Encyclopedia of ocean sciences*, 2nd ed. (pp. 726–731). Oxford, UK: Academic Press.
- Cox, D., Tseng, C.C., Bjekic, G. and Greenberg, S., 1999. A requirement for phosphatidylinositol 3-kinase in pseudopod extension. *Journal of Biological Chemistry*, 274(3), pp.1240-1247.
- Currais, A., Quehenberger, O., Armando, A.M., Daugherty, D., Maher, P. and Schubert, D., 2016. Amyloid proteotoxicity initiates an inflammatory response blocked by cannabinoids. *NPJ Aging and Mechanisms of Disease*, 2, p.16012.
- De Gregorio, D., McLaughlin, R.J., Posa, L., Ochoa-Sanchez, R., Enns, J., Lopez-Canul, M., Aboud, M., Maione, S., Comai, S. and Gobbi, G., 2019. Cannabidiol modulates serotonergic transmission and reverses both allodynia and anxiety-like behavior in a model of neuropathic pain. *Pain*, 160(1), p.136.
- De Petrocellis L., Melck, D., Bisogno, T. and Marzo, D.V., 2000. Endocannabinoids and fatty acid amides in cancer inflammation and related disorders. Elsevier. 108: 191-209.
- De Petrocellis, L., Ligresti, A., Schiano Moriello, A., Iappelli, M., Verde, R., Stott, C.G., Cristino, L., Orlando, P. and Di Marzo, V., 2013. Non-THC cannabinoids inhibit prostate carcinoma growth in vitro and in vivo: pro-apoptotic effects and underlying mechanisms. *British Journal of Pharmacology*, 168(1), pp.79-102.
- Desvergne, B. and Wahli, W., 1999. Peroxisome proliferator-activated receptors: nuclear control of metabolism. *Endocrine Reviews*, 20(5), pp.649-688.

- Devane, W.A., Hanus, L., Breuer, A., Pertwee, R.G., Stevenson, L.A., Griffin, G., Gibson, D., Mandelbaum, A., Etinger, A. and Mechoulam, R., 1992. Isolation and structure of a brain constituent that binds to the cannabinoid receptor. *Science*, 258(5090), pp.1946-1949.
- Devane, W.A., Dysarz, F.3., Johnson, M.R., Melvin, L.S. and Howlett, A.C., 1988. Determination and characterization of a cannabinoid receptor in rat brain. *Molecular Pharmacology*, 34(5), pp.605-613.
- Dey, R., Pierre, P., and Jacques, B. (2010) Endocannabinoids Inhibit the growth of free-living amoebae. *Antimicrobial Agents and Chemotherapy*. 54(7), pp.3065-3067.
- Di Marzo, V., Sepe, N., De Petrocellis, L., Berger, A., Crozier, G., Fride, E., & Mechoulam, R. (1998). Trick or treat from food endocannabinoids. *Nature*, 396(6712), pp.636-636.
- DiMarzo, V., Melck, D., Orlando, P., Bisogno, T., Zagoory, O., Bifulco, M., Vogel, Z. and de Petrocellis, L., 2001. Palmitoylethanolamide inhibits the expression of fatty acid amide hydrolase and enhances the anti-proliferative effect of anandamide in human breast cancer cells. *Biochemical Journal*, 358(1), pp.249-255.
- Dong, W., Liu, Y., Zhu, W., Mou, Q., Wang, J. and Hu, Y., 2014. Simulation of Swanson's literature-based discovery: Anandamide treatment inhibits growth of gastric cancer cells in vitro and in silico. *PLoS One*, 9(6), p.e100436.
- Dreyer, C., Krey, G., Keller, H., Givel, F., Helftenbein, G. and Wahli, W., 1992. Control of the peroxisomal β -oxidation pathway by a novel family of nuclear hormone receptors. *Cell*, 68(5), pp.879-887.
- Drickamer, K. and Taylor, M.E., 2015. Recent insights into structures and functions of C-type lectins in the immune system. *Current Opinion in Structural Biology*, 34, pp.26-34.
- Duhon, D. and Cardelli, J., 2002. The regulation of phagosome maturation in *Dictyostelium*. *Journal of Muscle Research & Cell Motility*, 23(7-8), pp.803-808.
- Duleh, S.N. and Welch, M.D., 2010. WASH and the Arp2/3 complex regulate endosome shape and trafficking. *Cytoskeleton*, 67(3), pp.193-206.
- Dürk, T., Panther, E., Müller, T., Sorichter, S., Ferrari, D., Pizzirani, C., Di Virgilio, F., Myrtek, D., Norgauer, J. and Idzko, M., 2005. 5-Hydroxytryptamine modulates cytokine and chemokine production in LPS-primed human monocytes via stimulation of different 5-HTR subtypes. *International Immunology*, 17(5), pp.599-606.
- Duvernay, M.T., Filipeanu, C.M. and Wu, G., 2005. The regulatory mechanisms of export trafficking of G protein-coupled receptors. *Cellular signalling*, 17(12), pp.1457-1465.

- Dyavanapalli, J., Byrne, P. and Mendelowitz, D., 2013. Activation of D2-like dopamine receptors inhibits GABA and glycinergic neurotransmission to pre-motor cardiac vagal neurons in the nucleus ambiguus. *Neuroscience*, 247, pp.213-226.
- Elbaz, M., Nasser, M.W., Ravi, J., Wani, N.A., Ahirwar, D.K., Zhao, H., Oghumu, S., Satoskar, A.R., Shilo, K., Carson III, W.E. and Ganju, R.K., 2015. Modulation of the tumor microenvironment and inhibition of EGF/EGFR pathway: Novel anti-tumor mechanisms of Cannabidiol in breast cancer. *Molecular Oncology*, 9(4), pp.906-919.
- Elvington, M., Liszewski, M.K. and Atkinson, J.P., 2016. Evolution of the complement system: from defense of the single cell to guardian of the intravascular space. *Immunological reviews*, 274(1), pp.9-15.
- Esteban, G.F., Finlay, B.J. and Warren, A., 2015. Free-living protozoa. In Thorp and Covich's *Freshwater Invertebrates* (pp. 113-132). Academic Press.
- Ezekowitz, R.A., Sastry, K., Bailly, P. and Warner, A., 1990. Molecular characterization of the human macrophage mannose receptor: demonstration of multiple carbohydrate recognition-like domains and phagocytosis of yeasts in Cos-1 cells. *The Journal of Experimental Medicine*, 172(6), pp.1785-1794.
- Fagundo, A.B., De la Torre, R., Jiménez-Murcia, S., Agüera, Z., Pastor, A., Casanueva, F.F., Granero, R., Baños, R., Botella, C., del Pino-Gutierrez, A. and Fernandez-Real, J.M., 2013. Modulation of the endocannabinoids N-arachidonylethanolamine (AEA) and 2-arachidonoylglycerol (2-AG) on executive functions in humans. *Plos one*, 8(6), p.e66387.
- Falkenstein, E., Norman, A.W. and Wehling, M., 2000. Mannheim classification of nongenomically initiated (rapid) steroid action (s). *The Journal of Clinical Endocrinology & Metabolism*, 85(5), pp.2072-2075.
- Ferguson, L.B., Zhang, L., Wang, S., Bridges, C., Harris, R.A. and Ponomarev, I., 2018. Peroxisome proliferator activated receptor agonists modulate transposable element expression in brain and liver. *Frontiers in Molecular Neuroscience*, 11, p.331.
- Fernández-López, D., Lizasoain, I., Moro, M.Á. and Martínez-Orgado, J., 2013. Cannabinoids: well-suited candidates for the treatment of perinatal brain injury. *Brain Sciences*, 3(3), pp.1043-1059.
- Fernández-Ruiz, J., Hernández, M. and Ramos, J.A., 2010. Cannabinoid–dopamine interaction in the pathophysiology and treatment of CNS disorders. *CNS neuroscience & therapeutics*, 16(3), pp. 72-e91.
- Fernstrom, J.D. and Fernstrom, M.H., 2007. Tyrosine, phenylalanine, and catecholamine synthesis and function in the brain. *The Journal of Nutrition*, 137(6), pp.1539S-1547S.

- Fezza, F., Bari, M., Florio, R., Talamonti, E., Feole, M. and Maccarrone, M., 2014. Endocannabinoids, related compounds and their metabolic routes. *Molecules*, 19(11), pp.17078-17106.
- Fitzner-Attas, C.J., Lowry, M., Crowley, M.T., Finn, A.J., Meng, F., DeFranco, A.L. and Lowell, C.A., 2000. Fcγ receptor–mediated phagocytosis in macrophages lacking the Src family tyrosine kinases Hck, Fgr, and Lyn. *The Journal of Experimental Medicine*, 191(4), pp.669-682.
- Fletcher, A., Bill, D.J., Bill, S.J., Cliffe, I.A., Dover, G.M., Forster, E.A., Haskins, J.T., Jones, D., Mansell, H.L. and Reilly, Y., 1993. WAY100135: a novel, selective antagonist at presynaptic and postsynaptic 5-HT_{1A} receptors. *European Journal of Pharmacology*, 237(2-3), pp.283-291.
- Frazer, A. and Hensler, J.G., 1999. Serotonin. *Basic Neurochemistry*, 6, pp.335-346.
- Freire-Garabal, M., Nunez, M.J., Balboa, J., López-Delgado, P., Gallego, R., García-Caballero, T., Fernández-Roel, M.D., Brenlla, J. and Rey-Méndez, M., 2003. Serotonin upregulates the activity of phagocytosis through 5-HT_{1A} receptors. *British Journal of Pharmacology*, 139(2), pp.457-463.
- Fu, J., Gaetani, S., Oveisi, F., Verme, J.L., Serrano, A., de Fonseca, F.R., Rosengarth, A., Luecke, H., Di Giacomo, B., Tarzia, G. and Piomelli, D., 2003. Oleylethanolamide regulates feeding and body weight through activation of the nuclear receptor PPAR-α. *Nature*, 425(6953), pp.90-93.
- Fux, M. and Belmaker, R.H. (1991). A controlled comparative study of chlorprothixene vs. haloperidol in chronic schizophrenia. *The Israel Journal of Psychiatry and Related Sciences*, [online] 28(1), pp.37–40.
- Gaetani, S., Oveisi, F. and Piomelli, D., 2003. Modulation of meal pattern in the rat by the anorexic lipid mediator oleylethanolamide. *Neuropsychopharmacology*, 28(7), pp.1311-1316.
- Gao, L. Y., Harb, O. S. & Abu Kwaik, Y. 1997. Utilization of similar mechanisms by *Legionella pneumophila* to parasitize two evolutionarily distant host cells, mammalian macrophages and protozoa. *Infection and Immunity*, 65, pp.4738-46.
- Garate, M., Cao, Z., Bateman, E. and Panjwani, N., 2004. Cloning and characterization of a novel mannose-binding protein of *Acanthamoeba*. *Journal of Biological Chemistry*, 279(28), pp.29849-29856.
- Garstecki, T., Brown, S. and De Jonckheere, J.F., 2005. Description of *Vahlkampfia signyensis* n. sp. (Heterolobosea), based on morphological, ultrastructural and molecular characteristics. *European Journal of Protistology*, 41(2), pp.119-127.

- Gbarah, A.W.N.I., Gahmberg, C.G., Ofek, I., Jacobi, U. and Sharon, N., 1991. Identification of the leukocyte adhesion molecules CD11 and CD18 as receptors for type 1-fimbriated (mannose-specific) *Escherichia coli*. *Infection and Immunity*, 59(12), pp.4524-4530.
- Giorgione, J. and Clarke, M., 2008. Heterogeneous modes of uptake for latex beads revealed through live cell imaging of phagocytes expressing a probe for phosphatidylinositol-(3, 4, 5)-trisphosphate and phosphatidylinositol-(3, 4)-bisphosphate. *Cell motility and the Cytoskeleton*, 65(9), pp.721-733.
- Girroir, E.E., Hollingshead, H.E., Billin, A.N., Willson, T.M., Robertson, G.P., Sharma, A.K., Amin, S., Gonzalez, F.J. and Peters, J.M., 2008. Peroxisome proliferator-activated receptor- β/δ (PPAR β/δ) ligands inhibit growth of UACC903 and MCF7 human cancer cell lines. *Toxicology*, 243(1-2), pp.236-243.
- Goley, E.D., Rodenbusch, S.E., Martin, A.C. and Welch, M.D., 2004. Critical conformational changes in the Arp2/3 complex are induced by nucleotide and nucleation promoting factor. *Molecular Cell*, 16(2), pp.269-279.
- Grassi, G. and McPartland, J.M., 2017. Chemical and Morphological Phenotypes in Breeding of *Cannabis sativa* L. In *Cannabis sativa* L.-Botany and Biotechnology (pp. 137-160). Springer, Cham.
- Grimaldi, C., Pisanti, S., Laezza, C., Malfitano, A.M., Santoro, A., Vitale, M., Caruso, M.G., Notarnicola, M., Iacuzzo, I., Portella, G. and Di Marzo, V., 2006. Anandamide inhibits adhesion and migration of breast cancer cells. *Experimental Cell Research*, 312(4), pp.363-373.
- Gross, B. and Staels, B., 2007. PPAR agonists: multimodal drugs for the treatment of type-2 diabetes. *Best Practice & Research Clinical Endocrinology & Metabolism*, 21(4), pp.687-710.
- Grotenhermen, F. (2004). Clinical pharmacodynamics of cannabinoids. *Journal of Cannabis Therapeutics*, 4(1), pp.29-78.
- Guevara Lora, I., Niewiarowska-Sendo, A., Polit, A. and Kozik, A., 2016. Hypothetical orchestrated cooperation between dopaminergic and kinin receptors for the regulation of common functions. *Acta Biochimica Polonica*, 63(3), pp.387–396.
- Gunduz-Bruce, H., Oliver, S., Gueorguieva, R., Forselius-Bielen, K., D'Souza, D.C., Zimolo, Z., Tek, C., Kaliora, S., Ray, S. and Petrides, G., 2013. Efficacy of pimozide augmentation for clozapine partial responders with schizophrenia. *Schizophrenia Research*, 143(2-3), pp.344-347.
- Gupta, A. and Gupta, G.S., 2012. C-Type Lectins Family. In *Animal Lectins: Form, Function and Clinical Applications* (pp. 473-482). Springer, Vienna.

- Haas, A., 2007. The phagosome: compartment with a license to kill. *Traffic*, 8(4), pp.311-330.
- Haile, C.N. and Kosten, T.A., 2017. The peroxisome proliferator-activated receptor alpha agonist fenofibrate attenuates alcohol self-administration in rats. *Neuropharmacology*, 116, pp.364-370.
- Hampson, A.J., Grimaldi, M., Axelrod, J. and Wink, D., 1998. Cannabidiol and (-) Δ^9 -tetrahydrocannabinol are neuroprotective antioxidants. *Proceedings of the National Academy of Sciences*, 95(14), pp.8268-8273.
- Hankir, M.K., Seyfried, F., Hintschich, C.A., Diep, T.A., Kleberg, K., Kranz, M., Deuther-Conrad, W., Tellez, L.A., Rullmann, M., Patt, M. and Teichert, J., 2017. Gastric bypass surgery recruits a gut PPAR- α -striatal D1R pathway to reduce fat appetite in obese rats. *Cell Metabolism*, 25(2), pp.335-344.
- Hansen, H. S., Petersen, G., Artmann, A., & Madsen, A. N. (2006). Endocannabinoids. *European Journal of Lipid Science and Technology*, 108(10), 877-889.
- Happyana, N., Agnolet, S., Muntendam, R., Van Dam, A., Schneider, B. and Kayser, O., 2013. Analysis of cannabinoids in laser-microdissected trichomes of medicinal *Cannabis sativa* using LCMS and cryogenic NMR. *Phytochemistry*, 87, pp.51-59.
- Harb, O.S., Venkataraman, C., Haack, B.J., Gao, L.Y. and Kwaik, Y.A., 1998. Heterogeneity in the attachment and uptake mechanisms of the Legionnaires' disease bacterium, *Legionella pneumophila*, by protozoan hosts. *Applied environmental Microbiology*, 64(1), pp.126-132.
- Hasbi, A., Madras, B.K., Bergman, J., Kohut, S., Lin, Z., Withey, S.L. and George, S.R., 2020. Δ -Tetrahydrocannabinol increases Dopamine D1-D2 receptor heteromer and elicits phenotypic reprogramming in adult primate striatal neurons. *iScience*, 23(1), p.100794.
- Hasenoehrl, C., Storr, M. and Schicho, R., 2017. Cannabinoids for treating inflammatory bowel diseases: where are we and where do we go? *Expert Review of Gastroenterology & Hepatology*, 11(4), pp.329-337.
- Hayes, A.C., Stupak, J., Li, J. and Cox, A.D., 2013. Identification of N-acylethanolamines in *Dictyostelium discoideum* and confirmation of their hydrolysis by fatty acid amide hydrolase. *Journal of Lipid Research*, 54(2), pp.457-466.
- Heaton, K, Drinkall, J, Minett, A, Hunt, AP & Parry, JD 2001, Amoeboid grazing on surface-associated prey. in P Gilbert, D Allison, M Brading, J Verran & J Walker (eds), *Biofilm community interactions : chance or necessity?*. Bioline, Cardiff, pp. 293-301.
- Hellstrand, K. and Hermodsson, S., 1993. Serotonergic 5-HT_{1A} receptors regulate a cell contact-mediated interaction between natural killer cells and monocytes. *Scandinavian Journal of Immunology*, 37(1), pp.7-18.

- Henriquez, F.L., Ingram, P.R., Muench, S.P., Rice, D.W. and Roberts, C.W., 2008. Molecular basis for resistance of *Acanthamoeba* tubulins to all major classes of antitubulin compounds. *Antimicrobial Agents and Chemotherapy*, 52(3), pp.1133-1135.
- Herant, M., Heinrich, V. and Dembo, M., 2005. Mechanics of neutrophil phagocytosis: behavior of the cortical tension. *Journal of Cell Science*, 118(9), pp.1789-1797.
- Hind, W.H., Tufarelli, C., Neophytou, M., Anderson, S.I., England, T.J. and O'Sullivan, S.E., 2015. Endocannabinoids modulate human blood–brain barrier permeability in vitro. *British Journal of Pharmacology*, 172(12), pp.3015-3027.
- Ho, W.S., Barrett, D.A. and Randall, M.D., 2008. 'Entourage' effects of N-palmitoylethanolamide and N-oleoylethanolamide on vasorelaxation to anandamide occur through TRPV1 receptors. *British Journal of Pharmacology*, 155(6), pp.837-846.
- Ho, B.Y., Uezono, Y., Takada, S., Takase, I. and Izumi, F., 1999. Coupling of the expressed cannabinoid CB1 and CB2 receptors to phospholipase C and G protein-coupled inwardly rectifying K⁺ channels. *Receptors & Channels*, 6(5), pp.363-374.
- Holdgate, G.A., 2017. Kinetics, Thermodynamics, and Ligand Efficiency Metrics in Drug Discovery, pp. 180-211
- Hourani, W. and Alexander, S.P., 2018. Cannabinoid ligands, receptors and enzymes: Pharmacological tools and therapeutic potential. *Brain and Neuroscience Advances*, 2, p.2398212818783908.
- Hoving, J.C., Wilson, G.J. and Brown, G.D., 2014. Signalling C-type lectin receptors, microbial recognition and immunity. *Cellular Microbiology*, 16(2), pp.185-194.
- Howlett, A.C., Barth, F., Bonner, T.I., Cabral, G., Casellas, P., Devane, W.A., Felder, C.C., Herkenham, M., Mackie, K., Martin, B.R. and Mechoulam, R., 2002. International Union of Pharmacology. XXVII. Classification of cannabinoid receptors. *Pharmacological Reviews*, 54(2), pp.161-202.
- Howlett, A.C., Blume, L.C. and Dalton, G.D., 2010. CB1 cannabinoid receptors and their associated proteins. *Current Medicinal Chemistry*, 17(14), pp.1382-1393.
- Huth, S., Revere, J.F., Leippe, M. and Selhuber-Unkel, C., 2017. Adhesion forces and mechanics in mannose-mediated *acanthamoeba* interactions. *PloS one*, 12(5), p.e0176207.
- Huws, S.A., McBain, A.J. and Gilbert, P., 2005. Protozoan grazing and its impact upon population dynamics in biofilm communities. *Journal of Applied Microbiology*, 98(1), pp.238-244.

- Ichinose, M. and Sawada, M., 1996. Enhancement of phagocytosis by calcitonin gene-related peptide (CGRP) in cultured mouse peritoneal macrophages. *Peptides*, 17(8), pp.1405-1414.
- Ilyas, R., Wallis, R., Soilleux, E.J., Townsend, P., Zehnder, D., Tan, B.K., Sim, R.B., Lehnert, H., Randevara, H.S. and Mitchell, D.A., 2011. High glucose disrupts oligosaccharide recognition function via competitive inhibition: a potential mechanism for immune dysregulation in diabetes mellitus. *Immunobiology*, 216(1-2), pp.126-131.
- Iyer, S.S., Barton, J.A., Bourgoin, S. and Kusner, D.J., 2004. Phospholipases D1 and D2 coordinately regulate macrophage phagocytosis. *The Journal of Immunology*, 173(4), pp.2615-2623.
- Jaggari, S.I., Hasnie, F.S., Sellaturay, S. and Rice, A.S., 1998. The anti-hyperalgesic actions of the cannabinoid anandamide and the putative CB2 receptor agonist palmitoylethanolamide in visceral and somatic inflammatory pain. *Pain*, 76(1-2), pp.189-199.
- Jaumouillé, V. and Waterman, C.M., 2020. Physical constraints and forces involved in phagocytosis. *Frontiers in Immunology*, 11, p.1097.
- Jaumouillé, V., Cartagena-Rivera, A.X. and Waterman, C.M., 2019. Coupling of β 2 integrins to actin by a mechanosensitive molecular clutch drives complement receptor-mediated phagocytosis. *Nature Cell Biology*, 21(11), pp.1357-1369.
- Jaumouillé, V., Farkash, Y., Jaqaman, K., Das, R., Lowell, C.A. and Grinstein, S., 2014. Actin cytoskeleton reorganization by Syk regulates Fc γ receptor responsiveness by increasing its lateral mobility and clustering. *Developmental Cell*, 29(5), pp.534-546.
- Johnson, S.A., Pleiman, C.M., Pao, L., Schneringer, J., Hippen, K. and Cambier, J.C., 1995. Phosphorylated immunoreceptor signaling motifs (ITAMs) exhibit unique abilities to bind and activate Lyn and Syk tyrosine kinases. *The Journal of Immunology*, 155(10), pp.4596-4603.
- Jones, N.A., Hill, A.J., Smith, I., Bevan, S.A., Williams, C.M., Whalley, B.J. and Stephens, G.J., 2010. Cannabidiol displays antiepileptiform and antiseizure properties in vitro and in vivo. *Journal of Pharmacology and Experimental Therapeutics*, 332(2), pp.569-577.
- Kang, S., Tice, A.K., Stairs, C.W., Lahr, D.J., Jones, R.E. and Brown, M.W., 2020. The integrin-mediated adhesome complex, essential to multicellularity, is present in the most recent common ancestor of animals, fungi, and amoebae.
- Kang, S., Tice, A.K., Spiegel, F.W., Silberman, J.D., Pánek, T., Čepička, I., Kostka, M., Kosakyan, A., Alcântara, D.M., Roger, A.J. and Shadwick, L.L., 2017. Between a pod and a hard test: the deep evolution of amoebae. *Molecular Biology and Evolution*, 34(9), pp.2258-2270.

- Karimian Azari, E., Ramachandran, D., Weibel, S., Arnold, M., Romano, A., Gaetani, S., Langhans, W. and Mansouri, A., 2014. Vagal afferents are not necessary for the satiety effect of the gut lipid messenger oleoylethanolamide. *American Journal of Physiology-Regulatory, Integrative and Comparative Physiology*, 307(2), pp.R167-R178.
- Karwad, M.A., Macpherson, T., Wang, B., Theophilidou, E., Sarmad, S., Barrett, D.A., Larvin, M., Wright, K.L., Lund, J.N. and O'Sullivan, S.E., 2017. Oleoylethanolamine and palmitoylethanolamine modulate intestinal permeability in vitro via TRPV1 and PPAR α . *The FASEB Journal*, 31(2), pp.469-481.
- Kassack, M.U., Höfgen, B., Decker, M., Eckstein, N. and Lehmann, J., 2002. Pharmacological characterization of the benz [d] indolo [2, 3-g] azecine LE300, a novel type of a nanomolar dopamine receptor antagonist. *Naunyn-Schmiedeberg's Archives of Pharmacology*, 366(6), pp.543-550.
- Kasten, C.R. and Boehm, S.L., 2016. Preclinical Medication Development: New Targets and New Drugs. *Alcoholism: Clinical and Experimental Research*, 40(7), pp.1418-1424.
- Kavia, R.B.C., De Ridder, D., Constantinescu, C.S., Stott, C.G. and Fowler, C.J., 2010. Randomized controlled trial of Sativex to treat detrusor overactivity in multiple sclerosis. *Multiple Sclerosis Journal*, 16(11), pp.1349-1359.
- Kerrigan, A.M. and Brown, G.D., 2009. C-type lectins and phagocytosis. *Immunobiology*, 214(7), pp.562-575.
- kilpatrick, D.C. (2003). Introduction to mannan-binding lectin. *Biochemical Society Transactions*, 31(4), pp.745–747.
- Kis, B., Ifrim, F.C., Buda, V., Avram, S., Pavel, I.Z., Antal, D., Paunescu, V., Dehelean, C.A., Ardelean, F., Diaconeasa, Z. and Soica, C., 2019. Cannabidiol—from plant to human body: A promising bioactive molecule with multi-target effects in cancer. *International Journal of Molecular Sciences*, 20(23), p.5905.
- Klein, M.O., Battagello, D.S., Cardoso, A.R., Hauser, D.N., Bittencourt, J.C. and Correa, R.G., 2019. Dopamine: functions, signaling, and association with neurological diseases. *Cellular and Molecular Neurobiology*, 39(1), pp.31-59.
- Koay L.C., Rigby, R.J and Wright, K.L. (2014) Cannabinoid-induced autophagy regulates suppressor of cytokine signaling-3 in the intestinal epithelium. *American Physiology Society*, 307, pp.140-148.
- Kremp, A. and Anderson, D.M., 2004. Lectin binding patterns of *Scripsiella lachrymosa* (Dinophyceae) in relation to cyst formation and nutrient conditions. *Journal of Experimental Marine Biology and Ecology*, 307(2), pp.165-181.

- Lambert, D.M., Vandevorde, S., Diependaele, G., Govaerts, S.J. and Robert, A.R., 2001. Anticonvulsant activity of N-palmitoylethanolamide, a putative endocannabinoid, in mice. *Epilepsia*, 42(3), pp.321-327.
- Lan, H., Vassileva, G., Corona, A., Liu, L., Baker, H., Golovko, A., Abbondanzo, S.J., Hu, W., Yang, S., Ning, Y. and Del Vecchio, R.A., 2009. GPR119 is required for physiological regulation of glucagon-like peptide-1 secretion but not for metabolic homeostasis. *Journal of Endocrinology*, 201(2), p.219.
- Larsen, E.C., Ueyama, T., Brannock, P.M., Shirai, Y., Saito, N., Larsson, C., Loegering, D., Weber, P.B. and Lennartz, M.R., 2002. A role for PKC- ϵ in Fc γ R-mediated phagocytosis by RAW 264.7 cells. *The Journal of Cell Biology*, 159(6), pp.939-944.
- Lazennec, G., Canaple, L., Saugy, D. and Wahli, W., 2000. Activation of peroxisome proliferator-activated receptors (PPARs) by their ligands and protein kinase A activators. *Molecular Endocrinology*, 14(12), pp.1962-1975.
- Lee, S.E., Chunsrivirod, S., Kamm, R.D. and Mofrad, M.R.K., 2008. Molecular dynamics study of talin-vinculin binding. *Biophysical Journal*, 95(4), pp.2027-2036.
- Lee, G., Elwood, F., McNally, J., Weiszmann, J., Lindstrom, M., Amaral, K., Nakamura, M., Miao, S., Cao, P., Learned, R.M. and Chen, J.L., 2002. T0070907, a selective ligand for peroxisome proliferator-activated receptor γ , functions as an antagonist of biochemical and cellular activities. *Journal of Biological Chemistry*, 277(22), pp.19649-19657.
- Leung, D., Saghatelian, A., Simon, G.M. and Cravatt, B.F., 2006. Inactivation of N-acyl phosphatidylethanolamine phospholipase D reveals multiple mechanisms for the biosynthesis of endocannabinoids. *Biochemistry*, 45(15), pp.4720-47
- Levin, R., Grinstein, S. and Canton, J., 2016. The life cycle of phagosomes: formation, maturation, and resolution. *Immunological Reviews*, 273(1), pp.156-179.
- Li, N.X., Brown, S., Kowalski, T., Wu, M., Yang, L., Dai, G., Petrov, A., Ding, Y., Dlugos, T., Wood, H.B. and Wang, L., 2018. GPR119 agonism increases glucagon secretion during insulin-induced hypoglycemia. *Diabetes*, 67(7), pp.1401-1413.
- Li, P., L Snyder, G. and E Vanover, K., 2016. Dopamine targeting drugs for the treatment of schizophrenia: past, present and future. *Current topics in Medicinal Chemistry*, 16(29), pp.3385-3403.
- Ligresti, A., Moriello, A.S., Starowicz, K., Matias, I., Pisanti, S., De Petrocellis, L., Laezza, C., Portella, G., Bifulco, M. and Di Marzo, V., 2006. Antitumor activity of plant cannabinoids with emphasis on the effect of cannabidiol on human breast carcinoma. *Journal of Pharmacology and Experimental Therapeutics*, 318(3), pp.1375-1387.

- Lim, M.P., Devi, L.A. and Rozenfeld, R., 2011. Cannabidiol causes activated hepatic stellate cell death through a mechanism of endoplasmic reticulum stress-induced apoptosis. *Cell Death & Disease*, 2(6), pp. e170-e170.
- Lindsley, C.W. and Hopkins, C.R., 2017. Return of D4 Dopamine receptor antagonists in drug discovery: Miniperspective. *Journal of Medicinal Chemistry*, 60(17), pp.7233-7243.
- Lis, H. and Sharon, N., 1986. Lectins as molecules and as tools. *Annual Review of Biochemistry*, 55(1), pp.35-67.
- Ludewig-Klingner, A.K., Michael, V., Jarek, M., Brinkmann, H. and Petersen, J., 2018. Distribution and evolution of peroxisomes in alveolates (Apicomplexa, Dinoflagellates, Ciliates). *Genome Biology and Evolution*, 10(1), pp.1-13.
- Lueneberg, K., Domínguez, G., Arias-Carrión, O., Palomero-Rivero, M., Millán-Aldaco, D., Morán, J., Drucker-Colín, R. and Murillo-Rodríguez, E., 2011. Cellular viability effects of fatty acid amide hydrolase inhibition on cerebellar neurons. *International Archives of Medicine*, 4(1), p.28.
- Maccarrone, M., Bari, M., Battista, N., Di Rienzo, M. and Finazzi-Agrò, A. (2001). Endogenous cannabinoids in neuronal and immune cells: toxic effects, levels and degradation. *Functional Neurology*, [online] 16(4 Suppl), pp.53–60.
- Madras, B.K., 2015. Update of cannabis and its medical use. Geneva: World Health Organization.
- Marciano-Cabral, F., MacLean, R., Mensah, A. and LaPat-Polasko, L., 2003. Identification of *Naegleria fowleri* in domestic water sources by nested PCR. *Applied and Environmental Microbiology*, 69(10), pp.5864-5869.
- Marsden, C.A., 2006. Dopamine: the rewarding years. *British Journal of Pharmacology*, 147(S1), pp.S136-S144.
- Marshall, J.G., Booth, J.W., Stambolic, V., Mak, T., Balla, T., Schreiber, A.D., Meyer, T. and Grinstein, S., 2001. Restricted accumulation of phosphatidylinositol 3-kinase products in a plasmalemmal subdomain during Fcγ receptor-mediated phagocytosis. *The Journal of Cell Biology*, 153(7), pp.1369-1380.
- Masson, J., Emerit, M.B., Hamon, M. and Darmon, M., 2012. Serotonergic signaling: multiple effectors and pleiotropic effects. *Wiley Interdisciplinary Reviews: Membrane Transport and Signaling*, 1(6), pp.685-713.
- Mayes, D.F., Rogerson, A., Marchant, H. and Laybourn-Parry, J., 1997. Growth and consumption rates of bacterivorous Antarctic naked marine amoebae. *Marine Ecology Progress Series*, 160, pp.101-108.

- Mazák, K., Dóczy, V., Kökösi, J. and Noszál, B., 2009. Proton speciation and microspeciation of serotonin and 5-hydroxytryptophan. *Chemistry & Biodiversity*, 6(4), pp.578-590.
- Mazzari, S., Canella, R., Petrelli, L., Marcolongo, G. and Leon, A., 1996. N-(2-hydroxyethyl) hexadecanamide is orally active in reducing edema formation and inflammatory hyperalgesia by down-modulating mast cell activation. *European Journal of Pharmacology*, 300(3), pp.227-236.
- McBride, J., Ingram, P.R., Henriquez, F.L. and Roberts, C.W., 2005. Development of colorimetric microtiter plate assay for assessment of antimicrobials against *Acanthamoeba*. *Journal of Clinical Microbiology*, 43(2), pp.629-634.
- McCance, K.L. and Huether, S.E., 2014. *Pathophysiology: The biologic basis for disease in adults and children*. Elsevier Health Sciences.
- McPartland, J.M., Matias, I., Di Marzo, V. and Glass, M., 2006. Evolutionary origins of the endocannabinoid system. *Gene*, 370, pp.64-74.
- McNeil, C. and Singh, U., 2012. *Acanthamoeba* species. In: Long SS, Pickering LK, Prober GC, eds. *Principles and Practice of Pediatric Infectious Diseases*, fourth ed. Philadelphia: Churchill Livingstone, 2012: 1295-1298.
- Mechoulam, R. and Fride, E., 1995. The unpaved road to the endogenous brain cannabinoid ligands, the anandamides (pp. 233-258). Academic Press, London.
- Miao, R., Xu, T.A.O., Liu, L., Wang, M., Jiang, Y., Li, J. and Guo, R., 2011. Rosiglitazone and retinoic acid inhibit proliferation and induce apoptosis in the HCT-15 human colorectal cancer cell line. *Experimental and Therapeutic Medicine*, 2(3), pp.413-417.
- Microworld. 2019. Homepage - Microworld. [online] Available at: <<https://www.arcella.nl/>> [Accessed 16 November 2019].
- Mishra, A., Singh, S. and Shukla, S., 2018. Physiological and functional basis of dopamine receptors and their role in neurogenesis: possible implication for Parkinson's disease. *Journal of Experimental Neuroscience*, 12, p.1179069518779829.
- Miyamoto, A., Yamamoto, T., Ohno, M., Watanabe, S., Tanak, T., Morimoto, S. and Shoyama, Y., 1996 Roles of dopamine D1 receptors in Δ^9 -tetrahydrocannabinol-induced expression of Fos protein in the rat brain. *Brain Research* 710, pp.234-240.
- Muccioli, G.G., Sia, A., Muchowski, P.J. and Stella, N., 2009. Genetic manipulation of palmitoylethanolamide production and inactivation in *Saccharomyces cerevisiae*. *PLoS One*, 4(6), p.e5942.
- Mócsai, A., Ruland, J. and Tybulewicz, V.L., 2010. The SYK tyrosine kinase: a crucial player in diverse biological functions. *Nature Reviews Immunology*, 10(6), pp.387-402.

- Mohammad-Zadeh, L.F., Moses, L. and Gwaltney-Brant, S.M., 2008. Serotonin: a review. *Journal of Veterinary Pharmacology and Therapeutics*, 31(3), pp.187-199.
- Moraes, L.A., Spyridon, M., Kaiser, W.J., Jones, C.I., Sage, T., Atherton, R.E.L. and Gibbins, J.M., 2010. Non-genomic effects of PPAR γ ligands: inhibition of GPVI-stimulated platelet activation. *Journal of Thrombosis and Haemostasis*, 8(3), pp.577-587.
- Munro, S., Thomas, K. L., & Abu-Shaar, M. (1993). Molecular characterization of a peripheral receptor for cannabinoids.
- Nagatsu, T., Levitt, M. and Udenfriend, S., 1964. Tyrosine hydroxylase the initial step in norepinephrine biosynthesis. *Journal of Biological Chemistry*, 239(9), pp.2910-2917.
- Nakamura, K. and Hasegawa, H. (2009). Production and Peripheral Roles of 5-HTP, a Precursor of Serotonin. *International Journal of Tryptophan Research : IJTR*, 2, pp.37–43.
- Nannmark, U., Sennerby, L., Bjursten, L.M., Skolnik, G. and Bagge, U., 1992. Inhibition of leukocyte phagocytosis by serotonin and its possible role in tumour cell destruction. *Cancer Letters*, 62(1), pp.83-86.
- Neelamegan, D., Schoenhofen, I.C., Richards, J.C. and Cox, A.D., 2012. Identification and recombinant expression of anandamide hydrolyzing enzyme from *Dictyostelium discoideum*. *BMC Microbiology*, 12(1), p.124.
- Neve, K.A., Seamans, J.K. and Trantham-Davidson, H., 2004. Dopamine receptor signaling. *Journal of Receptors and Signal Transduction*, 24(3), pp.165-205.
- Ngo, R., 2019. The Endocannabinoidome. *USURJ: University of Saskatchewan Undergraduate Research Journal*, 5(2), pp. 1-11.
- Nichols, D.E. and Nichols, C.D., 2008. Serotonin receptors. *Chemical Reviews*, 108(5), pp.1614-1641.
- Northover, B.J., 1961. The effect of histamine and 5-hydroxytryptamine on phagocytosis of staphylococci in vitro by polymorphs and macrophages. *The Journal of Pathology and Bacteriology*, 82(2), pp.355-361.
- Ofek, I., Goldhar, J., Keisari, Y. and Sharon, N., 1995. Nonopsonic phagocytosis of microorganisms. *Annual Review of Microbiology*, 49(1), pp.239-276.
- Onaivi, E. S., Chakrabarti, A., & Chaudhuri, G. (1996). Cannabinoid receptor genes. *Progress in Neurobiology*, 48(4), pp.275-305.
- Onaivi, E.S., Sugiura, T. and Di Marzo, V. eds., 2005. *Endocannabinoids: the brain and body's marijuana and beyond*. CRC Press.

- Ortega, A., Rangel-López, E., Hidalgo-Miranda, A., Morales, A., Ruiz-García, E., Meneses-García, A., Herrera-Gómez, A., Aguilar-Ponce, J.L., González-Herrera, I.G., Guevara-Salazar, P. and Prospero-García, O., 2015. On the effects of CP 55-940 and other cannabinoid receptor agonists in C6 and U373 cell lines. *Toxicology in Vitro*, 29(7), pp.1941-1951.
- O'Sullivan, S.E. and Kendall, D.A., 2010. Cannabinoid activation of peroxisome proliferator-activated receptors: potential for modulation of inflammatory disease. *Immunobiology*, 215(8), pp.611-616.
- Pacher, P., Bátkai, S., & Kunos, G. (2006). The endocannabinoid system as an emerging target of pharmacotherapy. *Pharmacological Reviews*, 58(3), pp.389-462.
- Pacioni, G., Rapino, C., Zarivi, O., Falconi, A., Leonardi, M., Battista, N., Colafarina, S., Sergi, M., Bonfigli, A., Miranda, M. and Barsacchi, D., 2015. Truffles contain endocannabinoid metabolic enzymes and anandamide. *Phytochemistry*, 110, pp.104-110.
- Palazzoli, F., Citti, C., Licata, M., Vilella, A., Manca, L., Zoli, M., Vandelli, M.A., Forni, F. and Cannazza, G., 2018. Development of a simple and sensitive liquid chromatography triple quadrupole mass spectrometry (LC-MS/MS) method for the determination of cannabidiol (CBD), Δ^9 -tetrahydrocannabinol (THC) and its metabolites in rat whole blood after oral administration of a single high dose of CBD. *Journal of Pharmaceutical and Biomedical Analysis*, 150, pp.25-32.
- Palkar, P.S., Borland, M.G., Naruhn, S., Ferry, C.H., Lee, C., Sk, U.H., Sharma, A.K., Amin, S., Murray, I.A., Anderson, C.R. and Perdew, G.H., 2010. Cellular and pharmacological selectivity of the peroxisome proliferator-activated receptor- β/δ antagonist GSK3787. *Molecular Pharmacology*, 78(3), pp.419-430.
- Parry, J.D., 2004. Protozoan grazing of freshwater biofilms. *Advances in Applied Microbiology*, 54, pp.167-196.
- Pauwels, A.M., Trost, M., Beyaert, R. and Hoffmann, E., 2017. Patterns, receptors, and signals: regulation of phagosome maturation. *Trends in Immunology*, 38(6), pp.407-422.
- Payandemehr, B., Ebrahimi, A., Gholizadeh, R., Rahimian, R., Varastehmoradi, B., Gooshe, M., Aghaei, H.N., Mousavizadeh, K. and Dehpour, A.R., 2015. Involvement of PPAR receptors in the anticonvulsant effects of a cannabinoid agonist, WIN 55,212-2. *Progress in Neuro-Psychopharmacology and Biological Psychiatry*, 57, pp.140-145.
- Perry, A., Ofek, I. and Silverblatt, F.J., 1983. Enhancement of mannose-mediated stimulation of human granulocytes by type 1 fimbriae aggregated with antibodies on *Escherichia coli* surfaces. *Infection and Immunity*, 39(3), pp.1334-1345.

- Pertwee, R. G. (1997). Pharmacology of cannabinoid CB 1 and CB 2 receptors. *Pharmacology & Therapeutics*, 74(2), pp.129-180.
- Pertwee, R. G. (2001). Cannabinoid receptors and pain. *Progress in Neurobiology*, 63(5), pp.569-611.
- Pertwee, R., Griffin, G., Fernando, S., Li, X., Hill, A. and Makriyannis, A., 1995. AM630, a competitive cannabinoid receptor antagonist. *Life Sciences*, 56(23-24), pp.1949-1955.
- Petrosino, S., Puigdemont, A., Della Valle, M.F., Fusco, M., Verde, R., Allara, M., Aveta, T., Orlando, P. and Di Marzo, V., 2016. Adelmidrol increases the endogenous concentrations of palmitoylethanolamide in canine keratinocytes and down-regulates an inflammatory reaction in an in vitro model of contact allergic dermatitis. *The Veterinary Journal*, 207, pp.85-91.
- Pickup Z.L., Pickup, R. and Parry, J. (2007). A comparison of the growth and starvation responses of *Acanthamoeba castellanii* and *Hartmannella vermiformis* in the presence of suspended and attached *Escherichia coli* K12. *FEMS Microbiology Ecology*, 59(3), pp.556-63.
- Pithadia, A.B. and Jain, S.M., 2009. 5-Hydroxytryptamine receptor subtypes and their modulators with therapeutic potentials. *Journal of Clinical Medicine Research*, 1(2), p.72.
- ringle, H.L., Bradley, S.G. and Harris, L.S. (1979). Susceptibility of *Naegleria fowleri* to delta 9-tetrahydrocannabinol. *Antimicrobial Agents and Chemotherapy*, [16(5), pp.674–679.
- Rácz, I., Bilkei-Gorzo, A., Markert, A., Stamer, F., Göthert, M. and Zimmer, A., 2008. Anandamide effects on 5-HT₃ receptors in vivo. *European Journal of Pharmacology*, 596(1-3), pp.98-101.
- Raff, M., Alberts, B., Lewis, J., Johnson, A. and Roberts, K., 2002. *Molecular Biology of the Cell* 4th edition. *Annals of Botany*, [online] 91(3), pp.401–401.
- Rahn, E.J. and Hohmann, A.G., 2009. Cannabinoids as pharmacotherapies for neuropathic pain: from the bench to the bedside. *Neurotherapeutics*, 6(4), pp.713-737.
- Rajaram, M.V., Arnett, E., Azad, A.K., Guirado, E., Ni, B., Gerberick, A.D., He, L.Z., Keler, T., Thomas, L.J., Lafuse, W.P. and Schlesinger, L.S., 2017. *M. tuberculosis*-initiated human mannose receptor signaling regulates macrophage recognition and vesicle trafficking by FcRγ-Chain, Grb2, and SHP-1. *Cell Reports*, 21(1), pp.126-140.
- Ramoino, P., 1997. Lectin-binding glycoconjugates in *Paramecium primaurelia*: changes with cellular age and starvation. *Histochemistry and Cell Biology*, 107(4), pp.321-329.

- Ramoino, P., Fronte, P., Fato, M., Beltrame, F., Robello, M. and Diaspro, A., 2001. Fluid phase and receptor-mediated endocytosis in *Paramecium primaurelia* by fluorescence confocal laser scanning microscopy. *European Biophysics Journal*, 30(5), pp.305-312.
- Ramos, J., Cruz, V.L., Martínez-Salazar, J., Campillo, N.E. and Páez, J.A., 2011. Dissimilar interaction of CB1/CB2 with lipid bilayers as revealed by molecular dynamics simulation. *Physical Chemistry Chemical Physics*, 13(9), pp.3660-3668.
- Rashid, A.J., So, C.H., Kong, M.M., Furtak, T., El-Ghundi, M., Cheng, R., O'Dowd, B.F. and George, S.R., 2007. D1–D2 dopamine receptor heterooligomers with unique pharmacology are coupled to rapid activation of Gq/11 in the striatum. *Proceedings of the National Academy of Sciences*, 104(2), pp.654-659.
- Rigano, D., Sirignano, C. and Tagliatela-Scafati, O., 2017. The potential of natural products for targeting PPAR α . *Acta Pharmaceutica Sinica B*, 7(4), pp.427-438.
- Roberts, E.C., Zubkov, M.V., Martin-Cereceda, M., Novarino, G. and Wootton, E.C., 2006. Cell surface lectin-binding glycoconjugates on marine planktonic protists. *FEMS Microbiology Letters*, 265(2), pp.202-207.
- Rogers, D.C. and Thorp, J.H. eds., 2019. Thorp and Covich's Freshwater Invertebrates: Volume 4: Keys to Palaeartic Fauna. Academic Press.
- Rogerson, A., Hannah, F. and Gothe, G., 1996. The grazing potential of some unusual marine benthic amoebae feeding on bacteria. *European Journal of Protistology*, 32(2), pp.271-279.
- Romanelli, R.J., Williams, J.T. and Neve, K.A., 2010. Dopamine receptor signaling: intracellular pathways to behavior. In *The dopamine receptors* (pp. 137-173). Humana Press, Totowa, NJ.
- Romano, A., Tempesta, B., Provensi, G., Passani, M.B. and Gaetani, S., 2015. Central mechanisms mediating the hypophagic effects of oleoylethanolamide and N-acylphosphatidylethanolamines: different lipid signals? *Frontiers in Pharmacology*, 6, p.137.
- Rose, J.M., Vora, N.M., Countway, P.D., Gast, R.J. and Caron, D.A., 2009. Effects of temperature on growth rate and gross growth efficiency of an Antarctic bacterivorous protist. *The ISME Journal*, 3(2), pp.252-260.
- Ross, R.A., Brockie, H.C. and Pertwee, R.G., 2000. Inhibition of nitric oxide production in RAW264. 7 macrophages by cannabinoids and palmitoylethanolamide. *European Journal of Pharmacology*, 401(2), pp.121-130.
- Russo, E.B., Burnett, A., Hall, B. and Parker, K.K., 2005. Agonistic properties of cannabidiol at 5-HT_{1a} receptors. *Neurochemical Research*, 30(8), pp.1037-1043.

- Ryberg, E., Larsson, N., Sjögren, S., Hjorth, S., Hermansson, N.O., Leonova, J., Elebring, T., Nilsson, K., Drmota, T. and Greasley, P.J., 2007. The orphan receptor GPR55 is a novel cannabinoid receptor. *British Journal of Pharmacology*, 152(7), pp.1092-1101.
- Sailler, S., Schmitz, K., Jäger, E., Ferreiros, N., Wicker, S., Zschiebsch, K., Pickert, G., Geisslinger, G., Walter, C., Tegeder, I. and Lötsch, J., 2014. Regulation of circulating endocannabinoids associated with cancer and metastases in mice and humans. *Oncoscience*, 1(4), p.272.
- Samara, M.T., Cao, H., Helfer, B., Davis, J.M. and Leucht, S., 2014. Chlorpromazine versus every other antipsychotic for schizophrenia: a systematic review and meta-analysis challenging the dogma of equal efficacy of antipsychotic drugs. *European Neuropsychopharmacology*, 24(7), pp.1046-1055.
- Saukkonen, K., Cabellos, C., Burroughs, M., Prasad, S. and Tuomanen, E., 1991. Integrin-mediated localization of *Bordetella pertussis* within macrophages: role in pulmonary colonization. *The Journal of Experimental Medicine*, 173(5), pp.1143-1149.
- Schotte, A., Janssen, P.F.M., Megens, A.A.H.P. and Leysen, J.E., 1993. Occupancy of central neurotransmitter receptors by risperidone, clozapine and haloperidol, measured ex vivo by quantitative autoradiography. *Brain Research*, 631(2), pp.191-202.
- Schumann, J., 2016. It is all about fluidity: Fatty acids and macrophage phagocytosis. *European Journal of Pharmacology*, 785, pp.18-23.
- Schweizer, A., Stahl, P.D. and Rohrer, J., 2000. A di-aromatic motif in the cytosolic tail of the mannose receptor mediates endosomal sorting. *Journal of Biological Chemistry*, 275(38), pp.29694-29700.
- Schuff-Werner, P. and Splettstoesser, W., 1999. Antioxidative properties of serotonin and the bactericidal function of polymorphonuclear phagocytes. In *Tryptophan, Serotonin, and Melatonin* (pp. 321-325). Springer, Boston, MA.
- Scotchie, J.G., Savaris, R.F., Martin, C.E. and Young, S.L., 2015. Endocannabinoid regulation in human endometrium across the menstrual cycle. *Reproductive Sciences*, 22(1), pp.113-123.
- Seeman, P., 2016. Cannabidiol is a partial agonist at dopamine D2High receptors, predicting its antipsychotic clinical dose. *Translational Psychiatry*, 6(10), pp.e920-e920.
- Shao, Z., Yin, J., Chapman, K., Grzemska, M., Clark, L., Wang, J. and Rosenbaum, D.M., 2016. High-resolution crystal structure of the human CB1 cannabinoid receptor. *Nature*, 540(7634), pp.602-606.
- Shinzaki, S., Ishii, M., Fujii, H., Iijima, H., Wakamatsu, K., Kawai, S., Shiraishi, E., Hiyama, S., Inoue, T., Hayashi, Y. and Kuwahara, R., 2016. N-acetylglucosaminyltransferase V

- exacerbates murine colitis with macrophage dysfunction and enhances colitic tumorigenesis. *Journal of Gastroenterology*, 51(4), pp.357-369.
- Silver, R.J., 2019. The Endocannabinoid System of Animals. *Animals*, 9(9), p.686.
- Singh, N., Hroudová, J. and Fišar, Z., 2015. Cannabinoid-induced changes in the activity of electron transport chain complexes of brain mitochondria. *Journal of Molecular Neuroscience*, 56(4), pp.926-931.
- Skaper, S.D., Facci, L., Zusso, M. and Giusti, P., 2018. An inflammation-centric view of neurological disease: beyond the neuron. *Frontiers in Cellular Neuroscience*, 12, p.72.
- Smirnov, A., 2008. Amoebas, lobose. *Encyclopedia of Microbiology*. Elsevier, Oxford, 558577.
- Smirnov, A.V., Chao, E., Nasonova, E.S. and Cavalier-Smith, T., 2011. A revised classification of naked lobose amoebae (Amoebozoa: Lobosa). *Protist*, 4(162), pp.545-570.
- Soethoudt, M., Grether, U., Fingerle, J., Grim, T.W., Fezza, F., De Petrocellis, L., Ullmer, C., Rothenhäusler, B., Perret, C., Van Gils, N. and Finlay, D., 2017. Cannabinoid CB2 receptor ligand profiling reveals biased signalling and off-target activity. *Nature Communications*, 8(1), pp.1-14.
- Stahl, P., Schlesinger, P.H., Sigardson, E., Rodman, J.S. and Lee, Y.C., 1980. Receptor-mediated pinocytosis of mannose glycoconjugates by macrophages: characterization and evidence for receptor recycling. *Cell*, 19(1), pp.207-215.
- Sternberg, E.M., Trial, J. and Parker, C.W., 1986. Effect of serotonin on murine macrophages: suppression of Ia expression by serotonin and its reversal by 5-HT₂ serotonergic receptor antagonists. *The Journal of Immunology*, 137(1), pp.276-282.
- Strange, P., 1997. Biochemical characterization of dopamine receptors. In *The dopamine receptors* (pp. 3-26). Humana Press, Totowa, NJ.
- Sugiura, T., Kondo, S., Kishimoto, S., Miyashita, T., Nakane, S., Kodaka, T., Suhara, Y., Takayama, H. and Waku, K., 2000. Evidence that 2-arachidonoylglycerol but not N-palmitoylethanolamine or anandamide is the physiological ligand for the cannabinoid CB2 receptor Comparison of the agonistic activities of various cannabinoid receptor ligands in HL-60 cells. *Journal of Biological Chemistry*, 275(1), pp.605-612.
- Sugiura, T., Kondo, S., Sukagawa, A., Nakane, S., Shinoda, A., Itoh, K., Yamashita, A. and Waku, K., 1995. 2-Arachidonoylglycerol: a possible endogenous cannabinoid receptor ligand in brain. *Biochemical and Biophysical Research Communications*, 215(1), pp.89-97.
- Sulak, D., 2015. Introduction to the endocannabinoid system. Arvutivõrgus kättesaadav: [\(http://norml.org/library/item/introduction-to-the-endocannabinoid-system\)](http://norml.org/library/item/introduction-to-the-endocannabinoid-system).(29.04.2017).

- Sultan, A.S., Marie, M.A. and Sheweita, S.A., 2018. Novel mechanism of cannabidiol-induced apoptosis in breast cancer cell lines. *The Breast*, 41, pp.34-41.
- Sun, Y. and Bennett, A. (2007). Cannabinoids: A New Group of Agonists of PPARs. *PPAR Research*, 2007, pp.1–7.
- Sun, Y., Alexander, S.P.H., Kendall, D.A. and Bennett, A.J. (2006). Cannabinoids and PPARalpha signalling. *Biochemical Society Transactions*, [online] 34(Pt 6), pp.1095–1097.
- Svíženská, I., Dubový, P. and Šulcová, A., 2008. Cannabinoid receptors 1 and 2 (CB1 and CB2), their distribution, ligands and functional involvement in nervous system structures—a short review. *Pharmacology Biochemistry and Behavior*, 90(4), pp.501-511.
- Szabo, B., Wallmichrath, I., Mathonia, P. and Pfreundtner, C., 2000. Cannabinoids inhibit excitatory neurotransmission in the substantia nigra pars reticulata. *Neuroscience*, 97(1), pp.89-97.
- Tambaro, S. and Bortolato, M., 2012. Cannabinoid-related agents in the treatment of anxiety disorders: current knowledge and future perspectives. *Recent patents on CNS drug discovery*, 7(1), pp.25-40.
- Tenenbaum, A., Motro, M. and Fisman, E.Z., 2005. Dual and pan-peroxisome proliferator-activated receptors (PPAR) co-agonism: the bezafibrate lessons. *Cardiovascular Diabetology*, 4(1), p.14.
- Thabuis, C., Destailats, F., Lambert, D.M., Muccioli, G.G., Maillot, M., Harach, T., Tissot-Favre, D. and Martin, J.C., 2011. Lipid transport function is the main target of oral oleoylethanolamide to reduce adiposity in high-fat-fed mice. *Journal of Lipid Research*, 52(7), pp.1373-1382.
- Thabuis, C., Tissot-Favre, D., Bezelgues, J.B., Martin, J.C., Cruz-Hernandez, C., Dionisi, F. and Destailats, F., 2008. Biological functions and metabolism of oleoylethanolamide. *Lipids*, 43(10), p.887.
- The Weed Blog. (2012). Best LED Grow Lights for Flowering Cannabis | LED Grow Lights for the Flowering Stage. [online] Available at: <https://theweedblog.com/growing/how-to-flower-cannabis-plants-with-led-grow-lights> [Accessed 31 March 2020].
- Tridandapani, S., Lyden, T.W., Smith, J.L., Carter, J.E., Coggeshall, K.M. and Anderson, C.L., 2000. The adapter protein LAT enhances Fcγ receptor-mediated signal transduction in myeloid cells. *Journal of Biological Chemistry*, 275(27), pp.20480-20487.
- Tripathy, S., Kleppinger-Sparace, K., Dixon, R.A. and Chapman, K.D., 2003. N-acylethanolamine signaling in tobacco is mediated by a membrane-associated, high-affinity binding protein. *Plant Physiology*, 131(4), pp.1781-1791.

- Tsuboi, K., Okamoto, Y., Rahman, I.A.S., Uyama, T., Inoue, T., Tokumura, A. and Ueda, N., 2015. Glycerophosphodiesterase GDE4 as a novel lysophospholipase D: a possible involvement in bioactive N-acylethanolamine biosynthesis. *Biochimica et Biophysica Acta (BBA)-Molecular and Cell Biology of Lipids*, 1851(5), pp.537-548.
- Tyagi, S., Gupta, P., Saini, A.S., Kaushal, C. and Sharma, S., 2011. The peroxisome proliferator-activated receptor: A family of nuclear receptors role in various diseases. *Journal of Advanced Pharmaceutical Technology & Research*, 2(4), p.236.
- Taylor, P.R., Martinez-Pomares, L., Stacey, M., Lin, H.H., Brown, G.D. and Gordon, S., 2005. Macrophage receptors and immune recognition. *Annual Review of Immunology*, 23, pp.901-944.
- Tyml, T., Skulinová, K., Kavan, J., Ditrich, O., Kostka, M. and Dyková, I., 2016. Heterolobosean amoebae from Arctic and Antarctic extremes: 18 novel strains of *Allovahlkampfia*, *Vahlkampfia* and *Naegleria*. *European Journal of Protistology*, 56, pp.119-133.
- Ud-Daula, A., Pfister, G. and Schramm, K.-W. (2012). Identification of Dopamine Receptor in *Tetrahymena thermophila* by Fluorescent Ligands. *Pakistan Journal of Biological Sciences*, 15(23), pp.1133–1138.
- Unsworth, A.J., Flora, G.D. and Gibbins, J.M., 2018. Non-genomic effects of nuclear receptors: insights from the anucleate platelet. *Cardiovascular Research*, 114(5), pp.645-655.
- Unsworth, A.J., Kriek, N., Bye, A.P., Naran, K., Sage, T., Flora, G.D. and Gibbins, J.M., 2017. PPAR γ agonists negatively regulate α II b β 3 integrin outside-in signaling and platelet function through up-regulation of protein kinase A activity. *Journal of Thrombosis and Haemostasis*, 15(2), pp.356-369.
- Vaughn, A.R., Davis, M.J., Sivamani, R.K. and Isseroff, R.R., 2018. A concise review of the conflicting roles of dopamine-1 versus dopamine-2 receptors in wound healing. *Molecules*, 23(1), p.50.
- Vauquelin, G. and Charlton, S.J., 2010. Long-lasting target binding and rebinding as mechanisms to prolong in vivo drug action. *British Journal of Pharmacology*, 161(3), pp.488-508.
- Venkataraman, C., Haack, B.J., Bondada, S. and Kwai, Y.A., 1997. Identification of a Gal/GalNAc lectin in the protozoan *Hartmannella vermiformis* as a potential receptor for attachment and invasion by the Legionnaires' disease bacterium. *The Journal of Experimental Medicine*, 186(4), pp.537-547.
- Verme, J.L., Fu, J., Astarita, G., La Rana, G., Russo, R., Calignano, A. and Piomelli, D., 2005. The nuclear receptor peroxisome proliferator-activated receptor- α mediates the anti-

- inflammatory actions of palmitoylethanolamide. *Molecular Pharmacology*, 67(1), pp.15-19.
- Vleugels, R., Verlinden, H. and Vanden Broeck, J., 2015. Serotonin, serotonin receptors and their actions in insects. *Neurotransmitter*, 2, pp.1-14.
- Vogel, G., Thilo, L., Schwarz, H. & Steinhart, R. 1980. Mechanism of phagocytosis in *Dictyostelium discoideum*: phagocytosis is mediated by different recognition sites as disclosed by mutants with altered phagocytotic properties. *The Journal of Cell Biology*, 86, pp.456-465.
- Wagner, J.A., J arai, Z., B atkai, S. and Kunos, G., 2001. Hemodynamic effects of cannabinoids: coronary and cerebral vasodilation mediated by cannabinoid CB1 receptors. *European Journal of Pharmacology*, 423(2-3), pp.203-210.
- Walochnik, J. and Mulec, J., 2009. Free-living amoebae in carbonate precipitating microhabitats of karst caves and a new vahlkampfiid amoeba, *Allovahlkampfia spelaea* gen. nov., sp. nov. *Acta Protozoologica*, 48(1), p.25.
- Wang, H., Xie, H., Sun, X., Kingsley, P. J., Marnett, L. J., Cravatt, B. F., & Dey, S. K. (2007). Differential regulation of endocannabinoid synthesis and degradation in the uterus during embryo implantation. *Prostaglandins & other Lipid Mediators*, 83(1), pp.62-74.
- Watkins, A.R., 2019. Cannabinoid interactions with ion channels and receptors. *Channels*, 13(1), pp.162-167.
- Watkins, R.A., Andrews, A., Wynn, C., Barisch, C., King, J.S. and Johnston, S.A., 2018. *Cryptococcus neoformans* escape from *Dictyostelium* amoeba by both WASH-mediated constitutive exocytosis and vomocytosis. *Frontiers in Cellular and Infection Microbiology*, 8, p.108.
- Weiel, J.E. and Piozzo, S.V., 1983. Down regulation of macrophage mannose/N-acetylglucosamine receptors by elevated glucose concentrations. *Biochimica et Biophysica Acta (BBA)-General Subjects*, 759(3), pp.170-175.
- Winkler, J., L unsdorf, H. and Jockusch, B.M., 1996. The ultrastructure of chicken gizzard vinculin as visualized by high-resolution electron microscopy. *Journal of Structural Biology*, 116(2), pp.270-277.
- Witkamp, R.F., 2018. The role of fatty acids and their endocannabinoid-like derivatives in the molecular regulation of appetite. *Molecular Aspects of Medicine*, 64, pp.45-67.
- Wootton, E.C., Zubkov, M.V., Jones, D.H., Jones, R.H., Martel, C.M., Thornton, C.A. and Roberts, E.C., 2007. Biochemical prey recognition by planktonic protozoa. *Environmental Microbiology*, 9(1), pp.216-222.

- Wormald, M.R. and Sharon, N. (2004). Carbohydrates and glycoconjugates: progress in non-mammalian glycosylation, glycosyltransferases, invertebrate lectins and carbohydrate-carbohydrate interactions. *Current Opinion in Structural Biology*, [online] 14(5), pp.591–592.
- Wright, S.D., Levin, S.M., Jong, M.T., Chad, Z. and Kabbash, L.G., 1989. CR3 (CD11b/CD18) expresses one binding site for Arg-Gly-Asp-containing peptides and a second site for bacterial lipopolysaccharide. *The Journal of Experimental Medicine*, 169(1), pp.175-183.
- Wu, J. (2019). Cannabis, cannabinoid receptors, and endocannabinoid system: yesterday, today, and tomorrow. *Acta Pharmacologica Sinica*, 40(3), pp.297–299.
- Xu, X., Wang, J., Jiang, H., Meng, L. and Lang, B. (2017). Rosiglitazone induces apoptosis on human bladder cancer 5637 and T24 cell lines. *International Journal of Clinical and Experimental Pathology*, [online] 10(10), pp.10197–10204.
- Yamauchi, S., Kawauchi, K. and Sawada, Y., 2012. Myosin II-dependent exclusion of CD45 from the site of Fcγ receptor activation during phagocytosis. *FEBS letters*, 586(19), pp.3229-3235.
- Yu, M., Lowell, C.A., Neel, B.G. and Gu, H., 2006. Scaffolding adapter Grb2-associated binder 2 requires Syk to transmit signals from FcεRI. *The Journal of Immunology*, 176(4), pp.2421-2429.
- Zanchi, R., Howard, G., Bretscher, M.S. and Kay, R.R., 2010. The exocytic gene *secA* is required for *Dictyostelium* cell motility and osmoregulation. *Journal of Cell Science*, 123(19), pp.3226-3234.
- Zeng, Z., Surewaard, B.G., Wong, C.H., Geoghegan, J.A., Jenne, C.N. and Kubes, P., 2016. CR1g functions as a macrophage pattern recognition receptor to directly bind and capture blood-borne gram-positive bacteria. *Cell Host & Microbe*, 20(1), pp.99-106.
- Zhou, J., Noori, H., Burkovskiy, I., Lafreniere, J.D., Kelly, M.E. and Lehmann, C., 2019. Modulation of the endocannabinoid system following central nervous system injury. *International Journal of Molecular Sciences*, 20(2), p.388.
- Zou, S. and Kumar, U., 2018. Cannabinoid receptors and the endocannabinoid system: signaling and function in the central nervous system. *International Journal of Molecular Sciences*, 19(3), p.833.

APPENDIX 1: Media formulations

Amoeba Saline (AS)

Stock 1:

NaCl	12.0g
MgSO ₄ ·7H ₂ O	0.4g
CaCl ₂ ·6H ₂ O	0.6g
Distilled water	500ml

Stock 2:

Na ₂ HPO ₄	14.2g
KH ₂ PO ₄	13.6g
Distilled water	500ml

Prepare stocks and store at 4°C. Add 5ml stock 1 and 5ml stock 2 to 990ml distilled water. Autoclave at 121°C for 15 min.

BG11 Broth

Stock 1:

NaNO ₃	15.0g
K ₂ HPO ₄	4.0g
MgSO ₄ ·7H ₂ O	7.5g
CaCl ₂ ·2H ₂ O	3.6g
Citric acid	0.6g
Ammonium ferric citrate green	0.6g
EDTANa ₂	0.1g
Na ₂ CO ₃	2.0g
Distilled water	1000 ml

Stock 2:

H ₃ BO ₃	2.86g
MnCl ₂ ·4H ₂ O	1.81g
ZnSO ₄ ·7H ₂ O	0.22g
Na ₂ MoO ₄ ·2H ₂ O	0.39g
CuSO ₄ ·5H ₂ O	0.08g
Co(NO ₃) ₂ ·6H ₂ O	0.05g
Distilled water	1000ml

Prepare stocks and store at 4°C. Add 10ml stock 1 and 1ml stock 2 to 989 ml distilled water. Adjust pH to 7.1 with 1M NaOH or HCl. Autoclave at 121°C for 15 minutes.

Diagnostic Sensitivity Test (DST) agar with chloramphenicol (at 30 µg/ml)

Add 37.5g of Diagnostic Sensitivity Test agar (MAST laboratories) to 1L distilled water. Autoclave at 121°C for 15 min. Cool to *ca.* 50°C before adding 1ml of filter sterilized chloramphenicol solution (30 mg/ml).

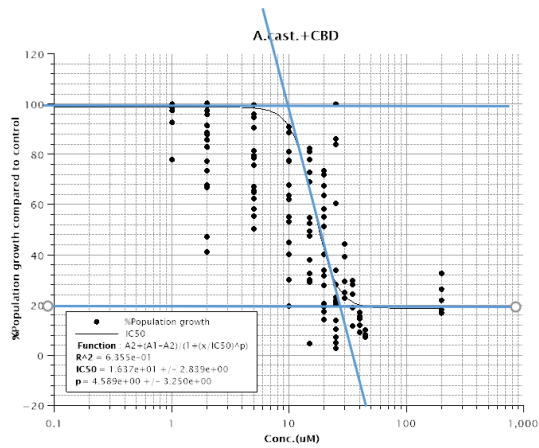
Non-Nutrient Agar with agar (NNA) or agarose (NNAg)

Add 15g of either Agar N° 2 (for NNA) or agarose (for NNAg) to 1L Amoeba Saline (AS). Autoclave at 121°C for 15 min.

Appendix 2: IC₅₀ graphs of all sensitive amoeba strains with AEA and CBD (Section 3.2.2)

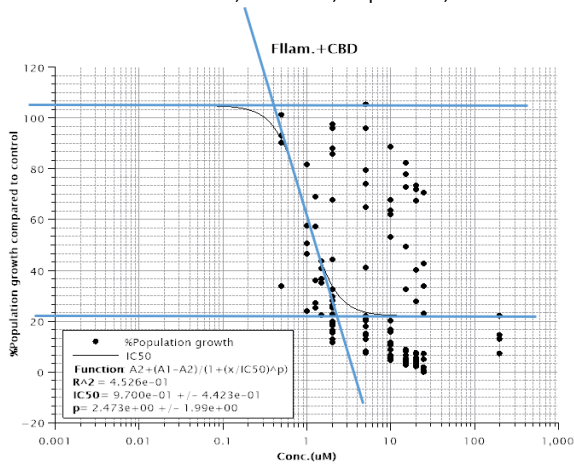
Acanthamoeba castellanii CCAP1501/1A (CBD only).

Estimated MIC =10.00, IC₅₀=16.37, Slope= 4.59, Lethal dose >27



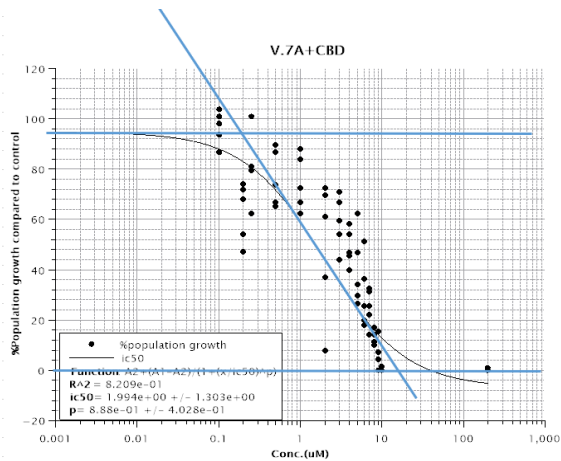
Flamella arnhemensis CCAP1525/2 (CBD only).

estimated MIC =0.40, IC₅₀=0.97, Slope= 2.47, Lethal dose >4



Vermamoeba vermiformis CCAP 1534/7A (CBD only, AEA in Fig. 3.2)

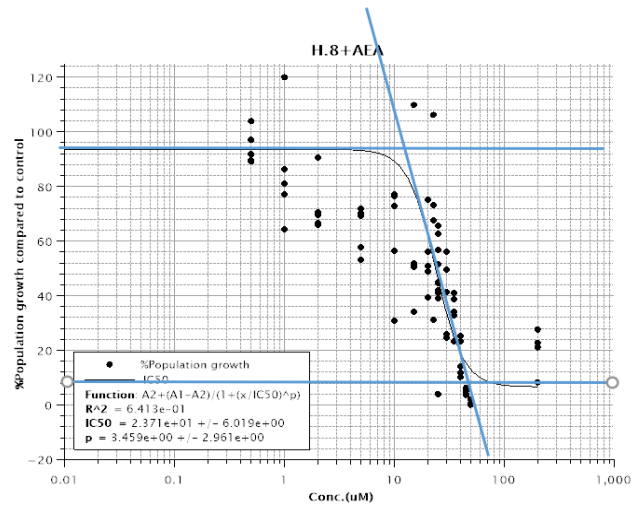
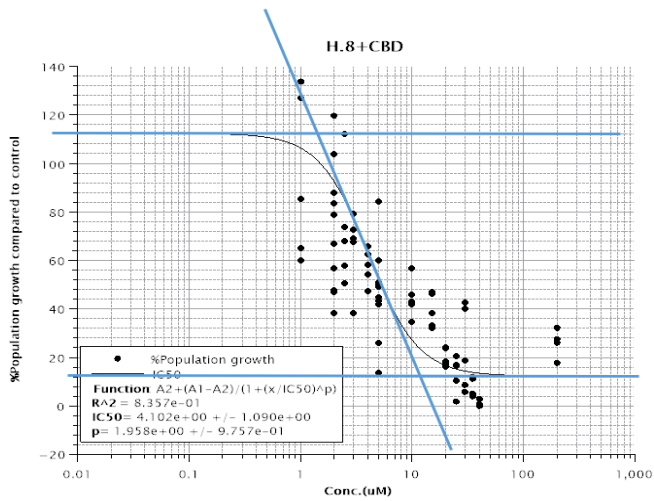
estimated MIC =0.20, IC₅₀=1.99, Slope=0.89, Lethal dose >16



Hartmannella cantabrigiensis CCAP1534/8

CBD: estimated MIC =1.50, IC50=4.10, Slope=1.96, Lethal dose >13

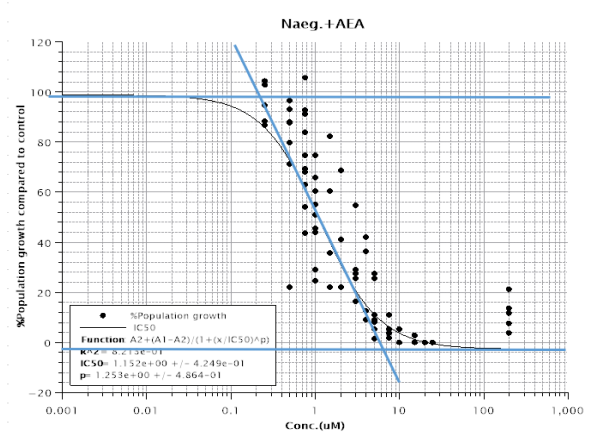
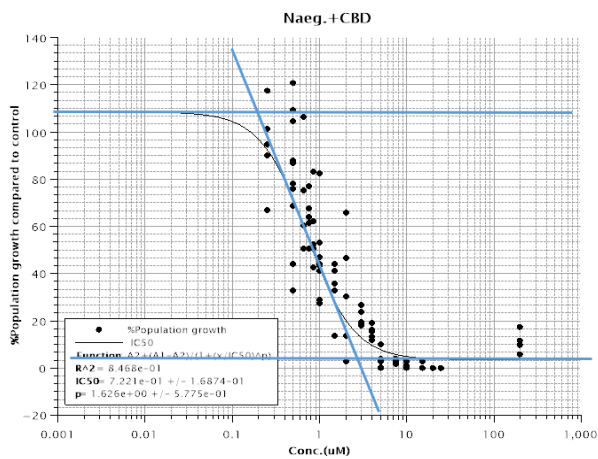
AEA: estimated MIC =14.00, IC50=23.10, Slope= 3.46, Lethal dose >41



Naegleria gruberi NEG-M

CBD: estimated MIC =0.20, IC50=0.75, Slope=1.63, Lethal dose >3

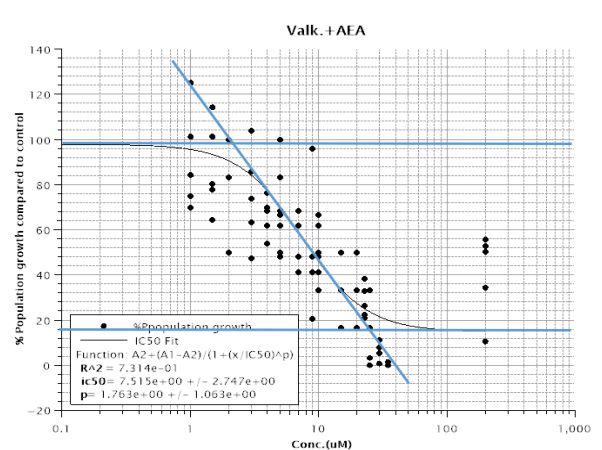
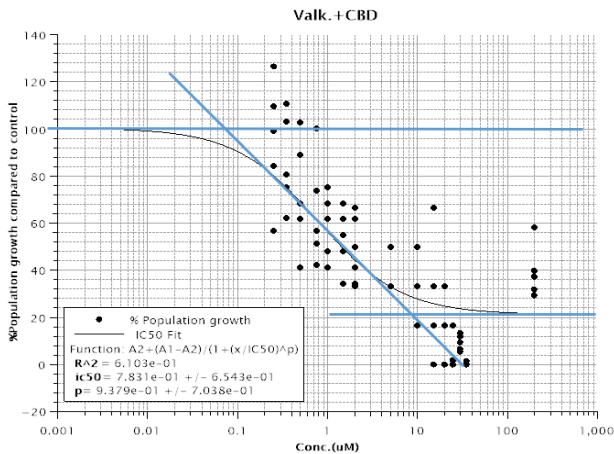
AEA: estimated MIC =0.21, IC50=1.15, Slope=1.25, Lethal dose >6



Vahlkampfia avara CCAP 1588/1A

CBD: estimated MIC =0.08, IC50=0.78, Slope=0.94, Lethal dose >9

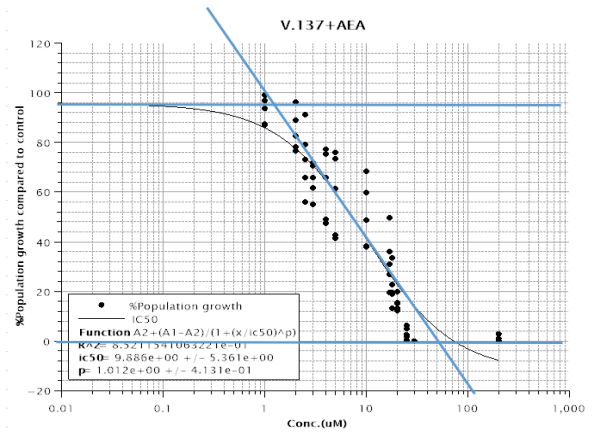
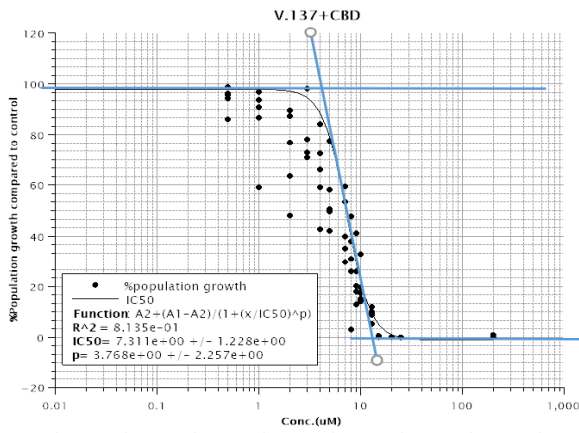
AEA: estimated MIC =2.10, IC50=7.52, Slope=1.76, Lethal dose >4



***Vermamoeba vermiformis* 137**

CBD: estimated MIC =4.00, IC50=7.31, Slope=3.77 , Lethal dose >14

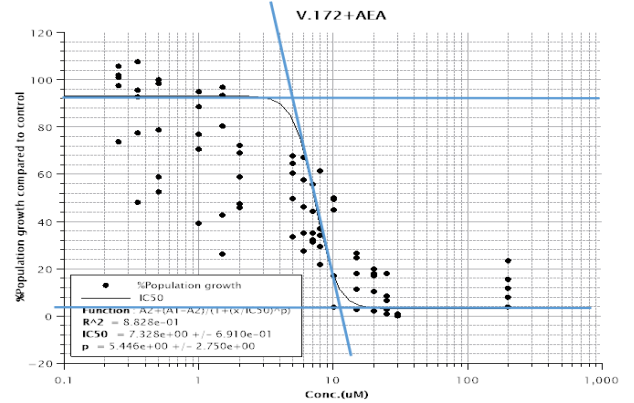
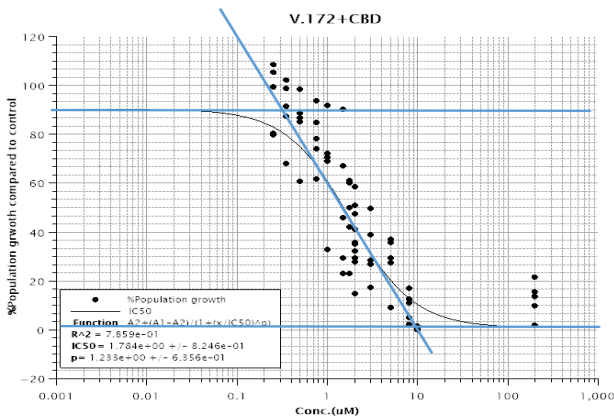
AEA: estimated MIC =1.30, IC50=9.89, Slope=1.01, Lethal dose >50



***Vermamoeba vermiformis* 172**

CBD: estimated MIC =0.30, IC50=1.78, Slope=1.23 , Lethal dose >10

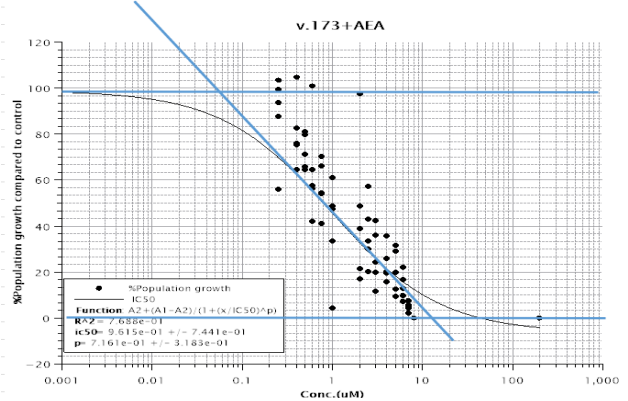
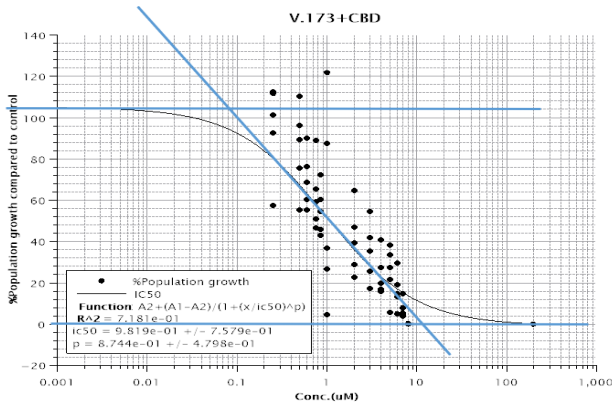
AEA: estimated MIC =5.00, IC50=7.33, Slope=5.45, Lethal dose >12



***Vermamoeba vermiformis* 173**

CBD: estimated MIC =0.08, IC50=0.98, Slope=0.87 , Lethal dose >10

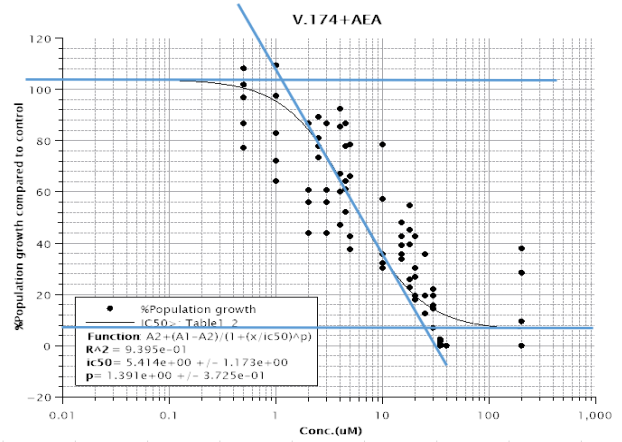
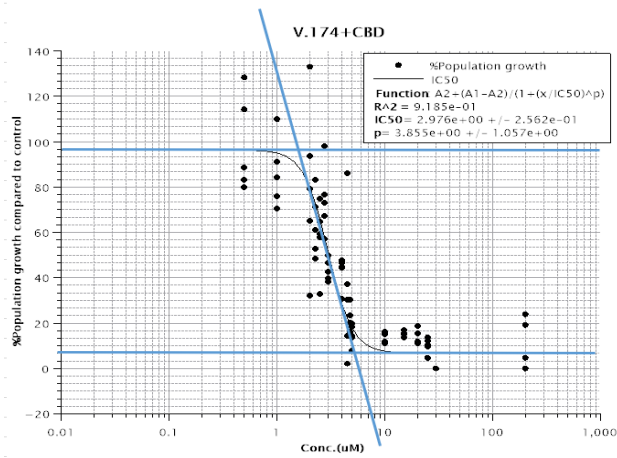
AEA: estimated MIC =0.06, IC50=0.96, Slope=0.72, Lethal dose >13



***Vermamoeba vermiformis* 174**

CBD: estimated MIC =1.60, IC50=2.98, Slope=3.86, Lethal dose >5

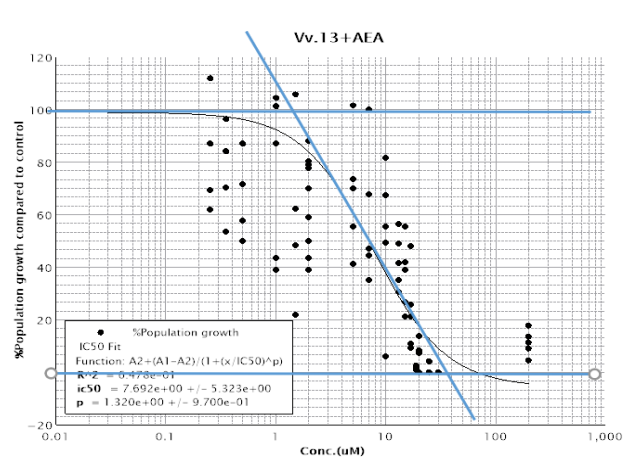
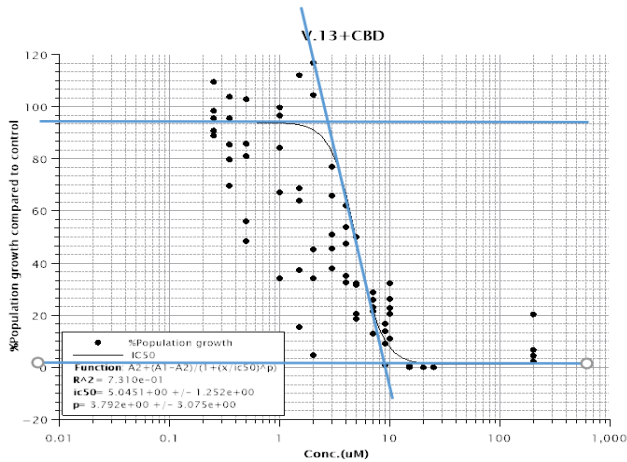
AEA: estimated MIC =1.20, IC50=5.41, Slope=1.23, Lethal dose >25



***Vermamoeba vermiformis* CCAP 1534/13**

CBD: estimated MIC =3.00, IC50=5.05, Slope=3.79, Lethal dose >9

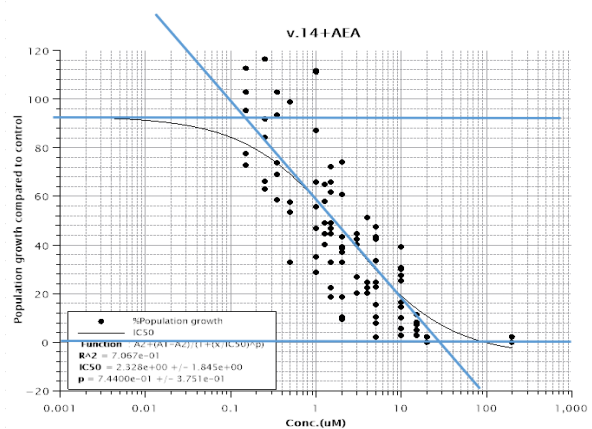
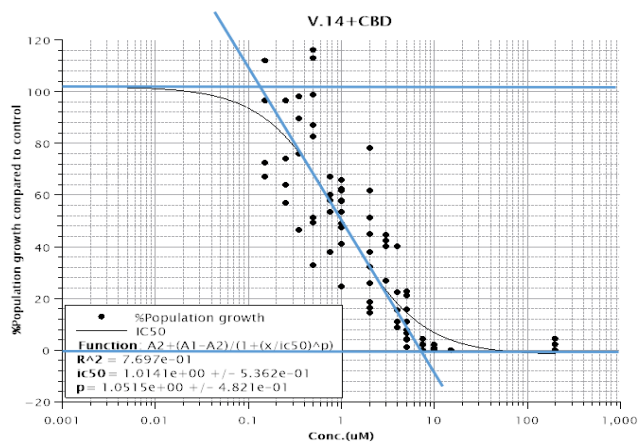
AEA: estimated MIC =1.50, IC50=7.69, Slope=1.32, Lethal dose >35



***Vermamoeba vermiformis* CCAP 1534/14**

CBD: estimated MIC =0.15, IC50=1.01, Slope=1.05, Lethal dose >8

AEA: estimated MIC =0.15, IC50=2.33, Slope=0.74, Lethal dose >30

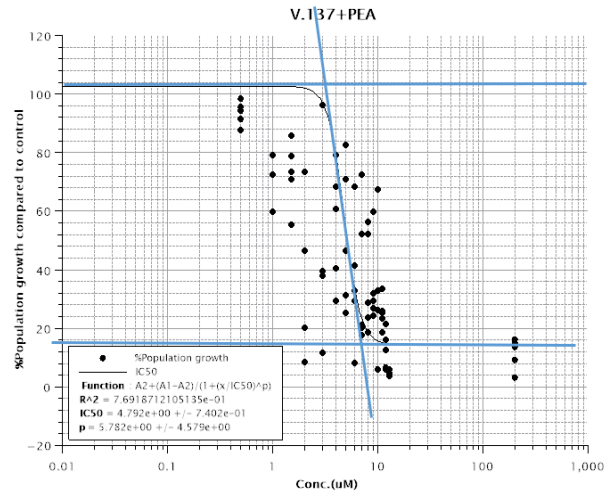
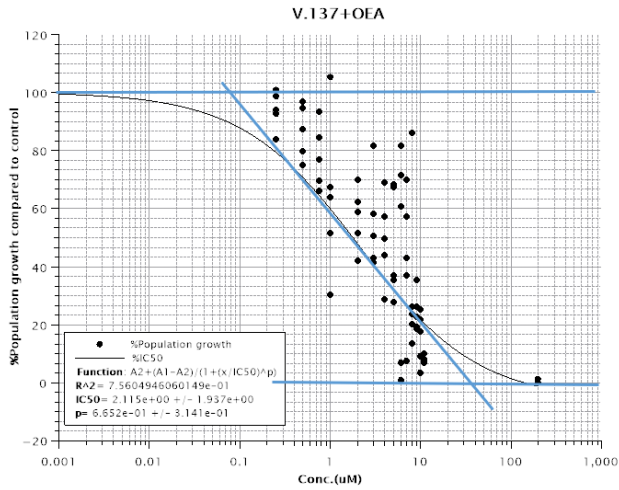


Appendix 3: IC50 graphs of all sensitive amoeba strains with OEA, PEA, GW0742 and Rosiglitazone (Section 5.2.1.1)

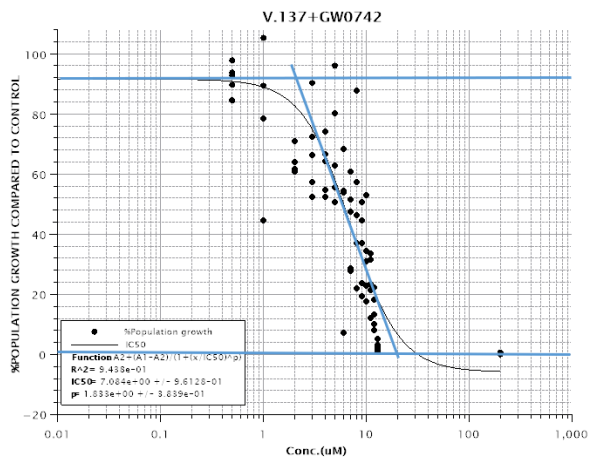
Vermamoeba vermiformis 137

OEA: estimated MIC = 0.08, IC50=2.12, Slope=0.67, Lethal dose >35

PEA: estimated MIC =3.10, IC50=4.79, Slope=5.78, Lethal dose >8



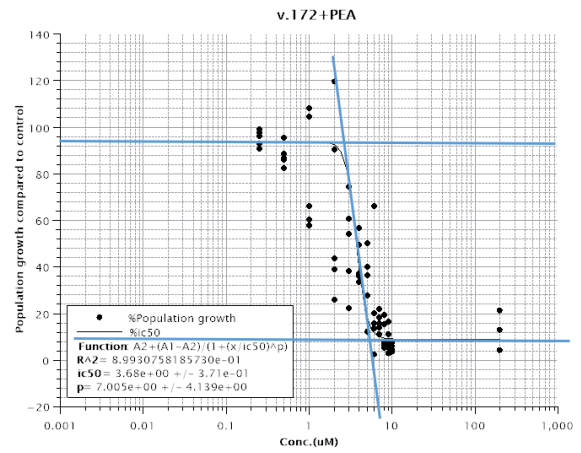
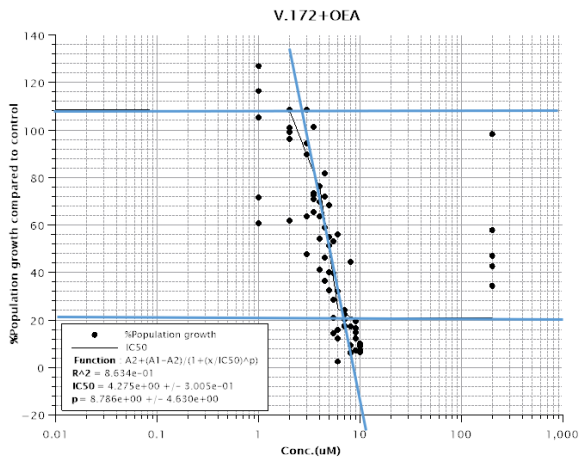
GW0742: estimated MIC =2, IC50=1.80, Slope=1.83, Lethal dose >20



Vermamoeba vermiformis 172

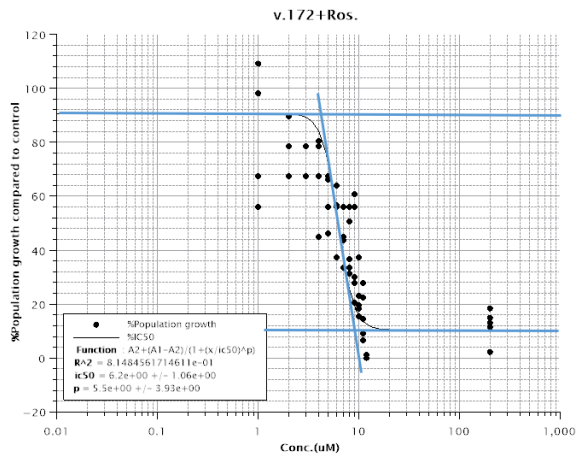
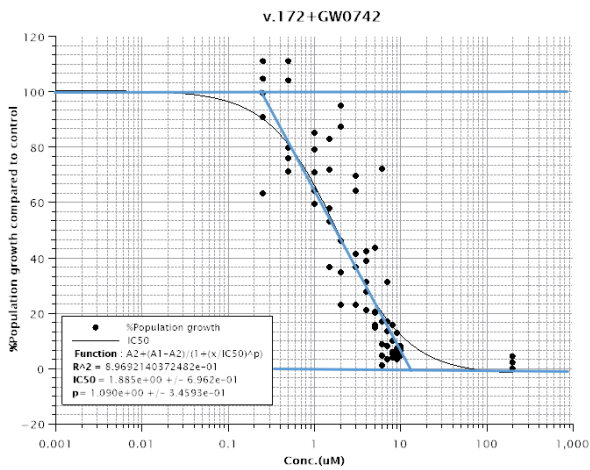
OEA: estimated MIC =2.70, IC50=4.28, Slope=8.79, Lethal dose >9

PEA: estimated MIC =2.70, IC50=3.68, Slope=7.00, Lethal dose >5



GW0742 estimated MIC =0.25, IC50=1.89, Slope=1.09, Lethal dose >14

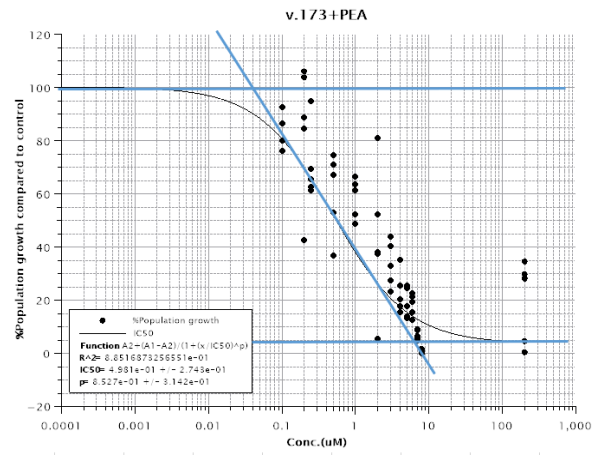
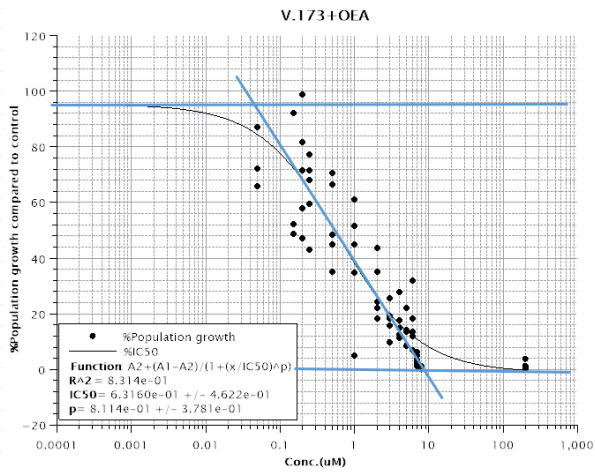
Rosiglitazone: estimated MIC =4.00, IC50=6.2, Slope=5.5, Lethal dose >9



Vermamoeba vermiformis 173

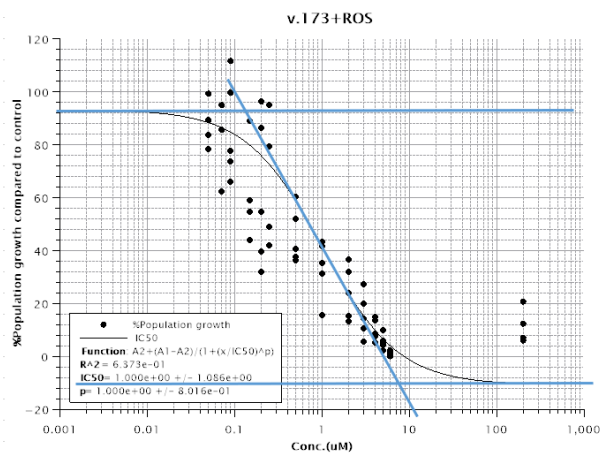
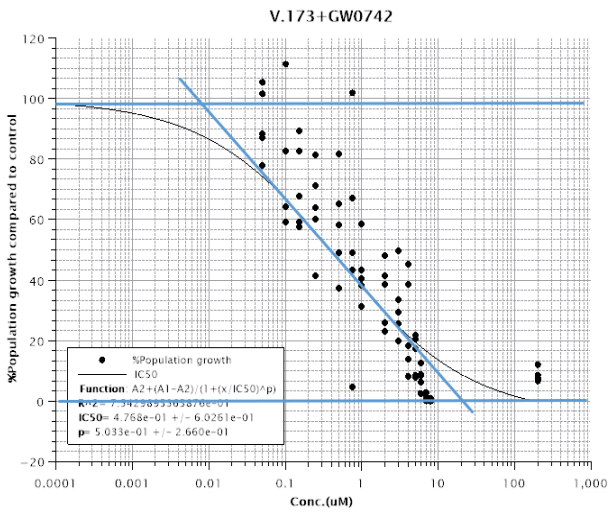
OEA: estimated MIC =0.04, IC50=0.63, Slope=0.81 , Lethal dose >10

PEA: estimated MIC =0.04, IC50=0.5, Slope=0.85, Lethal dose >8



GW0742 estimated MIC =0.01, IC50=0.48, Slope=0.5, Lethal dose >20

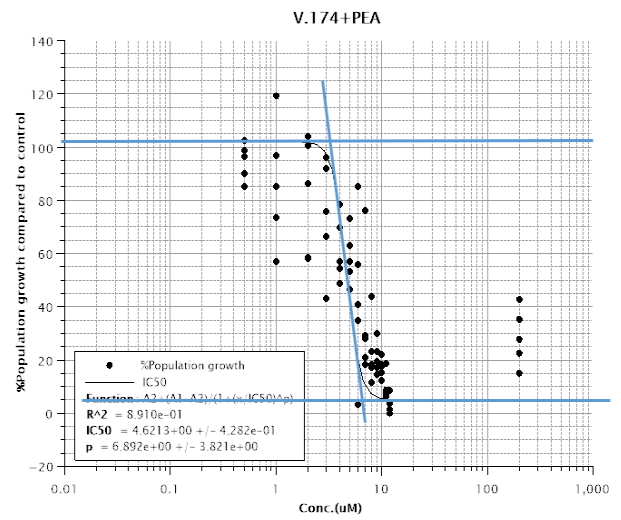
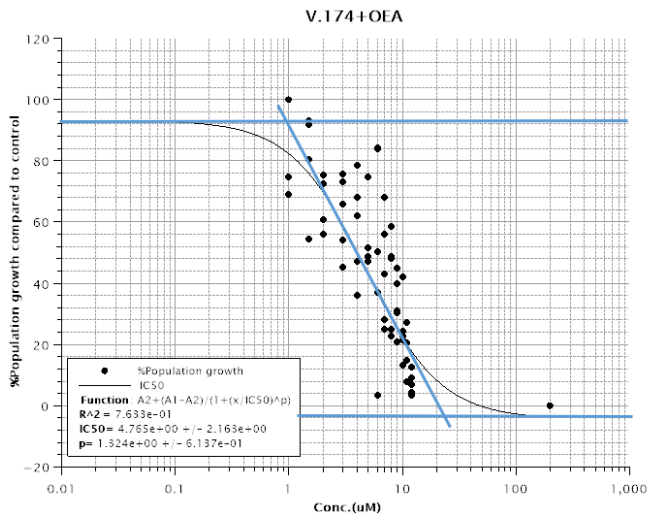
Rosiglitazone: estimated MIC =0.14, IC50=1, Slope=1, Lethal dose>8



Vermamoeba vermiformis 174

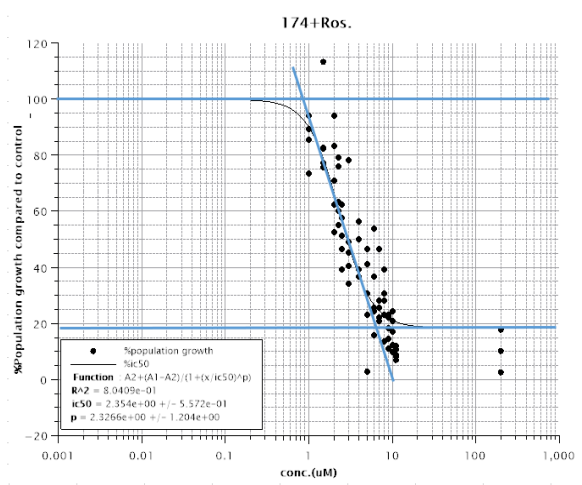
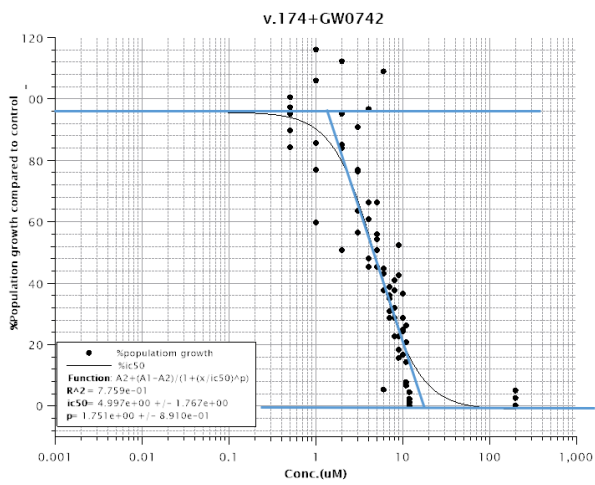
OEA: estimated MIC =1, IC50=4.77, Slope=1.32, Lethal dose >24

PEA: estimated MIC =3.20, IC50=4.62, Slope=6.89, Lethal dose >7



GW0742 estimated MIC =1.50, IC50=5.00, Slope=1.75, Lethal dose >19

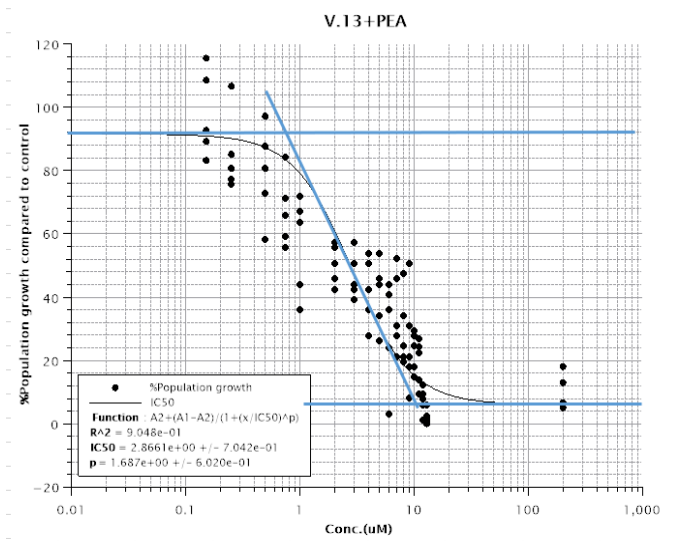
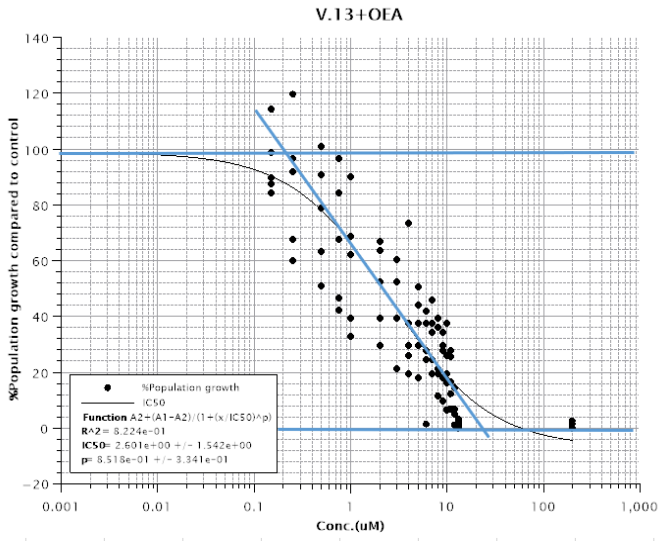
Rosiglitazone: estimated MIC =0.90, IC50=2.35, Slope=3.33, Lethal dose >6



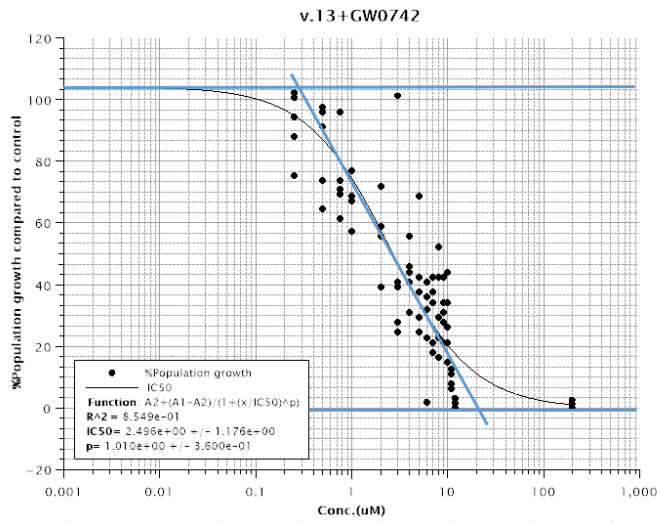
Vermamoeba vermiformis CCAP 1534/13

OEA: estimated MIC =0.20, IC50=2.60, Slope=0.85, Lethal dose >23

PEA: estimated MIC =0.75, IC50=2.87, Slope=1.69, Lethal dose >10



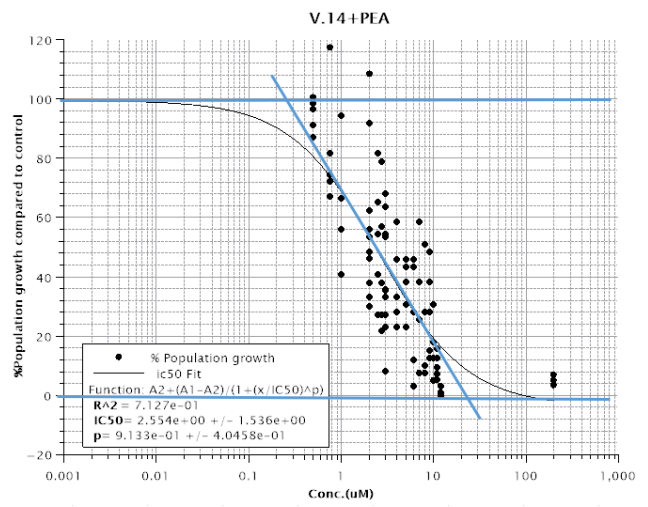
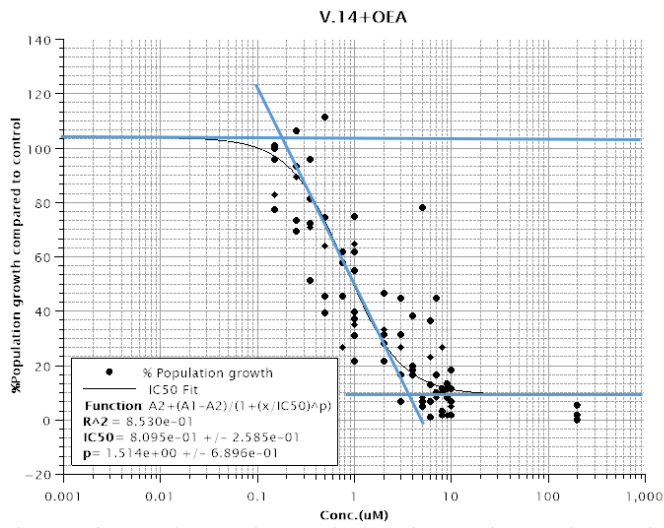
GW0742 estimated MIC =0.29, IC50=2.50, Slope=1.01, Lethal dose >20



Vermamoeba vermiformis CCAP 1534/14

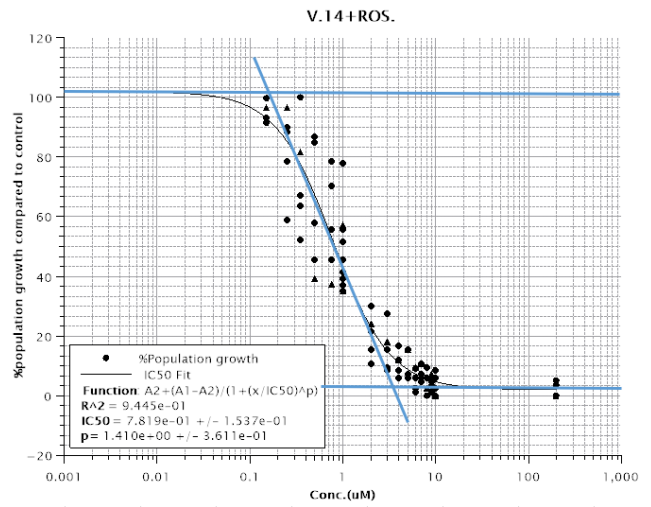
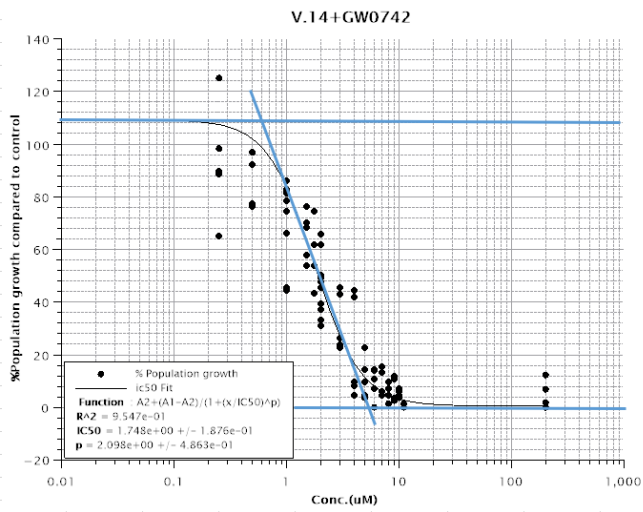
OEA: estimated MIC =0.19, IC50=0.81, Slope=1.51, Lethal dose >5

PEA: estimated MIC =0.25, IC50=2.55, Slope=0.91, Lethal dose >23



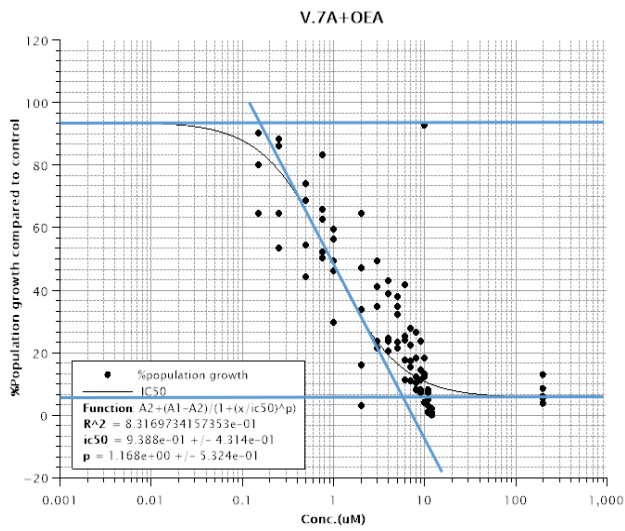
GW0742 estimated MIC =0.60, IC50=1.75, Slope=2.10, Lethal dose >5

Rosiglitazone: estimated MIC =0.16, IC50=0.78, Slope=1.41, Lethal dose >3

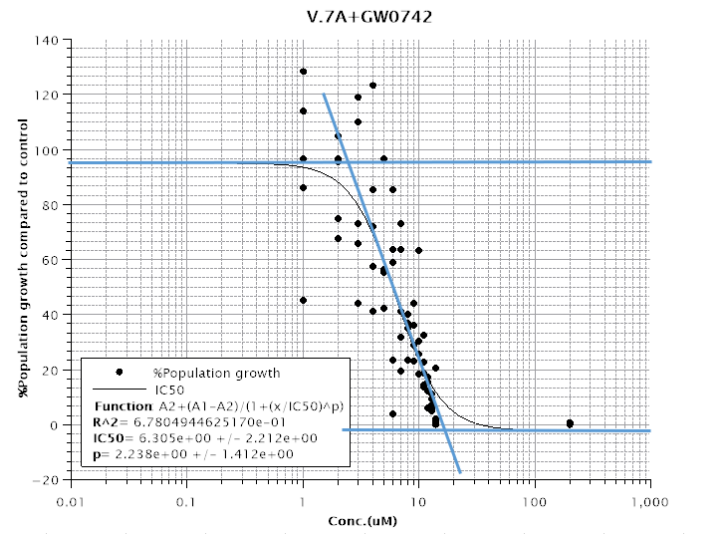


***Vermamoeba vermiformis* CCAP 1534/7A**

OEA: estimated MIC =0.60, IC50=0.94, Slope=1.17, Lethal dose >6



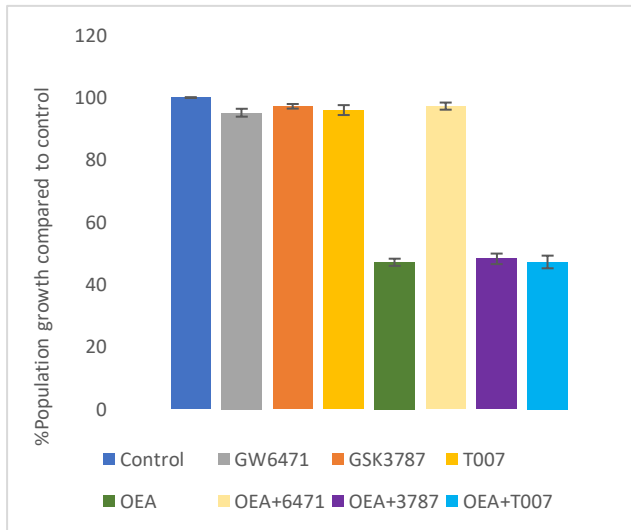
GW0742 estimated MIC =2.50, IC50=6.31, Slope=2.24, Lethal dose >17



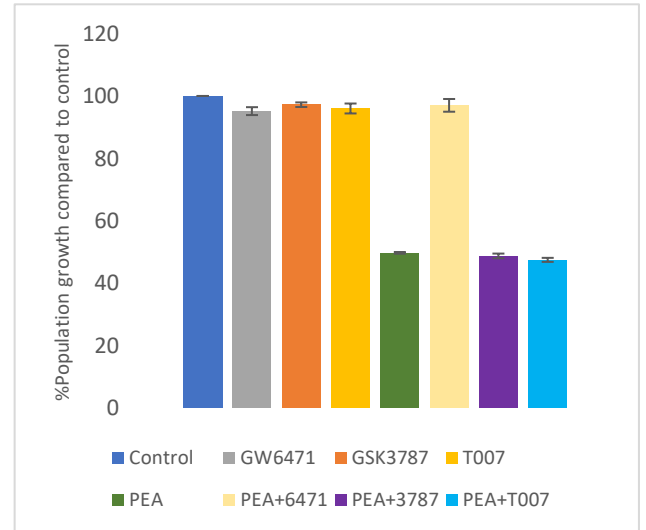
Appendix 4: Response of *Vermamoeba vermiformis* strains to PPAR agonists in the presence and absence of specific PPAR antagonists (Section 5.2.1.2)

V. vermiformis 137

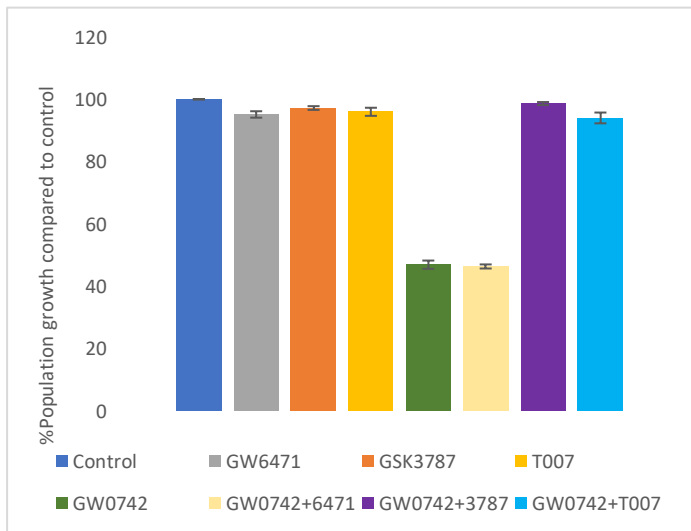
OEA



PEA

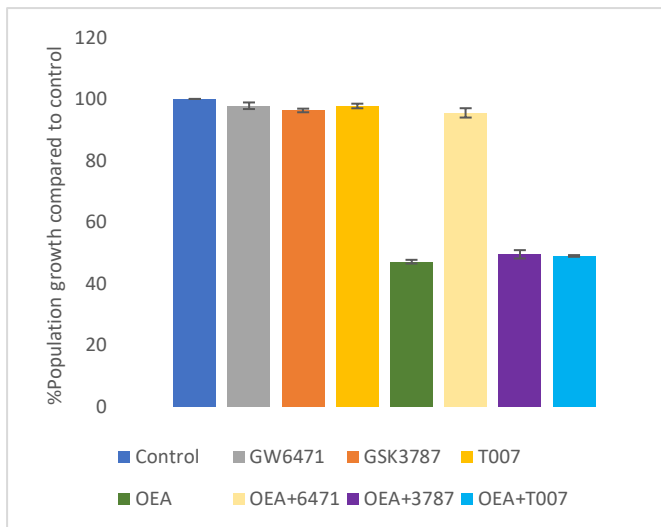


GW0742

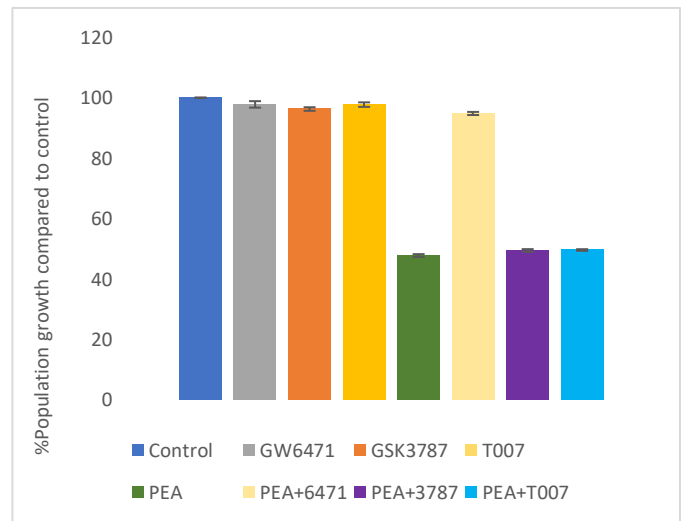


V. vermiformis 172

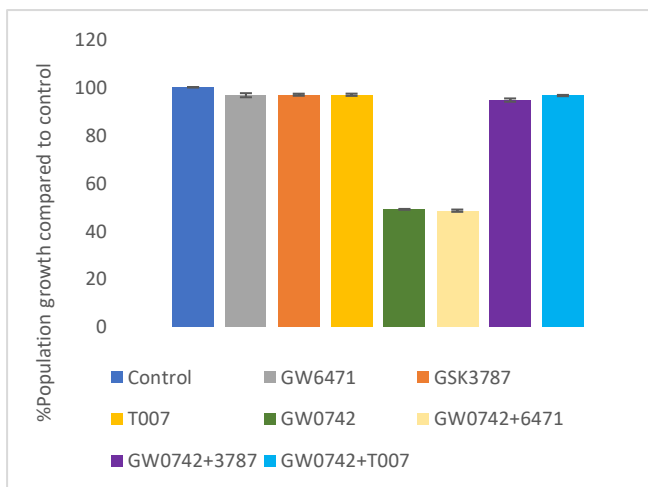
OEA



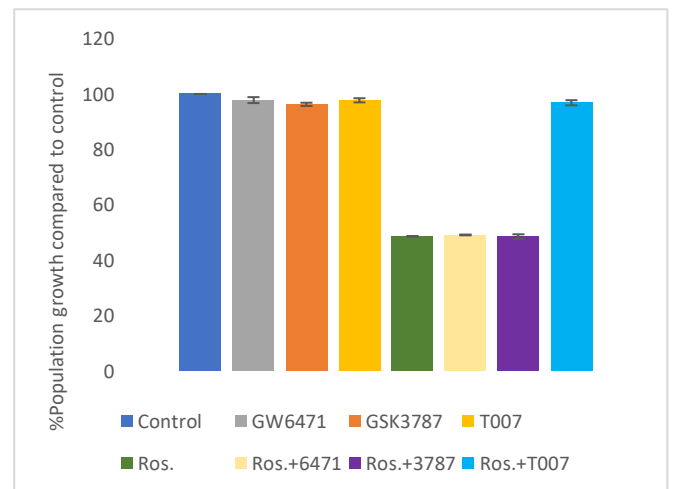
PEA



GW0742

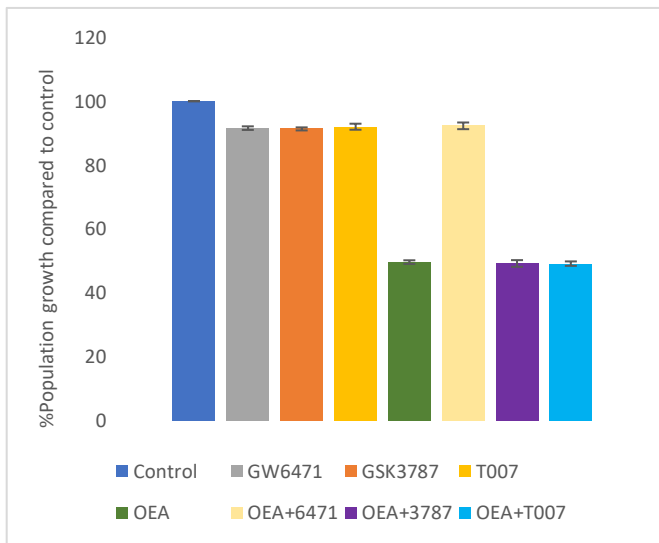


Rosiglitazone

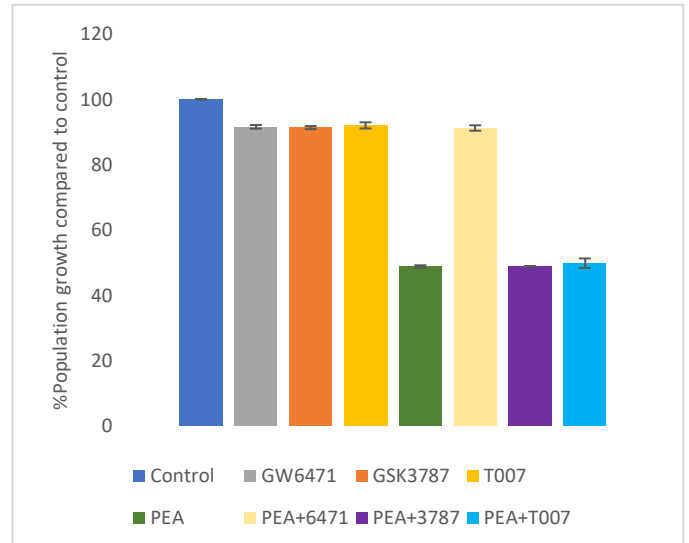


V. vermiformis 173

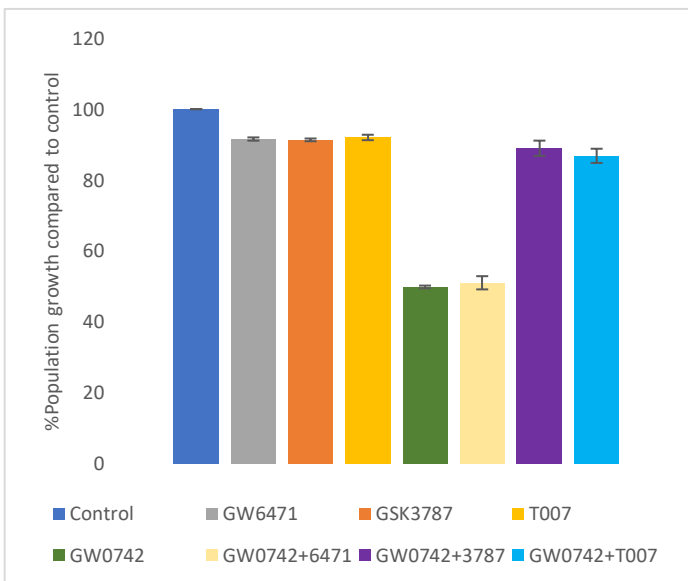
OEA



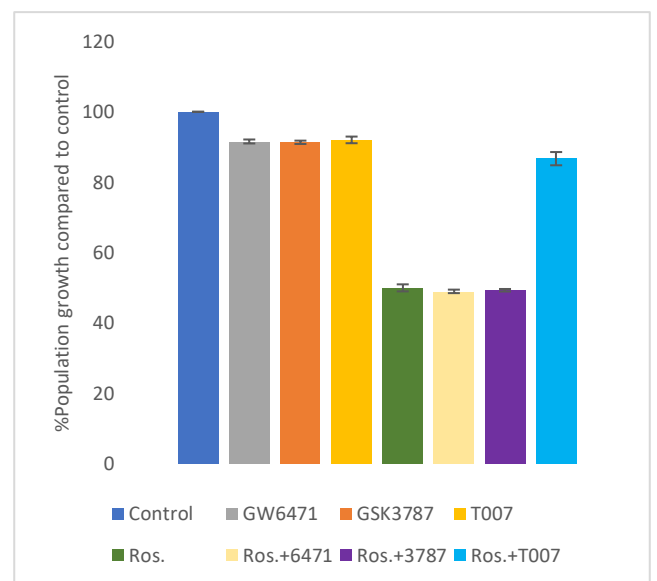
PEA



GW0742

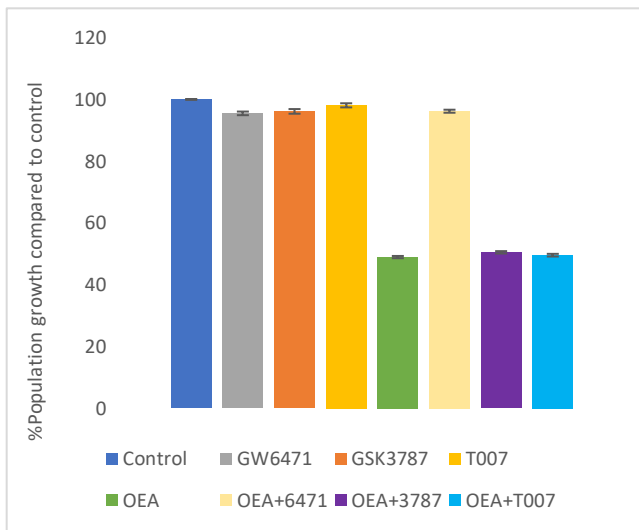


Rosiglitazone

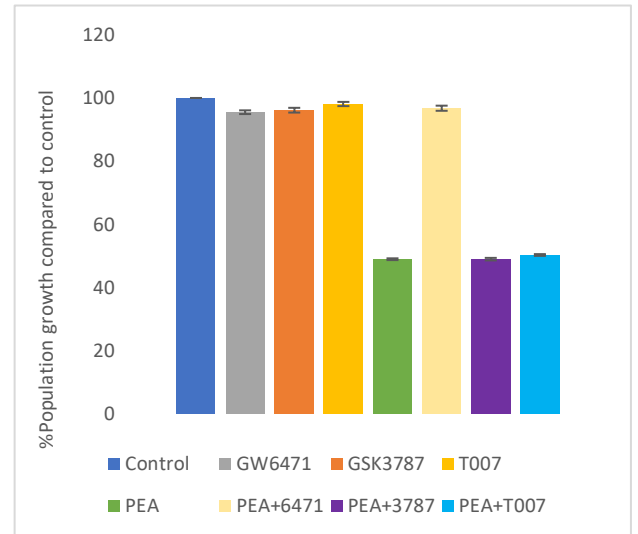


V. vermiformis 174

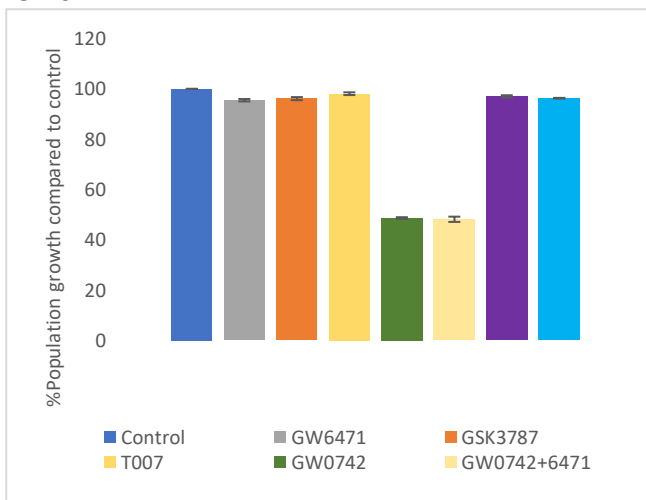
OEA



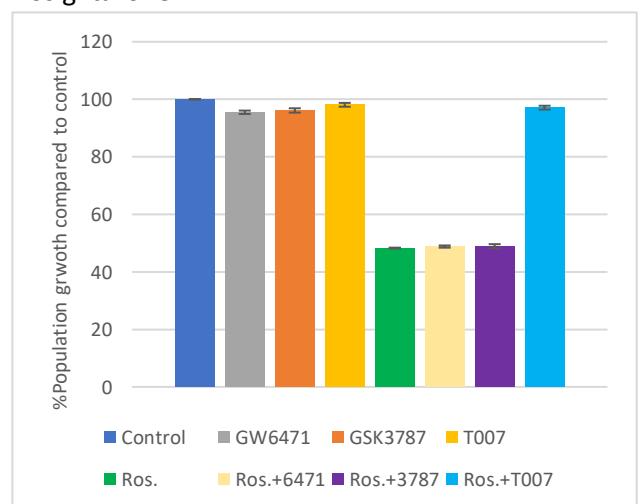
PEA



GW0742

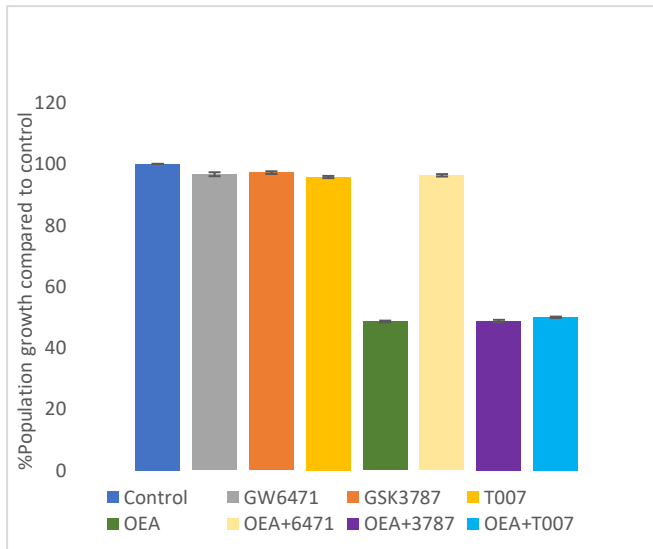


Rosiglitazone

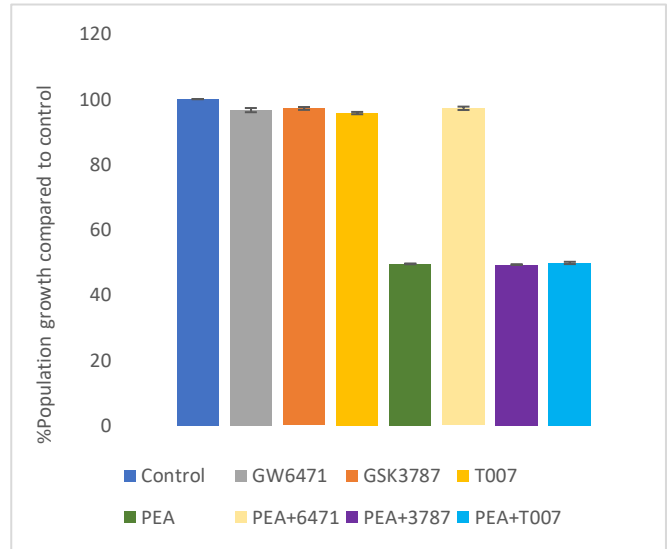


V. vermiformis CCAP 1534/13

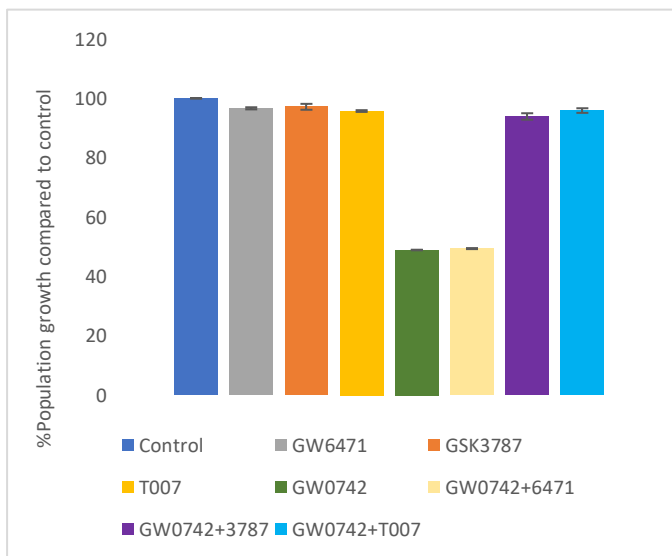
OEA



PEA

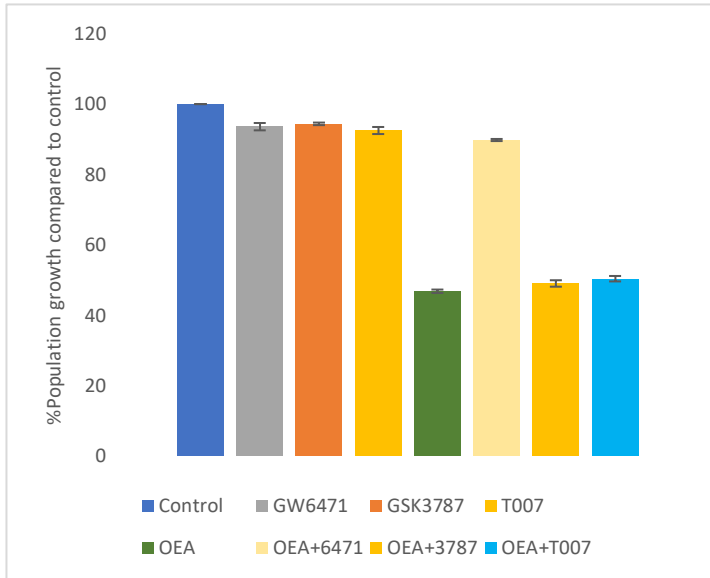


GW0742

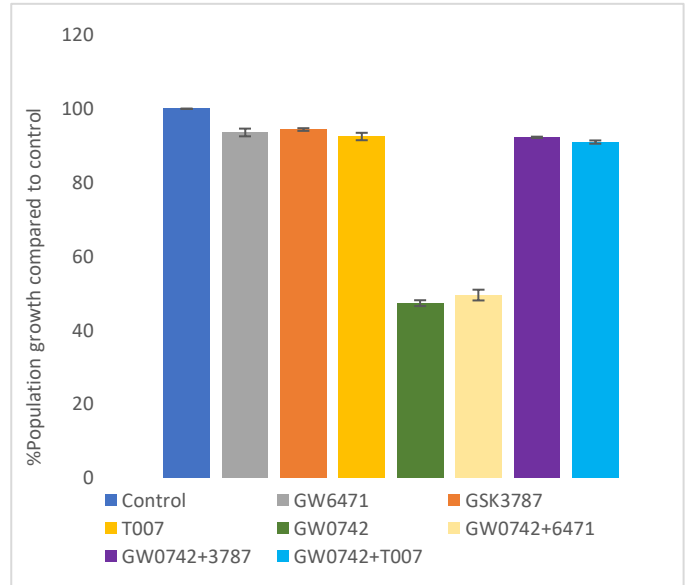


***V. vermiformis* CCAP 1534/7A**

OEA

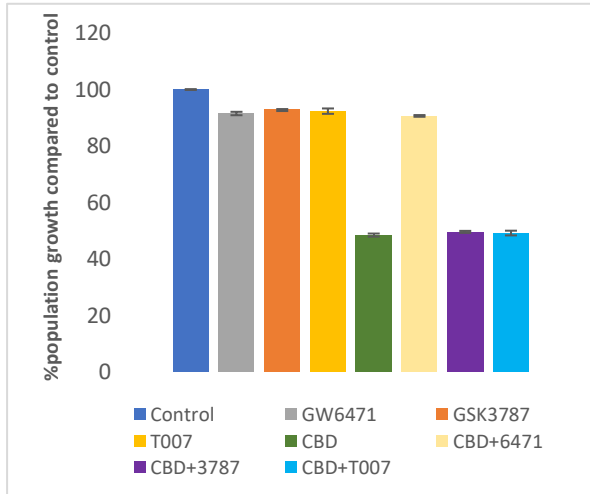


GW0742

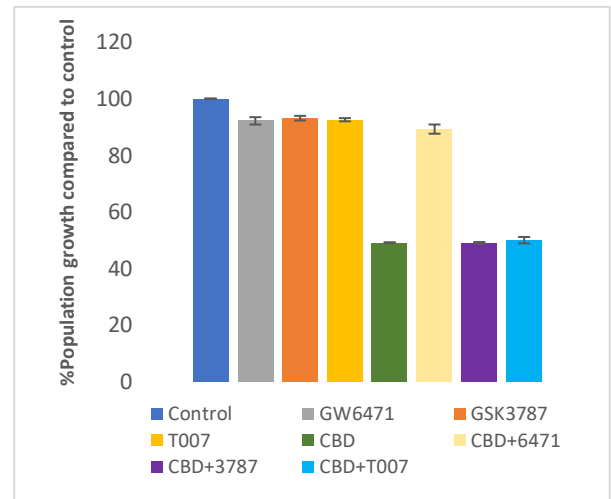


Appendix 5: Response of *Vermamoeba vermiformis* strains to CBD in the presence and absence of three PPAR antagonists (Section 5.2.1.3)

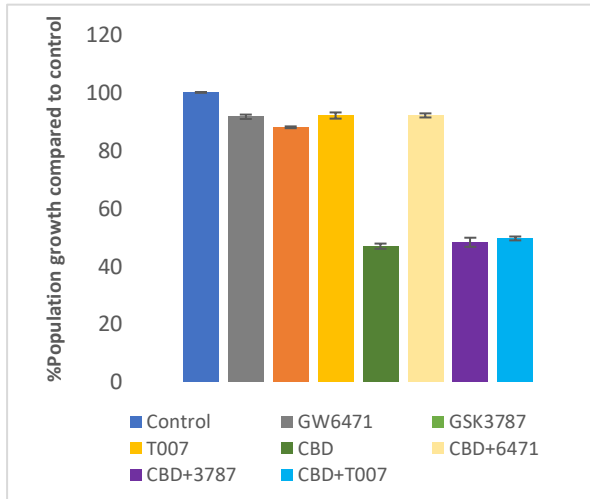
***V. vermiformis* 137**



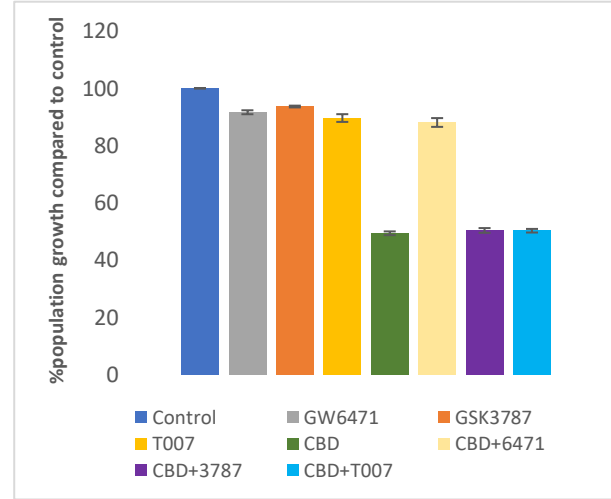
***V. vermiformis* 172**



***V. vermiformis* 173**

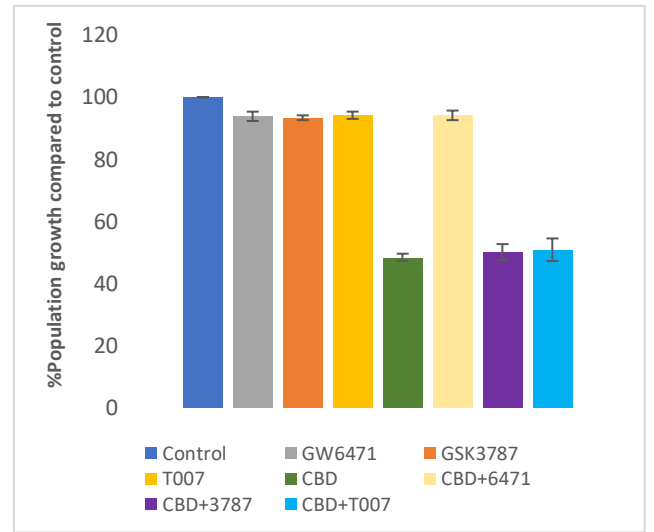
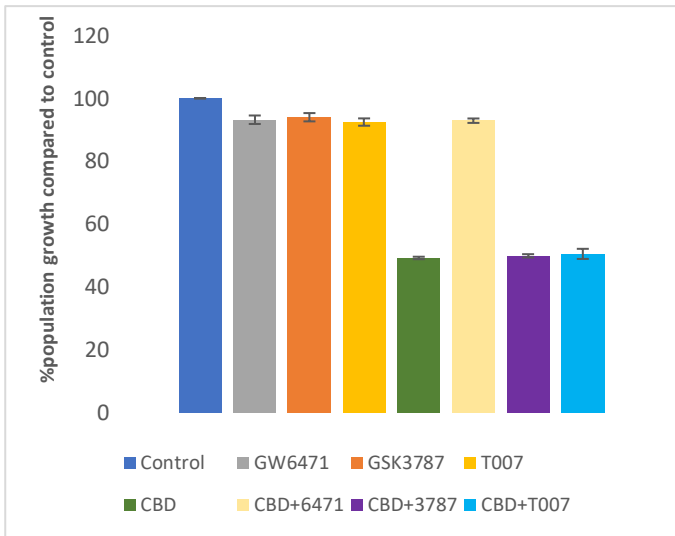


***V. vermiformis* 174**



***V. vermiformis* CCAP 1534/13**

***V. vermiformis* CCAP 1534/7A**

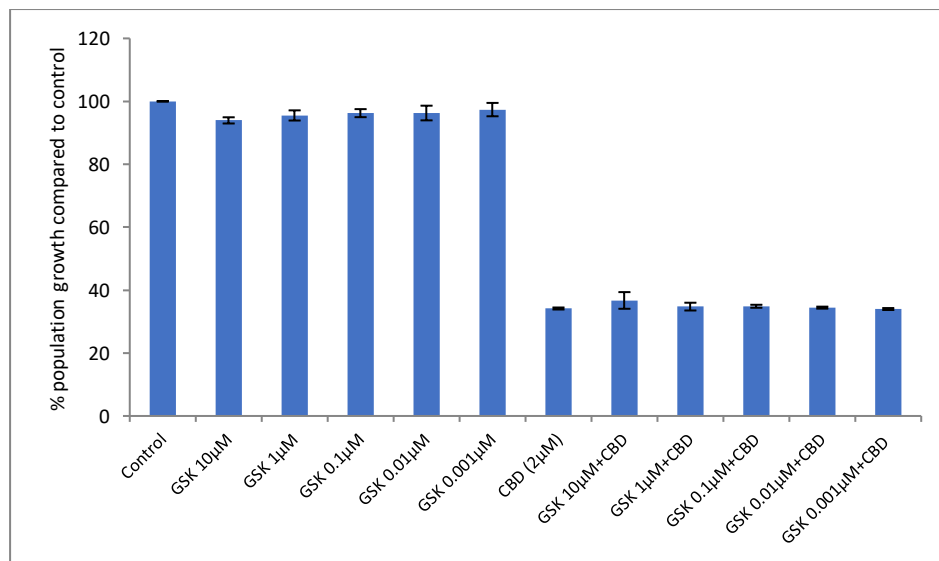


Key: GW6471 (antagonist for PPAR α), GSK3787 (antagonist for PPAR β/δ) and T007 (antagonist for PPAR γ)

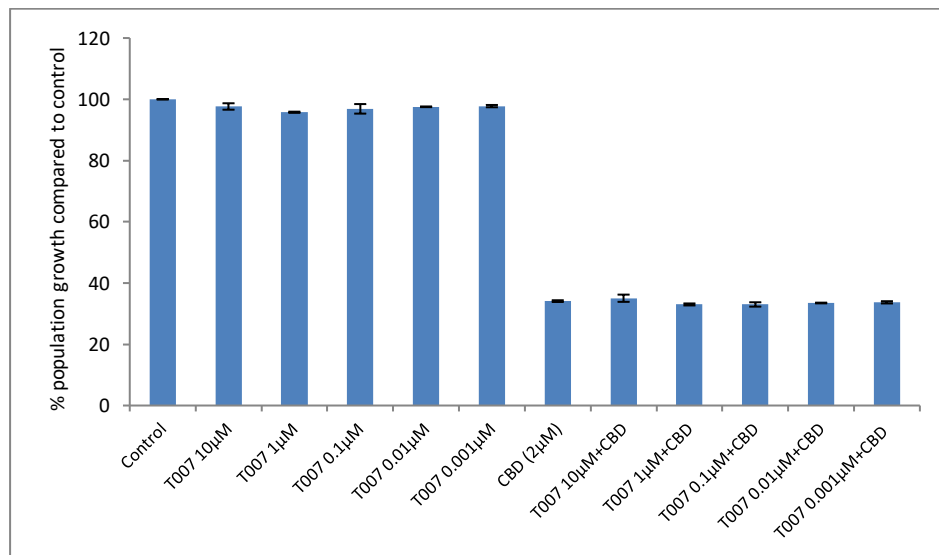
Appendix 6: Response of *Vermamoeba vermiformis* strains to CBD in the presence and absence of three PPAR antagonists at different concentrations (Section 5.2.1.4)

***V. vermiformis* CCAP 1534/14 (PPAR α response in Fig. 5.3)**

GSK3787 (PPAR β/δ)

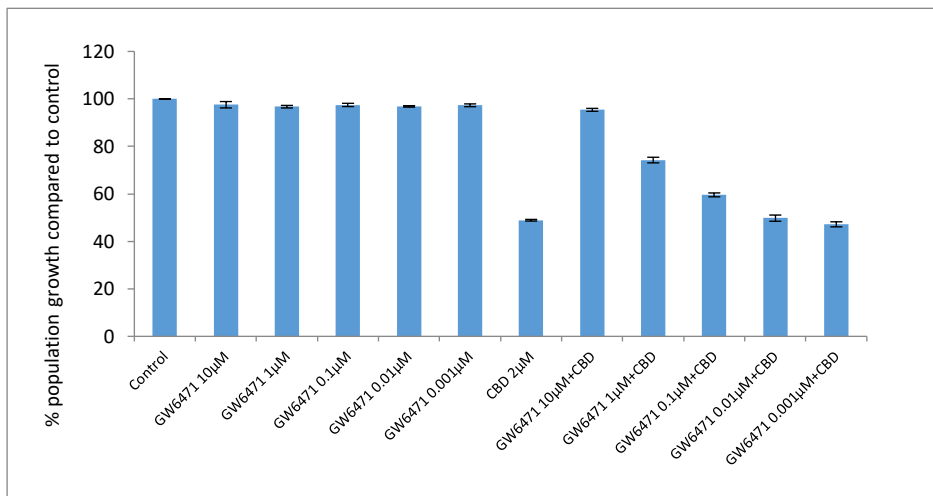


T0070907 (PPAR γ)

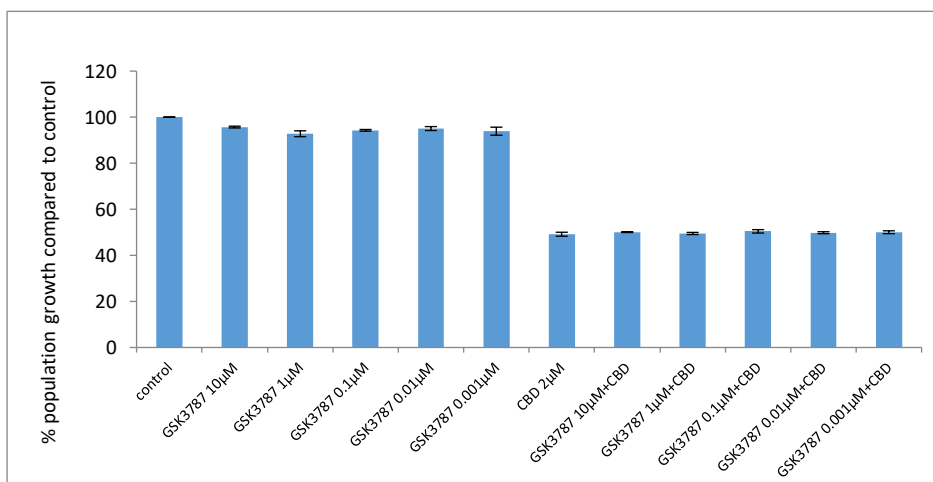


V. vermiformis 137

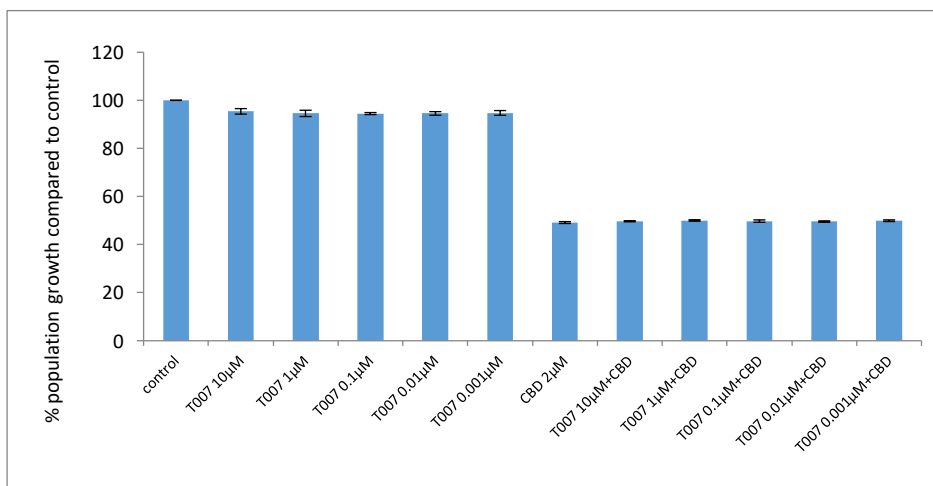
GW6471 (PPAR α)



GSK3787 (PPAR β/δ)

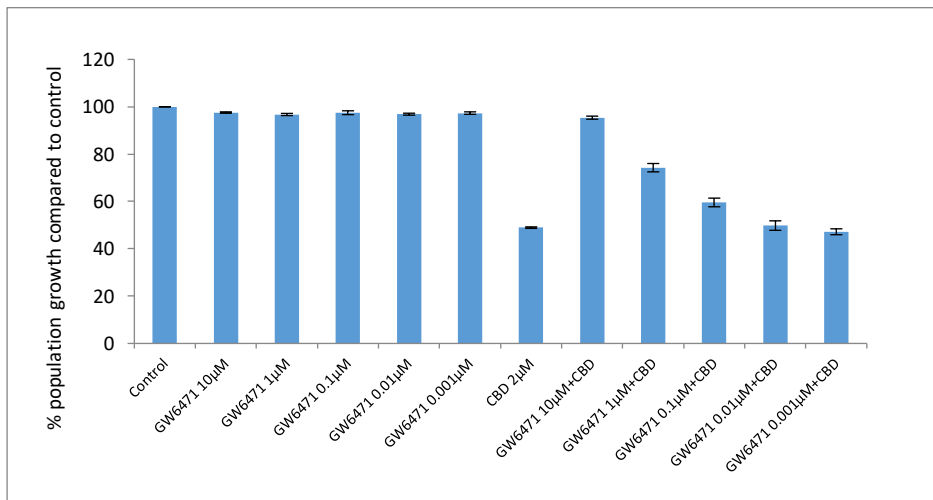


T0070907 (PPAR γ)

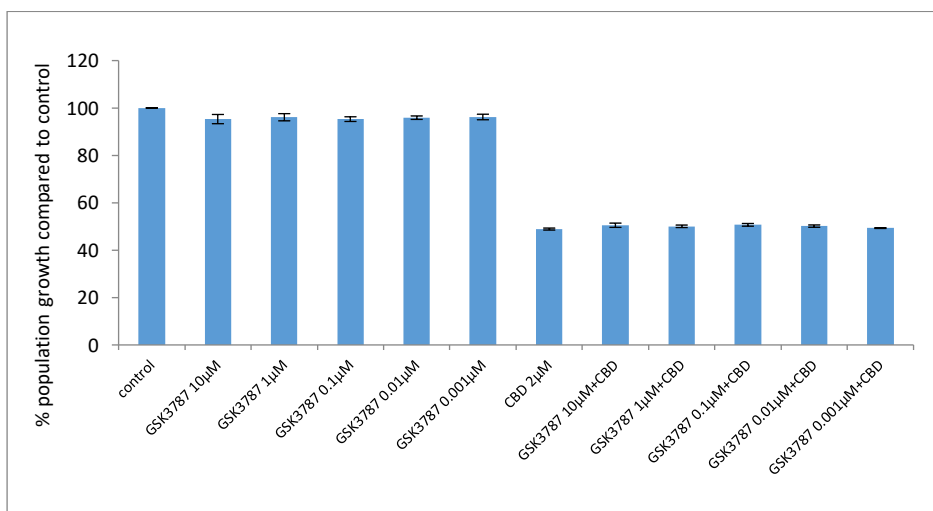


V. vermiformis 172

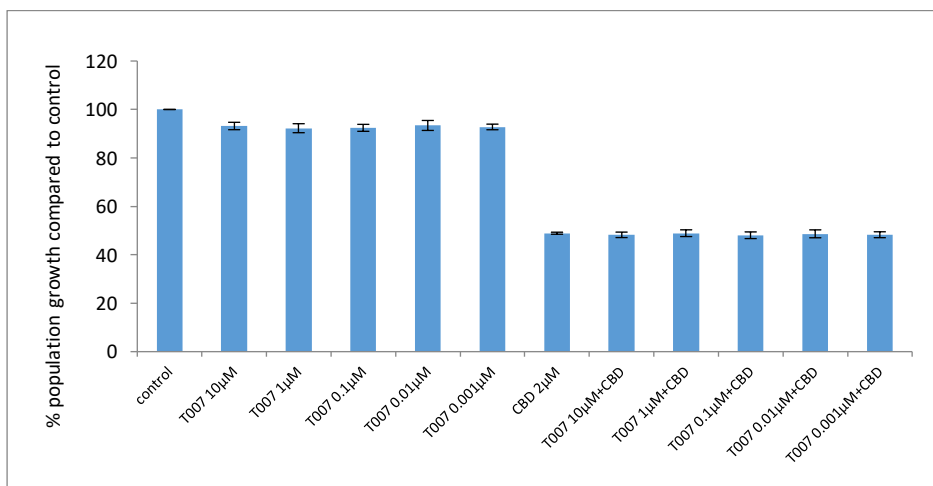
GW6471 (PPAR α)



GSK3787 (PPAR β/δ)

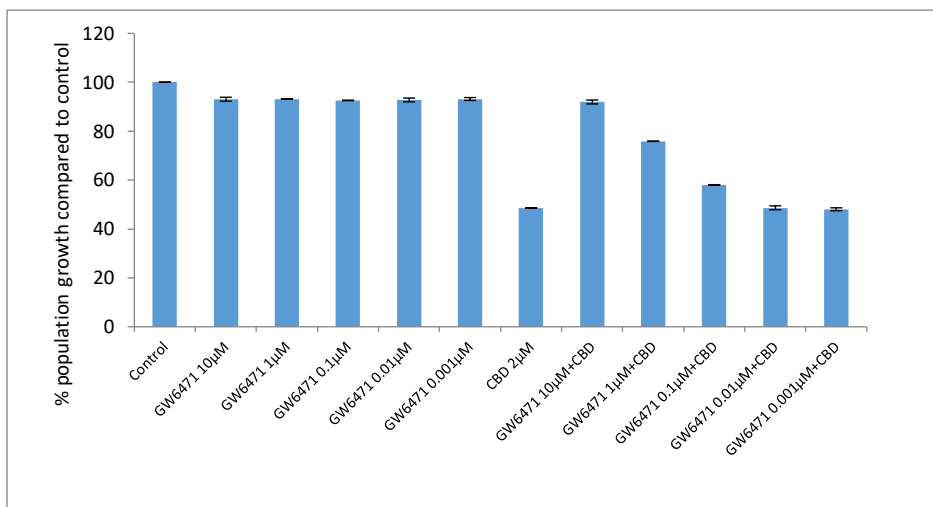


T0070907 (PPAR γ)

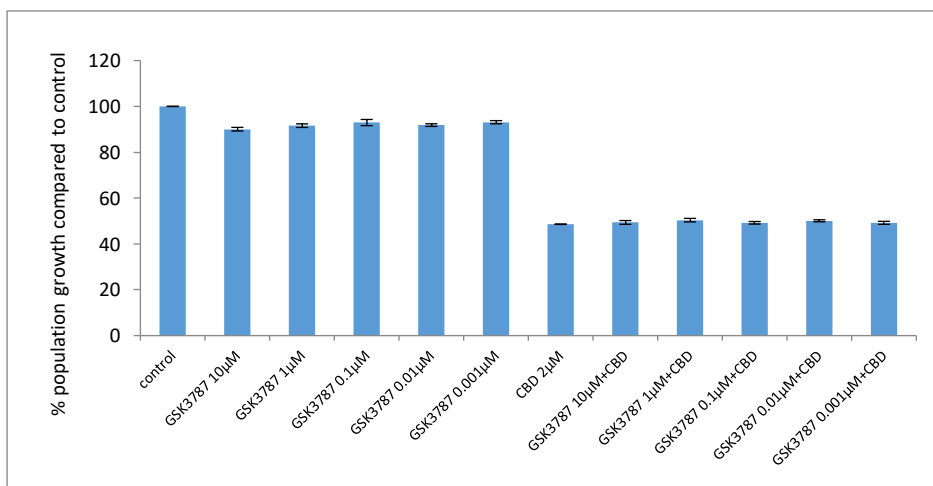


V. vermiformis 173

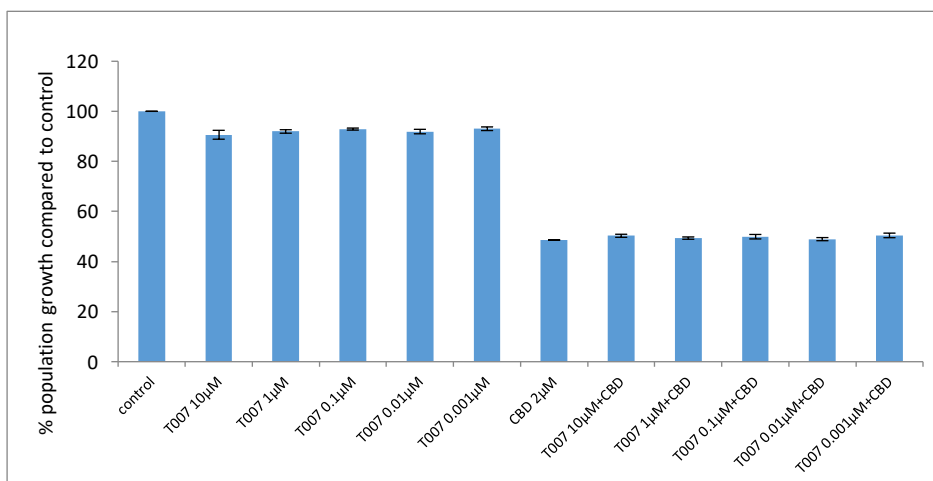
GW6471 (PPAR α)



GSK3787 (PPAR β/δ)

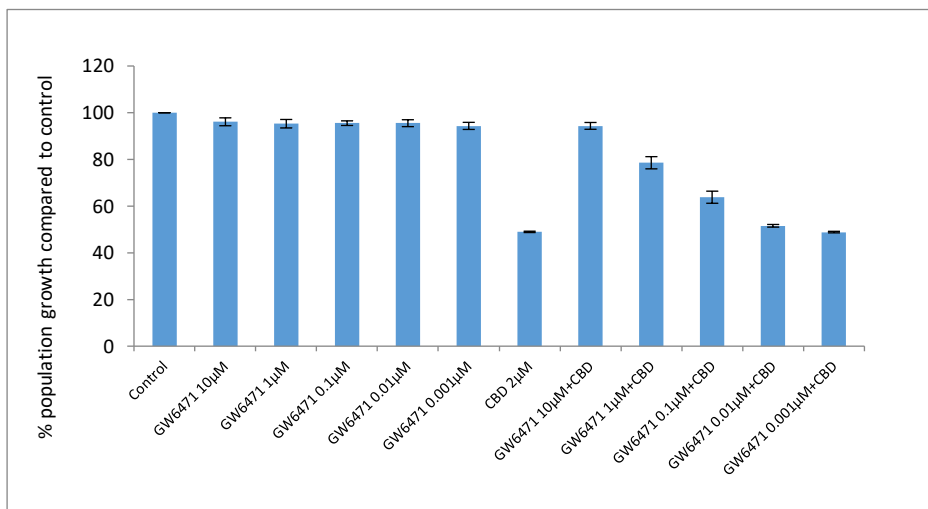


T0070907 (PPAR γ)

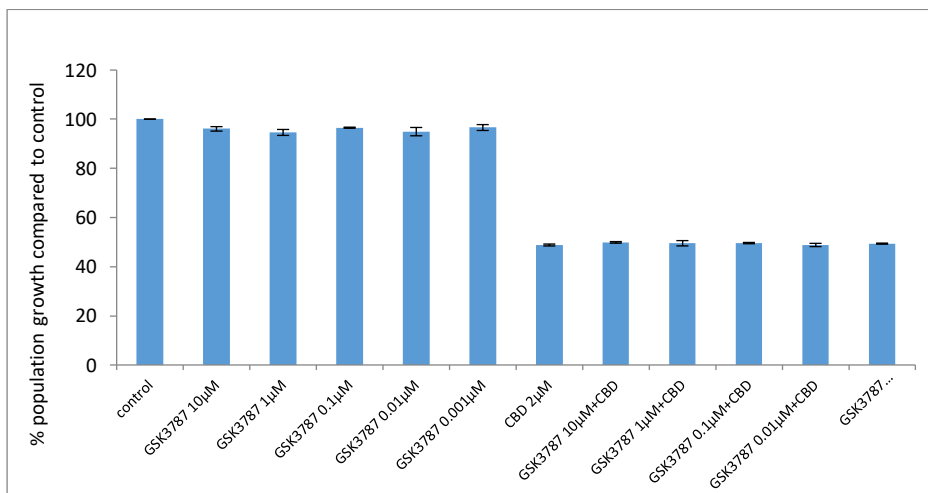


V. vermiformis 174

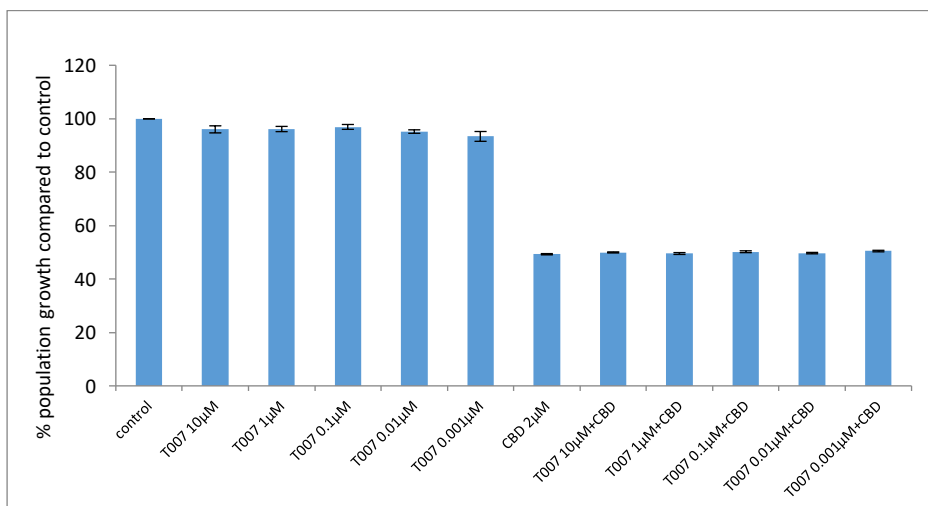
GW6471 (PPAR α)



GSK3787 (PPAR β/δ)

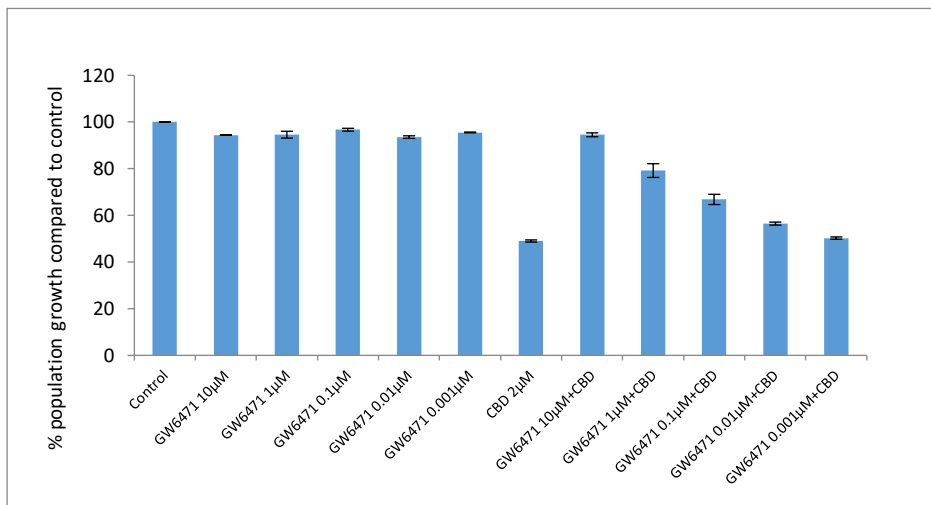


T0070907 (PPAR γ)

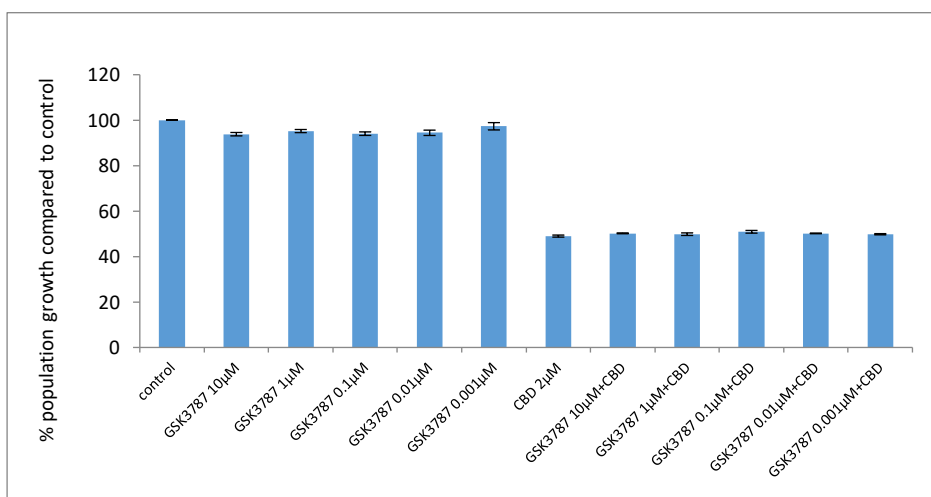


V. vermiformis CCAP 1534/13

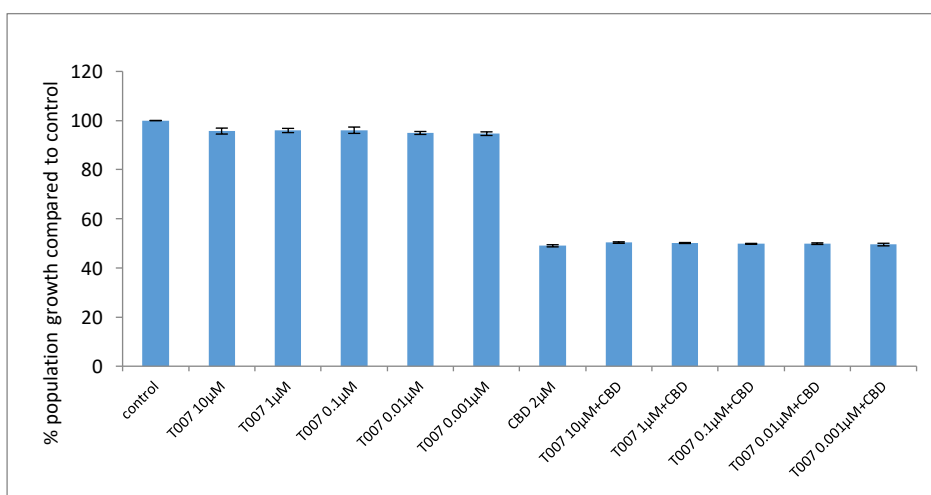
GW6471 (PPAR α)



GSK3787 (PPAR β/δ)

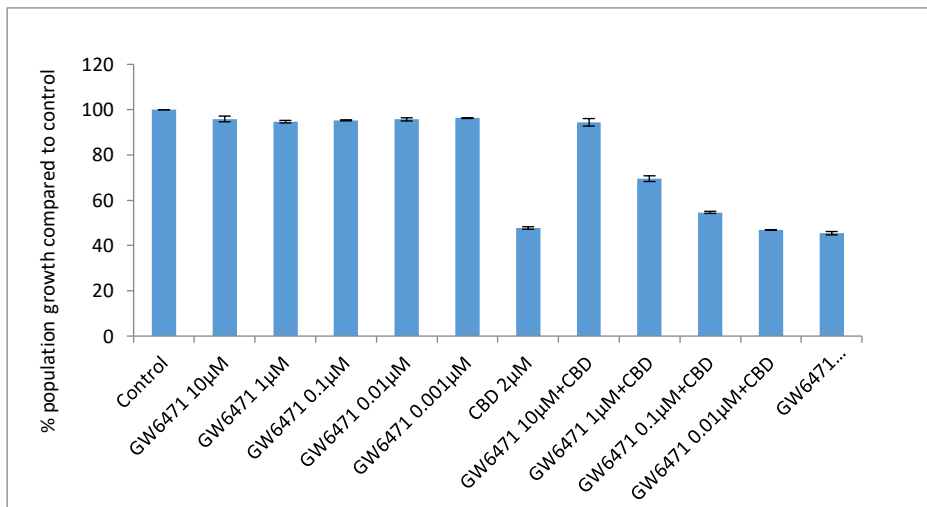


T0070907 (PPAR γ)

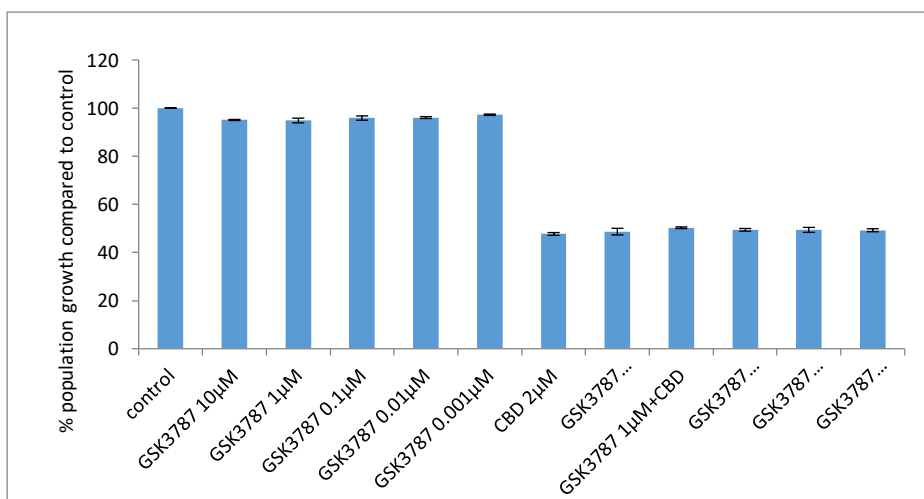


V. vermiformis CCAP 1534/7A

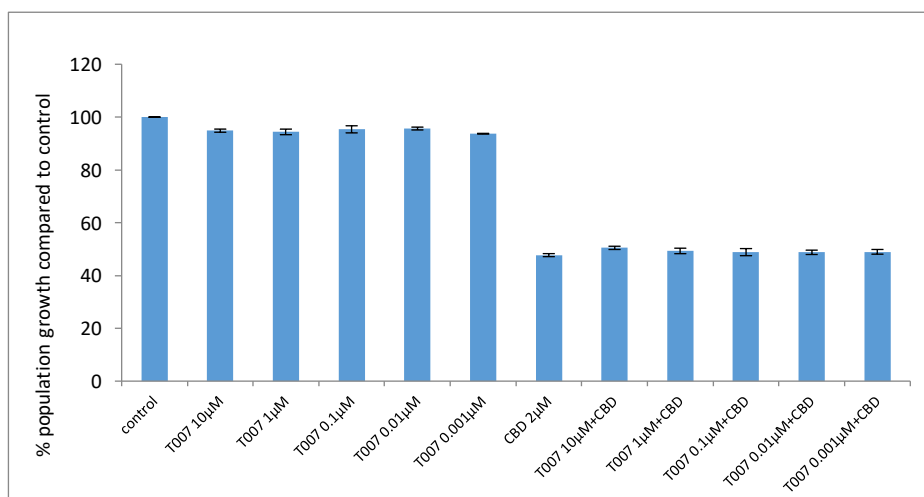
GW6471 (PPAR α)



GSK3787 (PPAR β/δ)

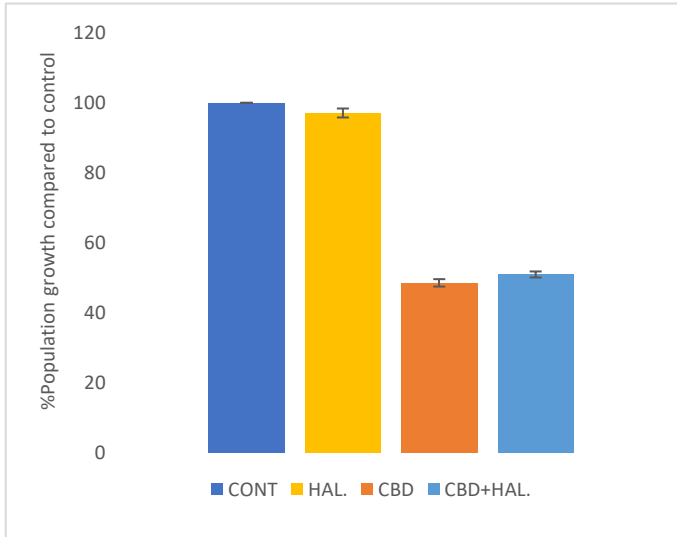


T007090 (PPAR γ)

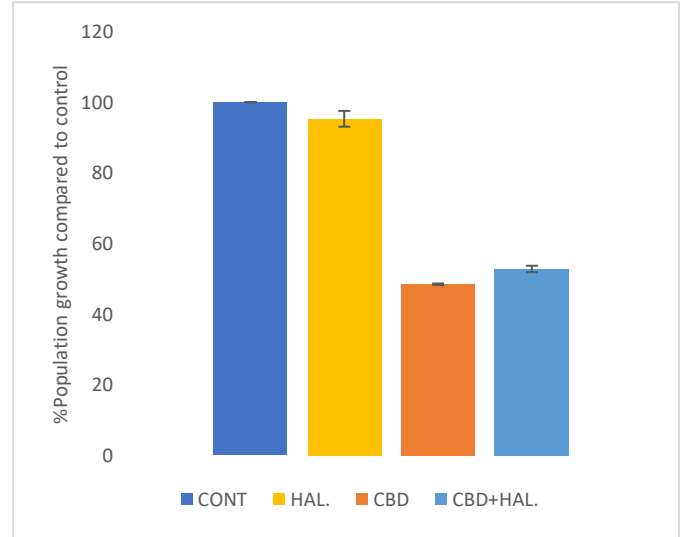


Appendix 7: Response of sensitive amoeba strains to CBD and AEA in the presence and absence of Haloperidol (Section 6.2.1.)

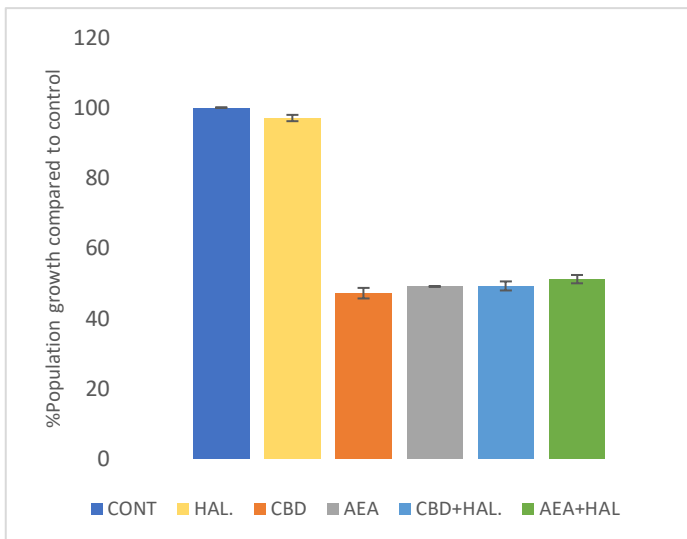
***Acanthamoeba castellanii* CCAP1501/1A .(CBD only).**



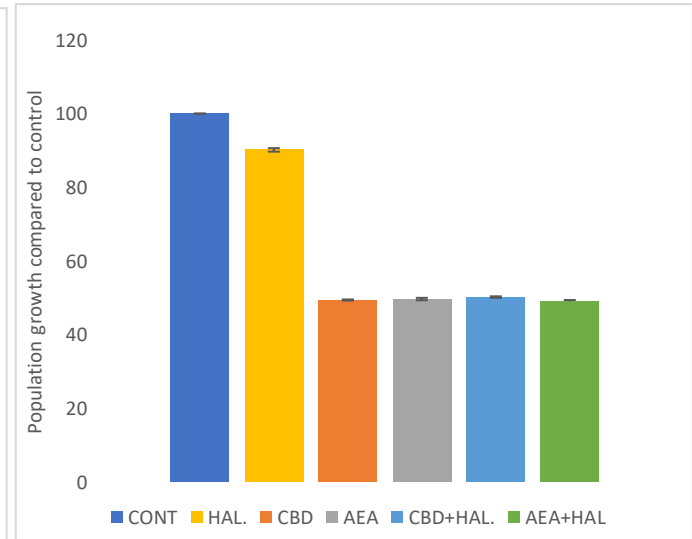
***Flamella arnhemensis* CCAP1525/2 (CBD only).**



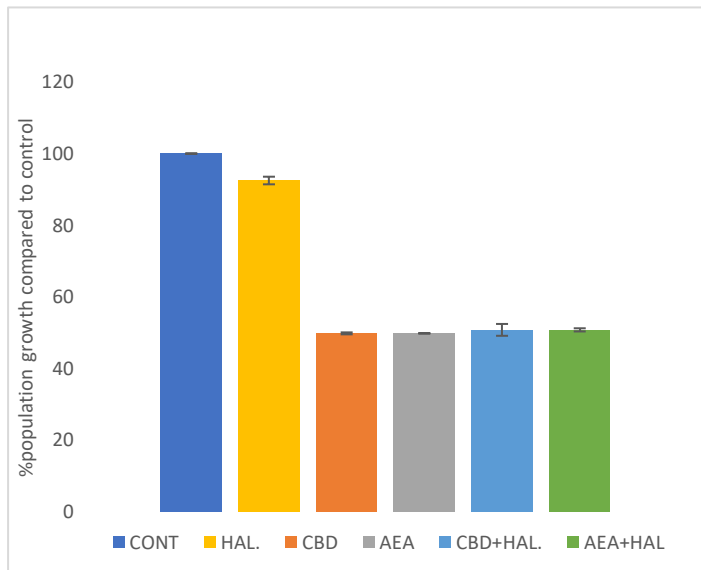
***Hartmannella cantabrigiensis* CCAP1534/8 +CBD/AEA**



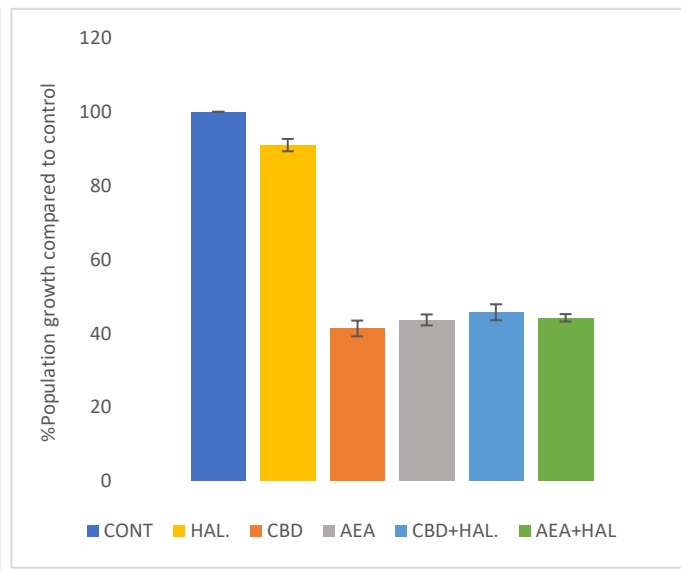
***Vermamoeba vermiformis* 137+ CBD/AEA**



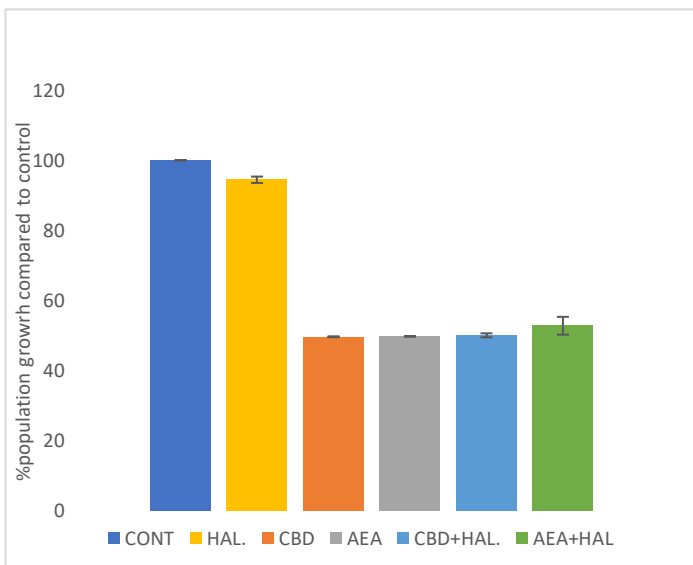
***Vermamoeba vermiformis* 172+ CBD/AEA**



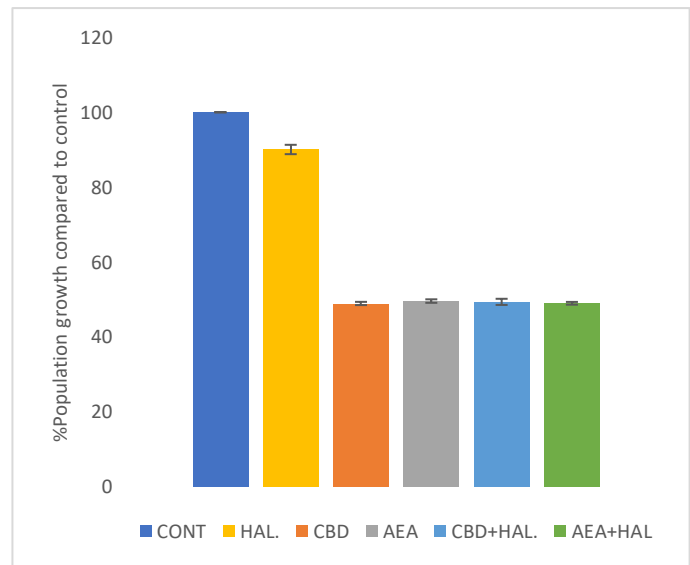
***Vermamoeba vermiformis* 173+ CBD/AEA**



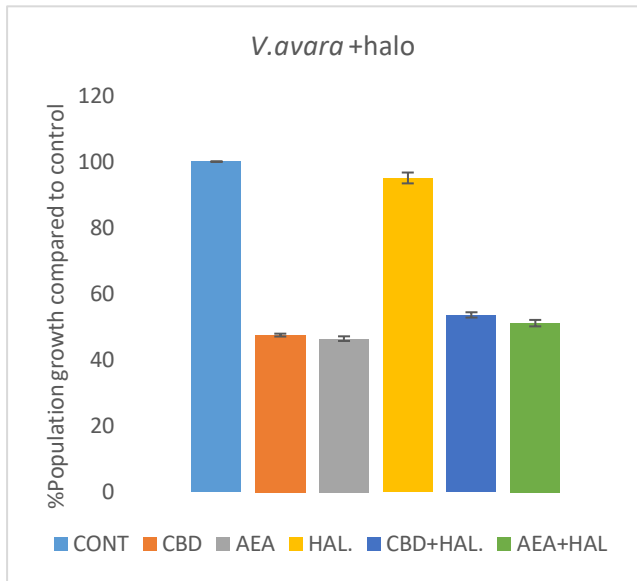
***Vermamoeba vermiformis* 174 + CBD/AEA**



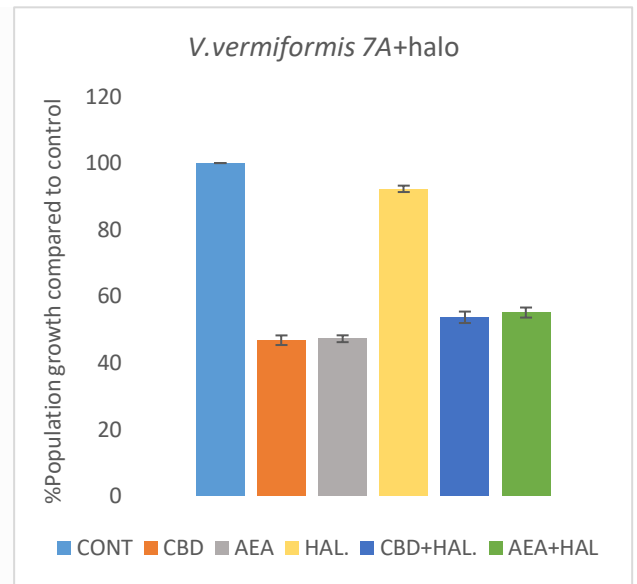
***Vermamoeba vermiformis* CCAP 1534/13+ CBD/AEA**



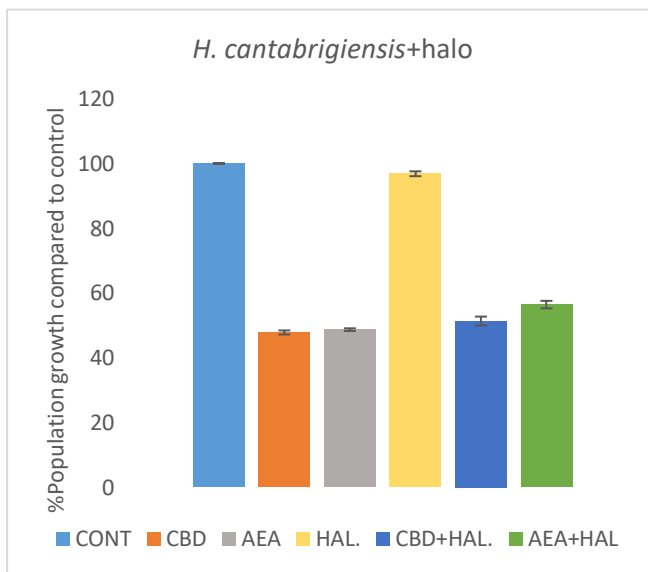
***Vahlkamphia avara* CCAP 1588/1A + CBD/AEA**



***Vermamoeba vermiformis* CCAP 1534/7A + CBD/AEA**



***Hartmannella cantabrigiensis* CCAP 1534/11 + CBD/AEA**



***Vermamoeba vermiformis* CCAP 1534/14 + CBD/AEA**

